

Regulation of specialized metabolites in *Photorhabdus* and *Xenorhabdus*

Dissertation

zur Erlangung des Doktorgrades
der Naturwissenschaften

vorgelegt beim Fachbereich für Biowissenschaften (15)
der Johann Wolfgang Goethe-Universität
in Frankfurt am Main

von

Nick Larry Valentin Neubacher
aus Weinheim

Frankfurt am Main 2020

D30

vom Fachbereich für Biowissenschaften (15) der
Johann Wolfgang Goethe-Universität als Dissertation angenommen.

Dekan: Prof. Dr. Sven Klimpel

Gutachter: Prof. Dr. Helge B. Bode

Zweitgutachter: Prof. Dr. Eckhard Boles

Datum der Disputation:

Table of contents

Table of abbreviations	V
Summary	VI
Zusammenfassung	VIII
1. Introduction	1
1.1. <i>Photorhabdus</i> and <i>Xenorhabdus</i>	2
1.2. Specialized metabolites – many “to rule them all”	4
1.3. Bacterial gene regulation	6
1.3.1. Regulation of transcription	6
1.3.2. Post-transcriptional regulation	10
1.3.3. Post-translational modifications	13
1.4. Regulatory network of SM production in <i>Photorhabdus</i> and <i>Xenorhabdus</i>	13
1.5. Motivation and aim of this work	15
2. Materials and methods	18
2.1. Topic A: Small RNA directs symbiosis, virulence, and natural products biosynthesis in entomopathogenic bacteria	18
2.1.1. Bacterial culture conditions	18
2.1.2. Microorganisms	19
2.1.3. Plasmids	21
2.1.4. Oligonucleotides	23
2.1.5. Construction of mutant strains	26
2.1.6. Creation of transposon mutant library	27
2.1.7. DNA extraction and sequencing	27
2.1.8. RNA extraction, sequencing and analysis	27
2.1.9. Northern blot analysis	28

2.1.10.	Compensatory base mutation and GFP fluorescence assay.....	28
2.1.11.	RIP-seq analysis	29
2.1.12.	ArcZ binding prediction.....	30
2.1.13.	SM analysis via HPLC-MS/MS.....	32
2.1.14.	Nematode development assay.....	32
2.2.	Topic B: Components of insect larvae modulate <i>Xenorhabdus</i> and <i>Photorhabdus</i> secondary metabolite production.....	33
2.2.1.	Bacterial culture conditions.....	33
2.2.2.	Preparation of insect homogenate.....	33
2.2.3.	Isolation of insect hemolymph	33
2.2.4.	RNA extraction, sequencing and analysis	33
2.2.5.	HPLC-MS/MS analysis.....	34
2.2.6.	GC-MS analysis.....	34
2.3.	Topic C: Identification of novel genes involved in SM production by transposon mutagenesis.....	35
2.3.1.	Cultivation of bacterial cultures.....	35
2.3.2.	Microorganisms	36
2.3.3.	Plasmids.....	37
2.3.4.	Oligonucleotides.....	38
2.3.5.	Transposon mutagenesis	38
2.3.6.	Construction of mutant strains.....	38
2.3.7.	HPLC-MS analysis	39
2.3.8.	RNA-seq.....	39
2.3.9.	Single-Molecule Real-Time sequencing	39
3.	Results.....	40
3.1.	Topic A: Small RNA directs symbiosis, virulence, and natural products biosynthesis in entomopathogenic bacteria	40

3.1.1.	sRNA identification in <i>P. laumondii</i> and <i>X. szentirmaii</i>	42
3.1.2.	RIPseq reveals Hfq dependent sRNAs	42
3.1.3.	ArcZ is essential for SM production in <i>P. laumondii</i> TTO1	44
3.1.4.	ArcZ specifically binds to a regulatory region in the 5'-UTR of <i>hexA</i> to control SM production.....	46
3.1.5.	A general mechanism? Effect of ArcZ in <i>Xenorhabdus</i>	48
3.1.6.	The ArcZ regulon in <i>Photorhabdus</i> and <i>Xenorhabdus</i>	50
3.1.7.	ArcZ in <i>P. laumondii</i> is essential for niche occupation.....	56
3.1.8.	Selective SM production in <i>X. szentirmaii</i> Δ <i>arcZ</i>	57
3.2.	Topic B: Components of insect larvae modulate SM production in <i>Xenorhabdus</i> and <i>Photorhabdus</i>	59
3.2.1.	<i>In vivo</i> Simulation	59
3.2.2.	RNA-sequencing	61
3.2.3.	The composition of <i>G. mellonella</i> homogenate and hemolymph.....	63
3.2.4.	Titration of SM production by addition of abundant insect components ..	65
3.3.	Topic C: Identification of novel genes involved in SM production by transposon mutagenesis	68
3.3.1.	Transposon mutagenesis	69
3.3.2.	SM profile of <i>dam1</i> deletion mutant in <i>P. laumondii</i>	72
3.3.3.	The deletion of the adenine-specific DNA-methyltransferase influences the growth behaviour of <i>P. laumondii</i>	73
3.3.4.	Transcriptomic profiling of <i>P. laumondii</i> Δ <i>dam1</i>	75
3.3.5.	The <i>dam1</i> methylome of <i>P. laumondii</i>	76
4.	Discussion and perspective	78
4.1.	Topic A: Implications of ArcZ in regulation of SM production	78
4.1.1.	The ArcZ regulon	78
4.1.2.	ArcZ and Hfq - shared and exclusive targets?	80

4.1.3.	ArcZ controls nematode development in <i>P. laumondii</i>	81
4.1.4.	The molecular basis of ArcZ mediated regulation	82
4.1.5.	ArcZ as a tool for SM production?	84
4.1.6.	The expanded regulatory network for SM production – A perspective	84
4.2.	Topic B: Sensing an insect host – a link to SM production	86
4.2.1.	“ <i>In vivo</i> simulation” alters SM profiles in <i>Photorhabdus</i> and <i>Xenorhabdus</i> strains	86
4.2.2.	The shared core response to an insect-like environment	87
4.2.3.	Insect signals link host recognition to metabolic adjustment	89
4.3.	Topic C: Identification of novel genes involved in SM production by transposon mutagenesis.....	91
4.3.1.	Characterization of the $\Delta dam1$ phenotype.....	91
4.3.2.	The Dam methylome of <i>P. laumondii</i>	93
	References	95
5.	Supporting information	110
6.	Appendix	114

Table of abbreviations

BGC	biosynthetic gene cluster
bp	base pairs
BPC	base peak chromatogram
CDS	coding sequence
CHIP-Seq	chromatin immunoprecipitation sequencing
CoA	coenzyme A
DNA	deoxyribonucleic acid
FDR	false discovery rate
GC-MS	gas chromatography-mass spectrometry
GFP	green fluorescent protein
Hfq	host factor of the RNA bacteriophage Q β
HK	histidine kinase
HPLC-MS	high performance liquid chromatography mass spectrometry
IJ	infective juvenile
LB	Lysogeny Broth
M-form	mutualistic form
mRNA	messenger RNA
Mtase	methyltransferase
NP	natural product
OD ₆₀₀	optical density at a wavelength of 600 nm
P-form	pathogenic form
PTM	post-translational modification
QS	quorum sensing
RBP	RNA binding protein
RBS	ribosome binding site
RIPseq	RNA immunoprecipitation followed by high-throughput sequencing
RNA	ribonucleic acid
RNAP	RNA polymerase
RR	response regulator
SM	specialized metabolite
SMRT	Single-Molecule Real-Time sequencing
TR	transcriptional regulator
tRNA	transfer RNA
UTR	untranslated region

Summary

Photorhabdus and *Xenorhabdus* bacteria live in a highly specific symbiosis with nematodes that belong to the genus of *Heterorhabditis* and *Steinernema*, respectively. These cruiser type nematodes actively search for soil-dwelling insects and infect them via natural openings. Inside of the insect, the bacteria are released into the hemocoel where they start producing an array of secondary metabolites to bypass the insect immune system and kill the prey within 48 hours. Many of those natural products possess bioactivities against other bacteria, fungi, protozoa or insects, which makes them interesting candidates for pharmaceutical applications. Even though advanced molecular biological methods in combination with bioinformatics tools can now be used to predict biosynthetic gene clusters (BGCs) and their products, there are still many BGCs with unknown products. Even for the plethora of natural products that were successfully identified in the last couple of years, the exact ecological function often remains elusive, as laboratory conditions can vary considerably from the natural environment of the bacteria. Knowledge about the natural conditions that stimulate, or repress production of certain natural products and their underlying regulatory mechanisms yield new approaches for natural product research and enables possibilities for selective manipulations of the regulatory cascades.

The overarching goal of this work was to examine the regulatory networks in *Photorhabdus* and *Xenorhabdus* strains. The first part of this work focused on the Hfq-dependent regulation of specialized metabolite production. In those genera, the RNA chaperone, Hfq, represses expression of *hexA*, which encodes for a global transcriptional regulator that acts as the master repressor for SM production. Multiple global approaches were used to identify the sRNA ArcZ, which targets a specific region in the 5'-untranslated region of the *hexA* mRNA and ultimately guides Hfq in order to repress its expression. It was shown that a deletion of *arcZ* led to a drastic reduction of SM production in *Photorhabdus* and *Xenorhabdus*, consistent with the phenotype of their respective *hfq* deletion mutants. Transcriptomic profiling revealed far-reaching effects on the transcriptome, with up to 735 coding sequences significantly affected in the *arcZ* deletion strain. Finally, it was shown that the resulting chemical background, devoid of SMs, in combination with targeted

promotor exchange can be used to exclusively overproduce a desired natural product, representing an alternative route of genetic manipulation.

The second part of this work focused on the influence and identification of insect related compounds that affect SM production in *P. laumondii*, *X. szentirmaii* and *X. nematophila*. Insect homogenate was generated from *G. mellonella* larvae, a model host for these bacteria. Supplementation of the cultivation medium with homogenate induced considerable shifts in the SM profiles of those bacteria. A global effect on the transcriptional output was determined by transcriptomic profiling. The core response to the simulation of an insect environment consisted of ten CDS, eight of which are involved in the degradation of fatty acids or the import of maltose and maltodextrin into the cells. Two abundant components in the insect homogenate, trehalose and putrescin, were added to the cultivation medium of those strains and subsequent HPLC-MS analysis revealed a direct correlation of their concentration in the medium and the production titres of certain SMs. These results indicated that the bacteria sense the insect environment via different insect specific components in order to initiate a metabolic adjustment, which is probably required for adaptation to the insect host.

The last part of this work examined the influence of other, so far not directly related genes on SM production, based on the isolation of *P. laumondii* transposon-insertion mutants with clear phenotypic alterations. Re-sequencing and SM profiling of the mutant strains revealed that a transposon-insertion in the gene encoding for a putative DNA-adenine methyltransferase affected SM production. The phenotype was confirmed by deleting this gene. Based on Single-Molecule Real-Time sequencing, the complete methylome of the WT, deletion- and complementation mutant were analysed (experimental work performed by Sacha J. Pidot, Melbourne, Australia). No obvious alterations were detected in the methylation patterns of the strains, indicating that the *dam* gene product does not methylate the adenine in GATC-motifs, as it was described in literature for *E. coli*. This data raises the question what the function of the putative DNA-adenine methyltransferase is in *P. laumondii* and how it can influence the secondary metabolism. Even though there is currently no clear evidence, the potential role of epigenetic gene regulation mechanisms should be considered in further work.

Zusammenfassung

Photorhabdus und *Xenorhabdus* sind zwei Vertreter von insektenpathogenen (entomopathogenen) Bakterien. In ihrem komplexen Lebenszyklus durchlaufen die Bakterien sowohl eine symbiotische Phase mit Fadenwürmern (Nematoden) der Gattung *Heterorhabditis* bzw. *Steinernema* als auch eine insektenpathogene Phase. Das „infektiöse Dauerform“ (infective juvenile) Stadium der Nematoden bietet den Bakterien durch die umgebende Cuticula Schutz vor äußeren Einflüssen. Nachdem der Fadenwurm ein im Erdreich lebendes Insekt aufgespürt hat, infiziert er es über natürliche Öffnungen oder Tracheen. Im Inneren des Insekts werden die Bakterien in die Hämolymphe entlassen, wo sie beginnen sich rasant zu vermehren. Es wird angenommen, dass die Bakterien insektenspezifische Signalmoleküle wahrnehmen, welche den Wechsel vom harmlosen Symbiosepartner des Nematoden zum hocheffizienten Insektenpathogen einleiten. Daraufhin produzieren die Bakterien eine Vielfalt von Naturstoffen, die zum einen der Überwindung des Immunsystems des Insekts dienen und dieses zum anderen innerhalb von 24-48 Stunden töten. Die enzymatische Zersetzung des Insekts liefert Nährstoffe für die Bakterien und Nematoden, welche daraufhin mehrere Entwicklungszyklen durchlaufen. Einige der produzierten Naturstoffe weisen eine biologische Aktivität gegen andere Bodenorganismen wie Bakterien, Pilze, Protozoen oder Insekten auf und dienen der Verteidigung des Insektenkadavers zur Sicherung der Nahrungsquelle. Andere Naturstoffe sind darüber hinaus auch für die Entwicklung der Nematoden notwendig. Sobald die Nährstoffquelle versiegt, reassoziieren Bakterien und Nematode und das Symbiosepaar bricht aus der Insektenhülle aus, um sich auf die Suche nach neuen Insektenwirten zu machen. Während die symbiotische Interaktion zwischen Bakterien und Nematoden hochspezifisch ist, können die Bakterien eine Vielzahl von Insektenarten töten, wovon einige Schädlinge in der Landwirtschaft darstellen. Dort werden die Nematoden bereits als Alternative zu Insektiziden eingesetzt.

Der außergewöhnliche Lebenszyklus qualifiziert *Photorhabdus* und *Xenorhabdus* als herausragenden Modelorganismus zur Untersuchung von Symbiose und Pathogenität, und vor allem dem Einfluss von Naturstoffen in den jeweiligen Phasen. Die Bakterien können in herkömmlichem Nährmedium bei 30°C kultiviert

werden, was die Untersuchung der bakteriellen Naturstoffe zusätzlich erleichtert. Darüber hinaus eignet sich die einfach kultivierbare Insektenlarve der Wachsmotte *Galleria mellonella* als Modelorganismus für die Untersuchung der Insektenpathogenität. Massenspektrometrische Verfahren wie „high performance liquid chromatography-mass spectrometry“ (HPLC-MS) werden zur Identifizierung und Analyse von Naturstoffen herangezogen.

Viele Genome von *Xenorhabdus* und *Photorhabdus* Stämmen sind mittlerweile sequenziert worden. Bioinformatische Werkzeuge wie antiSMASH ermöglichen die Analyse von Biosynthesegenclustern und eignen sich für eine erste Einschätzung der chemischen Struktur eines Naturstoffs. Obwohl fortgeschrittene molekularbiologische Methoden wie heterologe Expression und Promoteraustausch in den letzten Jahren wesentlich zur Identifizierung einer Vielzahl bakterieller Naturstoffe beigetragen haben, gibt es immer noch einige kryptische Gencluster in diesen Stämmen, für die bisher kein Produkt bekannt ist. So können beispielsweise fehlende Vorstufen oder Signalmoleküle im Standard-Kulturmedium dazu führen, dass die Produktion bestimmter Naturstoffe ausbleibt. Selbst für bereits identifizierte Naturstoffe ist die Erforschung der exakten ökologischen Funktion oft nur beschränkt möglich, da die Laborbedingungen häufig weit vom den natürlichen Umgebungsbedingungen der Bakterien abweichen. Oft ist unklar, welche Faktoren die Produktion von Naturstoffen unter natürlichen Bedingungen stimulieren und welchen Regulationsmechanismen diese unterliegen. Eine Identifizierung solcher Faktoren bietet die Möglichkeit, Kultivierungsbedingungen gezielt anzupassen, um die Produktion bestimmter Naturstoffe anzuregen. Die zugrundeliegenden Regulationsmechanismen können darüber hinaus manipuliert werden, um die Produktionstiter bekannter und unbekannter Naturstoffe zu erhöhen, was wiederum die Erforschung der natürlichen Funktion der Naturstoffe ermöglicht. Neben der Grundlagenforschung ist dies auch von pharmazeutischem Interesse, da einige Naturstoffe mit bekannter biologischer Funktion auch einen Startpunkt für die Entwicklung verbesserter Antibiotika oder sogar Alternativen zu Antibiotika darstellen können.

Das übergreifende Ziel dieser Arbeit war es, verschiedene Aspekte der Naturstoffregulation in *Photorhabdus* und *Xenorhabdus* zu untersuchen, um den Wissensstand über bereits bekannte regulatorische Netzwerke zu erweitern. Der erste Fokus dieser Arbeit lag auf der Untersuchung der Hfq-basierten Naturstoffproduktion in *Photorhabdus laumondii* und *Xenorhabdus szentirmaii*. Das RNA-Chaperon Hfq ist ein globaler Regulator, der in vielen Bakterien an der Ausprägung des Phänotyps beteiligt ist. Eine Deletion dieses Regulators zieht oft weitreichende phänotypische Veränderungen nach sich, die sich auf die bakterielle Virulenz, Motilität, Biofilmbildung und Naturstoffproduktion auswirken können. In *Photorhabdus* führt eine Deletion von Hfq zu einer dramatisch verminderten Naturstoffproduktion und gleichzeitig zu einem massiv erhöhten *hexA* Transkriptlevel. Darüber hinaus ist eine Δhfq Mutante nicht mehr in der Lage, die Symbiose zu seinem Nematodenwirt aufrechtzuerhalten. HexA ist ebenfalls als globaler Regulator bekannt und inhibiert in *Photorhabdus* die Produktion von Naturstoffen. Die Produktion von HexA wird wiederum durch Hfq unterbunden. Da Hfq seine regulatorische Wirkung durch sRNA-mRNA Interaktionen bewerkstelligt, wurde vermutet, dass eine sRNA an der Inhibierung von HexA beteiligt ist. Durch eine Vielzahl an globalen Ansätzen konnte in dieser Arbeit die Verbindung zwischen Hfq, HexA und der sRNA ArcZ identifiziert werden. Ebenso wie die Δhfq Mutante von *Photorhabdus*, war auch die $\Delta arcZ$ Mutante massiv in der Produktion von Naturstoffen beeinträchtigt und unterstützte die symbiotische Beziehung zum Nematodenwirt nicht mehr. Die Deletion von *arcZ* zog eine globale Modulation des Transkriptoms mit sich, welche 735 Gene betraf. Genau wie bei der Δhfq Mutante, war auch in dieser Mutante das Transkriptlevel von *hexA* stark erhöht. Die Analyse des Transkriptomvergleichs der Deletionsmutante mit dem WT ergab, dass das ArcZ Regulon sich nicht auf den Sekundärmetabolismus beschränkt, sondern auch darüber hinaus weitreichende Einflüsse auf Gene die in der Virulenz, Zellwand Biosynthese oder in anderen Zellprozessen beteiligt sind, hat. Durch eine Komplementierung der Deletion konnte die Naturstoffproduktion und das Transkriptom des WTs wiederhergestellt werden, was den Einfluss von ArcZ bestätigte. Mit Hilfe des bioinformatischen Werkzeugs CopraRNA wurden anschließend mögliche Bindepartner von ArcZ vorhergesagt. Eines der vorhergesagten Bindemotive lag im 5'-untranslatierten Bereich von *hexA*. Durch ein

gezieltes Austauschen der neun Basenpaare langen Sequenz zu einer *PacI* Restriktionsstelle konnte nachgewiesen werden, dass diese Sequenz notwendig ist, um HexA zu inhibieren. Zusätzlich wurde mit Hilfe von kompensatorischen Basenmutationen verifiziert, dass ArcZ spezifisch mit dem vorhergesagten Bindemotiv interagiert, um die Produktion von HexA zu inhibieren (durchgeführt von Michaela Huber, Papenfort Gruppe, Jena, Deutschland). Durch eine Deletion von ArcZ in *X. szentirmaii* konnte der Einfluss von ArcZ auf die Produktion von Naturstoffen auch artübergreifend gezeigt werden. Auch in diesem Stamm hatte die Deletion von ArcZ weitreichende Effekte auf den Sekundärmetabolismus und das Transkriptlevel von 191 Genen. Vergleiche mit anderen naturstoffproduzierenden Bakterien deuten an, dass es sich dabei um ein konserviertes System zur Regulation von Naturstoffen handeln könnte, was jedoch zukünftige Studien erst noch belegen müssen. Die drastische Reduzierung der Naturstoffproduktion in der Δhfq Mutante sorgt für einen klaren Hintergrund bei der Analyse der HPLC-MS Daten und wurde in Kombination mit Promoteraustauschen vor spezifischen Biosynthesegenclustern bereits erfolgreich verwendet, um gezielt gewünschte Naturstoffe anzureichern. Durch das Fehlen von anderen Naturstoffen mit ähnlichen Retentionszeiten wird zusätzlich die Identifizierung und Isolation des gewünschten Naturstoffs erleichtert. Am Beispiel von GameXPeptid wurde für die $\Delta arcZ$ Mutante von *X. szentirmaii* demonstriert, dass auch dieser Stamm sich potenziell für die gezielte Naturstoffüberproduktion eignet, was das Repertoire für die Erforschung von Naturstoffen erweitert und weitere neue Möglichkeiten zur gezielten Manipulation der Regulationskaskaden präsentiert.

Der zweite Teil dieser Arbeit beschäftigte sich mit dem Effekt von insektenspezifischen Faktoren auf den transkriptionellen Output sowie die Naturstoffproduktion von *P. laumondii*, *X. szentirmaii* und *X. nematophila*. Dazu wurde zunächst ein einfach übertragbares *in vitro* Experiment zur Untersuchung des Einflusses einer simulierten Insektenumgebung etabliert. Dieses basierte auf Insektenhomogenisat, welches aus dem Modelorganismus *Galleria mellonella* hergestellt wurde. Zunächst wurde Kultivierungsmedium mit dem Insektenhomogenisat supplementiert und anschließend der Einfluss auf die Naturstoffproduktion mittels HPLC-MS Analyse ermittelt. Dabei konnte gezeigt

werden, dass die Produktionstiter einiger Naturstoffe als Antwort auf das Insektenhomogenisat in allen drei verwendeten Stämmen wesentlich stimuliert oder reduziert wurden. Einer Reihe dieser Naturstoffe schreibt man wichtige Funktionen im Verlauf der Infizierung eines Insekts zu. Um Einblicke in die zugrundeliegenden bakteriellen Anpassungen als Reaktion auf das Insektenhomogenisat auf transkriptioneller Ebene zu erhalten, wurden RNA Sequenzierungen durchgeführt, nachdem den Kulturen Insektenhomogenisat hinzugefügt wurde. Interessanterweise wurde bei der Analyse eine umfangreiche Modulation des Transkriptom in allen drei Stämmen festgestellt, die 140 bis 259 Gene betraf. Artenübergreifend belief sich die Kernantwort auf das Insektenhomogenisat auf zehn Gene. Vier davon sind wichtig für den Abbau von Fettsäuren, während weitere vier Gene für den Import von Maltose und Maltodextrin in die Zelle verantwortlich sind. Damit korreliert die Kernantwort der drei Stämme gut mit der Zusammensetzung des Insektenhomogenisats, welches im Zuge dieser Arbeit mittels Gaschromatographie-gekoppelter Massenspektrometrie untersucht wurde. Das Insektenhomogenisat enthält viele Fettsäuren und verschiedene Kohlenhydrate (darunter viele Zucker), neben Aminosäuren und anderen Komponenten. Zwei der häufigsten Komponenten, Trehalose und Putrescin, wurden anschließend zu Kulturen der drei Stämme hinzugefügt, um etwaige Einflüsse auf die Naturstoffproduktion zu ermitteln. HPLC-MS Analysen von Proben mit steigenden Konzentrationen dieser Insektenkomponenten zeigten, dass die Produktionstiter einiger der analysierten Naturstoffe direkt mit der Konzentration der Komponenten im Medium korrelierten. Diese Funde liefern weitere Hinweise darauf, welche die essenziellen Anpassungen sind, die diese Bakterien zu so effizienten Insektenpathogenen machen.

Der abschließende Teil dieser Arbeit beschäftigt sich mit der Erforschung des Einflusses anderer, bisher unbekannter Gene, auf die Produktion von Naturstoffen in *P. laumondii*. Basierend auf einer Transposon-Mutagenese, wurden die Mutanten mit den offensichtlichsten phänotypischen Veränderungen isoliert und deren Naturstoffprofil untersucht. Mutanten mit beeinträchtigter Naturstoffproduktion wurden im Folgenden sequenziert, um die Insertion der Transposons zu lokalisieren. Anschließend wurde der Fokus auf eine Mutante mit der Transposon-

Insertion in einem Gen konzentriert, welches für eine putative DNA-Adenin Methyltransferase kodiert. Eine Deletion dieses Gens bestätigte den Einfluss auf die Naturstoffproduktion, die durch Komplementierung wiederhergestellt werden konnte. Der beobachtete Wachstumsdefekt der Deletion wurde dabei ebenso komplementiert. Transkriptomanalysen zeigten, dass die Deletion eine Vielzahl von Auswirkungen auf den transkriptionellen Output mit sich zog. In *E. coli* methyliert das Genprodukt des homologen *dam* Gens das Adenin in GATC-Motiven. Um zu überprüfen, ob die DNA-Adenin Methyltransferase in *P. laumondii* die gleiche Funktion erfüllt, wurde das Methylom des WTs sowie der Deletions- und Komplementationsmutante mittels „Single-Molecule Real-Time sequencing“ analysiert (Sequenzierung durchgeführt von Sacha J. Pidot, Melbourne, Australien). Die Analyse ergab keine offensichtlichen Unterschiede der Methylierungsmuster im Hinblick auf das GATC Motiv. Darüber hinaus wurden auch keine anderen offensichtlichen Unterschiede im Methylierungsmuster anderer Motive in den verschiedenen Stämmen detektiert. Diese Ergebnisse werfen die Frage auf, welche Funktion die putative DNA-Adenin Methyltransferase in *P. laumondii* erfüllt und wie diese den Sekundärmetabolismus der Bakterien beeinflussen kann. Obwohl es bisher keine eindeutigen Anzeichen dafür gibt, stellt sich darüber hinaus die Frage, ob der Δdam Phänotyp in *P. laumondii* möglicherweise auf epigenetische Genregulation zurückzuführen ist.

1. Introduction

The discovery of bacteria reaches back to the 17th century¹. Ever since, it has become more and more evident that bacteria utilize mutualistic relationships to all kinds of eukaryotes to shape many facets of the eukaryote life, such as development, fitness, immune system and many others^{2,3}. Moreover, microorganisms can support different hosts, or even parasites, and are thus regarded as a driving force for host-parasite interactions. Therefore, such interactions are relevant for evolutionary innovation, as they can contribute to an expansion of already existing ecological niches⁴. The high occurrence, number and diversity of microorganisms⁵ has led to the establishment of a more microbial ecology-centred view on all organisms, known as the holobiont concept⁶. A holobiont is defined as a discrete ecological unit that comprises a host and all of its symbionts⁷. Today, it is generally assumed that a broad understanding of microbiology is required to understand the general eukaryote⁸. Fortunately, microbe partners of eukaryote-microbe interactions are often amenable to manipulations with already established microbiological methods that allow investigation of the underlying basis of these interactions.

Sustaining a symbiotic interaction is often reliant on the formation of diverse natural products (NPs), as bacterial NPs can support their host and vice-versa⁹. Often, those NPs are specialized metabolites (SMs), which contribute to development, pathogenicity, or sustaining an ecological niche by repelling inter- and intra-species food competitors^{10,11}. Especially the latter point is of great (pharmaceutical) interest, as those SMs can possess bioactivities against fungi¹², bacteria^{13–15}, or sometimes even higher eukaryotes^{16–19}. The potential of NPs has already been recognized in the 1940s and 1950s. The discovery of the β -lactam antibiotic penicillin inaugurated the era of antibiotic and NP discovery, generally referred to as the “golden era”^{20,21}. With the game-changing discovery of broad-spectrum antibiotics like streptomycin (1943), chloramphenicol (1949), tetracycline (1949) and many others, efficient treatment of infectious diseases became possible^{22–24}. However, shortly after the introduction of the “wonder drugs”, some pathogenic bacteria developed a resistance against certain antibiotics²⁵. While antibiotic resistance can be acquired through mutations and horizontal gene transfer, over- and misuse of antibiotics clearly drives the evolution of resistance²⁶. In order to cope with this problem, many new antibiotics were introduced

from the late 1960s to the early 1980s²⁵. Since then however, the release of new drugs is in steep decline.

In modern times, the development of antibiotic resistance is – without a doubt – one of the most challenging health threats. The most recent “Antibiotic Resistance Threats Report” from 2019 presents estimates of ~2.87 million infections with antibiotic resistant bacteria or fungi in the United States every year²⁷. This results in approximately 36,000 deaths in the U.S.²⁷ and about 25,000 deaths in Europe per year²⁸.

To this day, it is assumed that only a very small fraction of all microorganisms can be cultivated under laboratory conditions^{28,29}. Although new techniques for culturing microorganisms are being developed with great effort, many potential NP sources are currently inaccessible. Even for cultivatable microorganisms, desired NPs are sometimes not produced under laboratory conditions, as external signals that promote their production are often missing^{30,31}.

While the number of sequenced genomes steadily increases and enables bioinformatics genome mining approaches to identify new NP biosynthetic gene clusters (BGCs), a lack of knowledge regarding the underlying regulation often hampers their potential because: (a) they might not be produced under standard cultivation conditions at all or; (b) the production titres are too low for detection. Gaining knowledge about the implications of regulators in SM production enables the possibility to exploit existing regulatory networks to promote production of (unknown) NPs, raise their production levels and elucidate their ecological function^{32–34}.

1.1. *Photorhabdus* and *Xenorhabdus*

Photorhabdus laumondii TTO1 (*P. laumondii*, previously known as *P. luminescens* TTO1) was first described more than four decades ago under the name of “*Xenorhabdus luminescens*”³⁵. The facultative anaerobic, motile, rod shaped, gram-negative bacterium was originally isolated from *Heterorhabditis bacteriophora* (*H. bacteriophora*)^{36,37}.

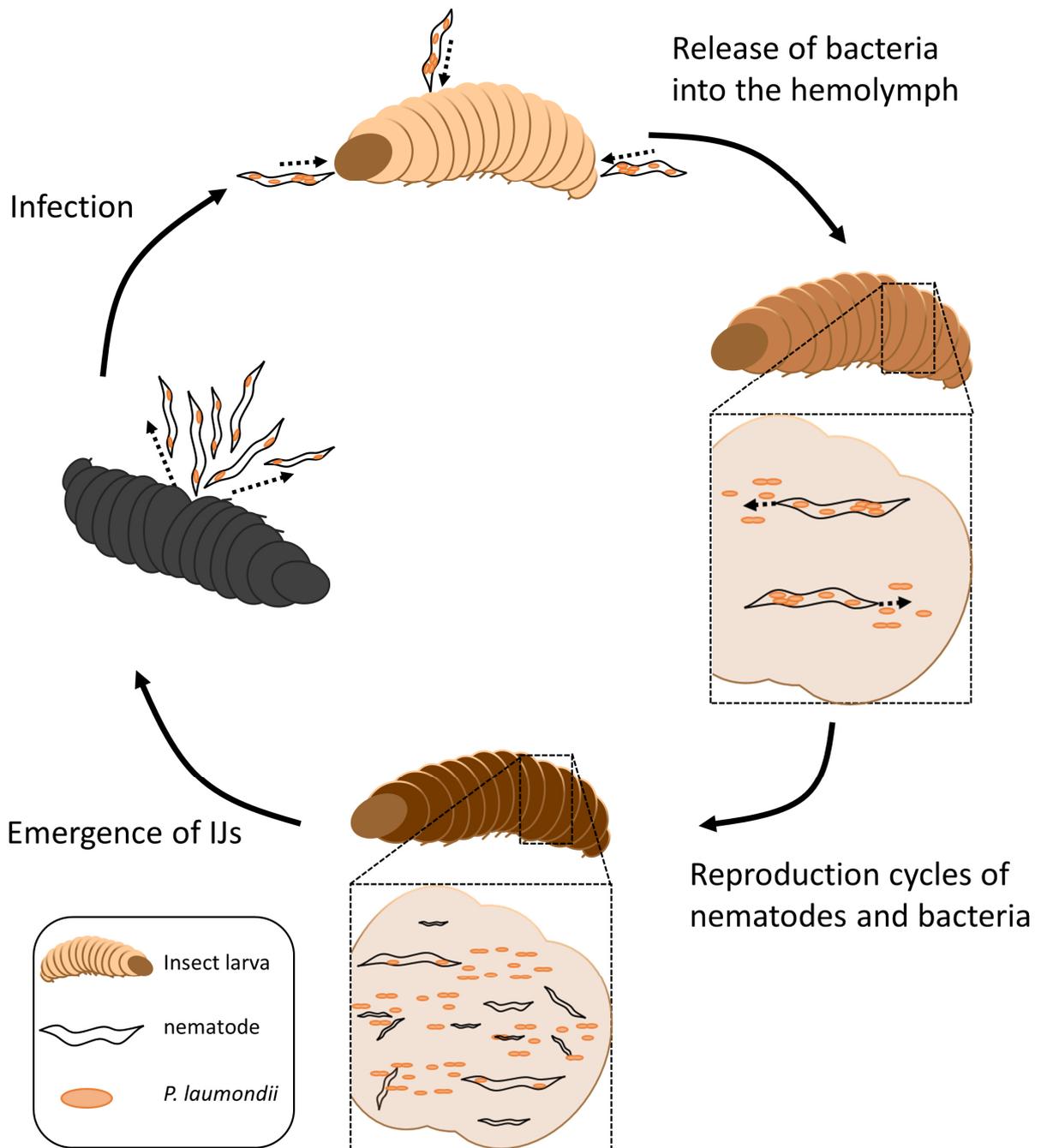


Figure 1. Life cycle of *P. laumondii*. IJ stage *H. bacteriophora* nematodes carry *P. laumondii* bacteria in their gut and actively search for insect larva in the soil. They enter the insect through natural openings or the cuticle and release the bacteria in the hemolymph of the insect (shown in the inset). Bacteria start reproducing quickly (shown in the inset) and kill the insect within 48 h. After multiple reproduction cycles bacteria and nematodes re-associate and emerge from the insect carcass to search for a new insect host.

Infective juvenile (IJ) stage *H. bacteriophora* nematodes carry *P. laumondii* in their gut and cruise through the soil, to actively search for insect larvae³⁸ (Figure 1). Upon entering the insect larvae through natural openings or the cuticle, the mutualistic bacteria are released into the insect hemocoel, where they start to reproduce

quickly^{39,40}. Unknown insect specific signals are assumed to trigger a switch from the mutualistic form (M-form) of the bacteria to the pathogenic form (P-form). This phase switch is, among other phenotypic traits, defined by the production of a plethora of SMs that contribute to suppressing the insect immune system and killing the insect prey^{41,42}. The phase switch is connected to the inversion of a promoter region upstream of the *mad* (**maternal adhesion defective**) locus⁴³. Activation of the *mad* locus leads to fimbriae production, which is necessary for adhesion of the bacteria to the intestine of the nematode host.

While the mutualistic interaction of bacteria and nematodes is very specific and the nematode development depends on the presence of the cognate bacterial species, the entomopathogenic bacteria are able to kill a broad range of different insect larvae, many of which belong to the order *Lepidoptera*⁴⁴ and represent agricultural pests, within one to two days^{37,45,46}. Conversion of the insect carcass provides nutrients for bacteria and nematodes, allowing them to replicate. After the nutrient source is depleted, bacteria and IJ-stage nematodes re-associate and emerge from the dead insect larvae, to search for a new suitable insect host⁴⁷ (Figure 1).

The life cycles of *Xenorhabdus szentirmaii* (*X. szentirmaii*) and *Xenorhabdus nematophila* (*X. nematophila*) are similar to the life cycle of *P. laumondii*. Both bacteria also live in a specific mutualistic interaction with nematodes and are capable of killing insect larvae. *X. szentirmaii* was isolated from *Steinernema rarum* (*S. rarum*), while *X. nematophila* was identified in the gut of *Steinernema carpocapsae* (*S. carpocapsae*)^{48,49}. Just like *P. laumondii*, they too produce a variety of SMs whose functions will be discussed in the next section.

1.2. Specialized metabolites – many “to rule them all”

The symbiosis of *Photorhabdus* and *Xenorhabdus* with their nematode hosts is not obligate. Although these bacteria have only been isolated from infected insect hosts or from their nematode hosts, they can be easily cultivated without their hosts in conventional LB medium⁵⁰, which makes them a remarkable model organism for ecology and pathogenesis studies. The whole genome of *P. laumondii* TTO1 was sequenced in 2003, and it became evident that the genome of *Photorhabdus* does not only encode a high number of protein toxins, but also an exceptional number of BGCs for NP production⁵¹.

A NP is defined as a small molecule that is produced by a living organisms found in nature⁵². This includes compounds that originate from the primary as well as secondary metabolism. Primary metabolites are central metabolites with assigned physiological functions in the respective organism and include carbohydrates, proteins, nucleic acids and lipids. The viability of organisms is usually dependent on the presence of primary metabolites⁵³. Conversely, secondary metabolites are not directly involved in growth, development or reproduction of organisms and their absence usually does not lead to the immediate death of the organism. However, compounds that derive from the secondary metabolism are often highly diverse specialized metabolites with important ecological functions. Hence, absence of those compounds can impair long-term survivability, reproduction or fitness of an organism^{54–57}.

Although advanced molecular biology methods like promoter exchange or heterologous expression have been successfully applied to identify several SMs produced by *Photorhabdus* and *Xenorhabdus*, there are still cryptic BGCs with unknown products^{31,58–60}. Even for the known SMs, precise elucidation of their ecological functions is often hindered because the conditions in nature can differ considerably from laboratory conditions. Unravelling the conditions under which a specific compound is produced and the regulation thereof opens the door for identification of the genuine role of SMs.

SMs produced by *Photorhabdus* and *Xenorhabdus*, whose role within the life cycle could be identified so far, have assigned functions in one of the following categories: cell-cell communication⁶¹ (dialkyresorcinols), nematode development^{62,63} (isopropylstilbene), insect pathogenicity^{41,64} (rhabduscin, rhabdopeptides) or defense against food competitors^{65–67} (glidobactin). Many of those bioactive molecules exist in small derivative libraries that differ in amino acid composition, methylation patterns, fatty acid residues, or can form both linear or cyclic versions. From an ecological point of view, those libraries are believed to facilitate adaptation to constantly fluctuating environmental conditions that come along with the challenges of different insect hosts and different food competitors. A quick response to those fluctuations requires a fully functional and finely-tuned regulatory system. The basic possibilities for regulatory inferences of bacterial gene regulation are explained in the following sections.

1.3. Bacterial gene regulation

Transcription and translation, the two steps that occur in gene expression, are tightly coupled in space and time in bacteria⁶⁸. Coupling of those processes is of great importance, as bacterial messenger RNA (mRNA) molecules usually have a relatively short half-life, with an average of a few minutes⁶⁹. Due to the limited availability of resources and energy, regulation of gene expression is pivotal for optimal energy management in bacteria. As described in the following sections, all processes from the DNA template to a fully functional protein can be targets for regulatory interference.

1.3.1. Regulation of transcription

Regulation of transcription is crucial because it avoids wasteful consumption of energy and resources and accumulation of pathway intermediates. As transcription is the very first step for protein production, it is the first potential target for regulatory interference to generate a swift and adapted metabolic response to stress and changing environmental conditions⁷⁰ (Figure 2A).

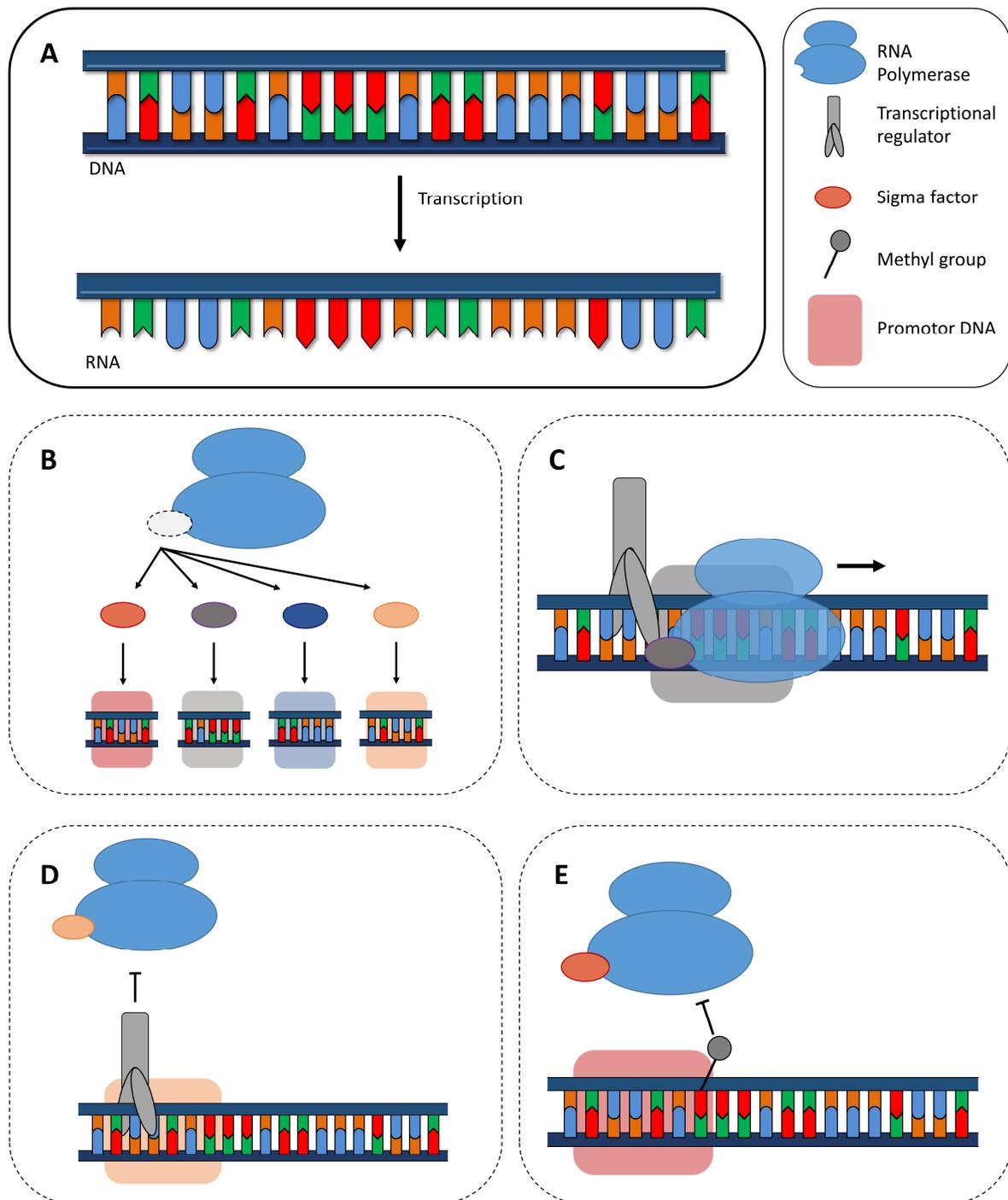


Figure 2. Transcriptional gene regulation in bacteria. **A.** Transcription of a DNA template yields RNA. **B.** The RNA polymerase binds different sigma factors that allow for specific recognition of different genes or sets of genes. **C.** Transcriptional activators can stimulate transcription rate by binding upstream of the promoter through recruitment of the RNA polymerase. **D.** Transcriptional repressors can inhibit transcription rate of certain genes by preventing binding of the RNA polymerase. **E.** Methylation of nucleotides in the promotor region can serve as epigenetic signals for gene regulation by reducing the affinity of the RNA polymerase to bind.

The RNA polymerase (RNAP) is responsible for all transcription and is therefore the central component in transcriptional regulation in bacteria. The activity of the RNAP is

dependent on the interaction with σ -subunits, which leads to the formation of a holoenzyme⁷¹. The σ -subunit is required for the specific recognition of a promoter sequence, positioning the RNAP at this target promoter and subsequently facilitating the unwinding of the DNA near the transcriptional start site⁷². Bacteria usually contain multiple σ -factors that compete for binding to the RNAP and enable the recognition of a different set of promoters (Figure 2B). Besides the housekeeping σ factor, which is required in all growth conditions, a variable number of alternative σ factors are used to ensure adaptability and evolvability, especially in response to stress conditions⁷³.

The vast majority of bacterial genes is, at least in parts, regulated by *trans*-acting transcriptional regulators (TRs)⁷⁰. Those accessory proteins bind to specific DNA sequences and thereby positively (activator) or negatively (repressor) regulate the initiation of transcription to control the expression of a gene, or often, a set of genes⁷⁴.

Repressors can achieve negative regulation of promoter activity through different mechanisms. In steric hindrance, the repressor inhibits transcription by preventing RNAP binding⁷⁴ (Figure 2D). Repressors can also bind downstream of the promoter element and physically inhibit RNAP progression. Moreover, binding of a repressor can result in deformation of the DNA, which prevents RNAP binding to the promoter. Interference of a repressor with an activator can further lead to anti-activation. Finally, repressors with strong contacts to both DNA and RNAP can impair RNAP movement^{70,74}.

Conversely, activators stimulate promoter activity and transcription rate. In class I and II activation, the activator binds upstream of the promoter or to a site overlapping the -35 promoter element and recruits the RNAP by interacting with one of the polymerase subunits (Figure 2C). Some activators can also bind between the -10 and -35 sequences of a promoter and stimulate promoter activity by untwisting the DNA helix, which generates a better alignment of the promoter elements for RNAP binding. The sum of all genes regulated by one TR is summarized as a regulon⁷⁵.

TRs consist of at least two domains, which are required for their function as regulatory switches⁷⁴. One domain contains a DNA binding motif (usually a helix-turn-helix motif) that directly interacts with specific DNA regions^{76,77}. The second domain serves as a signal sensor for specific ligands. Binding of a ligand modulates the DNA-binding affinity of the TFs. In many cases, this ligand is a physiochemical signal that is used to

couple gene expression to environmental signals. While TRs contain both domains required for modulation of gene expression, bacteria also possess two-component systems⁷⁸. In these systems, a histidine kinase (HK), usually located in the periplasm, phosphorylates itself and its cytoplasmic partner protein after sensing an exogenous signal⁷⁹. Following phosphorylation, the cytoplasmic protein, referred to as a response regulator (RR), is activated and modulates the transcriptional output of specific genes. In a more complex version of this system, the phosphate is not directly transferred from the HK to RR, instead it is transferred to various other proteins before it reaches the terminal RR that directly affects transcription initiation frequency. Those cascades of phosphotransfer are referred to as phosphor-relay systems⁸⁰.

Other possibilities for transcriptional regulation include oxidation/reduction of regulatory proteins⁸¹ and nucleotide associated proteins with gene silencing or anti-silencing activities (for detailed review see^{82,83}). Additionally, small ligands can directly interact with the bacterial RNAP to enable swift responses to environmental conditions^{84,85}.

Finally, the activity of promoters can be regulated through (reversible) chemical modifications. Epigenetic gene expression is heritable and does not require a change in the DNA sequence⁸⁶. Just like in eukaryotes, post-replicative DNA methylation is used by bacteria to control DNA-protein interactions⁸⁷. Most commonly, bacteria make use of DNA adenine methylation as an epigenetic signal (Figure 2E). Those DNA modifications are described to modulate virulence, DNA replication, transposase activity, mismatch repair and many other cellular processes of certain bacteria⁸⁸⁻⁹¹. The hemi-methylated state of newly replicated DNA is decisive for all of these events⁸⁷.

Most epigenetic systems in bacteria rely on a DNA methylase and a DNA binding protein that binds to a DNA sequence that overlaps with the methylation site of the methylase^{86,87}. If a target site is methylated, the DNA binding protein is usually unable to bind, and, vice versa, the DNA binding protein can block the methylation site. The methylases designated for epigenetic regulation are referred to as “orphan” methylases because they lack a cognate restriction enzyme. The first orphan DNA methyltransferase discovered was the **d**eoxy**a**denosine **m**ethyl**t**ransferase (Dam) of *E. coli*, which methylates the adenine in the palindromic 5'-GATC-3' motif^{92,93}. Absence of *dam* in *E. coli* leads to an increased spontaneous mutation rate, suggesting a role

of epigenetic regulation in DNA repair⁹⁴. While *dam* deficient *E. coli* cells were still viable, the gene products of *dam* homologues in *Yersinia pseudotuberculosis*, *Yersinia enterocolitica* and *Vibrio cholera* are essential for those strains. One theory suggests that Dam might be essential for the coordination of DNA replication in bacteria with two or more chromosomes⁹⁵. At least for Dam, transcriptional repression through epigenetic signals appears to be more common than transcriptional activation⁸⁷.

1.3.2. Post-transcriptional regulation

Gene expression in bacteria is also regulated on a post-transcriptional level, that is, after the mRNA has been synthesized but prior to post-translational regulatory events (Figure 3A). Post-transcriptional regulation is mainly controlled by small regulatory RNAs (sRNAs) and provides a faster response than transcriptional regulation. The stability of transcripts plays a key role in regulation of gene expression in bacteria. Decay rates of mRNAs differ from less than a minute to more than an hour⁶⁹.

Introduction

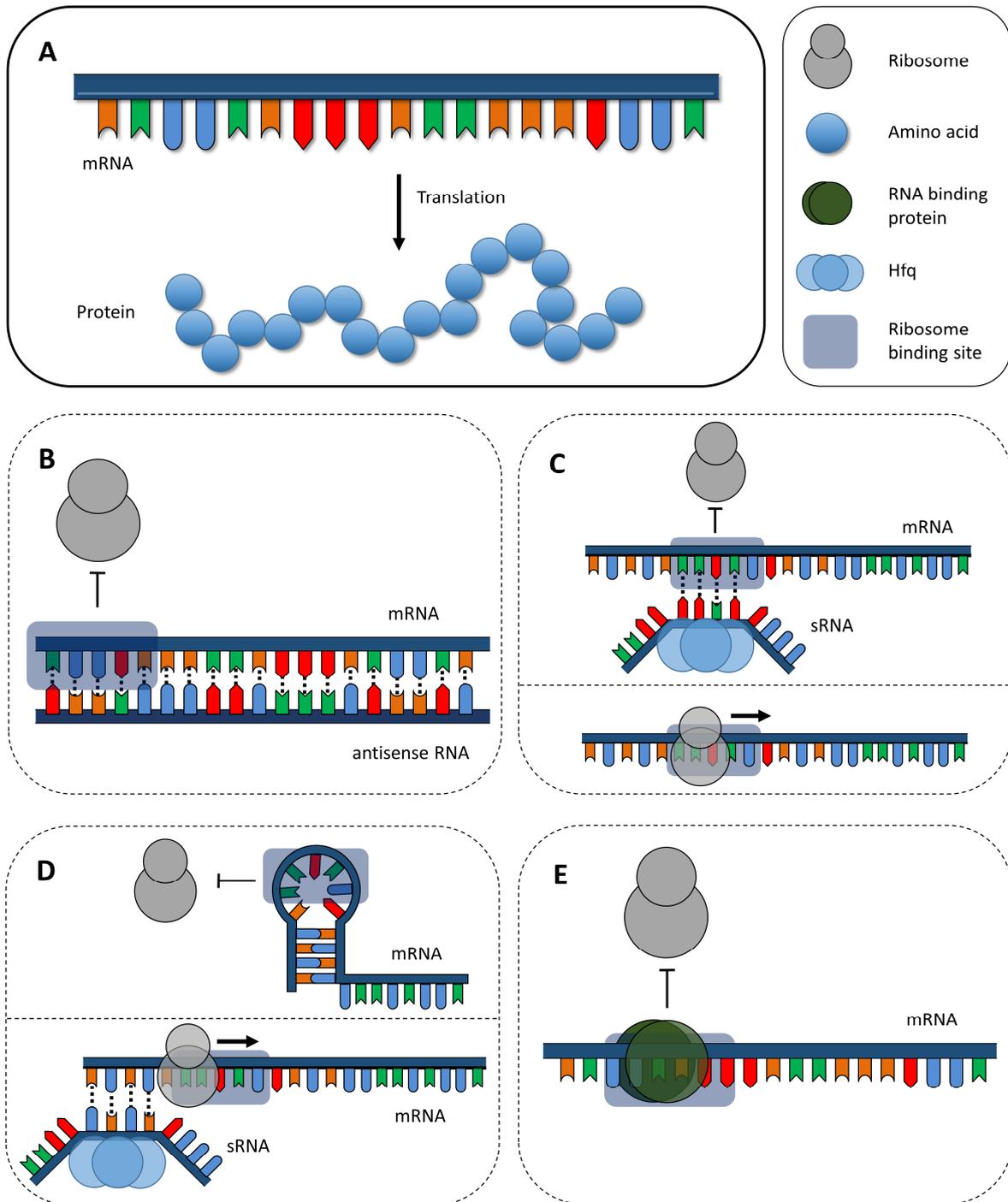


Figure 3. Post-transcriptional gene regulation in bacteria. **A.** Translation of mRNA yields a protein. **B.** Binding of *cis*-acting antisense RNAs to mRNAs inhibits binding of the ribosome to the ribosome binding site and thereby prevents translation. **C.** A *trans*-acting sRNA can bind to the ribosome binding site to prevent ribosome binding (top). In the absence of that sRNA, the ribosome can bind successfully and translation is initiated (bottom). **D.** An inhibitory secondary structure in the mRNA prevents ribosome binding to the ribosome binding site (top). Binding of a sRNA close to the ribosome binding site resolves the inhibitory stem loop and enables ribosome binding and subsequent translation (bottom). **E.** RNA binding proteins inhibit binding of the ribosome to the ribosome binding site and thereby prevent translation of the mRNA.

Many mRNAs possess structures that can be sensed by sRNAs. This can also lead to modulation of gene expression through RNA-RNA interactions⁹⁶. Generally, those interactions can be achieved through *cis*- and *trans*-acting anti-sense RNAs. *Cis*-acting sRNAs are transcribed from the opposite DNA strand and therefore show perfect complementarity and specificity to their target. Formation of an RNA-RNA duplex can sequester the ribosome-binding site (RBS), which leads to an inhibition of translation and, in some cases, degradation of the target mRNA by endo- or exoribonucleases⁹⁷(Figure 3B). Alternatively, transcription can be attenuated by formation of a terminator induced by *cis*-acting sRNAs.

Conversely, *trans*-acting sRNAs are encoded from loci other than their target genes and usually exhibit only limited complementarity to their targets⁷⁰. The seed region that allows interaction with target mRNAs is usually short (7-12 nucleotides) and is the most conserved part of the sRNA. Due to their often imperfect complementarity as well as their relatively small size (50-500 nucleotides), many sRNAs can act on multiple mRNA targets in response to environmental cues such as temperature, nutrient depletion or pH. Likewise, a single transcript can also be targeted by multiple sRNAs, which creates a dense regulatory network^{98,99}.

In *E. coli*, sRNA-mRNA hybrid formation is usually dependent on the mediator protein Hfq (**h**ost **f**actor of the RNA bacteriophage **Q β**)¹⁰⁰. Hfq acts as an RNA chaperone that stabilizes sRNAs against degradation and facilitates the formation of sRNA-mRNA hybrids^{101,102}. Due to its central role in post-transcriptional regulation, it is not surprising that deletion of Hfq in many bacterial species can lead to drastic phenotypic alterations. Implications of Hfq were already demonstrated for virulence, stress tolerance, growth, motility, biofilm formation and SM production^{103,104}.

sRNAs utilize a variety of mechanisms to fulfil their regulatory functions. Direct binding to the RBS is the easiest example for repression of translation (Figure 3C). As with other regulatory mechanisms, repression of translation may induce mRNA decay. In a similar manner, binding of an sRNA to an mRNA can also resolve self-inhibitory secondary structures of the mRNA that would usually repress translation and thereby facilitate protein production (Figure 3D). Furthermore, sRNAs can guide Hfq to a binding site and directly inhibit translation. Finally, binding of sRNAs to RNA binding

proteins can lead to (indirect) stimulation of translation by titration/sequestration of RNA binding proteins (RBPs)^{70,105,106}.

RBPs provide another level of both transcriptional and translational regulation of gene expression (Figure 3E). Generally, regulation through RBPs is achieved by: (a) modification of RBS accessibility, (b) modulation of RNA stability, (c) alteration of transcription terminator/anti-terminator structures or (d) chaperone activity of the RBP to allow interaction of the target with other effector molecules. All regulatory mechanisms and possible outcomes are summarized in a recently published review⁷⁰.

Some mRNAs are able to switch between alternative mRNA conformations that can act as sensors for different signal inputs. mRNAs that change their conformation upon binding small ligands are referred to as riboswitches¹⁰⁷, while other mRNAs, generally known as RNA thermometers, change their conformation in response to changing temperatures to control gene regulation^{108–110}. As with many of the above-described regulatory mechanisms, conformational changes of riboswitches and RNA thermometers can positively and negatively influence gene expression.

1.3.3. Post-translational modifications

Post-translational modifications (PTMs) play a central role in many cellular processes in eukaryotes¹¹¹. Only recently, advances in mass-spectrometry-based proteomics revealed that prokaryotes, too, are capable of modifying proteins using an extensive range of PTM with a profound influence on virulence and bacterial physiology¹¹². PTMs of eukaryotic proteins are often required for their functionality¹¹¹. The best-known examples of this are the RRs of two-component systems, which require phosphorylation in order to be active. However, the prokaryotic repertoire of PTMs is not limited to phosphorylation but also includes acetylation, methylation, carboxylation, glycosylation and many more¹¹¹.

The advantage of PTM is that it allows bacteria to rapidly adjust to external signals in a fashion that cannot be met with regulation of gene expression. Moreover, PTMs are often energy efficient and reversible¹¹³.

1.4. Regulatory network of SM production in *Photorhabdus* and *Xenorhabdus*

Even though *P. laumondii* is one of the best investigated bacteria with regards to SM production, some SMs are not detectable after cultivation under laboratory conditions.

Understanding the underlying regulatory mechanisms may lead to improved methods for NP identification. One good example for the latter point are cyclic GameXPptides. The main derivatives of this insecticidal compound are only produced in the insect, as the biosynthesis relies on the presence of p-amino phenylalanine⁵⁹. The bacteria can produce this precursor, but they only do so in the insect, suggesting a need to find cultivation conditions that are closer to the natural background of these bacteria, in order to access their full potential^{114,115}. In line with this idea, Crawford and colleagues were able to link the production of certain compounds in *P. laumondii* to the addition of L-proline (an abundant amino acid in the hemolymph of insects) to the culture medium.

In order to maintain their ecological niche, *Photorhabdus* and *Xenorhabdus* species rely on the production of SMs. As of today, their ecological role often remains elusive^{116,117}. The regulation of SM production in these strains so far mainly implicates the global regulators LeuO, Lrp, HexA and Hfq although other global and pathway-specific regulators have been described. Lrp and LeuO, both of which act as transcriptional regulators, influence SM production positively or negatively, depending on the class of SM¹¹⁸. HexA, another transcriptional regulator, is part of a regulatory cascade that controls SM production globally, controlled by Hfq. Recent work on Hfq in *Photorhabdus* revealed that a *hfq* deletion mutant was no longer able to maintain the mutualistic relation to their host nematode¹⁰⁴. Moreover, the deletion of *hfq* led to an abolishment of SM production, which correlated with a strong upregulation of the transcriptional *hexA* output. A double deletion of both *hfq* and *hexA* restored SM production and confirmed that, within this regulatory network, HexA acts as a repressor of SM production, and that transcription of *hexA* in the WT is controlled in a Hfq dependent manner.

Recently, the implications of Hfq in SM production could be expanded to *Xenorhabdus* and *Pseudomonas*¹¹⁹. The potential of exploiting this regulatory cascade has been demonstrated and led to the establishment of the easyPACId approach (**easy Promoter Activated Compound Identification**)¹¹⁹. Even though microorganisms have been, and still are, important sources for bioactive compounds, low production titres of the desired compounds or co-isolation with other compounds with similar retention times often hinder their identification. Deletion of Hfq leads to a chemical background devoid of NPs, which, in combination with exchanging the native promoter against an

inducible promoter, facilitates almost exclusive production of the desired NP. As described above, Hfq mainly fulfils its regulatory function by mediating sRNA-mRNA interactions. Despite its central position in regulation, the molecular mechanism underlying SM regulation, as well as the role of sRNAs in those processes in bacteria are so far unknown.

As of today, evidence for epigenetic mechanisms that affect gene regulation in *Photobacterium* is scarce. The genome of *Photobacterium* contains 47 putative methylases or methyltransferases, 12 of which are supposed to be involved in DNA methylation, suggesting that epigenetic mechanisms might be more abundant than assumed¹²⁰. Methyltransferases catalyse the transfer of a methyl group from a universal donor (often S-adenosylmethionine) to, for example, a nucleotide¹²¹. As described above, methylation can affect the activity of certain promoters. One example of *E. coli* is the *pap* operon, which encodes for pili¹²². The activity of the *pap* promoter depends on the methylation state. The DNA-methyltransferase Dam as well as the transcriptional regulator Lrp compete for binding to an overlapping DNA sequence in the promoter region of the operon. Binding of Lrp blocks the methylation of the 5'-GATC-3' motif, which ultimately influences promoter activity of the operon. Conversely, methylation of the motif reduces the binding affinity of Lrp to this position and also leads to a modulation of promoter activity^{122,123}. Given the presence of Lrp and Dam in *P. laumondii*, it may be possible that similar epigenetic events occur in this strain.

Payelleville and colleagues demonstrated that a mutant of *P. laumondii* overexpressing *dam* showed significantly impaired motility and delayed virulence compared to the WT¹²⁴. They were also able to identify eight different methylation motifs which displayed a high rate of methylation (>94%)¹²⁰. However, the exact mechanism of how Dam-induced methylation influences gene expression remains unknown.

1.5. Motivation and aim of this work

The overarching goal of this work is to expand the knowledge regarding regulatory networks in *Photobacterium* and *Xenorhabdus* with respect to SM production. Recent research highlighted that this regulatory network can be exploited to manipulate production of desired compounds. Those strategies can be applied to increase the production titres of both known and unknown SMs and allow for subsequent isolation, structural characterisation and determination of their biological function.

Topic A – The role of ArcZ in Hfq-based regulation of SM production

The first chapter of this work (Chapter 3.1) focuses on the regulatory cascade that controls SM production in *Photorhabdus* and *Xenorhabdus*, which is driven by the master regulator Hfq. As mentioned above, Hfq acts as an important mediator to allow sRNA-mRNA interactions. Although this central RNA-chaperone has previously been studied in *Photorhabdus* and *Xenorhabdus*, the molecular basis of Hfq-based SM regulation, and especially the role of sRNAs in this regulatory network, remain unclear. We used an array of global methods to unravel this network and to identify one sRNA that connects Hfq and HexA to control SM production. We further demonstrate that the regulon of this sRNA, ArcZ, is not exclusively limited to SM production, but instead severely affects the transcriptional output on a global scale. We examined the implications of this sRNA in niche occupation and demonstrated an alternative route for specific SM production in a background devoid of other natural products. The results covered in this chapter are based on the manuscript “Small RNA directs symbiosis, virulence, and natural products biosynthesis in entomopathogenic bacteria”.

Topic B – Components of insect larvae modulate Xenorhabdus and Photorhabdus secondary metabolite production

Regulatory knowledge about SM production, and especially under which conditions they are produced, greatly improves our possibilities to determine the true scope of SMs. The second part of this work (Chapter 3.2) focuses on the simulation of *in vivo*-like conditions and its effect on the specialized metabolome and transcriptome of *Photorhabdus* and *Xenorhabdus*. We established an easily applicable *in vitro* assay that can be used to mimic the natural environment of the bacteria. We used this *in vitro* assay to demonstrate how addition of insect homogenate to culture medium can result in considerably altered SM profiles as well as global modulations on the transcriptional output in *P. laumondii*, *X. szentirmaii* and *X. nematophila*. In order to narrow down potential signal molecules in the insect hemolymph that trigger this transition, we analysed hemolymph as well as insect homogenate via GC-MS. Finally, we supplemented culture medium with abundant insect components to determine correlations between those components and the relative production titres of several SMs.

Topic C – Identification of novel genes involved in SM production by transposon mutagenesis

The third part of this work focused on the implications of novel genes in SM production in *P. laumondii*. A transposon mutagenesis was conducted to subsequently isolate strains with obvious phenotypic alterations. The transposon insertion was determined by re-sequencing the mutant strains and revealed severe effects of multiple genes on the growth and SM profiles. For further investigation, we focused on the influence of Dam on the phenotypic expression of *P. laumondii*. Deletion of *dam* in *P. laumondii* resulted in attenuated growth of the deletion strain as well as reduced SM production titres. As the homologous *dam* gene in *E. coli* encodes for a DNA-adenine methyltransferase, we applied Single-Molecule Real-Time sequencing (sequencing performed by Sacha J. Pidot, Melbourne, Australia) to determine the methylome of the WT, the Δdam mutant and a complementation mutant. Analysis of the methylomic data revealed that the *dam* gene product in *P. laumondii* does not have the same function as Dam in *E. coli*.

2. Materials and methods

2.1. Topic A: Small RNA directs symbiosis, virulence, and natural products biosynthesis in entomopathogenic bacteria

The following sections contain all materials and methods used for the experiments covered in topic A (chapter 3.1). All methods described herein (Chapter 2.1.1. - 2.1.14.) are part of the manuscript “Small RNA directs symbiosis, virulence, and natural products biosynthesis in entomopathogenic bacteria” (under revision in *Nat. Microbiol.*; see Chapter 6 for the submitted manuscript).

2.1.1. Bacterial culture conditions

When grown in liquid, all strains used were grown on orbital shakers (200 rpm). *E. coli* strains were grown in Lysogeny Broth (LB) medium (10 g/L tryptone, 5 g/L yeast extract and 5 g/L NaCl, pH 7.5) at 37°C. All *Photorhabdus* and *Xenorhabdus* strains were grown in LB at 30°C. *E. coli* strains were grown in LB for at least 16 hours at 37°C. Solid LB medium contained 1.5% (w/v) agar. When appropriate, the culture medium was supplemented with chloramphenicol (34 µg/ml), ampicillin (100 µg/ml), rifampicin (50µg/ml) or kanamycin (50 µg/ml). To induce promoter exchange mutants, 0.2% L-arabinose was added to the cultures.

2.1.2. Microorganisms

All used microorganisms for topic A, their genotype and reference are covered in the following table.

Table 1. Microorganisms used in chapter 3.1 with name, genotype and reference (see also Chapter 6, Supplementary Table S14).

Strain	Genotype/Description	Reference
<i>Escherichia coli</i> S17-1 λpir	Tp ^R Sm ^R <i>recA, thi, pro, hsdR</i> -M+RP4: 2- Tc:Mu:Km Tn7 λ pir	Invitrogen
S17-1 λ pir + pCKcipB_Δ <i>arcZ</i> _TTO1	S17-1 λ pir + pCKcipB_Δ <i>arcZ</i> _TTO1, Cm ^R , R6K ori	This study
S17-1 λ pir + pCKcipB_Δ <i>arcZ</i> _XSZ_DSM	S17-1 λ pir + pCKcipB_Δ <i>arcZ</i> _XSZ_DSM, Cm ^R , R6K ori	This study
S17-1 λ pir + pEB17_Δ <i>arcZ</i> _TTO1	S17-1 λ pir + pEB17_Δ <i>arcZ</i> _TTO1, Kan ^R , R6K ori	This study
S17-1 λ pir + pEB17_Δ <i>arcZ</i> _XSZ_DSM	S17-1 λ pir + pEB17_Δ <i>arcZ</i> _XSZ_DSM, Kan ^R , R6K ori	This study
S17-1 λ pir + pEB17_Δ <i>hexA</i> _XSZ_DSM	S17-1 λ pir + pEB17_Δ <i>hexA</i> _XSZ_DSM, Kan ^R , R6K ori	This study
S17-1 λ pir + pEB17_Δ <i>hexA</i> _Pacl_TTO1	S17-1 λ pir + pEB17_Δ <i>hexA</i> _Pacl_TTO1, Kan ^R , R6K ori	This study
S17-1 λ pir + pCEPKMR_ORF00346	S17-1 λ pir + pCEPKMR_ORF00346, Kan ^R , R6K ori	This study
<i>E. coli</i> Top10	<i>F</i> - <i>mcrA</i> Δ(<i>mrr-hsdRMS-mcrBC</i>) ϕ 80 <i>lacZ</i> Δ <i>M15</i> Δ <i>lacX74</i> <i>nupG</i> <i>recA1</i> <i>araD139</i> Δ(<i>ara-leu</i>)7697 <i>galE15</i> <i>galK16</i> <i>rpsL</i> (<i>StrR</i>) <i>endA1</i> λ -	Invitrogen
Top10 + pMH079 + p-ctr	Top10 + pXG10- <i>hexA</i> ::gfp+ p-ctr	M. Huber, AG Papenfort
Top10 + pMH079 + pMH078	Top10 + pXG10- <i>hexA</i> ::gfp+ p- <i>arcZ</i>	M. Huber, AG Papenfort

Strain	Genotype/Description	Reference
Top10 + pMH079 + pMH080	Top10 + pXG10- <i>hexA</i> ::gfp+ p- <i>arcZ</i> *	M. Huber, AG Papenfort
Top10 + pMH081 + p-ctr	Top10 + pXG10- <i>hexA</i> *::gfp+ p-ctr	M. Huber, AG Papenfort
Top10 + pMH081 + pMH078	Top10 + pXG10- <i>hexA</i> *::gfp+ p- <i>arcZ</i>	M. Huber, AG Papenfort
Top10 + pMH081 + pMH080	Top10 + pXG10- <i>hexA</i> *::gfp+ p- <i>arcZ</i> *	M. Huber, AG Papenfort
<hr/>		
<i>Photorhabdus laumondii</i> ssp. <i>laumondii</i> TTO1	WT, Rif ^R	125
TN:: <i>arcZ</i>	Mariner transposon insertion in <i>arcZ</i> (insertion site: 4692989)	This study
Δ <i>arcZ</i>	Deletion starting from 4692930 to 4693059	This study
Δ <i>arcZ</i> :: <i>arcZ</i>	Complementation of TTO1 Δ <i>arcZ</i> by insertion of full length ArcZ sequence	This study
Δ <i>hexA</i>	TTO1 Δ <i>hexA</i> (<i>plu3090</i>)	104
Δ <i>hexA</i> :: <i>hexA</i> _Pacl_UTR	Knockin of <i>hexA</i> with an altered sequence in the 5'-UTR	This study
Hfq ^{3xFLAG}	Δ <i>hfq</i> :: <i>hfq</i> ^{3xFLAG}	This study
<hr/>		
<i>Xenorhabdus szentirmaii</i> DSM16338	WT, Amp ^R	126
Δ <i>hfq</i>	Δ <i>hfq</i> (<i>Xsze_00563</i>)	119
Δ <i>hfq</i> ::pCEP_GXPS	Promoter exchange in front of <i>gxpS</i>	This study
Δ <i>arcZ</i>	Deletion starting from 3833948 to 3833859	This study
Δ <i>arcZ</i> :: <i>arcZ</i>	Complementation of XSZ Δ <i>arcZ</i> by insertion of full length ArcZ sequence	This study
Δ <i>arcZ</i> ::pCEP_GXPS	Promoter exchange in front of <i>gxpS</i>	This study
Δ <i>hexA</i>	Δ <i>hexA</i> (<i>Xsze_03702</i>)	This study

2.1.3. Plasmids

The following table provides an overview of all plasmids used for the conducted experiments of topic A (see also Chapter 6).

Table 2. Plasmids used in chapter 3.1 with name, genotype and reference (see also Chapter 6, Supplementary Table S13).

Plasmid	Genotype	Reference
pSAM_BT	R6K ori, Amp ^R , oriT, Himar1C9 transposase, transposon containing <i>ermG</i>	127
pSAM_KAN	R6K ori, Amp ^R , oriT, Himar1C9 transposase, mariner transposon containing Kan ^R	This study
pCK_cipB	R6K ori, CM ^R , oriT, <i>sacB</i> , <i>tral</i>	128
pCOLA_ara_tacl	cola oriR, Kan ^R	129
pCKcipB_Δ <i>arcZ</i> _TTO1	R6K ori, CM ^R , oriT, <i>sacB</i> , <i>tral</i> , containing a 1083 bp upstream and a 994 bp downstream region of <i>arcZ</i>	This study
pCKcipB_Δ <i>arcZ</i> _XSZ_DSM	R6K ori, CM ^R , oriT, <i>sacB</i> , <i>tral</i> , containing a 860 bp upstream 965 bp downstream region of <i>arcZ</i>	This study
pEB17	R6K ori, Kan ^R , oriT, <i>sacB</i> , <i>tral</i>	This study
pEB17_Δ <i>arcZ</i> _TTO1	R6K ori, Kan ^R , oriT, <i>sacB</i> , <i>tral</i> , containing a 2207 bp fragment including a 1083 bp upstream and a 994 bp downstream region of <i>arcZ</i> and the full version of <i>arcZ</i>	This study
pEB17_Δ <i>arcZ</i> _XSZ_DSM	R6K ori, Kan ^R , oriT, <i>sacB</i> , <i>tral</i> , containing a 1915 bp fragment including a 860 bp upstream and a 965 bp downstream region of <i>arcZ</i> and the full version of <i>arcZ</i>	This study
pEB17_Δ <i>hexA</i> _XSZ	R6K ori, Kan ^R , oriT, <i>sacB</i> , <i>tral</i> , containing a 1110 bp upstream 1036 bp downstream region of <i>hexA</i>	This study

Plasmid	Genotype	Reference
pEB17_HexA_Pacl_TTO1	R6K ori, Kan ^R , oriT, <i>sacB</i> , <i>tral</i> , containing a 2141 bp fragment (includes upstream region of <i>hexA</i> , the complete <i>hexA</i> gene and downstream region of <i>hexA</i> with the introduced <i>Pacl</i> restriction site instead of the predicted ArcZ binding site)	This study
pCEPKMR_ORF00346	R6K ori, Kan ^R , oriT, <i>tral</i> , containing a 618 bp fragment homologous to <i>gxpS</i> required for homologous recombination	This study
pMH078	p- <i>arcZ</i> , constitutive sRNA expression plasmid, P15A, Kan ^R	This study
pMH079	pXG10- <i>hexA</i> :: <i>gfp</i> , containing the 5'UTR and the first 20 aa of <i>hexA</i> , pSC101*, Cm ^R	This study
pMH080	p- <i>arcZ</i> * (G79C), constitutive sRNA expression plasmid, P15A, Kan ^R	This study
pMH081	pXG10- <i>hexA</i> *:: <i>gfp</i> (C-46G), containing the 5'UTR and the first 20 aa of <i>hexA</i> , pSC101*, Cm ^R	This study
p-ctr	pCMW-1, control plasmid, P15A, Kan ^R	130

2.1.4. Oligonucleotides

All oligonucleotides used for conducting the experiments described in chapter 3.1 are listed subsequently.

Table 3. Oligonucleotides used in chapter 3.1 with name, sequence and purpose (see also Chapter 6, Supplementary Table S15).

Name	Sequence (5'-3')	Purpose
NN191	TATAACCTCTCCTTAATTTATTGC	Linearization of pSAM_Bt
NN192	AAACAATAGGCCACATGC	
NN193	TAAATTAAGGAGAGGTTATACTGC GTCTAGCATGCCTA	Amplification of Kan ^R
NN194	TTGCATGTGGCCTATTGTTTTTAGA AAAACATCATCGAGCATC	
NN276	ATCGATCCTCTAGAGTCGACCCTG AATGATTTTGATTACGCT	Deletion of <i>arcZ</i> : amplification of <i>upstream</i> region of <i>arcZ</i> (TTO1)
NN277	GACGCTGAAAAAAAAATAACCCAAA GATAAGATTTTTTGTACAAGATTC	
NN278	GGTTATTTTTTTTCAGCGTCC	Deletion of <i>arcZ</i> : amplification of <i>downstream</i> region of <i>arcZ</i> (TTO1)
NN279	TCCCGGGAGAGCTCAGATCTCGAT GTATTATCAAGTGAAAGGC	
NN281	GGCAGACTCCTGTAGAACG	Verification primer for TTO1Δ <i>arcZ</i>
NN282	CGCATAAGATAAAAGGTGCTGC	
NN315	TCCTCTAGAGTCGACCTGCACGAA AAACGATAAAGTTGTGAGC	Deletion of <i>arcZ</i> : amplification of <i>upstream</i> region of <i>arcZ</i> (XSZ DSM)
NN316	GGAACACAAGTACCAACATAGC	
NN317	TATGTTGGTACTTGTGTTCCCACCC CAACTTCGGTTGG	Deletion of <i>arcZ</i> : amplification of <i>downstream</i> region of <i>arcZ</i> (XSZ DSM)
NN318	GGAATTCCCGGGAGAGCTCAGCAA CAGGAACGGGCATTG	
NN329	CGACACTTCAGCACCAAG	Verification primer for XSZΔ <i>arcZ</i>
NN330	GCGAGAGATCAGAAAGGAATTAC	

Material and methods - Topic A

Name	Sequence (5'-3')	Purpose
NN333	ATCGATCCTCTAGAGTCGACGCAC TGCTAAAACGTGTCAG	Knock-in of <i>hexA_PacI</i> _UTR: amplification of <i>upstream</i> region of <i>arcZ</i> (TTO1)
NN334	TTAGTTAGTAATTAATAAATCAAAAA AAGTGATG	
NN335	TGATTTTAATTACTAATAAATTAATT AATTTACGTAAGCACTATCAAATTA AATTAACATC	Knock-in of <i>hexA_PacI</i> _UTR: amplification of <i>downstream</i> region of <i>arcZ</i> (TTO1)
NN336	GGAATTCCCGGGAGAGCTCACCTC CCTCTGAATGTTTTGAAG	
NN346	ATCGATCCTCTAGAGTCGACGCTT TGCGTGCAGAATAAATAC	Deletion of <i>hexA</i> : amplification of <i>upstream</i> region of <i>hexA</i> (XSZ DSM)
NN347	CCTGGTGTTTTTACTTCAGC	
NN348	GCTGAAGTAAAAACACCAGGGTAT TACGTATTTATAGGCTAATGTTTTCC	Deletion of <i>hexA</i> : amplification of <i>downstream</i> region of <i>hexA</i> (XSZ DSM)
NN349	GGAATTCCCGGGAGAGCTCACCAA TAACACCAAATGAAAATGC	
NN359	CAGAATAAGGTGAATTTAGTTGATG	Sequencing of <i>hexA_PacI</i> _UTR knockin part 1
NN357	GATGCAGAAGGTGAACTAAG	
NN358	CCAGCATACTTTCAATAAACTG	Sequencing of <i>hexA_PacI</i> _UTR knockin part 2
NN356	GGTTCAATAGGTAAAAAACAGC	
X.sz_Cl2_ORF0 0346_fw_gib_LP	TTTGGGCTAACAGGAGGCTAGCAT ATGAAAGATAGCAAGGTTGCT	Promotor exchange in front of <i>gxpS</i>
X.sz_Cl2_ORF0 0346_rv_gib_LP	TCTGCAGAGCTCGAGCATGCACAT GGTATACATGATGTACGCTGG	
X.sz_Cl2_ORF0 0346_ver_fw_LP	GGCTGCTGGGAATGACAAT	Verification primer for pCEPKMR_ORF00346
X.sz_Cl2_ORF0 0346_ver_rv_LP	GATAACGAGCCGGACTACAGC	
KPO-0092	CCACACATTATACGAGCCG	construction of pMH078 (p- <i>arcZ</i>)
KPO-1397	GATCCGGTGATTGATTGAGC	

Material and methods - Topic A

Name	Sequence (5'-3')	Purpose
KPO-1702	ATGCATGTGCTCAGTATCTCTATC	construction of pMH079 (pXG10- <i>hexA::gfp</i>)
KPO-1703	GCTAGCGGATCCGCTGG	
KPO-3024	CAATATGGGGATATCAAAGAAAAG C	RybB oligoprobe (TTO1)
KPO-3109	GGACTACACACAGCAATATAGG	RprA oligoprobe (TTO1)
KPO-3110	GCTGATTCACTTTTTCGTTCCG	GcvB oligoprobe (TTO1)
KPO-3111	CTTACCTCTGTACCCTACGC	Spot 42 oligoprobe (TTO1 and XSZ)
KPO-5989	GAATACTGCGCCAACACCAG	ArcZ oligoprobe (TTO1 and XSZ)
KPO-6007	ACACTACCATCGGCGCTAC	5S oligoprobe (TTO1 and XSZ)
KPO-6061	CTAAAGTAAACACTGGAAGCAATG	RyhB oligoprobe (TTO1)
KPO-6062	GCCTGTTGTTTATCTACAGTCAG	GlmZ oligoprobe (TTO1)
KPO-6130	AGACAGGGATGGTGTCTATG	CpxQ oligoprobe (XSZ)
KPO-6132	TTAAGAGCCGTGCGCTAAAAG	RyeB (SdsR) oligoprobe (TTO1)
KPO-6145	GAGATACTGAGCACATGCATGTCA GAAAACAAAATAACCAAACCT	construction of pMH079 (pXG10- <i>hexA::gfp</i>)
KPO-6146	CCAGCGGATCCGCTAGCAACAAAA GTTCTTAGCAGATCG	
KPO-6147	GGCTCGTATAATGTGTGGGTATGA TGTACGGAGAATTCC	construction of pMH078 (p- <i>arcZ</i>)
KPO-6148	GCTCAATCAATCACCGGATCCAAG AATGGAGAAAGGATACG	
KPO-6149	CAATATGGGGACATCAAAGAAAAG	RybB oligoprobe (XSZ)
KPO-6156	GTTTTCCCTGCTGTTGGCGCAGTA TTCGCG	construction of pMH080 (p- <i>arcZ</i> *)
KPO-6157	GCGCCAACAGCAGGGAAAACTTTT TACACGC	

Name	Sequence (5'-3')	Purpose
KPO-6164	CGTAAAAACAGCAGGTTAGTTAGT AATTTAAATC	construction of pMH081 (pXG10- <i>hexA</i> *:: <i>gfp</i>)
KPO-6165	CTAACTAACCTGCTGTTTTTACGTA AGCACTATC	
KPO-6166	CTGGTGTGACGGAAATAAGC	sRNA_00243 oligoprobe (TTO1)
KPO-6169	GAGGTGGTTCCTAGTCTTAC	CyaR oligoprobe (TTO1 and XSZ)

2.1.5. Construction of mutant strains

The $\Delta arcZ$ mutant of *P. laumondii* was generated as described in the following section: A 1123 bp upstream and a 1014 bp downstream fragment were amplified by PCR using the primer pairs NN 276/NN277 and NN278/NN279, respectively. The complementary overhangs introduced by the primers were used to clone the PCR products into the previously linearized plasmid pEB17. The verified plasmid was used for transformation of *E. coli* S17-1 λpir cells. Conjugation and the generation of the deletion strain through homologous combination were performed as previously described¹¹⁷. Desired deletion mutants were verified by PCR using the primer pair NN282/NN282, yielding a 632 bp fragment. To complement the *arcZ* deletion strain of *P. laumondii*, the full and intact version of *arcZ* was inserted at the original locus as follows: A 2207 bp fragment was amplified by PCR with the primer pair NN276/NN279 which included the upstream and downstream region required for homologous recombination as well as the full length *arcZ* gene. The fragment was cloned in pEB17 as described above. *E. coli* S17-1 λpir cells were transformed with the verified plasmid construct. Plasmid transfer and integration into the genome of *P. laumondii* $\Delta arcZ$ was achieved by conjugation and homologous recombination. A second homologous recombination through counter selection with 6% sucrose in the selection media was used to generate the final knock-in mutant. Knock-in mutants were verified as described above. The same strategies were applied for the construction of *X. szentirmaii* mutant strains. Promoter exchange mutants in front of *gxpS* in *X. szentirmaii* $\Delta arcZ$ and *X. szentirmaii* Δhfq were generated by conjugational transfer and homologous recombination of the plasmid pCEPKMR_ORF00346 from *E. coli* S17-1 λpir + pCEPKMR_ORF00346 into the recipient strain.

2.1.6. Creation of transposon mutant library

The plasmid pSAM_BT¹²⁷ was used as a template to generate pSAM_Kan. The kanamycin resistance cassette was amplified by PCR with the primer pair NN193/NN194 using pCOLA_ara_tacl as a template for PCR. The PCR fragment was cloned into the pSAM_BT plasmid, which was previously linearized by PCR with the oligonucleotides NN191/NN192. Complementary overhangs of the kanamycin cassette fragment introduced by the primers were utilized to fuse the PCR product and the linearized plasmid to generate pSAM_Kan. *E. coli* ST18 was transformed with pSAM_Kan. Transfer of pSAM_Kan into *P. laumondii* via conjugation then generated the transposon mutant library. Transposon-insertion mutants were selected by addition of kanamycin to the medium.

2.1.7. DNA extraction and sequencing

The Genra Puregene Yeast/Bact Kit was used for extraction of genomic DNA following the manufacturer's instructions. The DNeasy Blood & Tissue Kit (Qiagen) was used for DNA extraction for sequencing of transposon-insertion mutants. Sequencing was performed on the Illumina NextSeq platform by Sacha J. Pidot from the Steinar lab (Melbourne, Australia). Briefly, DNA libraries were constructed using the Nextera XT DNA preparation kit (Illumina). Whole genome sequencing was performed using 2x 150 bp paired-end chemistry with a sequencing depth of >50x as a target for each sample. Genome assembly was performed using SPAdes¹³¹ (v 3.10.1). Annotations were added with Prokka¹³² (v 1.12).

2.1.8. RNA extraction, sequencing and analysis

Overnight cultures of *X. szentirmaii* DSM16338, *P. laumondii* TTO1 and their respective *arcZ* deletion and knock-in mutants were used to inoculate fresh LB medium at an optical density measured at a wavelength of 600 nm (OD₆₀₀) of 0.3. Cultures were incubated at 30°C with shaking until mid-exponential phase was reached (Supplementary Table 1).

The RNeasy Mini Kit (Qiagen) was used for extraction of total RNA following manufacturer's instructions. Cells were pelleted and snap frozen in liquid nitrogen to facilitate cell lysis. After thawing, cells were resuspended in lysis buffer and vortexed

for 30 sec before proceeding with the protocol. Total RNA was isolated in duplicates for each sample.

The (150bp paired-end) RNA sequencing was performed by Novogene after rRNA depletion with a RiboZero kit and preparation of strand-specific libraries following the Illumina protocol. Bowtie2¹³³ (v2.3.4.3) was used to map the raw reads to the reference genome downloaded from NCBI (NC_005126.1 for *P. laumondii* and NZ_NIBV00000000.1 for *X. szentirmaii*) after trimming the raw data using Trimmomatic¹³⁴. The resulting .sam files were converted to .bam files using samtools¹³⁵ (v1.8). FeatureCounts¹³⁶ was used to count the reads mapped to annotated genes. Degust (<http://degust.erc.monash.edu/>) was used for analysis of the count files using the voom/limma normalization method. Coding sequences with a change of the transcriptomic output >2 and a false discovery rate (FDR) <0.01 were considered significantly regulated.

2.1.9. Northern blot analysis

Northern blot analysis was performed by Michaela Huber in the Papenfort lab (Jena, Germany) as described previously¹³⁷. Briefly, RNA samples were separated on 6% polyacrylamide / 7 M urea gels. Subsequently, RNA samples were transferred to Hybond–XL membranes (GE Healthcare) by electro-blotting. Membranes were hybridized at 42°C with gene-specific [³²P] end-labeled DNA oligonucleotides in Roti-Hybri-Quick buffer (Roth). The membranes were washed in three subsequent steps with SSC (5x, 1x, 0.5x) / 0.1% SDS wash buffer. A Typhoon FLA 7000 phosphorimager (FUJIFILM) were used to visualize the signals. All Oligonucleotides for Northern blot analyses are listed in Table 3.

2.1.10. Compensatory base mutation and GFP fluorescence assay

This compensatory base mutation study was performed by Michaela Huber in the Papenfort lab (Jena, Germany). Gibson assembly¹³⁸ was used to generate the plasmids pMH078 and pMH079. To generate the plasmid pMH078, the *arcZ* gene was amplified with oligonucleotides KPO-6147 and KPO-6148 using *P. laumondii* TTO1 genomic DNA. The PCR fragments were fused into pEVS143 vector backbone¹³⁹ which was previously linearized with KPO-0092 and KPO-1397. The 5'UTR and the first 20 aa of *hexA* were amplified using KPO-6145 and KPO-6146 to generate plasmid

pMH079. The pXG10-*gfp*¹⁴⁰ vector was linearized with KPO-1702 and KPO-1703. The plasmids pMH078 and pMH079 were used as templates to insert single point mutations in the *hexA* 5'UTR or in the *arcZ* gene using site-directed mutagenesis, yielding plasmids pMH080 and pMH081.

The GFP reporter fusion assay to measure target regulation was analysed as described previously¹⁴⁰. Briefly, three independent *E. coli* Top10 cells were grown overnight in LB medium (37°C, 200 rpm shaking conditions) for each strain. A Spark Microplate Reader (TECAN) was used to determine the GFP fluorescence intensity. Control samples were used to subtract background fluorescence.

2.1.11. RIP-seq analysis

Experimental work for RIP-seq analysis was performed by Xiaofeng Cai (Bode group) and Michaela Huber in the Papenfort lab (Jena, Germany). Fresh LB medium was inoculated with overnight cultures of *P. laumondii* TTO1 (WT and Hfq^{3xFLAG}) in duplicate and grown at 30°C with shaking. The cells were harvested at 4°C at 4000 rpm for 15 minutes at two different growth phases (OD₆₀₀ of 0.5 and 5, respectively). Cell pellets were resuspended in 1 ml lysis buffer (20 mM Tris pH8.0, 150 mM KCl, 1 mM MgCl₂, 1 mM DTT) and centrifuged at 4 °C for 5 min at 11,200 xg. Cell pellets were snap-frozen in liquid nitrogen. After thawing on ice, the pellets were resuspended in 800 µl lysis buffer and transferred into vials with 300 µl glass beads to facilitate cell lysis with a Bead Ruptor (2x 150 sec with 2 min break on ice). Subsequently, the cell lysates were centrifuged at 15,000 and 4°C, and the supernatant was transferred into a new precooled tube. The same procedure was repeated for the remaining samples using 400 µl lysis buffer. The supernatants were combined and centrifuged at 15,200 rpm for 30 min at 4°C. 800 µl of supernatant was transferred into a new tube. 35 µl Flag antibody (Monoclonal ANTI-FLAG M2, Sigma, #F 1804) was added to the samples and incubated with rotation for 45 min at 4°C. 75 µl Protein G sepharose (#6649, Sigma), prewashed with 1 ml lysis buffer, was added to the tubes and incubated with rotation for 45 min at 4°C. 800 µl of supernatant was transferred into a new tube and 35 µl Flag antibody (Monoclonal ANTI-FLAG M2, Sigma, #F 1804) was added to the tubes. Again, 75 µl Protein G Sepharose beads, prewashed with 1 ml wash buffer, were added to the tube and incubated for 45 min at 4°C. The Protein G Sepharose beads were washed with lysis buffer five times at 4°C and resuspended in 500 µl lysis buffer. Subsequently, the beads were extracted by addition of 500 µl

Phenol:Chloroform:Isoamylalcohol (P:C:I; 25:24:1, pH 4.5, Roth) at RT for 5 min, followed by centrifugation at 15,200 rpm for 30 min at 15 °C. The supernatant was precipitated with 1.5 ml EtOH:Na(acetate) (30:1) and 1.5 µl GlycoBlue (#AM9516, Ambion) overnight, after transfer into a fresh tube. On the following day, the samples were centrifuged at 11,200 rpm for 30 min at 4°C. The pellets were washed with 500 µl 70% EtOH, dried and resuspended in 15.5 µl nuclease-free H₂O. The samples were then treated with 0.5µl RNase inhibitor and 2 µl DNase in DNase buffer at 37°C for 30 min. Afterwards, 100 µl H₂O was added and the samples were transferred into a phase lock tube. The samples were extracted with 120 µl of P:C:I for 5 min at RT and centrifuged at 15,200 rpm for 30 min at 15°C. After transferring the supernatants into new tubes, ~350 µl of EtOH:Na(acetate) (30:1) were added and the samples were stored at -20°C overnight. For extraction of total sRNAs, the pellet was harvested at 13,300 rpm for 30 min at 4°C, washed with 500 µl 70% EtOH and finally dissolved in nuclease-free H₂O. The NEBNext Small RNA Library Prep Set for Illumina (Multiplex Compatible) was used for sRNA library construction according to the manual.

Enriched/Control sample pairs were normalized by the number of raw reads after trimming. Samtools¹³⁵ (v 1.8) was used to obtain depth counts of all samples. A region was considered to be enriched if the enrichment factor was at least three and the corresponding 'enriched' nucleotide was present in both sample pairs. Only nucleotide positions with a read count of at least 50 in the enriched samples were used for the analysis. Finally, a region was only defined as enriched, if more than five consecutive nucleotides were identified as enriched.

2.1.12. ArcZ binding prediction

The boundaries of *arcZ* in *Photorhabdus* and *Xenorhabdus* were defined based on *arcZ* from *E. coli*. The annotated *arcZ* sequence, together with homologs from other *Enterobacteriaceae*, were used for mRNA target prediction using the online CopraRNA tool with default parameters. ArcZ sequences used for CopraRNA¹⁴¹ analysis are listed in the following table (Table 4).

2.1.13. SM analysis via HPLC-MS/MS

An overnight culture was used to inoculate fresh LB medium at an OD₆₀₀ of 0.1. After 72 h of cultivation at 30°C with shaking, 1 ml of the culture was removed and spun down for 20 min at 13,300 rpm. The supernatant was then directly subjected for HPLC-UV/MS analysis using a Dionex Ultimate 3000 system with a Bruker AmaZon X mass spectrometer. Peak areas of the compounds of interest were quantified using TargetAnalysis (v1.3, Bruker). All analysed SMs are included in Supplementary Table 2.

2.1.14. Nematode development assay

Nematode bioassays were performed as described elsewhere¹⁰⁴. Briefly, overnight cultures of *P. luminescens* WT, *X. szentirmaii* WT and mutant strains were diluted to an OD₆₀₀ of 5. 200 µl of the culture was spread on lipid agar plates (0.5% (w/v) yeast extract, 1% (w/v) corn syrup, 2.5% (w/v) nutrient agar, 0.5% (v/v) cod liver oil and 0.2% (w/v) MgCl₂·6H₂O) in a “Z”-shape and incubated for 3 d at 30°C. Following incubation, approximately 50 surface sterilized infective juveniles (IJs) of *H. bacteriophora* or *S. rarum* were added to the lipid agar plates. The number of hermaphrodites was determined after another incubation of 4 d at 30°C using a dissecting microscope at 8x magnification. Ten biological replicates were performed.

2.2. Topic B: Components of insect larvae modulate *Xenorhabdus* and *Photorhabdus* secondary metabolite production

All materials and methods used for the conducted experiments covered in topic B (chapter 3.2) are described in the following sections. All herein described methods are part of the manuscript in preparation “Components of insect larvae modulate *Xenorhabdus* and *Photorhabdus* secondary metabolite production” by Nick Neubacher[#] ([#]first author), Nicholas J. Tobias, Martina Wurster, Michael Lalk and Helge B. Bode* (*corresponding author).

2.2.1. Bacterial culture conditions

X. szentirmaii, *X. nematophila* and *P. laumondii* cultures were grown in LB medium at 30°C with shaking. Solid LB medium contained 1.5% (w/v) agar.

2.2.2. Preparation of insect homogenate

Insect homogenate was obtained as previously described¹⁴². Briefly, *G. mellonella* larvae were snap frozen in liquid nitrogen, homogenized and freeze-dried for 18 h.

2.2.3. Isolation of insect hemolymph

G. mellonella larvae were frozen for 18 h at –20°C. On the following day, the larvae were thawed and the posterior segment was removed with a scalpel. The larvae were centrifuged for 1 min at 500 rpm at 4°C to collect the hemolymph. The hemolymph was transferred into a new reaction tube and freeze-dried for 18 h.

2.2.4. RNA extraction, sequencing and analysis

Overnight cultures of *X. szentirmaii*, *X. nematophila* and *P. laumondii* were used to inoculate fresh LB medium to an OD₆₀₀ of 0.35. The cultures were cultivated at 30°C with shaking until mid-exponential growth phase was reached (Individual OD₆₀₀ values are listed in Supplementary Table 3). Insect homogenate (5 mg/ml) was added and the cultures were cultivated for another 60 min. RNA extraction was performed as previously described¹⁴³. Data were analysed as described in 2.1.8. Reference genomes were downloaded from NCBI (NC_005126.1 for *P. laumondii*, NZ_LN681227.1 for *X. nematophila* and NZ_NIUA00000000.1 for *X. szentirmaii*).

2.2.5. HPLC-MS/MS analysis

Cultures of *X. szentirmaii*, *X. nematophila* and *P. laumondii* were grown overnight and used to inoculate fresh LB medium to an OD₆₀₀ of 0.1 on the next day. After 72 h of cultivation with or without addition of insect homogenate, 1 ml of the culture was transferred to a new reaction tube and centrifuged for 20 min at 13,300 rpm. The supernatant was used for HPLC-UV/MS analysis (Dionex Ultimate 3000 system coupled with a Bruker Amazon X mass spectrometer). Compound peak areas were quantified using TargetAnalysis (v1.3, Bruker). All analysed SMs are included in Supplementary Table 2.

2.2.6. GC-MS analysis

The GC-MS analysis of insect homogenate and insect hemolymph was performed by Martina Wurster in the Lalk lab (Greifswald, Germany). Briefly, freeze-dried insect hemolymph and insect homogenate were derivatized for 90 min at 37°C in 40 µl of 20 mg ml⁻¹ methoxyamine hydrochloride in pyridine, followed by a 30 min treatment with 80 µl of *N*-methyl-*N*-(trimethylsilyl)trifluoroacetamide (MSTFA) at 37°C. Injection was performed with an Agilent (series 7890B) gas chromatograph (Split 25:1 at 230°C, 2 µl injection volume, carrier gas: helium 1 ml/min). The MS was operated in the electron ionization mode with an ionization energy of 70 eV. Full mass scan was acquired from 50 to 500 m/z at a rate of 2.74 scans/s. The detected compounds were identified by processing of the raw GC-MS data with MassHunter version B 8.00 software (Agilent, USA) and comparing retention times and mass spectra of detected metabolites with those of standard compounds. Unknown peaks were analysed using the Fiehn library (Kind et al. 2009) and NIST 2017 mass spectral database 2.0 d (National Institute of Standards and Technology, USA) and were listed with the respective score.

2.3. Topic C: Identification of novel genes involved in SM production by transposon mutagenesis

The following sections cover all materials and methods used for the conducted experiments described in topic C (chapter 3.3).

2.3.1. Cultivation of bacterial cultures

Cultures of *P. laumondii* were cultivated in LB medium at 30°C with shaking. For solid growth medium, agar (1.5% w/v) was added.

2.3.2. Microorganisms

The following table shows all strains used for the experiments conducted in chapter 3.3.

Table 5. Microorganisms used in chapter 3.2 with name, genotype and reference.

Strain	Genotype/Description	Reference
<i>Escherichia coli</i> S17-1 λpir	Tp ^R Sm ^R <i>recA</i> , <i>thi</i> , <i>pro</i> , <i>hsdR</i> -M+RP4: 2- Tc:Mu:Km Tn7 λ pir	Invitrogen
S17-1 λ pir + pCKcipB_Δ <i>dam1</i>	S17-1 λ pir + pCKcipB_Δ <i>dam1</i> _TTO1, Cm ^R , R6K ori	This study
S17-1 λ pir + pCKcipB_knock-in_Δ <i>dam1</i>	S17-1 λ pir + pCKcipB_knock-in_Δ <i>dam1</i> , Cm ^R , R6K ori	This study
<i>Escherichia coli</i> ST18 λpir	Tp ^r Sm ^r , <i>recA thi hsdR</i> ⁺ RP4-2-Tc::Mu-Km::Tn7, λ pir phage lysogen, Δ <i>hemA</i>	144
ST λ pir + pSAM_Bt ¹²⁷	R6K ori, Amp ^R , oriT, Himar1C9 transposase, transposon containing <i>ermG</i>	This study
ST λ pir + pSAM_Kan	R6K ori, Amp ^R , oriT, Himar1C9 transposase, mariner transposon containing Kan ^R	This study
<i>Photorhabdus laumondii</i> ssp. <i>laumondii</i>	WT, Rif ^R	125
TN:: <i>dam1</i>	Mariner transposon insertion in <i>dam1</i> (insertion site: 82285)	This study
Δ <i>dam1</i>	Deletion of PLU_RS_00430	This study
Δ <i>dam1</i> :: <i>dam1</i>	Complementation of TTO1Δ <i>dam1</i> by insertion of full length <i>dam1</i> sequence	This study

2.3.3. Plasmids

The subsequent table covers all plasmids that were used for mutant construction covered in chapter 3.3.

Table 6. Plasmids used in chapter 3.1 with name, genotype and reference.

Plasmid	Genotype	Reference
pSAM_BT	R6K ori, Amp ^R , oriT, Himar1C9 transposase, transposon containing <i>ermG</i>	127
pSAM_KAN	R6K ori, Amp ^R , oriT, Himar1C9 transposase, mariner transposon containing Kan ^R	This study
pCK_cipB	R6K ori, CM ^R , oriT, <i>sacB</i> , <i>tral</i>	128
pCKcipB_Δ <i>dam1</i>	R6K ori, CM ^R , oriT, <i>sacB</i> , <i>tral</i> , containing a 980 bp upstream and a 1036 bp downstream region of <i>dam1</i>	This study
pCKcipB_knock-in_Δ <i>dam1</i>	R6K ori, Kan ^R , oriT, <i>sacB</i> , <i>tral</i> , containing a 2829 bp fragment including a 980 bp upstream and a 1036 bp downstream region of <i>dam1</i> and the full version of <i>dam1</i> (813 bp)	This study

2.3.4. Oligonucleotides

Table 7. Oligonucleotides used in chapter 3.3 with name, sequence and purpose.

Name	Sequence (5´-3´)	Purpose
NN191	TATAACCTCTCCTTAATTTATTGC	Linearization of pSAM_Bt
NN192	AAACAATAGGCCACATGC	
NN193	TAAATTAAGGAGAGGTTATACTGC GTCTAGCATGCCTA	Amplification of Kan ^R
NN194	TTGCATGTGGCCTATTGTTTTTAG AAAACTCATCGAGCATC	
NN255	ATCGATCCTCTAGAGTCGACCCA GATACCTCAGATCGCC	Deletion of <i>dam1</i> : amplification of <i>upstream</i> region of <i>dam1</i>
NN246	GCAAAAGGGGAGTGGATAAAGCT GTCAATTAATTACTCAATCATTCC	
NN247	TTTATCCACTCCCCTTTTGC	Deletion of <i>dam1</i> : amplification of <i>downstream</i> region of <i>dam1</i>
NN248	TCCCGGGAGAGCTCAGATCTCCA ATGTAACCTTTGACTTCCGG	
NN281	GCAGTACAGAATCTGAATCAAGC	Verification primer for TTO1Δ <i>dam1</i>
NN282	GGTGCAGTGATACCATAATCTCT	

2.3.5. Transposon mutagenesis

Creation of the transposon library was performed as described in 2.1.6

2.3.6. Construction of mutant strains

The Δ*dam1* mutant was generated as described in 2.1.5. Briefly, the upstream and downstream regions of *dam1* were amplified with the primer pairs NN 255/NN246 and NN247/NN248, respectively. The fragments were cloned into pCK_cipB resulting in the plasmid pCK_cipB_Δ*dam1*. pCK_cipB_Δ*dam1* was transferred and integrated into the genome of *P. laumondii* via conjugation. Deletion mutants were verified using the primer pair NN281/NN282 after counterselection on selective agar. The knock-in complementation was achieved as described in 2.1.5 using the primer pair NN255/NN248 to generate the fragment required for homologous recombination.

2.3.7. HPLC-MS analysis

HPLC-MS data were acquired and analysed as described in 2.1.11. All analysed SMs are covered in Supplementary Table S2.

2.3.8. RNA-seq

Overnight cultures of *P. laumondii* WT, $\Delta dam1$ and $\Delta dam1::dam1$ were used to inoculate fresh LB medium to an OD₆₀₀ of 0.35. The cultures were cultivated at 30°C with shaking until mid-exponential growth phase (OD₆₀₀ 3.5-4) was reached. RNA extraction, sequencing and analysis were performed as described in 2.1.8.

2.3.9. Single-Molecule Real-Time sequencing

Single-Molecule Real-Time sequencing was performed by Sacha J. Pidot (Melbourne, Australia). Determination of methylation patterns was performed on a Pacbio Sequel system. DNA was extracted using the Genomic Tip 100/G kit and the Genomic DNA buffer set (Qiagen) according to the manufacturer's protocol. Extracted DNA was submitted to the Australian Genome Research Facility (AGRF) for sample preparation, size selection and sequencing.

3. Results

3.1. Topic A: Small RNA directs symbiosis, virulence, and natural products biosynthesis in entomopathogenic bacteria

The following chapter is based on the manuscript “Small RNA directs symbiosis, virulence, and natural products biosynthesis in entomopathogenic bacteria” by Nick Neubacher[#], Nicholas J. Tobias[#], Michaela Huber[#] ([#]co-first authors), Xiaofeng Cai, Sacha J. Pidot, Timothy P. Stinear, Anna Lena Lütticke, Kai Papenfort and Helge B. Bode* (*corresponding author). This chapter covers the results included in this manuscript (under revision in *Nat. Microbiol.*; see Chapter 6 for the submitted manuscript). When results from other co-authors are described, these authors are mentioned.

So far, the regulation of SM production in *Photorhabdus* and *Xenorhabdus* implicates the regulators HexA, Hfq, LeuO and Lrp. To achieve its regulatory role, the RNA chaperone Hfq mediates base pairing of sRNAs and their respective mRNA targets, which leads to improved stability or accelerated degradation of sRNAs or transcripts. Deletion of Hfq in bacteria often leads to pleiotropic phenotypes. Common phenotypic alterations include impaired virulence, decreased motility and stress tolerance as well as deficits in antibiotic production^{103,145}. In *P. laumondii*, disruption of Hfq leads to abolishment of SM production, which correlates with an upregulation of the *hexA* mRNA¹⁰⁴ (Figure 4).

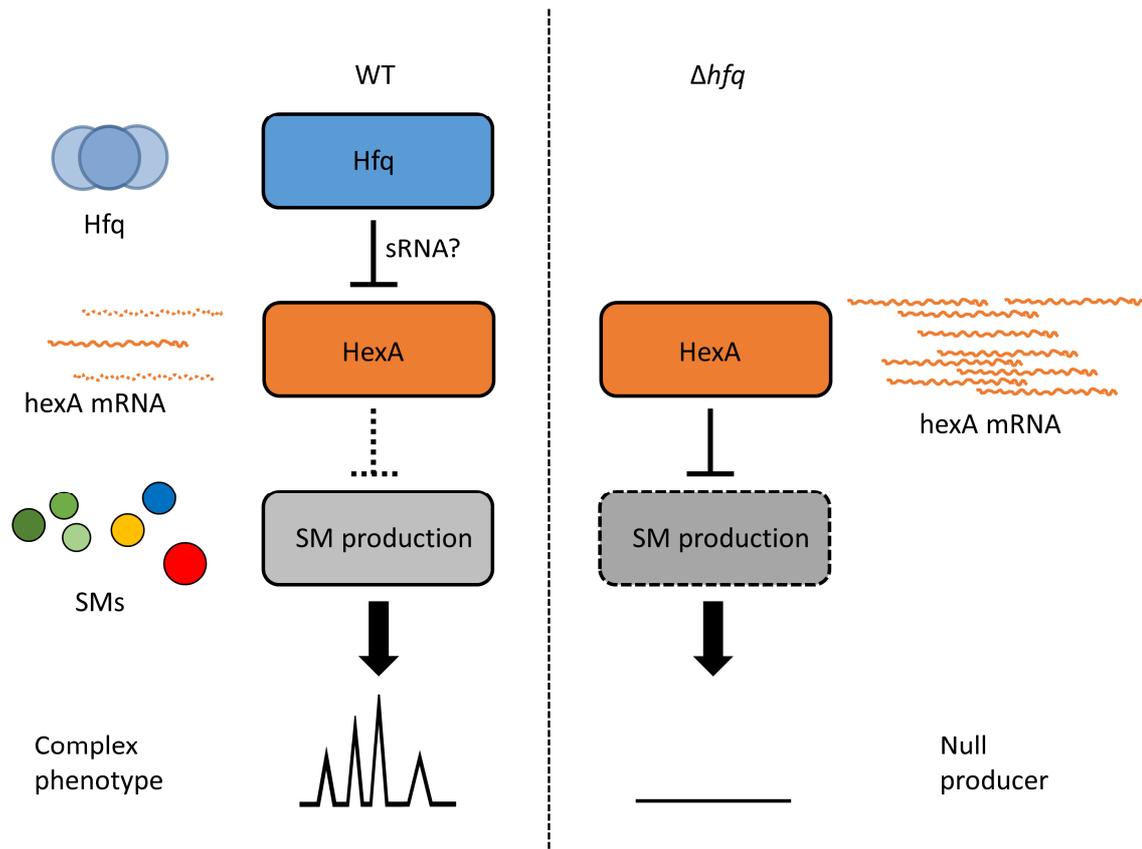


Figure 4. Hfq-based regulation of SM production in *Photorhabdus*. In the WT, Hfq inhibits HexA production, presumably by increasing degradation of the *hexA* mRNA. If HexA is not produced, SM production can occur. In the Δhfq mutant, *hexA* mRNA is strongly upregulated which results in production of HexA and in turn repression of the secondary metabolism.

Deletion of HexA in *P. laumondii* Δhfq restores SM production, suggesting a direct connection between Hfq, HexA and SM production, most likely through a sRNA. In this study, different global approaches were applied to unravel this connection and to expand the scope of Hfq based regulation of SM production in these genera.

3.1.1. sRNA identification in *P. laumondii* and *X. szentirmaii*

So far, very little is known about sRNAs in entomopathogenic bacteria like *Photorhabdus* and *Xenorhabdus*. Therefore, we decided to conduct a RNA sequencing protocol specifically customized for the identification of sRNAs to identify novel sRNAs in our strains (experiment performed by Nicholas Tobias, Bode group, Frankfurt, Germany). The analysis revealed a total of 130 and 242 previously unidentified sRNAs in *Xenorhabdus* and *Photorhabdus*, respectively. We used the Bacterial sRNA Database (BSRD) to search for our sRNA candidates and found a total of 51 sRNAs that have previously been described in other bacteria.

3.1.2. RIPseq reveals Hfq dependent sRNAs

We used RNA immunoprecipitation followed by high-throughput sequencing (RIPseq) to determine Hfq dependent sRNAs in *P. laumondii*. We used a Hfq^{3xFLAG} integrated into the genome of *P. laumondii* and performed the RIPseq experiment at different cell densities, which correspond to the early and late exponential growth phase (OD₆₀₀ of 0.5, and 5, respectively, experiment performed by Xiaofeng Cai, Bode group, Frankfurt, Germany and Michaela Huber, Papenfort group, Jena, Germany, see Chapter 6, Appendix). The previously generated sRNA list was used to search for sRNA candidates that were specifically enriched in the tagged samples compared to the control (untagged sample). We were able to identify 37 putative sRNAs in the early exponential growth phase and 37 putative sRNAs in the late exponential growth phase respectively, that were enriched only in the tagged samples (Figure 5).

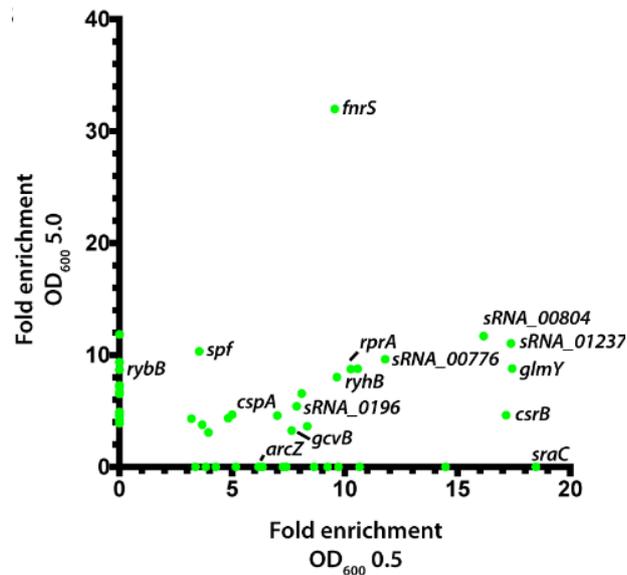


Figure 5. RIPseq enrichment in regions of sRNAs in *P. laumondii* Hfq^{3xFLAG} compared to untagged samples at OD₆₀₀ 0.5 and 5. Adapted from Neubacher et al., under revision (see Chapter 6, Figure 1B).

At OD₆₀₀ 0.5, eleven sRNAs are known to associate with Hfq while at OD₆₀₀ 5, ten sRNAs have been described to associate with Hfq. In order to verify the identified sRNAs, we performed northern blot analysis and probed for several different candidates including conserved sRNAs in *P. laumondii* and *X. szentirmaii* (northern blot analysis was performed by Michaela Huber, Papenfort group, Jena, Germany, see Appendix). The expression of several sRNAs (Spot 42, RybB, RhyB, GcvB, RprA, CyaR, RyeB (SdrS), GlmZ, sRNA_00243, sRNA_01262 and sRNA_00408) could be verified by analysis of northern blots. Excluding RyeB and GcvB, all of the tested sRNAs were identified in the WT of *P. laumondii* across all time points in varying concentrations. A Hfq-dependency was demonstrated for Spot 42, RybB, RyhB, sRNA_00243, RprA and CyaR, whose abundance was considerably reduced in the Δhfq strain compared to the WT (Neubacher et al., under revision, see Chapter 6, Supplementary Figure S1).

Five conserved sRNAs (CpxQ, RyhB, RybB, Spot 42 and CyaR) were probed for *X. szentirmaii*. In the WT, the concentration of Spot 42 was highest in the early exponential growth phase and decreased at later time points. CpxQ and RybB were most abundant in the early- to late-exponential growth phase and considerably reduced after 24 h of growth, while CyaR was most abundant in the mid-exponential phase in the WT. RyhB was only detected in WT samples after 24 h of growth. Hfq

appeared to be important for all of the tested sRNAs, as their abundance was considerably reduced in the Δhfq background (Neubacher et al., under revision, see Chapter 6, Supplementary Figure S2).

3.1.3. ArcZ is essential for SM production in *P. laumondii* TTO1

Instead of individually deleting the total of 69 Hfq associated sRNAs (across both ODs) identified by RIPseq, we decided to perform a transposon mutagenesis protocol based on the plasmid pSAM-BT. The orange to red color afforded to *P. laumondii* colonies by anthraquinone production makes the strain suitable for transposon mutagenesis, as mutants that are defective in AQ biosynthesis can be easily screened. We screened about 60,000 transposon mutants for obvious phenotypic alterations. We identified one transposon insertion mutant that was not able to produce any SMs, consistent with the phenotype of the Δhfq strain. By re-sequencing this strain, we could identify the transposon insertion site in an intergenic region (position 4692988, between PLU_RS_19855 and PLU_RS_19850; sequencing performed by Sacha J. Pidot and Timothy P. Stinear, University of Melbourne, Australia), which correlated to the annotation for *arcZ*.

ArcZ also showed up in our list of Hfq-associated sRNAs that were found to be enriched in the RIPseq experiment. We generated a $\Delta arcZ$ strain by deleting the major part of the gene to confirm that the observed phenotype is linked to the determined transposon insertion site. Indeed, deletion of *arcZ* led to an abolishment of SM production, as observed for the transposon insertion mutant. By introducing an intact version of *arcZ* at the original locus, we were able to restore SM production to WT level (Figure 6; see also Chapter 6, Figure 2C-H).

Results - Topic A

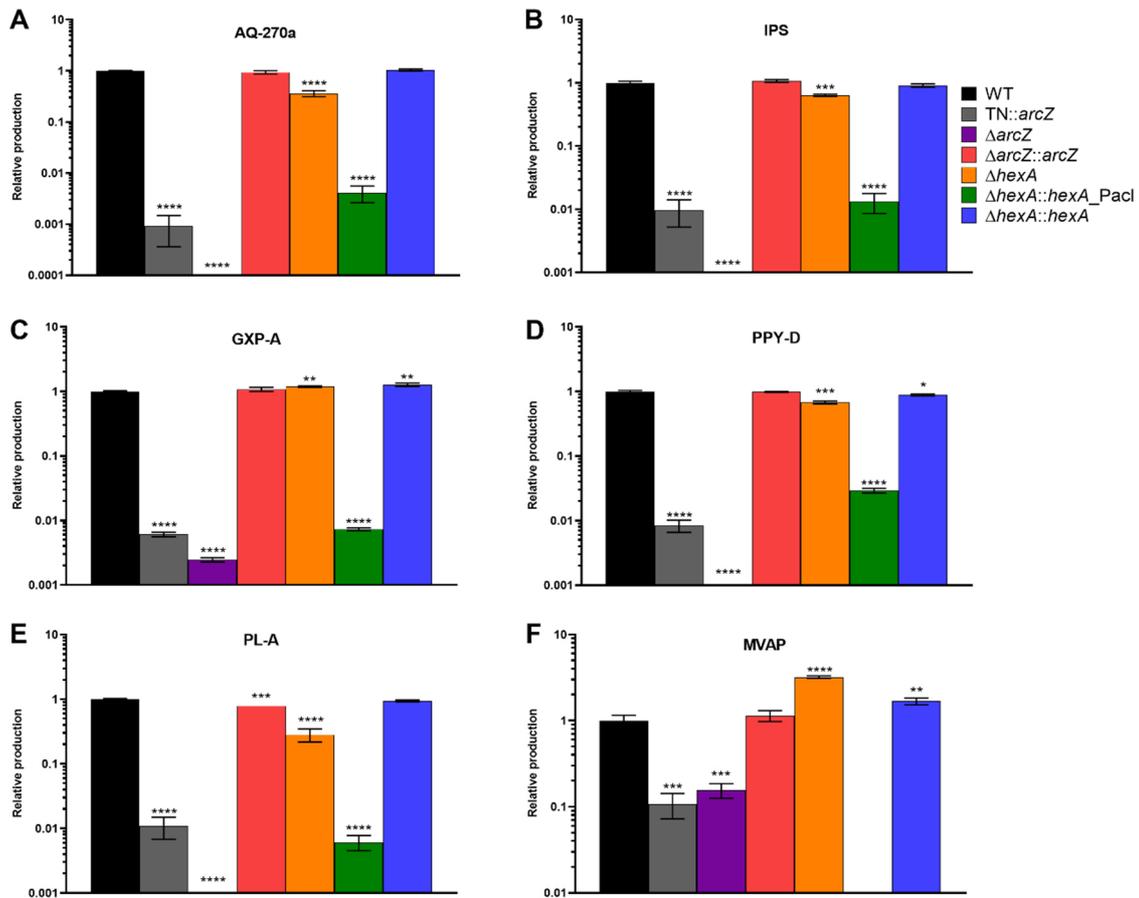


Figure 6. Quantification of major SM derivatives produced by *P. laumondii* WT (black), TN::arcZ (grey), ΔarcZ (purple), ΔarcZ::arcZ (red), ΔhexA (orange), ΔhexA::hexA_Pacl (green) and ΔhexA::hexA (blue). Depicted are the relative production titres of **A.** anthraquinone (AQ-270a), **B.** isopropylstilbene (IPS), **C.** GameXPepitide A, **D.** photopyrone D (PPY-D), **E.** phurealipid A (PL-A) and **F.** mevalagmapeptid (MVAP) generated from biological triplicates. Error bars represent the standard error of the mean. Asterisks indicate statistical significance (* p<0.05, ** p<0.005, *** p<0.0005, **** p<0.00005) of relative production compared to WT production levels. Adapted from Neubacher et al., under revision (see Chapter 6, Fig 2C-H).

Subsequently, *P. laumondii* WT, ΔarcZ and ΔarcZ::arcZ were tested for expression of ArcZ using northern blot analysis (northern blot analysis performed by Michaela Huber, Papenfort group, Jena, Germany). Expression of the processed form of ArcZ (around 50 nt) was demonstrated for the WT and complementation mutant across all tested time points (see Chapter 6, Figure 2A). A clearly visible signal was already present at early-exponential growth phase (OD₆₀₀=0.5). The ArcZ concentration increased during exponential growth phase and presumably hit its maximum concentration after 24 h of growth. As expected, no ArcZ expression was detected for the ΔarcZ strain.

3.1.4. ArcZ specifically binds to a regulatory region in the 5'-UTR of *hexA* to control SM production

To underpin the role of ArcZ in SM production, we predicted mRNA targets of ArcZ by using CopraRNA¹⁴¹, a tool for sRNA target prediction. Although not the top hit of the target prediction, we found a proposed 9 bp binding motif in the 5'-untranslated region (UTR) of *hexA*, a known repressor of SM production in both *P. laumondii*¹⁴⁶ and *X. szentirmaii*. We developed the hypothesis that ArcZ might bind to a regulatory region in the *hexA* mRNA to allow SM production by preventing HexA production. In accordance with this hypothesis, we found a corresponding enriched stretch of RNA upstream of *hexA* in the RIPseq experiment at OD₆₀₀ 0.5 (Figure 7).

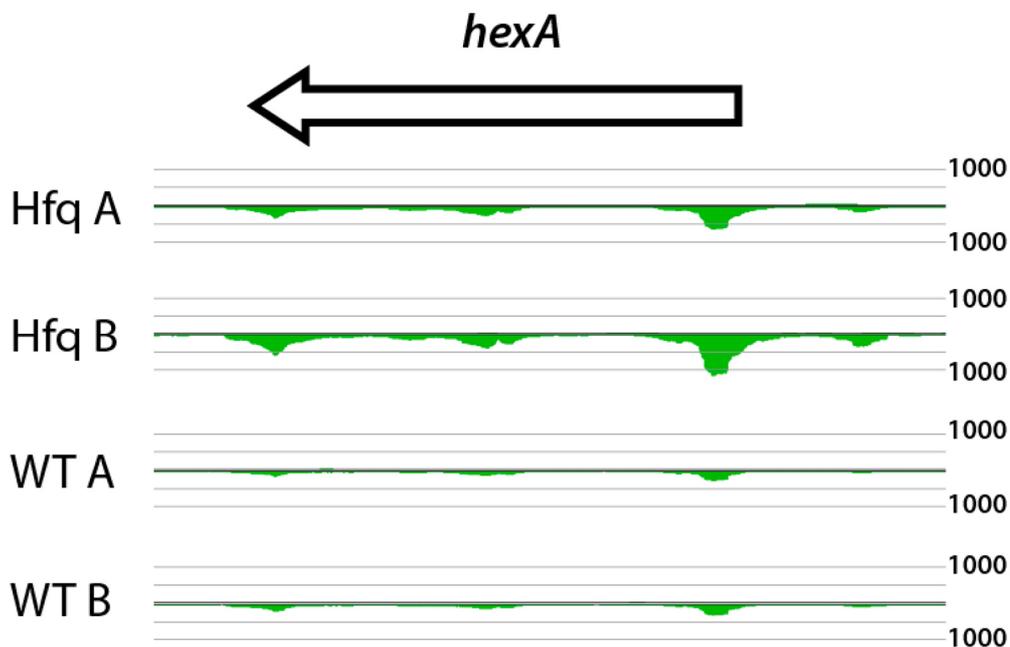


Figure 7. Enrichment around the region of *hexA* in Hfq^{3xFLAG} samples (Hfq A & B) compared to untagged samples (WT A & B). The plots indicate the mapped reads to the reverse strand (bottom) and forward strand (top). Adapted from Neubacher et al., under revision (see Chapter 6, Supplementary Figure S5).

To verify this idea, we decided to introduce an altered sequence at the predicted ArcZ binding site in the 5'-UTR of *hexA*. We created a knock-in mutant with a modified 5'-UTR upstream of *hexA* in *P. laumondii*. Specifically, we altered the native 5'-AACACCAGG motif to a *PacI* restriction site (5'-TTAATTAA). We chose to perform the insertion in a $\Delta hexA$ background because this strain has no defect in

SM production. The final strain, *P. laumondii* Δ *hexA::hexA_Pacl*, produced significantly reduced amounts of all analysed SMs (Figure 6), which supports our theory. To confirm that no other mutations were introduced during the construction of the strain, we sequenced the entire region containing the knock-in, including HexA.

In order to verify the proposed interaction region, we conducted a compensatory base mutation study (experiment performed by Michaela Huber, Papenfort group, Jena, Germany, see Chapter 6, Figure 3A-C). The fifth nucleotide of the proposed interaction region was exchanged in the *arcZ* sequence, the *hexA* UTR, or both, by site directed mutagenesis (see Chapter 6, Figure 3A). The *hexA* UTR sequence was fused to *gfp*. The GFP output was measured to determine inhibition of *hexA*. The measured green fluorescent protein (GFP) signal derived from the expression of p-ctr (*hexA::gfp*) was set to 1 and used to determine the efficiency of inhibition. Co-expression of p-*arcZ* and *hexA::gfp* led to a 5.7-fold increase of repression compared to the control, confirming that ArcZ binds to the UTR of *hexA* to inhibit the production. Additionally, when p-*arcZ*^{*} (G79C) was expressed, ArcZ^{*} was no longer able to repress *hexA::gfp*. The combination of *hexA::gfp* (C46G) with the native ArcZ led to a slightly increased *hexA::gfp* repression compared to the control, suggesting that ArcZ can still bind to the UTR of *hexA* but with reduced efficiency. When combining p-*arcZ*^{*} (G79C) with *hexA::gfp* (C46G), the fold repression of *hexA::gfp* increased almost 10-fold (see Chapter 6, Figure 3B). Overall, these experiments confirmed the interaction between ArcZ and the UTR of *hexA* as well as the region of interaction.

3.1.5. A general mechanism? Effect of ArcZ in *Xenorhabdus*

Among enterobacterial species, *arcZ* and its genomic organization are highly conserved¹⁴⁷ (Figure 8).

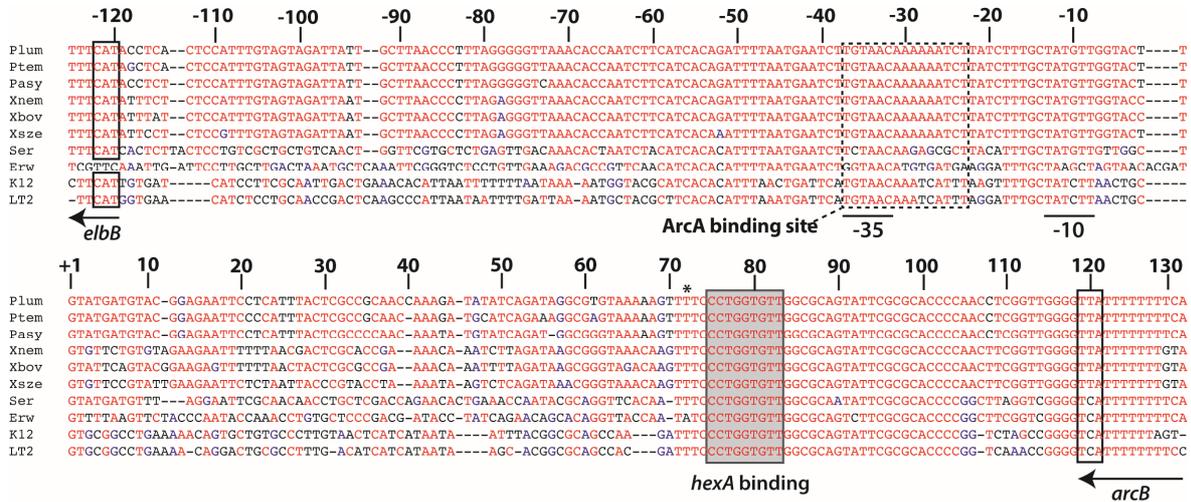


Figure 8. Conservation of ArcZ among diverse bacterial species. Depicted is an alignment of bacterial *arcZ* sequences including upstream promoter region (Plum: *P. laumondii*, Ptem: *P. temperate*, Pasy: *P. asymbiotica*, Xnem: *X. nematophila*, Xbov: *X. bovienii*, Xsze: *X. szentirmaii*, Ser: *Serratia marsecens* Db11, Erw: *Erwinia amylovora* CFBP1430, K12: *E. coli* K12, LT2: *Salmonella typhimurium* LT2). The putative -10 and the -35 promoter regions are indicated. The start codon of *elbB* and the stop codon of *arcB*, as well as the conserved ArcA binding region is also indicated. '+1' denotes the transcriptional start site of *arcZ*. The asterisk shows the proposed processing site of ArcZ. The *hexA* binding region is highlighted in a box. Adapted from Neubacher et al., under revision (see Chapter 6, Figure 1A).

Since we could attribute a clear-cut phenotype concerning SM production to the deletion of *arcZ* in *P. laumondii*, we decided to investigate whether the same mechanism to control SM production is applied in *Xenorhabdus*.

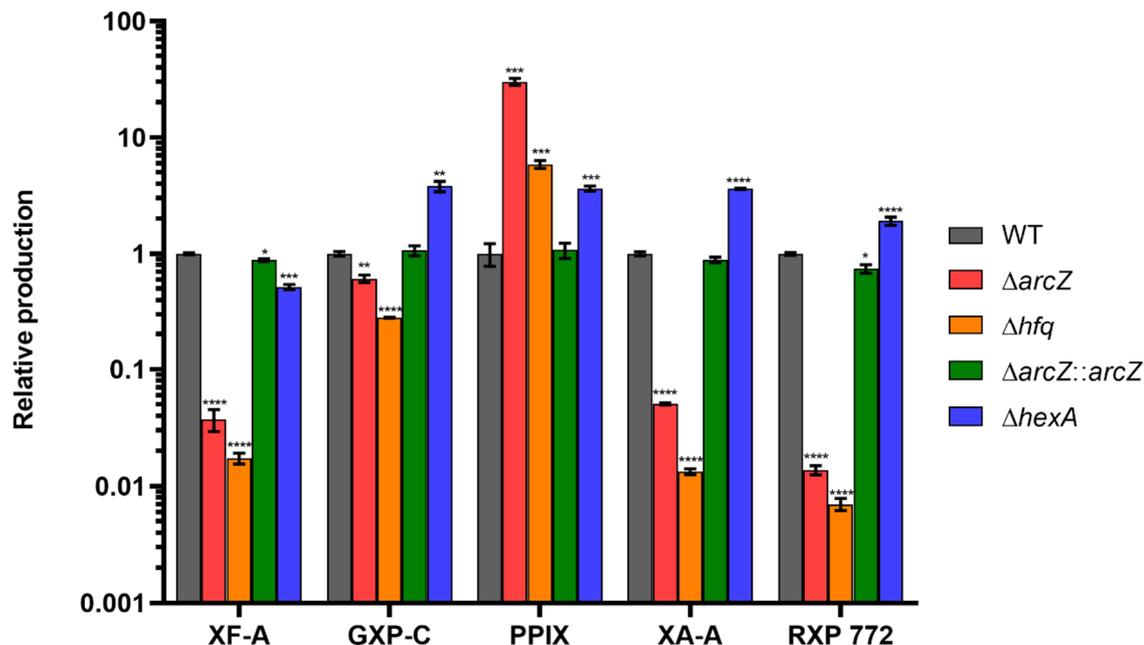


Figure 9. Quantification of SM production in *X. szentirmaii* WT (grey), $\Delta arcZ$ (red), Δhfq (orange), $\Delta arcZ::arcZ$ (green), and $\Delta hexA$ (blue). All bars represent relative production compared to the WT (production =1) generated from biological triplicates. The compounds xenofuranone A (XF-A), GameXPeptide C (GXP-C), protoporphyrin IX (PPIX), xenoamicin A (XA-A) and rhabdopeptide 772 (RXP-772) were analysed. Error bars represent the standard error of the mean. Asterisks indicate statistical significance (* $p < 0.05$, ** $p < 0.005$, *** $p < 0.0005$, **** $p < 0.00005$) of relative production compared to WT production levels. Adapted from Neubacher et al., under revision (see Chapter 6, Figure 3E).

In accordance with the previously observed phenotype after deletion of *hfq* in *P. laumondii*, the Δhfq mutant in *X. szentirmaii* also exhibited severely reduced SM titres. We constructed a $\Delta arcZ$ mutant in *X. szentirmaii* by deleting a major part of the ArcZ coding sequence, in a similar fashion to the *P. laumondii* deletion mutant. A drastic effect on SM production was also observed in *X. szentirmaii* (Figure 9). Although all SM were found to be down-regulated upon deletion of *arcZ*, we observed that production of protoporphyrin IX (PPIX), a compound derived from the primary metabolism, was strongly increased (~30-fold) compared to the WT. As already demonstrated for *P. laumondii*, knock-in of *arcZ* at the original gene locus in *X. szentirmaii* complemented the observed phenotype. Production of PPIX was also reduced back to WT level upon deletion, suggesting that the regulon of ArcZ is possibly not restricted to SM regulation. The deletion of *hexA* led to an increase of most analysed compounds except XF-A. As shown for *P. laumondii*, we tested *X. szentirmaii* WT, $\Delta arcZ$ and $\Delta arcZ::arcZ$ for ArcZ expression (experiment

performed by Michaela Huber, Papenfort group, Jena, Germany, see Chapter 6, Supplementary Figure S2).

For the WT of *X. szentirmaii* and the $\Delta arcZ::arcZ$ mutant, an ArcZ signal was detected at all analysed time points. ArcZ levels were low in the early-exponential growth phase and highest in the mid- to late-exponential growth phase. Opposed to *P. laumondii*, ArcZ concentrations appeared to be decreasing after prolonged growth, as only a faint signal for ArcZ was detected after 24 h of cultivation. In contrast to *Photorhabdus*, a clear signal for the primary (unprocessed) form of ArcZ around 130 nt was visible for the samples taken at OD₆₀₀ 2 and 4. Again, no ArcZ expression was detected for the $\Delta arcZ$ mutant (Neubacher et al., under revision, see Chapter 6, Supplementary Figure S2).

3.1.6. The ArcZ regulon in *Photorhabdus* and *Xenorhabdus*

To determine possible implications of ArcZ in other regulatory circuits, we conducted RNA sequencing experiments of WT, $\Delta arcZ$ and complementation strains of *P. laumondii* and *X. szentirmaii* at mid exponential growth phase (OD₆₀₀ of 4). Including our previous RNA sequencing results for the Δhfq mutants¹⁰⁴, we aimed to unravel the differences in regulation between these genera and underpin the observed pleiotropic phenotypes by transcriptomic profiling. Strikingly, the deletion of the sRNA significantly affected the transcript level of 735 coding sequences (CDS) in *P. laumondii* (FDR<0.01; log₂ fold change >2). In an attempt to identify broader effects, we compared the data set generated for the $\Delta arcZ$ strain with the data for the Δhfq strain. First, we generated a scatter plot with the RNA sequencing data for the *hfq* deletion strain on the y-axis and the $\Delta arcZ$ data on the x-axis (Figure 10A).

Results - Topic A

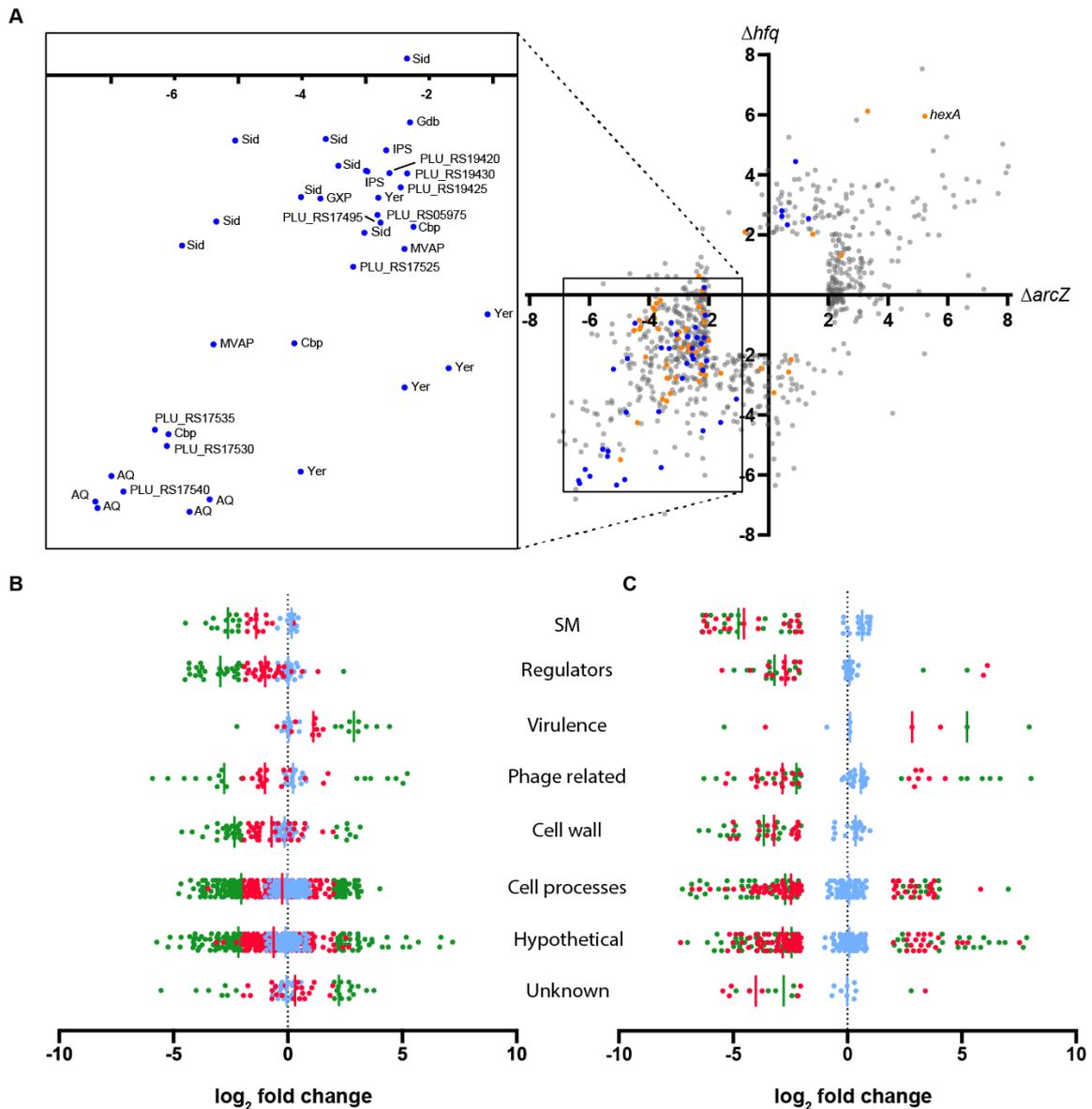


Figure 10. Comparison of Hfq and ArcZ regulon in *P. laumondii*. **A.** Relative transcript level modulation of individual CDS compared to the WT strain in the $\Delta arcZ$ (x-axis) and Δhfq mutants (y-axis). Regulators are depicted as orange dots and CDS involved in SM production are shown as blue dots. The CDS involved in the production of anthraquinone (AQ), mevalgmapeptide (MVAP), cabapenem (Cbp), yersiniabactin (Yer), GameXPepptide (GXP), isopropylstilbene (IPS), siderophore (Sid) and glidobactin (Gdb) are shown in the inset. **B.** Significantly altered CDS in *P. laumondii* $\Delta arcZ$ and not in Δhfq or **C** significantly affected CDS in both strains. All affected CDS associated with *P. laumondii* $\Delta arcZ$ (green), *P. laumondii* Δhfq (red) and *P. laumondii* $\Delta arcZ::\Delta arcZ$ (blue) were grouped into one of eight different categories: specialized metabolites (SM), regulators, virulence, phage related, cell wall, cell processes, hypothetical and unknown based on their annotations. The median is represented as a vertical line. Adapted from Neubacher et al., under revision (see Chapter 6, Supplementary Figure S9).

In accordance with our theory that *hfq* and *arcZ* regulate SM production by repressing HexA production, we found strongly elevated transcript levels of *hexA* when either part of the regulatory network was deleted. Consistent with the severe

effect on SM production, the vast majority of SM related CDS were also found to be downregulated.

All significantly affected CDS were grouped into eight different categories based on their proposed or known function: Regulators, SM related, virulence, cell wall, phage related, unknown and hypothetical proteins. We focused on CDS that were significantly regulated exclusively in the *arcZ* deletion mutant and not in the *hfq* deletion mutant (Figure 10B). Except for the categories ‘virulence’ and ‘unknown’, a clear trend towards down-regulation of the transcriptional output was observed upon deletion of *arcZ* (green dots). Although somewhat weakened, a similar trend was also observed for the *hfq* deletion mutant (red dots). The vast majority of transcript level alterations were complemented back to WT level in the knock-in strains (blue dots). Finally, we looked at genes whose expression was significantly altered in both the *arcZ* and *hfq* deletion strain. The individual categories clustered very closely together as indicated by the median (Figure 10C). The significantly affected regulators are listed below (Table 8).

Table 8. List of affected regulators in *P. laumondii* upon deletion of *arcZ* or *hfq* with locus tag, annotation and log₂ fold change in the respective strains. For a complete list of affected genes see also Chapter 6, Supplementary Tables S7 & S8 (digitally available on the attached CD).

Locus tag	Annotation	WT	$\Delta arcZ$	Δhfq
PLU_RS04575	transcriptional regulator	0	-2,99	-1,76
PLU_RS04580	transcriptional regulator	0	-2,74	-1,71
PLU_RS04585	transcriptional regulator	0	-2,34	-2,62
PLU_RS04590	transcriptional regulator	0	-3,36	-3,29
PLU_RS04595	transcriptional regulator	0	-2,72	-1,85
PLU_RS04600	transcriptional regulator	0	-3,47	-2,77
PLU_RS04605	transcriptional regulator	0	-3,62	-3,47
PLU_RS04610	transcriptional regulator	0	-3,48	-3,54
PLU_RS06355	transcriptional regulator	0	-3,47	-2,34
PLU_RS07630	transcriptional regulator	0	-2,60	-2,13
PLU_RS09890	LuxR family transcriptional regulator	0	-2,39	-2,89
PLU_RS09905	RpiR family transcriptional regulator	0	-2,27	-1,77
PLU_RS09980	LuxR family transcriptional regulator	0	-2,22	-1,42
PLU_RS09985	LuxR family transcriptional regulator	0	-2,83	-1,13
PLU_RS09995	LuxR family transcriptional regulator	0	-3,75	-1,14
PLU_RS10000	LuxR family transcriptional regulator	0	-4,56	-1,18

Results - Topic A

Locus tag	Annotation	WT	$\Delta arcZ$	Δhfq
PLU_RS10005	LuxR family transcriptional regulator	0	-4,38	-1,14
PLU_RS10010	LuxR family transcriptional regulator	0	-4,36	-1,08
PLU_RS10015	LuxR family transcriptional regulator	0	-4,11	-0,88
PLU_RS10020	LuxR family transcriptional regulator	0	-4,39	-0,84
PLU_RS10030	LuxR family transcriptional regulator	0	-3,88	-0,78
PLU_RS10035	LuxR family transcriptional regulator	0	-3,93	-0,43
PLU_RS10040	LuxR family transcriptional regulator	0	-3,88	-0,51
PLU_RS10045	LuxR family transcriptional regulator	0	-4,06	-0,16
PLU_RS10050	LuxR family transcriptional regulator	0	-3,82	-0,28
PLU_RS10055	LuxR family transcriptional regulator	0	-3,69	-0,18
PLU_RS10885	fumarate/nitrate reduction transcriptional regulator	0	-2,32	-2,33
PLU_RS11350	transcriptional regulator	0	-2,07	-1,52
PLU_RS12080	CysB family transcriptional regulator	0	-2,51	-1,91
PLU_RS12870	SlyA family transcriptional regulator	0	-4,18	-2,07
PLU_RS13075	AraC family transcriptional regulator	0	-5,03	-5,49
PLU_RS13485	transcriptional regulator	0	-4,45	-4,26
PLU_RS15150	Cro/CI family transcriptional regulator	0	-3,17	-2,77
PLU_RS15385	transcriptional regulator LrhA (HexA)	0	5,16	5,95
PLU_RS15820	two-component system response regulator	0	-2,22	-0,91
PLU_RS16025	LuxR family transcriptional regulator	0	-3,05	-1,23
PLU_RS16030	LuxR family transcriptional regulator	0	-3,11	-1,44
PLU_RS17390	transcriptional regulator	0	3,25	6,12
PLU_RS18510	LuxR family transcriptional regulator	0	-2,17	-2,67
PLU_RS18745	AraC family transcriptional regulator	0	2,37	1,32
PLU_RS21065	transcriptional regulator	0	-2,25	-0,59
PLU_RS21135	LuxR family transcriptional regulator	0	-2,40	-0,39
PLU_RS21200	LuxR family transcriptional regulator	0	-2,40	0,63
PLU_RS23620	transcriptional regulator	0	-2,29	0,15

A global effect of the *arcZ* deletion was also observed for *X. szentirmaii*, albeit only 191 CDS were affected in this strain. Similar to *P. laumondii*, the majority of affected CDS were downregulated. Transcript levels of CDS involved in the synthesis of SMs were also found to be reduced significantly in both *X. szentirmaii* $\Delta arcZ$ and *X. szentirmaii* Δhfq (Figure 11).

Results - Topic A

Table 9. List of affected regulators in *X. szentirmaii* upon deletion of *arcZ* or *hfq* with locus tag, annotation and log₂ fold change in the respective strains. For a complete list of affected genes, see also Chapter 6, Supplementary Tables S1 & S12 (digitally available on the attached CD).

Locus tag	Annotation	WT	$\Delta arcZ$	Δhfq
Xsze_RS00440	molecular chaperone HtpG	0	-2.47	-0.84
Xsze_RS01205	AraC family transcriptional regulator	0	-1.08	-2.28
Xsze_RS01245	molecular chaperone	0	-1.61	-3.01
Xsze_RS02645	transcriptional regulator	0	1.68	2.68
Xsze_RS04235	LuxR family transcriptional regulator	0	-2.91	-4.00
Xsze_RS04880	LysR family transcriptional regulator	0	1.16	2.01
Xsze_RS09420	winged helix-turn-helix transcriptional regulator	0	-1.10	-2.24
Xsze_RS09965	AraC family transcriptional regulator	0	-1.29	-2.40
Xsze_RS10390	LuxR family transcriptional regulator	0	-3.42	-2.91
Xsze_RS13130	trifunctional transcriptional regulator/proline dehydrogenase/L-glutamate gamma-semialdehyde dehydrogenase	0	-0.44	2.41
Xsze_RS13275	ANR family transcriptional regulator	0	2.32	-0.43
Xsze_RS13320	XRE family transcriptional regulator	0	2.34	0.18
Xsze_RS15160	helix-turn-helix domain-containing protein	0	-3.18	-3.36
Xsze_RS15790	LysR family transcriptional regulator	0	-3.14	-2.80
Xsze_RS16700	molecular chaperone	0	-2.24	-1.24
Xsze_RS17120	hypothetical protein	0	-7.57	-9.24
Xsze_RS17920	molecular chaperone	0	-0.95	-2.90
Xsze_RS18135	transcriptional regulator LrhA (HexA)	0	3.61	3.07
Xsze_RS20560	XRE family transcriptional regulator	0	-1.91	-2.82

Consistent with the data for *P. laumondii*, *hexA* transcript levels were strongly elevated when either part of the regulatory system was deleted.

3.1.7. *ArcZ* in *P. laumondii* is essential for niche occupation

Controlling SM production relays a fundamental ability for *Photorhabdus* and *Xenorhabdus* to occupy their niche, as SMs are required for supporting development of their nematode hosts, repellents for competitors or for full virulence¹⁰. The ability to retain their niche upon deletion of *arcZ* was analysed in a nematode development assay (Figure 12).

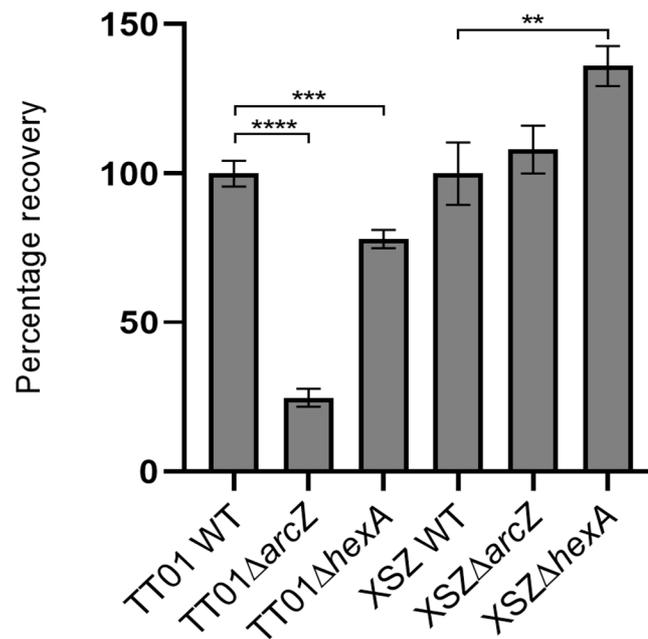


Figure 12. Recovery of hermaphrodites with strains of *P. laumondii* and *X. szentirmaii*. Each bar represents a mean value of 10 individual experiments with standard deviations also shown. Error bars represent the standard error of the mean. Asterisks indicate statistical significance (* $p < 0.05$, ** $p < 0.005$, *** $p < 0.0005$, **** $p < 0.00005$) of relative production compared to WT production levels. Adapted from Neubacher et al., under revision (see Chapter 6, Supplementary Figure S8).

Interestingly, the ability of *P. laumondii* $\Delta arcZ$ to support nematode development was significantly ($p < 0.0005$) reduced to approximately 25% of WT level, while *X. szentirmaii* $\Delta arcZ$ was still able to support nematode development (Figure 12). The deletion of *hexA* appeared to have a slight effect on nematode development in both strains. For *P. laumondii* $\Delta hexA$ the percentage of recovered hermaphrodites was reduced, whereas the opposite was observed for *X. szentirmaii* $\Delta hexA$.

3.1.8. Selective SM production in *X. szentirmaii* Δ *arcZ*

The deletion of *hfq* and *arcZ* provides a chemical background that is devoid of SMs. Isolation of desired compounds is often hindered by production of other compounds with similar retention times. Combined with the specific activation of the desired compound by promoter exchanges, those strains represent a powerful tool for production, isolation, and identification of new natural products. Understanding SM-based regulation in *Photorhabdus* and *Xenorhabdus* has recently allowed us to exploit the regulatory cascade for production of specific SM in Δ *hfq* strains of *Photorhabdus*, *Xenorhabdus*, but also *Pseudomonas*¹¹⁹. The Δ *arcZ* strain of *X. szentirmaii* was tested for its suitability to serve as an alternative strain for specific natural product production. As a proof of concept, the native promoter of *gxpS* was exchanged with an arabinose inducible promoter in *X. szentirmaii* Δ *arcZ*. The relative production of GameXPeptide was measured after HPLC-MS analysis and compared to the WT and a promoter exchange mutant in front of *gxpS* in *X. szentirmaii* Δ *hfq* (Figure 13).

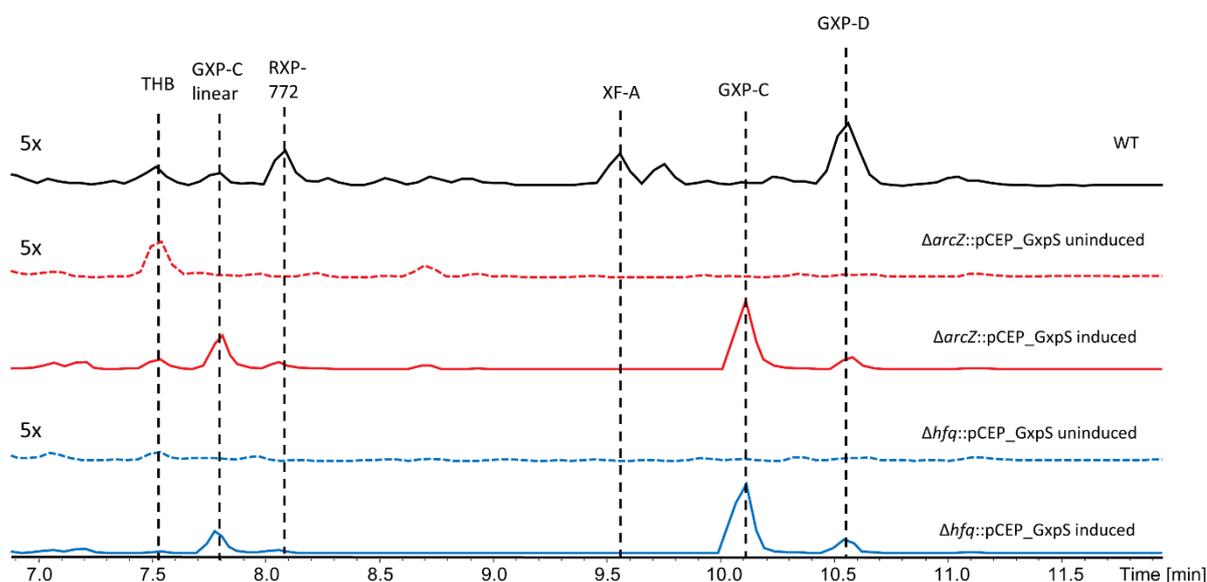


Figure 13. Base peak chromatograms (BPCs) of *X. szentirmaii* WT (black), Δ *arcZ*::pCEP_GxpS uninduced (red dotted line), Δ *arcZ*::pCEP_GxpS induced (red solid line), Δ *hfq*::pCEP_GxpS uninduced (blue dotted line) and Δ *hfq*::pCEP_GxpS induced (blue solid line). Peaks corresponding to (cyclo)tetrahydroxybutyrate (THB)¹⁴, Linear GameXPeptide C (GXP-C), rhabdopeptide 772 (RXP), xenofuranone A (XF-A), as well as cyclic GXP-C and GXP-D. BPCs of WT and uninduced mutants have been zoomed in 5x compared to the induced mutants. Adapted from Neubacher et al., under revision (see Chapter 6, Figure 4C).

Compared to the WT, a 90-fold overproduction of GXP-C was measured after induction of *gxpS* in *X. szentirmaii* Δ *arcZ* compared to the WT. In the uninduced culture, only trace amounts of GXP-C were measured. For *X. szentirmaii* Δ *hfq*, a 138-fold GXP-C overproduction was observed after inducing the promoter exchange mutant, with no GXP-C detectable in the non-induced culture. In general, both strains appeared to be suitable for activation of specific natural products, as almost no other peaks that could hinder isolation were observed in the base peak chromatogram (BPC).

3.2. Topic B: Components of insect larvae modulate SM production in *Xenorhabdus* and *Photorhabdus*

This chapter is based on the manuscript in preparation “Components of insect larvae modulate SM production in *Xenorhabdus* and *Photorhabdus*” by Nick Neubacher[#] ([#]first author), Nicholas J. Tobias, Martina Wurster, Michael Lalk and Helge B. Bode* (*corresponding author). The results shown in this chapter are covered in the manuscript.

Photorhabdus and *Xenorhabdus* exist in a mutualistic form (in symbiosis with their nematode host) and in a pathogenic form (in the insect host). The P-form is, among other characteristics, defined by production of an array of SMs, which are required for full virulence against the insect host and to support the development of their nematode host. Upon transmission of the bacteria from their nematode vector into the insect hemolymph, the phase switch from M-form to P-form is initiated. Signal molecules from the insect hemolymph are assumed to trigger this transition. In this chapter, an easily applicable *in vitro* assay to determine the response of entomopathogenic bacteria to their insect hosts is presented. The influence of simulating the insect host environment was assayed for alterations on SM as well as on the transcriptome. Furthermore, GC-MS analysis was used to determine the components of *G. mellonella* hemolymph as well as insect homogenate (samples were measured by Martina Wurster, Lalk group, Greifswald, Germany). Finally, the most abundant components of insect hemolymph were tested for their potential to serve as a signal molecule for the bacteria by supplementing culture media with increasing concentrations and subsequent HPLC-MS analysis.

3.2.1. *In vivo* Simulation

In order to determine the effect of simulating the environment of an insect host on their respective SM profile, cultures of *P. laumondii*, *X. szentirmaii* and *X. nematophila* were supplemented with insect homogenate. The insect homogenate was made from *G. mellonella* larvae, a potential host for these bacteria. Indeed, addition of insect homogenate to the cultures shifted the SM profiles of the tested bacteria, as displayed in Figure 14.

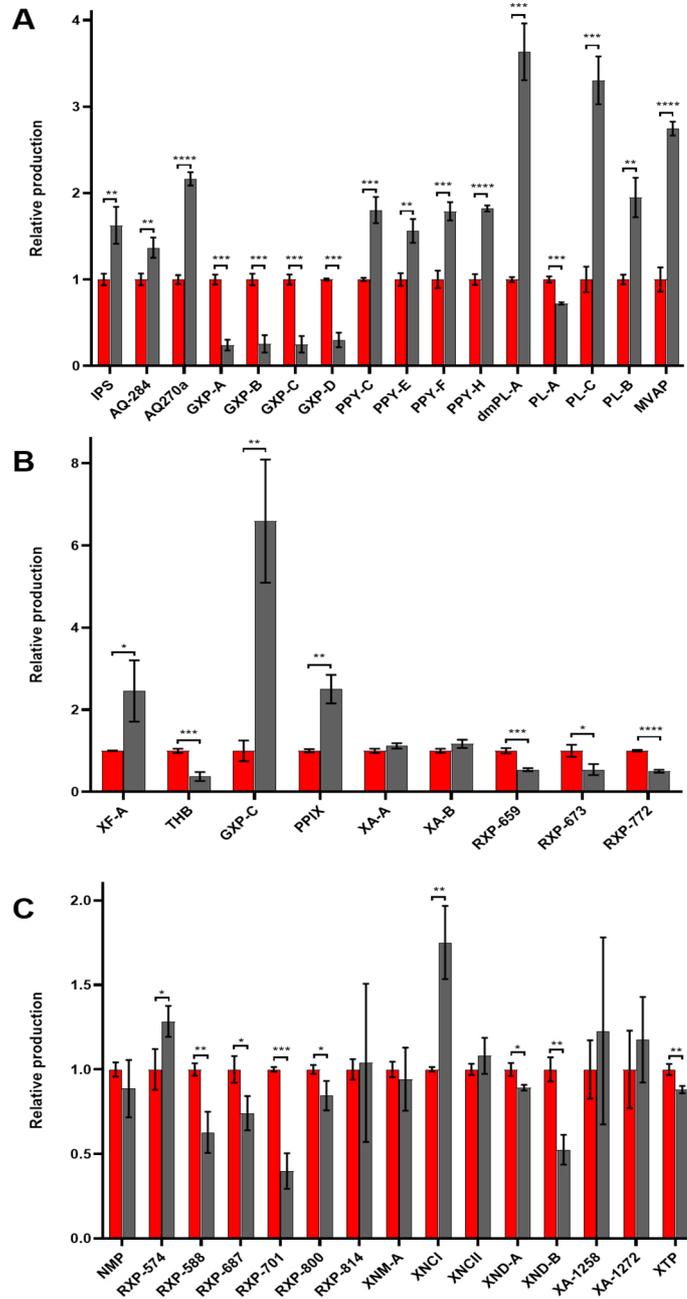


Figure 14. SM profiles of **A.** *P. laumondii* TTO1, **B.** *X. szentirmaii* and **C.** *X. nematophila*. Depicted are the relative amounts of isopropylstilbene (IPS), anthraquinone (AQ), GameXPeptide (GXP), photopyrone (PPY), desmethyl-phurealipid A (dmPL-A), phurealipid (PL) and mevalagmapeptide (MVAP) produced by *P. laumondii*, xenofuranone A (XF-A), tetrahydrobutyrate (THB), GameXPeptide C (GXP-C), protoporphyrin IX (PPIX), xenoamicin (XA), and rhabdopeptide (RXP) produced by *X. szentirmaii* and nematophin (NMP), rhabdopeptide (RXP), xenematide A (XNM-A), xenocoumacin (XNC), xenortid (XND), xenoamicin (XA) and xenotrapeptide produced by *X. nematophila* after addition of insect homogenate and cultivation for 72 h at 30°C with shaking. The data was generated from three biological replicates. Asterisks indicate statistical significance (* p<0.05, ** p<0.005, *** p<0.0005, **** p<0.00005) of relative production compared to WT production levels.

The most severe alterations were detected for *P. laumondii*, where all analysed SMs were significantly ($p < 0.05$) affected. Relative production titres of all GameXPepptide (GXP) derivatives were reduced to about 25 % compared to WT levels. In contrast, isopropylstilbene (IPS), anthraquinones (AQs), mevalagmapeptide (MVAP), all photopyrones (PPYs) and most phurealipids (PLs) were overproduced by a factor of 1.3 to 3.5-fold compared to the WT level. For *X. szentirmaii*, relative production of xenofuranone A(XF-A), GameXPepptide C (GXP-C) and protoporphyrin IX (PPIX) was increased up to 6.5-fold in comparison to the WT samples, while a relative decrease in production was observed for all other analysed compounds. Addition of insect homogenate to *X. nematophila* cultures had the most limited effect on SM production, with the most prominent change being an increase of xenocoumacin I (XNCI) production and the decrease of four rhabdopeptides (RXP-588, RXP-687, RXP-701, RXP-800) as well as xenortide B (XND-B).

3.2.2. RNA-sequencing

RNA sequencing was performed to investigate the influence of adding insect homogenate to the medium on the transcriptomic profile of those genera. To do this, insect homogenate was added at mid-exponential growth phase. Total RNA was extracted 1 h after adding the insect homogenate to the cultures and subsequently sequenced. Interestingly, the *in vivo* simulation had a global effect on the transcriptome, significantly affecting up to 6% of the global transcriptomic output (Figure 15A, trimming, counting and mapping of raw reads performed by Nicholas J. Tobias, Bode group, Frankfurt, Germany).

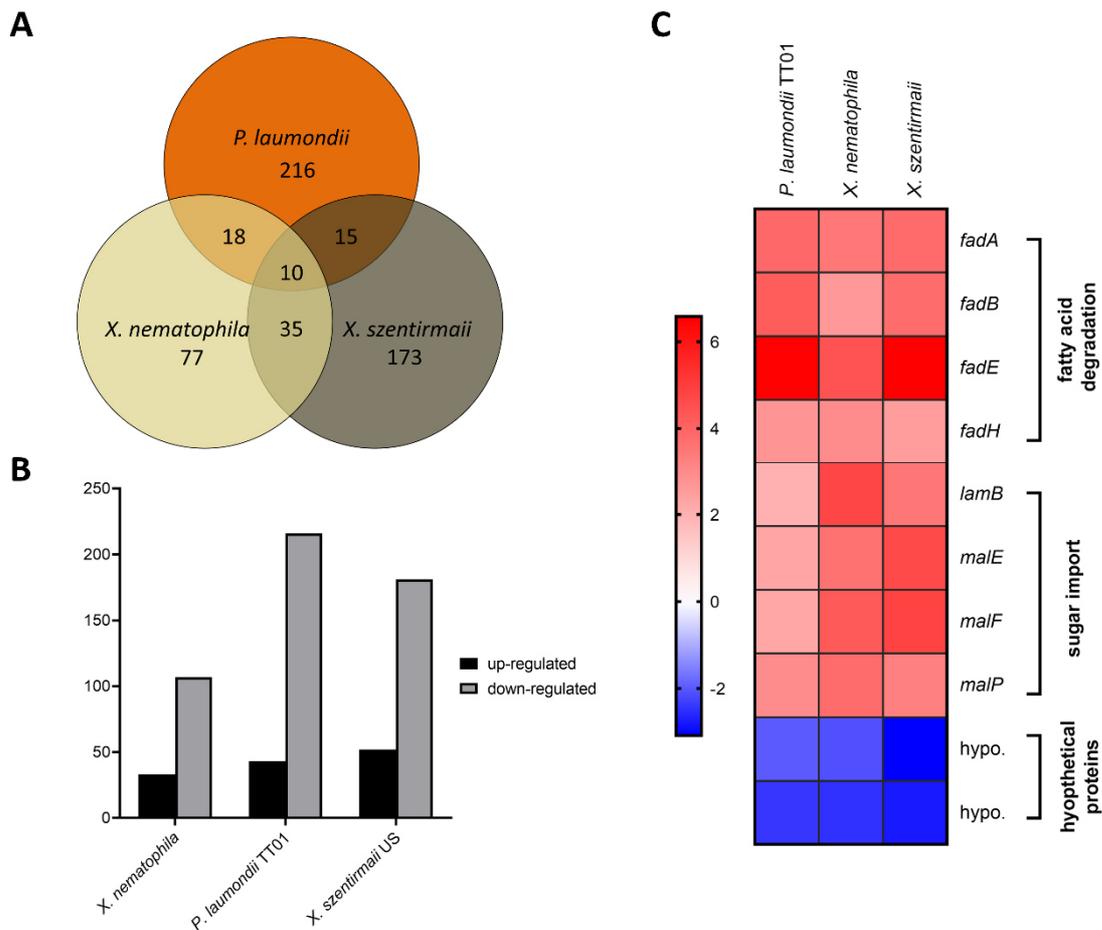


Figure 15. Transcriptomic profiles of *P. laumondii*, *X. szentirmaii* and *X. nematophila* after addition of insect homogenate to the cultures. **A.** Significantly affected CDS (FDR > 0.01; log₂ fold change > 2) and overlap across strains. **B.** Ratio of upregulated to downregulated CDS. **C.** The core response across all three strains in response to addition of insect homogenate to the culture medium.

In response to addition of insect homogenate, the transcriptional level of 259, 233 and 140 CDS were found to be significantly altered in *P. laumondii*, *X. szentirmaii* and *X. nematophila*, respectively (FDR < 0.01; log₂ fold change > 2). The majority of affected CDS were found to be down regulated and only 16 to 23% of affected genes were up-regulated (Figure 15B). With the aim to identify a general core response across the investigated strains, we took a more detailed look on the orthologous coding sequences that were affected in all three strains simultaneously (Figure 15C). The core response consisted of ten CDS, eight of which were up regulated. Based on annotations generated with a reciprocal BLAST approach, four CDS were classified as components for fatty acid degradation and four for sugar import. The remaining two affected CDS, both of which were down regulated, could not be

classified based on homology and were therefore described as hypothetical proteins.

3.2.3. The composition of *G. mellonella* homogenate and hemolymph

Changing environmental conditions, e.g. changing hosts, requires fast adaptation of the bacteria in order to retain their niche. Although a signalling molecule present in the insect host is assumed to trigger this transition, the nature of that signal molecule is unknown. To develop an idea of the components in the insect with potential signal characteristics, gas chromatography-mass spectrometry (GC-MS) analysis was performed with isolated insect hemolymph and complete insect homogenate (samples were measured by Martina Wurster, Lalk group, Greifswald, Germany). All analysed compounds were grouped in different classes: Fatty acids, amino acids, carbohydrates or other. The differences between hemolymph and whole insect homogenate are illustrated in a pie chart (Figure 16A). An additional heat map displays the components identified by GC-MS analysis (Figure 16B). Grey bars indicate that a component was not identified in the respective sample.

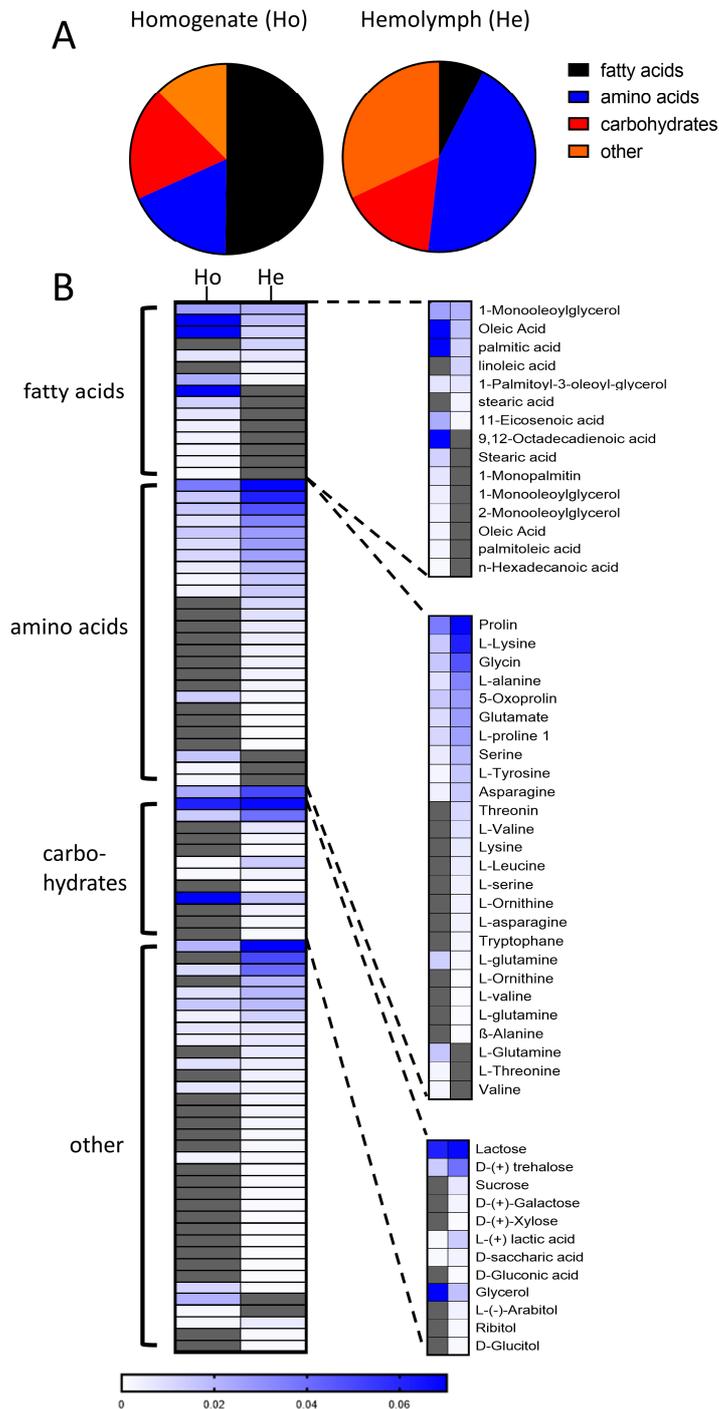


Figure 16. GC-MS analysis of insect homogenate (Ho) and insect hemolymph (He). **A.** Relative abundance of fatty acids (black), amino acids (blue), carbohydrates (red) and other components (orange) in insect homogenate and insect hemolymph. **B.** Most abundant components of insect homogenate (left column) and insect hemolymph (right column) based on GC-MS analysis. Depicted is the relative abundance based on integration of the respective peak signal. Grey rectangles indicate absence of a compound in one of the samples.

For the insect hemolymph samples, 76 compounds could be identified, whereas only 47 compounds were identified for the insect homogenate. Out of those compounds, 34 were found in both samples. Fatty acids and amino acids made up the majority of identified compounds for the insect homogenate, whereas the hemolymph mainly comprises amino acids and carbohydrates. The most abundant fatty acids for insect homogenate are oleic acid and palmitic acid, whereas only traces of fatty acids were identified for hemolymph samples. For both sample types, proline was the most abundant amino acid. Interestingly, besides trehalose, high relative amounts of lactose and glycerol were also detected in both samples. Furthermore, putrescine was detected in very high amounts in the insect homogenate.

3.2.4. Titration of SM production by addition of abundant insect components

Two of the most abundant compounds identified by GC-MS, trehalose and putrescine, were used as media supplements in increasing concentrations to determine the dose dependent influence of those compounds on SM production titres. Cultures of *P. laumondii* were supplemented with putrescine (1-100 mM) and grown for 72 h in triplicates. Trehalose was added to cultures of *X. szentirmaii* and *X. nematophila* in increasing concentrations from 1-50 mM. After 72 h of growth, the samples were subjected to HPLC-MS analysis. Relative SM production profiles were determined using TargetAnalysis (Figure 17A-C).

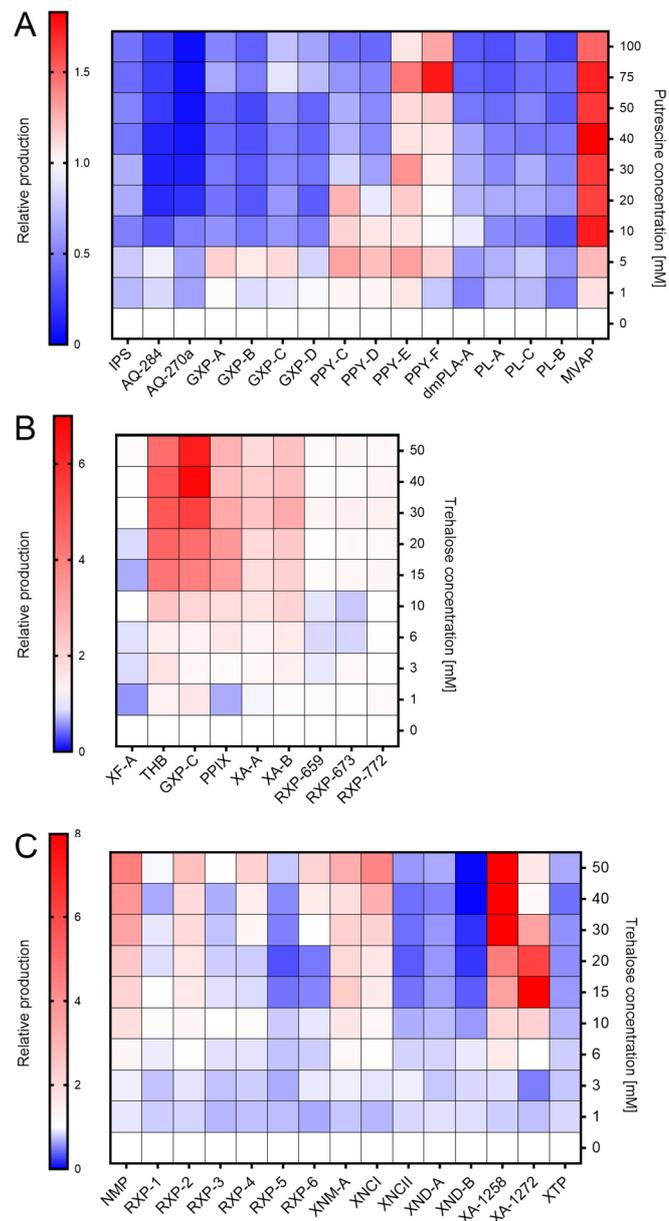


Figure 17. SM profiles of *P. laumondii*, *X. szentirmaii* and *X. nematophila* after supplementing medium with abundant insect components and 72 h of growth in an orbital shaker at 30°C. *P. laumondii* cultures were supplemented with 0-100 mM putrescine. Trehalose (0-50 mM) was added to cultures of *X. szentirmaii* and *X. nematophila*. **A.** Depicted are the relative amounts of isopropylstilbene (IPS), anthraquinone (AQ), GameXPeptide (GXP), photopyrone (PPY), desmethylphurealipid A (dmPLA-A), phurealipid (PL) and mevalagmapeptide (MVAP) produced by *P. laumondii*. **B.** Relative amounts of xenofuranone A (XF-A), tetrahydrobutyrate (THB), GameXPeptide C (GXP-C), protoporphyrin IX (PPIX), xenoamicin (XA), and rhabdopeptide (RXP) produced by *X. szentirmaii*. **C.** Relative amounts of nematophin (NMP), rhabdopeptide (RXP), xenematide A (XNM-A), xenocoumacin (XNC), xenortid (XND), xenoamicin (XA) and xenotetrapeptide produced by *X. nematophila*. Relative SM production of the cultures without addition of insect components (=0 mM) was set to 1. All data were generated from biological triplicates of liquid cultures after 72 h of growth at 30°C.

Interestingly, in many cases, raising concentrations of either putrescine or trehalose in the culture medium directly correlated with the production of certain SMs in a dose dependent manner. For *P. laumondii*, increased putrescine concentration in the culture medium led to strongly reduced SM production titres for most analysed compounds, e.g. for AQs, GXPs, PLs and IPS. Increasing concentrations were observed for relative MVAP amounts. The putrescine concentration was determined to be 55 mM in the insect hemolymph of *G. mellonella*¹⁴⁸. Upon addition of 50 mM putrescine to cultures of *P. laumondii*, GXP and MVAP titre alterations are comparable to samples where complete insect homogenate was added to the cultures (see Figure 14).

For *X. szentirmaii*, relative XF-A and RXP production titres remained largely unchanged, whereas the production titres of all other SMs were elevated with increasing trehalose concentrations. Consistent with the HPLC-MS data set after adding insect homogenate to the cultures, GPX-C, PPIX, XA-A and XA-B production titres were also increased with increasing concentrations of trehalose.

For *X. nematophila*, the effect of adding trehalose was not as broad as for the other tested strains, although clear alterations were detected. The strongest effect was observed for xenoamicin (XA-1258), with a 22-fold increase in production compared to the WT. Interestingly, XA-1272 production was also increased up to a trehalose concentration of 15 mM, but decreased at higher trehalose concentrations. Opposed to this observation, XA-1258 amounts steadily increased, even at maximum trehalose concentration. Likewise, an increase in production (up to 4.5-fold of WT levels) was also observed for nematophin (NMP), xenematide A (XNM-A) and XNCI. In contrast, XND-A and XND-B production correlated negatively with increasing trehalose concentration.

3.3. Topic C: Identification of novel genes involved in SM production by transposon mutagenesis

Transposon mutagenesis is a powerful method for near-random mutation of bacterial genomes and is often utilized to shed light on the implication of one or multiple genes in different aspects of a bacterium's biology. This chapter displays the most obvious phenotypic alterations (of 60,000 transposon insertion mutants) observed after conducting transposon mutagenesis in *P. laumondii*. For subsequent analysis, this chapter focuses on one isolated mutant with a transposon insertion in *dam1*. This gene encodes for an adenine-specific DNA-methyltransferase, which is responsible for the methylation of GATC motifs in *E. coli*¹⁴⁹. A combination of HPLC-MS-analysis, RNA sequencing and Single-Molecule Real-Time sequencing (SMRT) sequencing was used to characterize the influence of a deletion on SM production, the transcriptomic profile and the methylome of *P. laumondii*.

3.3.1. Transposon mutagenesis

The transposon mutagenesis described in Chapter 3.1.3 resulted in a variety of distinct phenotypes. In order to examine a potential influence of the transposon mutagenesis on secondary metabolism, the SM profiles of the most prominent phenotypes were investigated (Figure 18).

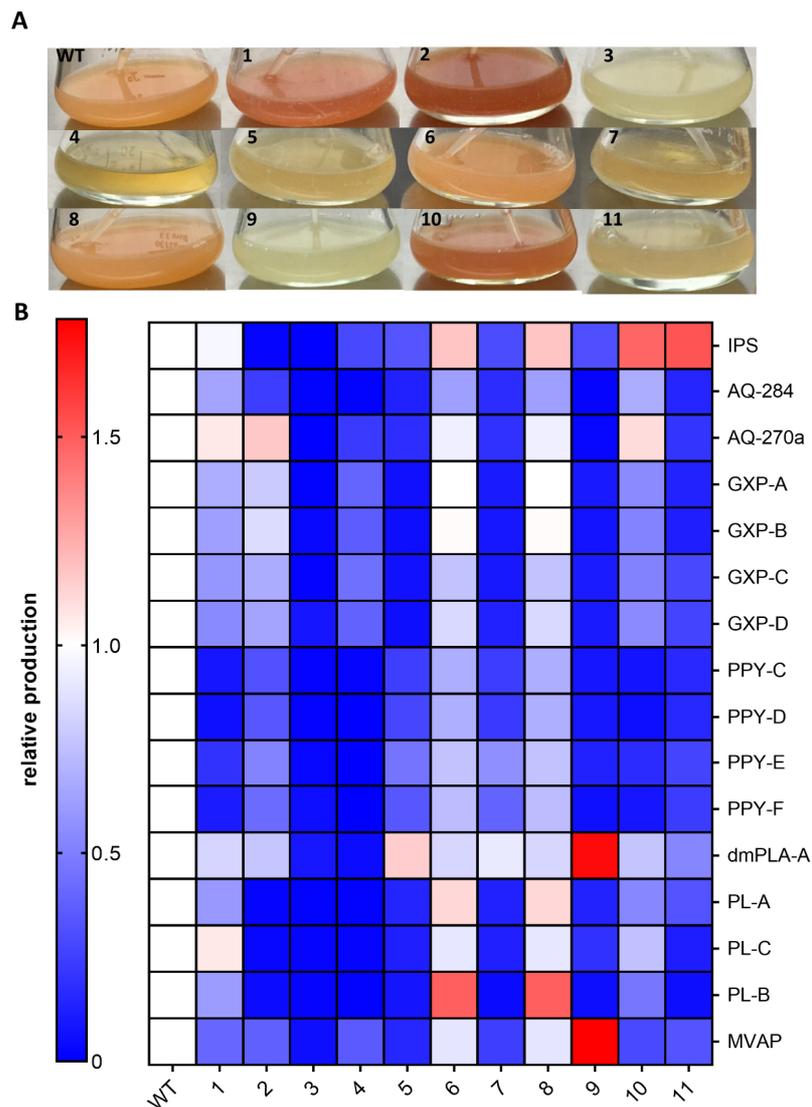


Figure 18. Phenotype of transposon insertion mutants of *P. laumondii*. **A.** Differences in pigmentation of transposon insertion mutant liquid cultures compared to WT. Depicted are eleven transposon insertion mutants and a WT culture after 3 d of cultivation at 30°C with shaking. **B.** SM-profiles of the transposon insertion mutants. Relative amounts of isopropylstilbene (IPS), anthraquinone (AQ), GameXPepptide (GXP), photopyrone (PPY), desmethyl-phurealipid A (dmPLA-A), phurealipid (PL) and mevalagmapeptide (MVAP) produced by *P. laumondii* were quantified from duplicates using TargetAnalysis (Bruker) and compared to the WT of *P. laumondii* after 72 h cultivation at 30°C with shaking. Adapted from Neubacher et al., under revision (see Chapter 6, Supplementary Figure S3).

Many of the analysed mutant strains (hereafter referred to as TN-mutants) showed severely reduced SM production titres in comparison to the WT strain. In most cases, multiple SM classes were affected by the transposon insertion. On rare occasions, the transposon insertion led to an increase in production of certain SMs. For example, dmPLA-A and MVAP levels were elevated in mutant strain 9 and IPS titres were slightly raised in the TN-mutant strains 10 and 11. Interestingly, the remaining SMs were negatively affected in those strains. As the growth appeared to be mildly to severely affected by the transposon insertion (Table 10), it remains uncertain how the growth defects correlate with SM production.

Table 10. OD₆₀₀ of *P. laumondii* WT and TN-mutants after 72 h of cultivation.

Strain	WT	1	2	3	4	5	6	7	8	9	10	11
OD ₆₀₀	14.5	9.8	8.9	7.6	1.7	3.9	12.5	3.5	14.8	5.4	9.2	4.8

To gain insights into the genotypes associated to the observed phenotypes, the genomes of TN- mutants 1-11 were sequenced (sequencing performed by Sacha J. Pidot, University of Melbourne, Australia). The identified transposon insertion sites in the genome as well as the affected coding sequences are summarized in the following table (Table 11).

Table 11. Identification of transposon insertion site, including position of transposon insertion, affected genes and their annotation.

Strain	TN insertion site	Locus tag	Annotation
1	82287	PLU_RS00430	adenine-specific DNA-methyltransferase
2	2080933	PLU_RS08760	TetR/AcrR family transcriptional regulator
3	4692989	PLU_RS25655	ArcZ
4	1721292	PLU_RS07195	dihydrolipoyllysine-residue succinyltransferase
5	1748702	PLU_RS07320	hypothetical protein
6	3733339	PLU_RS15790	tRNA pseudouridine(38-40) synthase
7	1745650	PLU_RS07305	colicin transporter
8	5144552	PLU_RS21740	unknown
9	5360182	PLU_RS22705	oligoribonuclease
10	82608	PLU_RS00430	adenine-specific DNA-methyltransferase
11	225040	PLU_RS01055	phosphate ABC transporter ATP-binding protein

For further analysis, we decided to focus on strains that showed only moderate growth defects while at the same time producing reduced SM titres. Strain 3 has been thoroughly described in chapter 3.1. For strains 1 and 10 the transposon insertion was identified in the same gene at different positions and in the reverse orientation. In order to confirm the observed phenotype, the adenine-specific DNA-methyltransferase (PLU_RS0430) was deleted as a first step. Additionally, a knock-in mutant was created by inserting the deleted gene at the original position to complement the phenotype and the mutants were examined for alterations in their SM profiles.

3.3.2. SM profile of *dam1* deletion mutant in *P. laumondii*

The SM production was determined over the course of three consecutive days. Clear alterations were observed in the relative production of many SMs between the deletion mutant and the WT/complementation mutant (Figure 19).

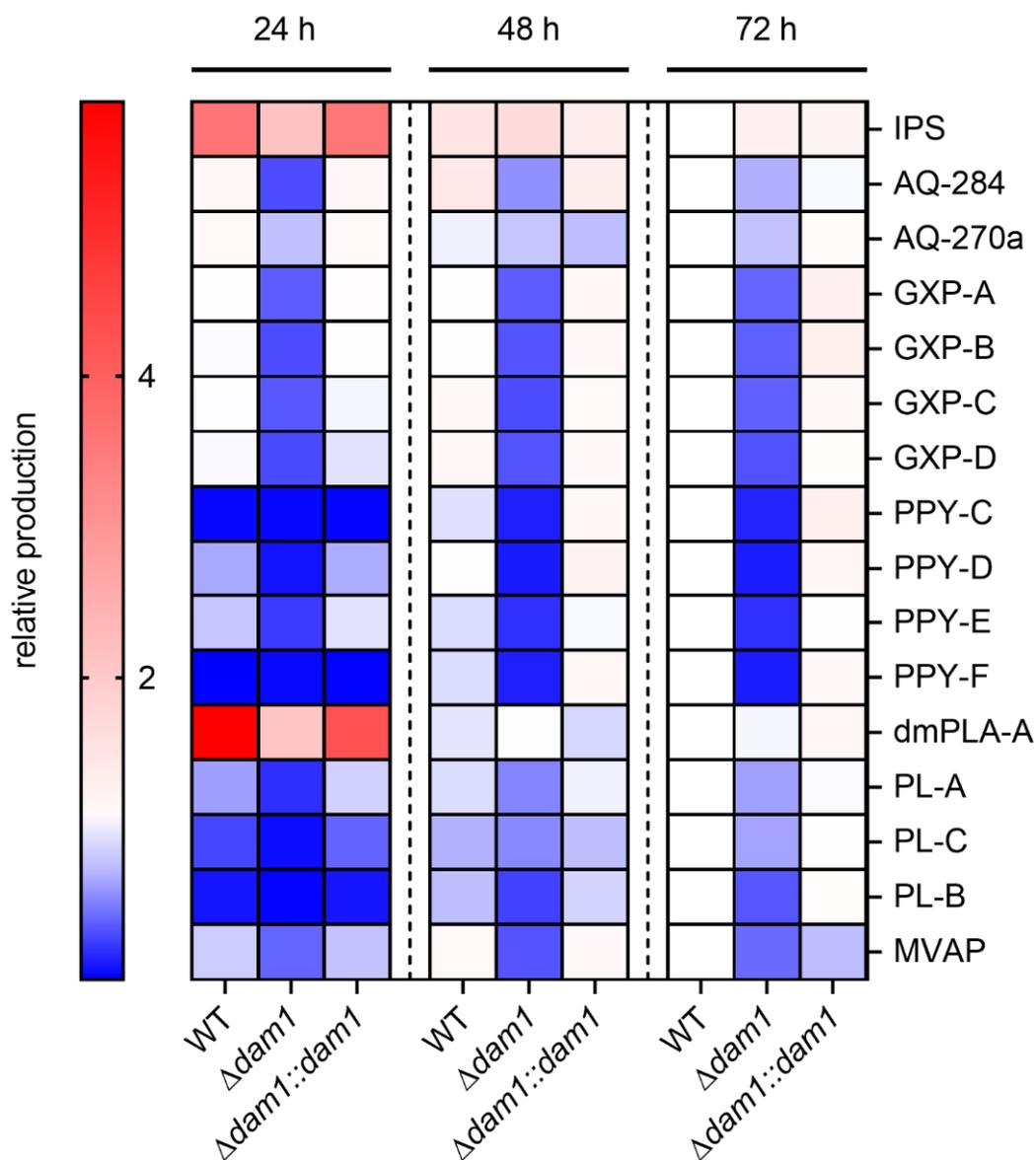


Figure 19. SM profiling of *P. laumondii*. Depicted are the relative amounts of isopropylstilbene (IPS), anthraquinone (AQ), GameXPepptide (GXP), photopyrone (PPY), desmethyl-phurealipid A (dmPLA-A), phurealipid (PL) and mevalagmapeptide (MVAP) produced by *P. laumondii* WT, $\Delta dam1$ and $\Delta dam1::dam1$ after 24, 48 and 72 h of cultivation. The production titre of the WT after 72 h of growth was set to 1 (white) and all other values were normalized to the WT production titres on day 3. A relative reduction of a compound is shown in blue and a relative increase in production is shown in red. The data is based on biological triplicates.

Throughout the data set, production titres of SMs in the WT and the knock-in complementation mutant were very similar. Interestingly, maximum relative production of certain SMs can be seen at different time points of the cultivation. For example, the highest relative amounts of IPS and dmPLA-A were detected after 24 h of growth and decreased after prolonged cultivation. Conversely, the highest PPY-C, PPY-F and phurealipid production was observed after 72 h of growth. For the $\Delta dam1$ mutant, considerable reduction in GXP, PPY, PL and MVAP production was observed for all time points, as already observed in the transposon insertion mutants (Figure 18).

3.3.3. The deletion of the adenine-specific DNA-methyltransferase influences the growth behaviour of *P. laumondii*

Consistent with previous observations, the deletion of *dam1* appeared to affect the growth behaviour of the strain. After 1 d of cultivation, the deletion mutant appeared as a pale yellow colour compared to the intensive orange colour of the WT. After 3 d of cultivation however, the culture of the deletion mutant showed a strong red pigmentation compared to the typical orange to red colour of the WT (Figure 20A).

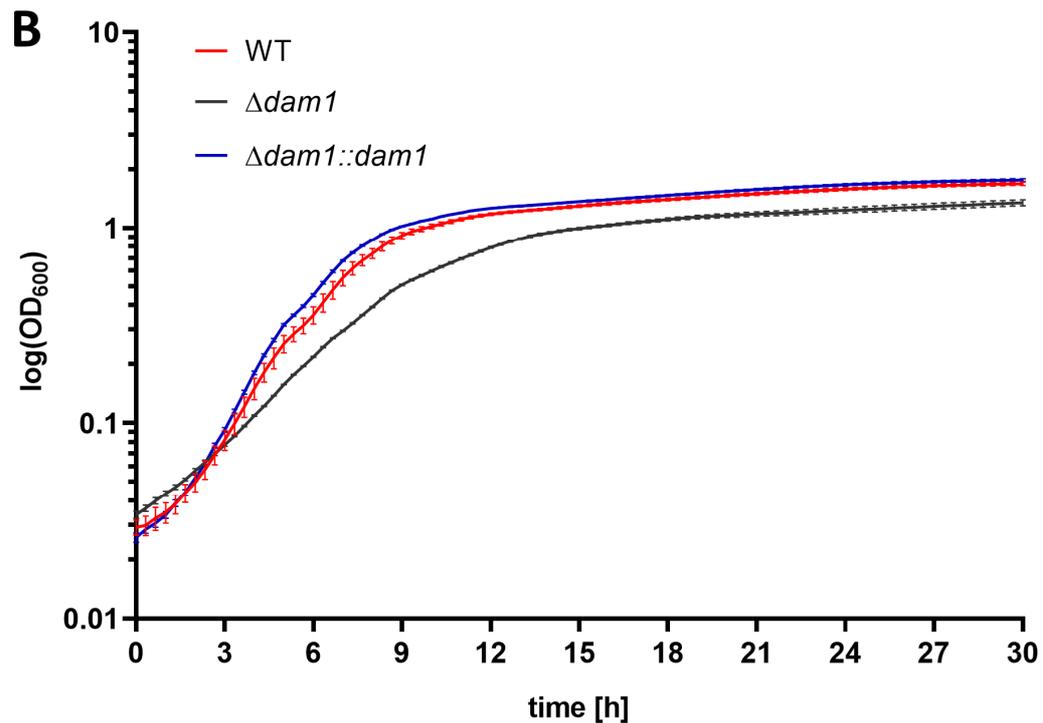
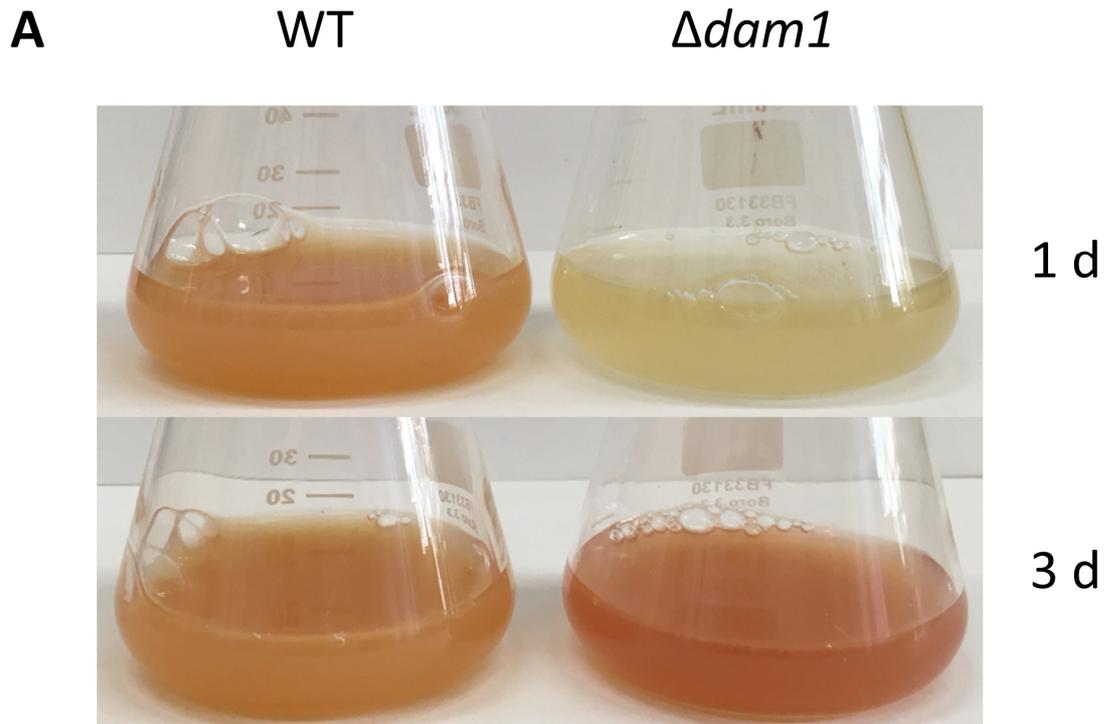


Figure 20. Phenotypic differences of the $\Delta dam1$ mutant compared to the WT of *P. laumondii*. **A.** Pigmentation of the $\Delta dam1$ mutant compared to the WT after 1d and 3d of cultivation. **B.** Growth curve of *P. laumondii* WT (red), $\Delta dam1$ (grey) and $\Delta dam1::dam1$ (blue). The growth curve was measured in triplicates over the course of 30 h in 20 min intervals using a Tecan reader. Error bars indicate the standard deviation of the triplicates.

The growth behaviour was examined by measuring a growth curve. The $\Delta dam1$ mutant grew slower and reached a lower final OD₆₀₀ than the WT and complementation mutant (1.35 compared to ~1.7; Figure 20B). Noticeably, the deletion mutant entered early stationary phase after around 10 h of cultivation while both WT and complementation mutant reached early stationary phase after ~7 h. Although minor differences can be observed between the WT and the complementation mutant, the growth defect appeared to be successfully complemented by creating the *dam1* knock-in.

3.3.4. Transcriptomic profiling of *P. laumondii* $\Delta dam1$

Transcriptomic profiling was performed to determine significant alterations in the transcriptional output of the $\Delta dam1$ mutant compared to the WT in duplicates (trimming, counting and mapping of raw reads performed by Nicholas J. Tobias, Bode group, Frankfurt). Further samples of the knock-in complementation were also analysed. The transcription level of 353 CDS was significantly (FDR<0.01; log₂-fold change >2) affected upon deletion of *dam1*. Surprisingly, the knock-in mutant failed to restore transcript levels of 152 CDS back to WT level (log-fold change in the knock-in mutant >1 or <-1, respectively), although growth behaviour and SM profiles were successfully restored (Figure 19, Figure 20). Based on their annotations, the affected CDS were grouped into different categories (Table 12).

Table 12. Significantly affected CDS in *P. laumondii*Δ*dam1* compared to the WT. The affected CDS have been grouped in different categories based on their annotation.

Category	Significantly affected CDS	Upregulated	Downregulated
Cell processes	53	37	16
Cell wall	18	10	8
Unknown	9	8	1
Regulators	4	4	0
tRNAs	11	0	11
transposases	7	7	0
Hypothetical proteins	142	131	11
Motility related	43	39	4
Other	65	53	12

For almost every category, clear tendencies were observed. For the categories cell processes, unknown, regulators, transposases, hypothetical proteins, motility related and other, transcript levels of most CDS were elevated. All CDS related to tRNAs were found to be downregulated.

3.3.5. The *dam1* methylome of *P. laumondii*

In a next step, *P. laumondii* WT, Δ*dam1* and Δ*dam1*::*dam1* were subjected to SMRT sequencing using the Pacbio platform in order to determine the methylation patterns of the respective mutant (sequencing performed by Sacha J. Pidot, University of Melbourne, Australia). The methylation motifs GATC, TGGCCA, AGGCCT and CTCGAG were predicted using Motif maker (v 0.3). The following table summarizes the abundance of each motif as well as the percentage of methylated motifs in all three strains (Table 13).

Table 13. Identified methylation motifs including their abundance in the genome, as well as number and percentage of methylated motifs in *P. laumondii* WT, $\Delta dam1$ and $\Delta dam1::dam1$. The methylated nucleotide within a motif is represented in bold.

Motif	n(genome)	n(WT)	[%]	n($\Delta dam1$)	[%]	n($\Delta dam1::dam1$)	[%]
GATC	37500	35486	94.6	35364	94.3	35459	94.6
TGGCCA	1256	1153	91.8	1152	91.7	1155	92.0
AGGCCT	184	175	95.1	175	95.1	175	95.1
CTCGAG	28	24	85.7	24	85.7	24	85.7

The most abundant methylation motif in the genome of *P. laumondii* is GATC. In the WT, 94.6% of GATC motifs were methylated. In the deletion and complementation mutants, 94.3% and 94.6% of all GATC motifs were methylated, respectively. Only minor differences in the methylation of TGGCCA, AGGCCT and CTGAG motifs were observed when comparing all strains with a percentage of approximately 92%, 95% and 86% of the total amount of motifs that were found to be methylated.

4. Discussion and perspective

4.1. Topic A: Implications of ArcZ in regulation of SM production

Previous work on *Photorhabdus* revealed that deletion of *hfq* resulted in a dramatically reduced ability to produce SMs and severe perturbations of gene networks, which included numerous regulators¹⁰⁴. Moreover, Δhfq mutants of *P. laumondii* were unable to support the mutualistic relationship to their nematode hosts. Hfq is widely spread throughout the bacterial kingdom and several pleiotropic phenotypes have been attributed to the RNA chaperone^{103,145,150–152}. Hfq achieves its regulatory roles by stabilizing transcripts or sRNAs, mediating base-pairing of sRNAs and their targets, modulating mRNA translation rates, as well as accelerating or preventing degradation of mRNAs and sRNAs¹⁵³. However, the molecular basis of Hfq-based regulation of SM production, as well as the implication of sRNAs in this process, remained unknown. In the first chapter (3.1) of this work, we demonstrated that SM biosynthesis hinges upon the action of Hfq and ArcZ to inhibit production of HexA.

HexA is a transcriptional repressor that controls SM production in *Photorhabdus*. In the WT of *P. laumondii*, transcription of *hexA* is negatively affected by regulatory interference through Hfq and ArcZ (Figure 4). Currently, it is unclear how exactly HexA regulates its targets, which results in the repression of SM production. Unravelling the next layer of this regulatory network requires experimental data to map the global binding sites of HexA in the genome. One possibility to analyse those DNA-protein interactions is chromatin immunoprecipitation sequencing (CHIP-Seq). Analysis of the HexA binding sites would provide a deeper understanding of the implications of HexA in SM production, as it would reveal the next layer of regulation in this complex regulatory network.

4.1.1. The ArcZ regulon

Consistent with literature¹⁵⁴, ArcZ exists in a primary full length form and a processed form in *P. laumondii* (and *X. szentirmaii*, Neubacher et al., under revision, Chapter 6, Figure 3A & Supplementary Figure S2). Just like the deletion of *hfq*,

deletion of *arcZ* also resulted in significant decreases in SM production in both *Photorhabdus* and *Xenorhabdus* (Figure 6, Figure 9). ArcZ is a *trans*-acting sRNA that has been extensively studied in other bacteria such as *E. coli* and *Salmonella*^{147,155}. In *E. coli*, ArcZ has been found to increase levels of σ^S , an alternative σ factor that is produced in the stationary growth phase and under stress conditions¹⁵⁶. ArcA represses ArcZ under anaerobic conditions. The regulatory sRNA can respond to a range of environmental conditions by fine-tuning σ^S levels. In *Salmonella*, ArcZ acts as a post-transcriptional regulator that represses genes for serine uptake (*sdaCB*), oxidative stress (*tpx*) and a methyl-accepting chemotaxis protein (STM3216)¹⁴⁷. Although ArcZ and its genomic organisation are conserved among enteric bacteria, the targets and magnitude of its regulon appear to be very different in the entomopathogenic bacteria *Photorhabdus* and *Xenorhabdus*. While a deletion of ArcZ in *Salmonella* significantly affects the expression of five genes, deletion in these genera affects up to ~15% of the transcriptional output. Strikingly, the deletion of *arcZ* was even more dramatic than the deletion of *hfq* and significantly (FDR<0.01; log2-fold change >2) affected the transcriptional output of 735 CDS in *P. laumondii* Δ *arcZ* compared to 520 CDS in *P. laumondii* Δ *hfq*. In *X. szentirmaii*, the effect of deleting *arcZ* was not as broad and affected the mRNA levels of 191 CDS. Despite a similar overall trend for the affected CDS in *P. laumondii*, noticeable differences were observed between the Δ *arcZ* and Δ *hfq* mutants. When comparing the data sets, only 239 CDS were significantly altered in both strains and therefore likely represent functional overlaps. This leaves 281 CDS that are only significantly affected upon deletion of *hfq*. Possibly, the regulation of those genes is controlled by sRNAs other than ArcZ, guided by Hfq. Out of 735 CDS, 419 CDS are only significantly affected in the Δ *arcZ* mutant of *P. laumondii*.

One possible hypothesis to explain the observed differences is that in absence of Hfq, ArcZ can still, theoretically, interact with targets and exert its regulatory functions, albeit at lower efficiency. Conversely, in the absence of ArcZ, Hfq lacks the complementary RNA required to guide to the appropriate target sequences. Recent work on another sRNA, DsrA, supports this hypothesis. Kim and colleagues demonstrated that, regardless of Hfq, physiological concentrations of DsrA enhance translation rate and stability of the *rpoS* mRNA in *E. coli*. However, in the Δ *hfq*

mutant, DsrA degradation was greatly accelerated which ultimately led to decreased *rpoS* mRNA stability. This suggests that translational activation of the *rpoS* mRNA through DsrA is independent of Hfq. However, further experiments are required to prove this hypothesis in *Photorhabdus* and *Xenorhabdus*.

4.1.2. ArcZ and Hfq - shared and exclusive targets?

The biosynthesis of IPS is a good example to demonstrate how Hfq and ArcZ act, together or alone, to repress key enzymes required for the biosynthesis of SM. The biosynthesis of IPS starts with the phenylalanine-ammonium lyase, *stlA*, which converts phenylalanine (PAL) into cinnamic acid, a precursor of IPS⁶². It has been shown previously that at least three different regulators, TyrR, Lrp and RpoS, control *stlA* expression¹⁵⁷. Nutrient availability appears to be the determining factor for *stlA* expression modulation. Expression levels of TyrR were reduced in the *hfq* and *arcZ* deletion mutants, both of which only produce traces of IPS. This functional overlap is also mirrored in a strong downregulation of *stlA* in both strains.

The expression level of *rpoS*, however, was only reduced in the *arcZ* deletion mutant and slightly increased in the *hfq* deletion mutant. This finding supports previous studies that determined ArcZ as a positive regulator of *rpoS* and shows that absence of one partner in this network can result in a different regulatory outcome^{99,158}. RpoS is a central regulator with functions assigned to virulence, stress adaptation, biofilm development, flagella biosynthesis and others¹⁵⁹. As RpoS is involved in so many different regulation pathways and seems to be an ArcZ specific target, it is not very surprising that an *arcZ* deletion affects ~200 genes more than a deletion of *hfq*.

In order to get a better understanding of the ArcZ regulon, the CDS that were exclusively affected in the $\Delta arcZ$ mutant were grouped into different categories, based on their known or proposed functions. The transcript levels of 29 regulators were modulated upon deletion of *arcZ*, 19 of which belong to the LuxR type transcriptional regulators. Among those, 14 CDS are clustered in the genome of *P. laumondii*. *Photorhabdus* strains contain an exceptional amount of LuxR type regulators with up to 40 different homologues in one strain¹⁶⁰. Bacterial communication circuits via quorum sensing (QS) make use of small diffusible

molecules, e.g. acyl-homoserine lactones (AHLs), which are synthesized by LuxI-like autoinducers. A LuxR-type receptor senses those signal molecules and controls expression of specific genes after detection, usually in a concentration dependent manner¹³⁰. In *Photorhabdus* strains, however, this counterpart is often missing. Due to their abundance, those LuxR solos are assumed to be involved in cell-cell and/or inter-kingdom communication¹⁶¹. Therefore, a reduced transcription level of LuxR solos, as observed for the *arcZ* deletion strain of *P. laumondii*, may affect the bacteria's fitness. Potentially, this could extensively impair ecologically relevant circuits such as biofilm formation, motility and antibiotic production.

The genome of *X. szentirmaii* contains fewer LuxR homologs, suggesting that those bacteria might use alternative mechanisms to control these processes. On the same note, this might also explain why the overall effect of deleting *arcZ* in *X. szentirmaii* is not as broad as observed for *P. laumondii*.

In the *ArcZ* deletion of *P. laumondii*, the expression of 29 different ribosomal proteins was significantly upregulated. It has recently been shown that Hfq is not only capable of binding sRNAs and mRNAs, but also ribosomal RNAs, which potentially hints towards an important role of *ArcZ* in ribosome biogenesis^{162,163}. Our data suggests that *ArcZ* might be involved in repressing ribosome biogenesis under tested conditions in late exponential phase which might be important to guarantee the optimal amount of ribosomes in the cell and to avoid unnecessary energy loss, as the ribosome biogenesis consumes a major proportion of the cellular energy^{164,165}.

4.1.3. *ArcZ* controls nematode development in *P. laumondii*

Consistent with the previously published Δhfq mutant¹⁰⁴, the $\Delta arcZ$ mutant in *P. laumondii*, too, was incapable of supporting nematode development. Interestingly, *X. szentirmaii* $\Delta arcZ$ was still able to support nematode development (Figure 12). One possible explanation might be the observed overproduction of protoporphyrin IX (PPIX) in this strain (Figure 9). PPIX is a precursor of heme, which is an important cofactor for many key biological processes. This includes protein translation¹⁶⁶, maintaining protein stability¹⁶⁷, oxidative metabolism¹⁶⁸ and other

processes. *Caenorhabditis elegans* and other nematodes cannot synthesize PPIX *de novo*¹⁶⁹. PPIX positively affects growth, reproduction and development of the nematodes¹⁷⁰. Therefore, the nematodes rely on external sources for PPIX (such as symbiotic bacteria). Although *P. laumondii* also produces PPIX, *Heterorhabditis* development was attenuated with both $\Delta arcZ$ and Δhfq strains. Isopropylstilbene has been shown to be essential for the development of *Heterorhabditis bacteriophora*⁶², whereas no analogous compound is known yet for *Steinernema* nematodes. Potentially, this is indicative of the nematode specific requirements for reproduction.

4.1.4. The molecular basis of ArcZ mediated regulation

Taken together, we demonstrated that ArcZ binds to the 5'-UTR of *hexA*, guided by Hfq, which results in an inhibition of *hexA* transcription (Figure 21A). Under laboratory conditions, inhibition of *hexA* enables SM biosynthesis and successful symbiosis with nematodes. In the absence of either Hfq or ArcZ, *hexA* is no longer repressed (Figure 21B and C). Production of HexA in turn represses SM production. By exchanging a predicted ArcZ binding motif in the 5'-UTR of *hexA* to a *PacI* restriction site, we identified the interaction site of ArcZ (Figure 21D). Compensatory base mutation studies have been used to validate the mRNA-sRNA interaction and confirm the interaction region (Neubacher et al., under revision, see Chapter 6, Figure 3B, experiment performed by Michaela Huber, Papenfort group, Jena, Germany).

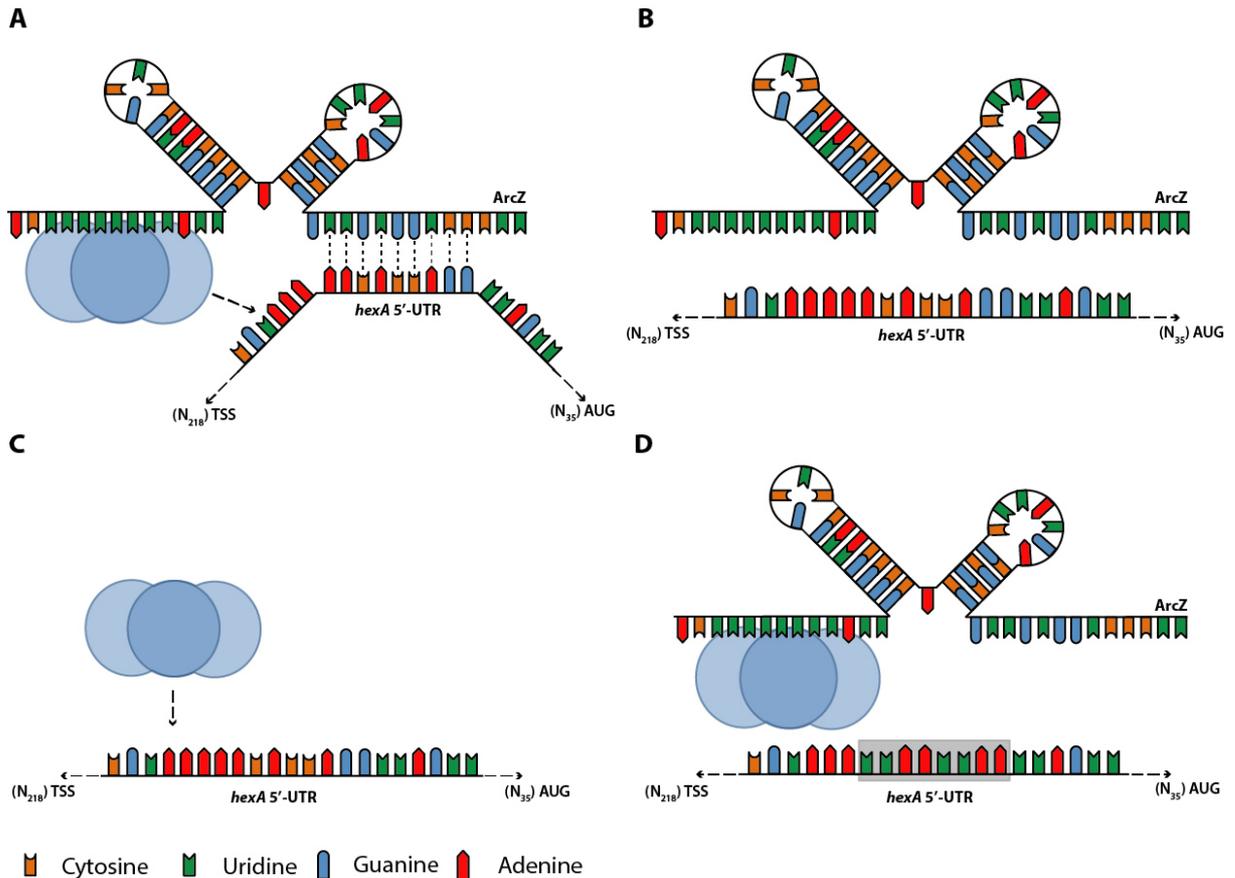


Figure 21. Schematic of Hfq-mediated binding of ArcZ to the 5'-UTR of *hexA*. **A.** The processed form of ArcZ is bound by the proximal face of Hfq. ArcZ is used as a guide to allow sRNA-mRNA duplex formation (dotted lines) overall resulting in very low HexA levels which facilitates SM production. **B.** In the Δhfq strain both interaction partners are still present, but the absence of Hfq as a mediator leads to reduced duplex formation resulting in high HexA levels which inhibit SM production. **C.** Post-transcriptional regulation of *hexA* can no longer occur in the absence of ArcZ, which also leads to high HexA levels and strongly reduced SM production. **D.** Alteration of the proposed ArcZ binding motif to a *PacI* restriction site (TTAATTAA, highlighted in grey) in the 5'-UTR of *hexA* disrupts native duplex formation. ArcZ can no longer inhibit HexA production, which in turn leads to inhibition of SM production.

It remains to be determined if ArcZ regulates *hexA* on a transcriptional or translational level. To test a possible model of translational inhibition, an additional *in vitro* protein synthesis experiment could be performed. The assay would contain a reconstituted 70S ribosome and *in vitro* transcribed ArcZ and *hexA* mRNA. In this assay, synthesis of HexA could be visualized through, for example, a fluorescence label.

4.1.5. ArcZ as a tool for SM production?

As shown in chapter 3.1, deletion of *arcZ* provides a clear chemical background devoid of SMs (Figure 13). Understanding the regulatory mechanisms in *Photorhabdus* and *Xenorhabdus* allows for exploitation of the regulatory cascade for specific activation of SM gene clusters. A recent study with the Δhfq strain revealed that this exploitation method can be successfully applied to trigger almost exclusive production of the desired compounds in *Photorhabdus* and *Xenorhabdus*, but also in *Pseudomonas*¹¹⁹. By applying the same strategy in the $\Delta arcZ$ of *X. szentirmaii*, we demonstrated an alternative route to activation, without the additional sRNA perturbations associated with the deletion of the RNA chaperone Hfq. While further examples are needed to underpin the suitability of $\Delta arcZ$ strains for exclusive SM production, the herein presented results offer a novel powerful tool for the (over-) production, isolation and identification of known and unknown natural products.

Interestingly, comparisons can be drawn to other SM-producing bacteria. HexA serves a similar function in the plant pathogenic bacteria *Erwinia*, where it acts as a negative regulator of SM production in this genus¹⁷¹. Furthermore, both ArcZ and Hfq have been reported to be involved in virulence in these bacteria. Similar parallels can be seen for *Pseudomonas*¹⁷² and *Serratia*^{173–175}, two other SM producers. Further investigations are required to ascertain whether these apparent similarities represent identical mechanisms. However, similar regulatory systems in other SM-producing bacteria may yield fresh avenues for the investigation of SM biosynthesis in these taxa.

4.1.6. The expanded regulatory network for SM production – A perspective

With *hexA* identified as one target of ArcZ, the other ArcZ targets remain to be examined. One possible method to get a deeper insight into the regulon of ArcZ is a technique that was developed to map RNA-RNA interactions, referred to as UV cross-linking, ligation and sequencing of hybrids (CLASH)¹⁷⁶. This method was first used to provide an unbiased view of human miRNA targets. Recent advances made it possible to use this technique to uncover targets of Hfq-dependent sRNA targets¹⁷⁷. During this experiment, RNA ends of sRNA-target RNA bound by Hfq that

are close in proximity are ligated together. A previously introduced tagged version of Hfq is used to exclusively purify RNA bound to Hfq. In a next step, the protein is degraded and the resulting chimeric sequences are identified by high-throughput sequencing. By using this method, it is possible to examine all Hfq-dependent mRNAs and sRNAs and to elucidate their respective targets.

In the last ten years, substantial progress has been made towards developing sRNAs as avenues for controlling gene expression. Rational design of synthetic sRNAs can be applied for metabolic engineering. Man and colleagues established initial design principles for creating novel sRNAs that contain a Hfq-binding site and regulatory regions that target the enhanced green fluorescent protein and a native *E. coli* gene (*uidA*)¹⁷⁸. They found reduction in target gene expression up to 71%. This method can be advantageous for the functional investigation of especially essential bacterial genes, because the expression system of the synthetic sRNA can be finely tuned. Gene silencing through synthetic sRNAs has also been used successfully to engineer microbial strains that can produce high yields of desired metabolites in order to raise their production titres. As an example, repression of *murE* by a synthetic sRNA led to a 55% increase in cadaverine production in *E. coli*¹⁷⁹. Potentially, this method can also be applied to *Photorhabdus* and *Xenorhabdus* strains and might represent a powerful method for functional investigation of genes or modulation of SM production titres. However, the applicability of synthetic sRNAs in those taxa has to be addressed in future experiments.

4.2. Topic B: Sensing an insect host – a link to SM production

Production of SMs has been shown to be crucial to maintain the symbiosis of *Xenorhabdus* and *Photorhabdus* with their respective hosts, and especially for insecticidal activity. L-proline, an abundant component of insect hemolymph, links insect host recognition to bacterial metabolic regulation¹⁸⁰. This adjustment is required for the bacteria of these taxa for full virulence and insect immune-system evasive capabilities. As of now, the overall adjustment to create this regulatory response to the fluctuating environmental conditions upon entry of the insect larva is not well defined. In this topic, we aimed to define this regulatory response.

4.2.1. “*In vivo* simulation” alters SM profiles in *Photorhabdus* and *Xenorhabdus* strains

The focus of chapter 3.2 was to provide deeper insight in the modulations that occur on a metabolic and transcriptional level, based on an easily applicable *in vitro* assay. Homogenized insect larvae were supplemented to LB growth media in order to simulate an insect-like environment. Subsequent metabolic profiling of *X. szentirmaii*, *X. nematophila* and *P. laumondii* revealed significant alterations compared to a control (cultivated without insect homogenate, Figure 14). Many of the affected SMs have been assigned to important functions during the infection process or for maintaining the nematode symbiosis. Isopropylstilbene is assumed to be involved in repelling food competitors from the insect cadaver and serves as a cross-kingdom signal for the recovery of the IJ stage and is thus required for the development of *Heterorhabditis* nematodes^{62,63}. Phurealipids inhibit the juvenile hormone epoxide hydrolase, a key enzyme for the growth and development of insects. Inhibition of this enzyme leads to accumulation of juvenile hormone III, which in turn inhibits production of antimicrobial peptides¹²⁸. AQs are redox active compounds that are assumed to be involved in the protection against reactive oxygen species and PPYs are involved in cell-cell signalling via quorum sensing (QS)⁶¹. All SMs mentioned here were upregulated when insect homogenate was added to the culture and might hint towards adjustments of the bacteria to the changing environmental conditions.

Photorhabdus and *Xenorhabdus* share an ecological niche and have very similar life cycles. Therefore, it is conceivable that simulation of an insect environment might lead to comparable transcriptional modulations. Indeed, the transcriptome was greatly altered in *X. szentirmaii*, *X. nematophila* and *P. laumondii* (Figure 15), suggesting that the adjustment in response to the nutrient rich environment of an insect is rather extensive. Interestingly, the majority of significantly affected genes were negatively regulated. This suggests that certain metabolic pathways might not be required in the relatively nutrient rich environment of an insect larva.

GC-MS analysis showed that insect hemolymph mainly comprises carbohydrates and amino acids (GC-MS measurement performed by Martina Wurster, Lalk group, Greifswald, Germany, Figure 16), consistent with previous studies¹⁴⁸. For the insect homogenate, fatty acids represent the most abundant components, followed by amino acids and carbohydrates. As the quality of the model organism, *G. mellonella*, can vary dramatically and can therefore lead to considerable experimental deficits, this generated data could be used for future work to define an insect-like medium. Not only would such an insect medium increase reproducibility of experiments but it would also offer another possibility to look more closely into the underlying processes required for the bacterial adjustment to insect hosts. Potentially, even cryptic SM clusters might be stimulated by the insect components that are otherwise silent (repressed) under standard laboratory conditions.

4.2.2. The shared core response to an insect-like environment

When comparing the GC-MS data with the transcriptomic data, clear correlations can be observed. The two data sets harmonize well, as the core response to the simulated insect environment across all three strains shares significant upregulation of CDS involved in the import of sugars into the cell and degradation of fatty acids (Figure 16C).

The transcript levels of *fadA*, *fadB*, *fadE* and *fadH* were significantly elevated in response to insect homogenate. Those genes encode for key enzymes required for fatty acid degradation. In *E. coli*, the membrane proteins FadL and FadD import fatty acids into the cells. During β -oxidation, the initial acyl-coenzyme A (CoA) is

shortened by two carbon atoms, which yields acetyl-CoA¹⁸¹. FadE is required for the first step in the β -oxidation cycle. The enzyme converts acyl-CoA moieties to enoyl-CoA. A tetrameric complex consisting of two FadA and FadB copies performs the hydration, oxidation and finally thiolitic cleavage steps¹⁸². By coupling this process to the citric acid cycle, exogenously supplied fatty acids can serve as carbon and energy sources. FadH transforms 2,4-dienoyl-CoA derived from unsaturated fatty acids into enoyl-CoA. This step is required for the degradation of fatty acids with an unsaturation at the even-numbered carbon.

Acetyl-CoA is a precursor of Malonyl-CoA, which usually serves as a starter unit and elongation units for type II polyketide synthase systems (PKSII). PKSII systems are very rare in Gram-negative bacteria, with only a few published examples. Interestingly, three of those systems can be found in *Photorhabdus* and *Xenorhabdus*, one of which is responsible for the synthesis of AQs in *P. laumondii*^{10,60,183}. The synthesis of AQ requires seven malonate elongation units¹¹⁷. Due to an environment that is rich in fatty acids, acetyl-CoA (and in turn malonyl-CoA) oversupply might directly influence the production of AQs. However, further experimental proof is required to validate this hypothesis.

For many bacteria, glucose is the preferred carbon and energy source¹⁸⁴. Nevertheless, many bacteria can use other carbohydrates as energy or carbon sources as well. Their import is dependent on different transport systems. In *E. coli*, maltose and maltodextrins are imported through the outer membrane through a specific pore named LamB¹⁸⁵. The maltose binding protein MalE transports maltose across the periplasm. The intrinsic membrane protein MalF forms a translocation complex together with MalG and MalK, which transports the maltose into the cells. Although maltose was not identified as a component of insect hemolymph or insect homogenate using GC-MS analysis, it is known that glucose, derived from the metabolism of trehalose, induces the maltose transport system in *E. coli*¹⁸⁶. It appears that *Xenorhabdus* and *Photorhabdus* might utilize a similar system, as trehalose was identified in both insect samples in relative high amounts. Induction of an alternative pathway for the import of carbohydrates as seen for *Photorhabdus* and *Xenorhabdus* in response to insect homogenate might be advantageous for the

bacteria with regards to the overall energy supply. The significant upregulation of the maltose system across all three tested strains might hint towards an important function of the system. Particularly during the infectious phase of the bacteria, this system might be of importance, as bacteria and insect host compete for their nutrients.

4.2.3. Insect signals link host recognition to metabolic adjustment

Secondary metabolism in *Photorhabdus* and *Xenorhabdus* has been described to be directly linked to L-proline, an abundant amino acid in insect hemolymph¹⁸⁰. By adding L-proline to cultures and comparing SM production relative to cultures where insect hemolymph was added to the cultures, Crawford and colleagues showed that the production of one anthraquinone, two stilbenes and nematophin could be stimulated in both cases¹⁸⁰. In a similar manner, we added two abundant insect components, trehalose and putrescine to cultures of *Photorhabdus* and *Xenorhabdus*. We found that production rates of some of the analysed SMs directly correlated with increasing concentrations of those two compounds in the culture medium within the ecologically relevant concentration range (Figure 17). This suggests that beside L-proline, trehalose and putrescine, too, might be important for host recognition and adjustment of the bacterial metabolic status. As some of the affected SMs are assumed to be important in the context of the infection process, those findings reinforce the idea that insect components could serve as signals for the bacteria in order to switch to their pathogenic phase. Xenoamicin, for example, showed weak bioactivity against different protozoa¹⁸⁷. Production of xenoamicin might therefore be important for the defence against food competitors. Xenocoumacin I is another compound produced by *X. nematophila* that exhibits a broad spectrum antibiotic activity against bacteria and some fungi and was also found to be strongly upregulated after trehalose supplementation of the growth medium. As already described for amicoumacins¹⁵, xenocoumacins might be involved in inhibition of the bacterial protein biosynthesis¹⁸⁸. For future work, it would be interesting to analyse samples of *Xenorhabdus* and *Photorhabdus* strains using a proteomic approach after supplementation of the culture medium with insect homogenate. Potentially, this data could be used to directly link SM production to

the abundance of proteins relevant for SM synthesis. RNA sequencing and proteome analysis could further be used for *Xenorhabdus* and *Photorhabdus* strains after adding trehalose or putrescine to the cultures to determine the bacterial adjustment to a specific component of the insect.

Taken together, we showed that insect homogenate could both stimulate and inhibit production of many different SMs in *Photorhabdus* and *Xenorhabdus*. Those bacteria respond to the simulation of an insect host environment by far reaching modulations of the transcriptional output. The shared core response contains ten CDS, eight of which might be required for efficient nutrient use. This suggests that each of the bacterial strains tested here adapt individually to the insect larva and highlights that the shared core response might be of great importance in this process.

4.3. Topic C: Identification of novel genes involved in SM production by transposon mutagenesis

Regulation of SM production in *Photorhabdus* was shown to be dependent on various exogenous factors, as well as regulatory proteins. As described above, previous studies focused on the implication of regulators like Hfq, LeuO, Lrp, HexA and insect specific factors like the abundant amino acid L-proline on SM production.

Transposon mutagenesis was used to gain deeper insights into the implications of other genes, which might be directly involved in SM production. *P. laumondii* is especially suitable for this approach, as phenotypic differences can be easily screened due to the intense orange to red colour of the colonies. Many mutant strains with distinct phenotypes were isolated (Figure 18A) and influences of SM production were demonstrated (Figure 18B). As many of the transposon insertions also impaired the growth behaviour of the strains, it remains unclear whether or not the observed reduction in SM production has to be attributed to the growth defects. Two of the isolated mutants had slightly reduced final OD₆₀₀ values and showed a strong reduction in the production of certain SMs. The transposon insertions were localized in the *dam* gene (Table 11).

4.3.1. Characterization of the $\Delta dam1$ phenotype

In *E. coli*, the adenine-specific DNA-methyltransferase Dam is responsible for methylation of GATC motifs¹⁸⁹. As such, the enzyme plays a pivotal role in DNA replication, mismatch repair and gene regulation^{89,190}. Previous studies suggested that the enzyme is essential for the viability of certain bacteria including *P. laumondii*^{124,191}. However, by constructing a transposon-insertion library with *P. laumondii*, we found a transposon insertion in *dam1* to be viable in two cases (sequencing performed by Sacha J. Pidot, Melbourne, Australia). Noticeably, those mutants showed impaired growth and reduced SM titres (Figure 18B, Figure 20). Opposed to the approaches presented in previous studies, deletion of the whole *dam1* gene in *P. laumondii* yielded a viable mutant. It has been shown before that the phenotype of *P. laumondii* can differ significantly when comparing strains from different labs which might be one explanation for this outcome¹⁹². In fact, a recent

study revealed that thousands of point mutations differentiate the widely used rifampicin-resistant *Photorhabdus* strain to the original isolate¹⁹³, suggesting that different mutations might accumulate in different labs long-term.

By creating *P. laumondii* Δ *dam1*, we confirmed the influence of Dam on SM production and growth behaviour. Additionally, complementation of the SM profile and growth curve was achieved by creating the knock-in complementation mutant *P. laumondii* Δ *dam1::dam1* (Figure 19). In order to determine the genes whose expression was affected by this deletion, we conducted an RNA sequencing experiment with the WT, deletion and complementation mutant. Surprisingly, the transcriptional output of the deletion mutant was globally affected (Table 12). A considerable number of CDS related to important cell processes (53) and transfer RNAs (tRNA; 11) were affected in the deletion mutant which might in part explain the observed growth defect. As the functionality of the primary metabolism is mandatory for all organisms, it can be expected that alterations in the metabolic flux might impair important cellular processes. The concentration of aminoacyl-tRNAs in the cell determines the speed of translation¹⁹⁴. As shown for *E. coli*, deletion of genes encoding for tRNAs can cause severe growth defects¹⁹⁵.

Interestingly, multiple transposases (7) were significantly affected by the deletion of *dam1*. Transposases represent mobile genetic elements and appear to have important functions in host adaptation and bacterial genome plasticity¹⁹⁶. Transposase genes are highly variable in prokaryotes¹⁹⁷ and facilitate genomic rearrangements and gene duplications through transposition events or enabling genetic recombination. It was shown in previous studies that hemimethylated GATC sites control rates of transposition of multiple insertion sequences^{198–200}. Although there is currently no clear evidence, a potential increase in transposition events might explain why the knock-in mutant failed to restore parts of the transcriptome back to the WT level. Generally, little is known about transposases and additional experiments are required to establish their implications in the life cycle of *Photorhabdus*.

4.3.2. The Dam methylome of *P. laumondii*

SMRT sequencing was performed to identify the *dam1* methylome of *P. laumondii* (sequencing was performed by Sacha J. Pidot, Melbourne, Australia). Surprisingly, we found no striking differences in the abundance of methylated GATC motifs (Table 13). This suggests that Dam does not methylate GATC motifs in *P. laumondii*, even though the gene displays a ~71% identity and ~86% similarity with the *E. coli dam1* gene¹²⁴. However, the enzyme also does not methylate any of the other predicted motifs. The genome of *P. laumondii* contains 47 genes that are annotated as methylase or methyltransferase¹²⁰. Only eight of those are annotated as DNA methyltransferase (MTase) or DNA methylase while most of the other genes encode for putative RNA MTases. Therefore, it is likely that one of the other eight MTases is responsible for this methylation. In order to prove this theory, further experiments should aim towards deleting the individual genes encoding for MTases and subsequently comparing SMRT data sets. We further tested if deletion of *dam1* has an impact on the abundance of RNA modifications but found no considerable alterations, suggesting that the *dam1* gene does encode for an RNA MTase (data not shown).

As of now, the functions that can be assigned to the putative DNA-methyltransferase Dam in *P. laumondii* and how this can affect the production of SMs and growth remains elusive. Potentially, the enzyme methylates a different motif than the ones predicted here, but further work is required to verify this.

In recent years, the idea of epigenetic gene regulation in bacteria has been increasingly supported. Multiple epigenetics based regulatory mechanisms used by bacteria have been described to date⁸⁷. Unlike eukaryotes, bacteria make use of DNA adenine methylation as an epigenetic signal⁸⁷. Those methylations were shown to be involved in virulence of many different pathogenic bacteria including *Vibrio*, *Yersinia*, *Salmonella* and others^{190,201}. In Alphaproteobacteria, adenine methylation of GANTC motifs by the CcrM methylase was also shown to be involved in the regulation of the cell cycle^{202,203}. In Gammaproteobacteria, adenine methylation at GATC sites is further involved in DNA replication, mismatch repair and regulation of gene expression^{204,205}. In most cases, Dam induced methylation

appears to lead to transcriptional repression rather than activation. As of now, epigenetic gene regulation in *Photorhabdus* has not been investigated. While our presented results hint towards possible epigenetic gene regulation mechanisms in this genus, it was not yet possible to support this hypothesis with experimental evidence. However, this work presents feasible starting points for the future examination of a potential epigenome.

References

1. Porter, J. R. Antony van Leeuwenhoek: tercentenary of his discovery of bacteria. *Bacteriol. Rev.* **40**, 260–269 (1976).
2. Sharon, G. *et al.* Specialized metabolites from the microbiome in health and disease. *Cell. Metab.* **20**, 719–730; 10.1016/j.cmet.2014.10.016 (2014).
3. Fischbach, M. A. & Segre, J. A. Signaling in Host-Associated Microbial Communities. *Cell* **164**, 1288–1300; 10.1016/j.cell.2016.02.037 (2016).
4. Dheilly, N. M., Poulin, R. & Thomas, F. Biological warfare: Microorganisms as drivers of host-parasite interactions. *Infect. Genet. Evol.* **34**, 251–259; 10.1016/j.meegid.2015.05.027 (2015).
5. McFall-Ngai, M. *et al.* Animals in a bacterial world, a new imperative for the life sciences. *Proc. Natl. Acad. Sci. USA* **110**, 3229–3236; 10.1073/pnas.1218525110 (2013).
6. Bordenstein, S. R. & Theis, K. R. Host Biology in Light of the Microbiome: Ten Principles of Holobionts and Hologenomes. *PLoS Biol.* **13**, e1002226; 10.1371/journal.pbio.1002226 (2015).
7. Rosenberg, E. & Zilber-Rosenberg, I. Microbes Drive Evolution of Animals and Plants: the Hologenome Concept. *mBio* **7**, e01395; 10.1128/mBio.01395-15 (2016).
8. Woese, C. R. Default taxonomy: Ernst Mayr's view of the microbial world. *Proc. Natl. Acad. Sci. USA* **95**, 11043–11046; 10.1073/pnas.95.19.11043 (1998).
9. Demain, A. L. & Fang, A. The natural functions of secondary metabolites. *Adv. Biochem. Eng. Biotechnol.* **69**, 1–39; 10.1007/3-540-44964-7_1 (2000).
10. Shi, Y.-M. & Bode, H. B. Chemical language and warfare of bacterial natural products in bacteria-nematode-insect interactions. *Nat. Prod. Rep.* **35**, 309–335; 10.1039/c7np00054e (2018).
11. Tobias, N. J. *et al.* New Vocabulary for Bacterial Communication. *Chembiochem* **21**, 759–768; 10.1002/cbic.201900580 (2020).
12. Fuchs, S. W., Grundmann, F., Kurz, M., Kaiser, M. & Bode, H. B. Fabclavines: bioactive peptide-polyketide-polyamino hybrids from *Xenorhabdus*. *Chembiochem* **15**, 512–516; 10.1002/cbic.201300802 (2014).
13. Ciche, T. A., Blackburn, M., Carney, J. R. & Ensign, J. C. Photobactin: a catechol siderophore produced by *Photorhabdus luminescens*, an entomopathogen mutually associated with Heterorhabditis bacteriophora NC1 nematodes. *Appl. Environ. Microbiol.* **69**, 4706–4713; 10.1128/aem.69.8.4706-4713.2003 (2003).
14. Li, J., Chen, G. & Webster, J. M. Nematophin, a novel antimicrobial substance produced by *Xenorhabdus nematophilus* (*Enterobacteriaceae*). *Can. J. Microbiol.* **43**, 770–773; 10.1139/m97-110 (1997).
15. Polikanov, Y. S. *et al.* Amicoumacin a inhibits translation by stabilizing mRNA interaction with the ribosome. *Mol. Cell.* **56**, 531–540; 10.1016/j.molcel.2014.09.020 (2014).

References

16. Groll, M. *et al.* A plant pathogen virulence factor inhibits the eukaryotic proteasome by a novel mechanism. *Nature* **452**, 755–758; 10.1038/nature06782 (2008).
17. Kisselev, A. F. Joining the army of proteasome inhibitors. *Chem. Biol.* **15**, 419–421; 10.1016/j.chembiol.2008.04.010 (2008).
18. Lang, G., Kalvelage, T., Peters, A., Wiese, J. & Imhoff, J. F. Linear and cyclic peptides from the entomopathogenic bacterium *Xenorhabdus nematophilus*. *J. Nat. Prod.* **71**, 1074–1077; 10.1021/np800053n (2008).
19. Proschak, A. *et al.* Biosynthesis of the insecticidal xenoclyoins in *Xenorhabdus bovienii*. *Chembiochem* **15**, 369–372; 10.1002/cbic.201300694 (2014).
20. Miller, E. L. THE PENICILLINS: A REVIEW AND UPDATE. *J. Midwifery Women's Health* **47**, 426–434; 10.1016/S1526-9523(02)00330-6 (2002).
21. Aminov, R. I. A brief history of the antibiotic era: lessons learned and challenges for the future. *Front. Microbiol.* **1**, 134; 10.3389/fmicb.2010.00134 (2010).
22. Clardy, J., Fischbach, M. A. & Walsh, C. T. New antibiotics from bacterial natural products. *Nat. Biotechnol.* **24**, 1541–1550; 10.1038/nbt1266 (2006).
23. Ribeiro da Cunha, B., Fonseca, L. P. & Calado, C. R. C. Antibiotic Discovery: Where Have We Come from, Where Do We Go? *Antibiotics (Basel, Switzerland)* **8**; 10.3390/antibiotics8020045 (2019).
24. Nussbaum, F. von, Brands, M., Hinzen, B., Weigand, S. & Häbich, D. Antibacterial natural products in medicinal chemistry--exodus or revival? *Angew. Chem. Int. Ed. Engl.* **45**, 5072–5129; 10.1002/anie.200600350 (2006).
25. Ventola, C. L. The Antibiotic Resistance Crisis: Part 1: Causes and Threats. *Pharm. Ther.* **40**, 277–283 (2015).
26. Read, A. F. & Woods, R. J. Antibiotic resistance management. *Evol. Med. Public Health* **2014**, 147; 10.1093/emph/eou024 (2014).
27. U.S. Centers for Disease Control and Prevention. *Antibiotic Resistance Threats in the United States* (2019).
28. Challinor, V. L. & Bode, H. B. Bioactive natural products from novel microbial sources. *Ann. NY Acad. Sci.* **1354**, 82–97; 10.1111/nyas.12954 (2015).
29. Connon, S. A. & Giovannoni, S. J. High-Throughput Methods for Culturing Microorganisms in Very-Low-Nutrient Media Yield Diverse New Marine Isolates. *Appl. Environ. Microbiol.* **68**, 3878–3885; 10.1128/AEM.68.8.3878-3885.2002 (2002).
30. Bibb, M. J. Regulation of secondary metabolism in streptomycetes. *Curr. Opin. Microbiol.* **8**, 208–215; 10.1016/j.mib.2005.02.016 (2005).
31. Brakhage, A. A. Regulation of fungal secondary metabolism. *Nat. Rev. Microbiol.* **11**, 21–32; 10.1038/nrmicro2916 (2013).
32. Scharf, D. H. & Brakhage, A. A. Engineering fungal secondary metabolism: a roadmap to novel compounds. *J. Biotechnol.* **163**, 179–183; 10.1016/j.jbiotec.2012.06.027 (2013).

References

33. Rutledge, P. J. & Challis, G. L. Discovery of microbial natural products by activation of silent biosynthetic gene clusters. *Nat. Rev. Microbiol.* **13**, 509–523; 10.1038/nrmicro3496 (2015).
34. Bode, H. B. & Müller, R. Analysis of myxobacterial secondary metabolism goes molecular. *J. Ind. Microbiol. Biotechnol.* **33**, 577–588; 10.1007/s10295-006-0082-7 (2006).
35. Thomas, G. M. & Poinar, G. O. *Xenorhabdus* gen. nov., a Genus of Entomopathogenic, Nematophilic Bacteria of the Family *Enterobacteriaceae*. *Int. J. Syst. Bacteriol.* **29**, 352–360; 10.1099/00207713-29-4-352 (1979).
36. Fischer-Le Saux, M., Mauléon, H., Constant, P., Brunel, B. & Boemare, N. PCR-Ribotyping of *Xenorhabdus* and *Photorhabdus* Isolates from the Caribbean Region in Relation to the Taxonomy and Geographic Distribution of Their Nematode Hosts. *Appl. Environ. Microbiol.* **64**, 4246–4254 (1998).
37. Waterfield, N. R., Ciche, T. & Clarke, D. *Photorhabdus* and a host of hosts. *Annu. Rev. Microbiol.* **63**, 557–574; 10.1146/annurev.micro.091208.073507 (2009).
38. Kaya, H. K. & Gaugler, R. Entomopathogenic Nematodes. *Annu. Rev. Entomol.* **38**, 181–206; 10.1146/annurev.en.38.010193.001145 (1993).
39. Ciche, T. The biology and genome of *Heterorhabditis bacteriophora*. *Wormbook*, 1–9; 10.1895/wormbook.1.135.1 (2007).
40. Ciche, T. A. & Ensign, J. C. For the insect pathogen *Photorhabdus luminescens*, which end of a nematode is out? *Appl. Environ. Microbiol.* **69**, 1890–1897; 10.1128/aem.69.4.1890-1897.2003 (2003).
41. Crawford, J. M., Portmann, C., Zhang, X., Roeffaers, M. B. J. & Clardy, J. Small molecule perimeter defense in entomopathogenic bacteria. *Proc. Natl. Acad. Sci. USA* **109**, 10821–10826; 10.1073/pnas.1201160109 (2012).
42. Reimer, D. *et al.* Rhabdopeptides as insect-specific virulence factors from entomopathogenic bacteria. *Chembiochem* **14**, 1991–1997; 10.1002/cbic.201300205 (2013).
43. Somvanshi, V. S., Kaufmann-Daszczuk, B., Kim, K.-S., Mallon, S. & Ciche, T. A. *Photorhabdus* phase variants express a novel fimbrial locus, *mad*, essential for symbiosis. *Mol. Microbiol.* **77**, 1021–1038; 10.1111/j.1365-2958.2010.07270.x (2010).
44. Georgis, R. *et al.* Successes and failures in the use of parasitic nematodes for pest control. *Biol.* **38**, 103–123; 10.1016/j.biocontrol.2005.11.005 (2006).
45. Han, R. & Ehlers, R. U. Pathogenicity, development, and reproduction of *Heterorhabditis bacteriophora* and *Steinernema carpocapsae* under axenic in vivo conditions. *J. Invertebr. Pathol.* **75**, 55–58; 10.1006/jipa.1999.4900 (2000).
46. Bowen, D. J. & Ensign, J. C. Purification and Characterization of a High-Molecular-Weight Insecticidal Protein Complex Produced by the Entomopathogenic Bacterium *Photorhabdus luminescens*. *Appl. Environ. Microbiol.* **64**, 3029–3035 (1998).

References

47. Goodrich-Blair, H. & Clarke, D. J. Mutualism and pathogenesis in *Xenorhabdus* and *Photorhabdus*: two roads to the same destination. *Mol. Microbiol.* **64**, 260–268; 10.1111/j.1365-2958.2007.05671.x (2007).
48. Forst, S. & Neelson, K. Molecular biology of the symbiotic-pathogenic bacteria *Xenorhabdus spp.* and *Photorhabdus spp.* *Microbiol. Rev.* **60**, 21–43 (1996).
49. Forst, S., Dowds, B., Boemare, N. & Stackebrandt, E. *Xenorhabdus* and *Photorhabdus spp.*: bugs that kill bugs. *Annu. Rev. Microbiol.* **51**, 47–72; 10.1146/annurev.micro.51.1.47 (1997).
50. Poinar, G. O. & Grewal, P. S. History of Entomopathogenic Nematology. *J. Nematol.* **44**, 153–161 (2012).
51. Duchaud, E. *et al.* The genome sequence of the entomopathogenic bacterium *Photorhabdus luminescens*. *Nat. Biotechnol.* **21**, 1307–1313; 10.1038/nbt886 (2003).
52. All natural. *Nat. Chem. Biol.* **3**, 351; 10.1038/nchembio0707-351 (2007).
53. Dewick, P. M. *Medicinal natural products. A biosynthetic approach*. 3rd ed. (Wiley a John Wiley and Sons Ltd, Chichester, 2009).
54. Ruiz, B. *et al.* Production of microbial secondary metabolites: regulation by the carbon source. *Crit. Rev. Microbiol.* **36**, 146–167; 10.3109/10408410903489576 (2010).
55. Singh, B. P., Rateb, M. E., Rodriguez-Couto, S., Polizeli, M. d. L. T. d. M. & Li, W.-J. Editorial: Microbial Secondary Metabolites: Recent Developments and Technological Challenges. *Front. Microbiol.* **10**, 914; 10.3389/fmicb.2019.00914 (2019).
56. Walsh, C. T. & Tang, Y. *Natural product biosynthesis. Chemical logic and enzymatic machinery* (Royal Society of Chemistry, London, UK, 2017).
57. Yan, Q. *et al.* Secondary Metabolism and Interspecific Competition Affect Accumulation of Spontaneous Mutants in the GacS-GacA Regulatory System in *Pseudomonas protegens*. *mBio* **9**; 10.1128/mBio.01845-17 (2018).
58. Dudnik, A., Bigler, L. & Dudler, R. Heterologous expression of a *Photorhabdus luminescens* syrbactin-like gene cluster results in production of the potent proteasome inhibitor glidobactin A. *Microbiol. Res.* **168**, 73–76; 10.1016/j.micres.2012.09.006 (2013).
59. Nollmann, F. I. *et al.* Insect-specific production of new GameXPptides in *photorhabdus luminescens* TTO1, widespread natural products in entomopathogenic bacteria. *Chembiochem* **16**, 205–208; 10.1002/cbic.201402603 (2015).
60. Tobias, N. J. *et al.* Natural product diversity associated with the nematode symbionts *Photorhabdus* and *Xenorhabdus*. *Nat. Microbiol.* **2**, 1676–1685; 10.1038/s41564-017-0039-9 (2017).
61. Brachmann, A. O. *et al.* Pyrones as bacterial signaling molecules. *Nat. Chem. Biol.* **9**, 573–578; 10.1038/nchembio.1295 (2013).
62. Joyce, S. A. *et al.* Bacterial biosynthesis of a multipotent stilbene. *Angew. Chem. Int. Ed. Engl.* **47**, 1942–1945; 10.1002/anie.200705148 (2008).

63. Ciche, T. A., Bintrim, S. B., Horswill, A. R. & Ensign, J. C. A Phosphopantetheinyl Transferase Homolog Is Essential for *Photorhabdus luminescens* To Support Growth and Reproduction of the Entomopathogenic Nematode *Heterorhabditis bacteriophora*. *J. Bacteriol.* **183**, 3117–3126; 10.1128/JB.183.10.3117-3126.2001 (2001).
64. Cai, X. *et al.* Entomopathogenic bacteria use multiple mechanisms for bioactive peptide library design. *Nat. Chem.* **9**, 379–386; 10.1038/nchem.2671 (2017).
65. Akhurst, R. J. Antibiotic activity of *Xenorhabdus spp.*, bacteria symbiotically associated with insect pathogenic nematodes of the families *Heterorhabditidae* and *Steinernematidae*. *J. Gen. Microbiol.* **128**, 3061–3065; 10.1099/00221287-128-12-3061 (1982).
66. Stein, M. L. *et al.* One-shot NMR analysis of microbial secretions identifies highly potent proteasome inhibitor. *Proc. Natl. Acad. Sci. USA* **109**, 18367–18371; 10.1073/pnas.1211423109 (2012).
67. Zhou, X., Kaya, H. K., Heungens, K. & Goodrich-Blair, H. Response of ants to a deterrent factor(s) produced by the symbiotic bacteria of entomopathogenic nematodes. *Appl. Environ. Microbiol.* **68**, 6202–6209; 10.1128/aem.68.12.6202-6209.2002 (2002).
68. McGary, K. & Nudler, E. RNA polymerase and the Ribosome: The Close Relationship. *Curr. Opin. Microbiol.* **16**, 112–117; 10.1016/j.mib.2013.01.010 (2013).
69. Rauhut, R. & Klug, G. mRNA degradation in bacteria. *FEMS Microbiol. Rev.* **23**, 353–370; 10.1111/j.1574-6976.1999.tb00404.x (1999).
70. Bervoets, I. & Charlier, D. Diversity, versatility and complexity of bacterial gene regulation mechanisms: opportunities and drawbacks for applications in synthetic biology. *FEMS Microbiol. Rev.* **43**, 304–339; 10.1093/femsre/fuz001 (2019).
71. Browning, D. F. & Busby, S. J. The regulation of bacterial transcription initiation. *Nat. Rev. Microbiol.* **2**, 57–65; 10.1038/nrmicro787 (2004).
72. Wösten, M. M. Eubacterial sigma-factors. *FEMS Microbiol. Rev.* **22**, 127–150; 10.1111/j.1574-6976.1998.tb00364.x (1998).
73. Binder, S. C. *et al.* Functional modules of sigma factor regulons guarantee adaptability and evolvability. *Sci. Rep.* **6**, 22212; 10.1038/srep22212 (2016).
74. Balleza, E. *et al.* Regulation by transcription factors in bacteria: beyond description. *FEMS Microbiol. Rev.* **33**, 133–151; 10.1111/j.1574-6976.2008.00145.x (20).
75. Maas, W. K. & Clark, A. J. Studies on the mechanism of repression of arginine biosynthesis in *Escherichia coli*. *J. Mol. Biol.* **8**, 365–370; 10.1016/S0022-2836(64)80200-X (1964).
76. Madan Babu, M. & Teichmann, S. A. Evolution of transcription factors and the gene regulatory network in *Escherichia coli*. *Nucleic Acids Res.* **31**, 1234–1244 (2003).
77. Seshasayee, A. S. N., Bertone, P., Fraser, G. M. & Luscombe, N. M. Transcriptional regulatory networks in bacteria: from input signals to output responses. *Curr. Opin. Microbiol.* **9**, 511–519; 10.1016/j.mib.2006.08.007 (2006).

78. Ulrich, L. E., Koonin, E. V. & Zhulin, I. B. One-component systems dominate signal transduction in prokaryotes. *Trends Microbiol.* **13**, 52–56; 10.1016/j.tim.2004.12.006 (2005).
79. Mascher, T., Helmann, J. D. & Uden, G. Stimulus Perception in Bacterial Signal-Transducing Histidine Kinases. *Microbiol. Mol. Biol. Rev.* **70**, 910–938; 10.1128/MMBR.00020-06 (2006).
80. Bijlsma, J. J.E. & Groisman, E. A. Making informed decisions: regulatory interactions between two-component systems. *Trends Microbiol.* **11**, 359–366; 10.1016/S0966-842X(03)00176-8 (2003).
81. Sevilla, E., Bes, M. T., González, A., Peleato, M. L. & Fillat, M. F. Redox-Based Transcriptional Regulation in Prokaryotes: Revisiting Model Mechanisms. *Antioxid. Redox Signal.* **30**, 1651–1696; 10.1089/ars.2017.7442 (2019).
82. Dillon, S. C. & Dorman, C. J. Bacterial nucleoid-associated proteins, nucleoid structure and gene expression. *Nat. Rev. Microbiol.* **8**, 185–195; 10.1038/nrmicro2261 (2010).
83. Dame, R. T. & Tark-Dame, M. Bacterial chromatin: converging views at different scales. *Curr. Opin. Cell. Biol.* **40**, 60–65; 10.1016/j.ceb.2016.02.015 (2016).
84. Artsimovitch, I. *et al.* Structural Basis for Transcription Regulation by Alarmone ppGpp. *Cell* **117**, 299–310; 10.1016/S0092-8674(04)00401-5 (2004).
85. Ross, W., Vrentas, C. E., Sanchez-Vazquez, P., Gaal, T. & Gourse, R. L. The Magic Spot: A ppGpp Binding Site on *E. coli* RNA Polymerase Responsible for Regulation of Transcription Initiation. *Mol. Cell.* **50**, 420–429; 10.1016/j.molcel.2013.03.021 (2013).
86. Adhikari, S. & Curtis, P. D. DNA methyltransferases and epigenetic regulation in bacteria. *FEMS Microbiol. Rev.* **40**, 575–591; 10.1093/femsre/fuw023 (2016).
87. Casadesús, J. & Low, D. Epigenetic gene regulation in the bacterial world. *Microbiol. Mol. Biol. Rev.* **70**, 830–856; 10.1128/MMBR.00016-06 (2006).
88. Calmann, M. A. & Marinus, M. G. Regulated expression of the *Escherichia coli* *dam* gene. *J. Bacteriol.* **185**, 5012–5014; 10.1128/jb.185.16.5012-5014.2003 (2003).
89. Løbner-Olesen, A., Skovgaard, O. & Marinus, M. G. Dam methylation: coordinating cellular processes. *Curr. Opin. Microbiol.* **8**, 154–160; 10.1016/j.mib.2005.02.009 (2005).
90. Wion, D. & Casadesús, J. N6-methyl-adenine: an epigenetic signal for DNA-protein interactions. *Nat. Rev. Microbiol.* **4**, 183–192; 10.1038/nrmicro1350 (2006).
91. Barras, F. & Marinus, M. G. The great GATC: DNA methylation in *E. coli*. *Trends Genet.* **5**, 139–143; 10.1016/0168-9525(89)90054-1 (1989).
92. Brooks, J. E., Blumenthal, R. M. & Gingeras, T. R. The isolation and characterization of the *Escherichia coli* DNA adenine methylase (*dam*) gene. *Nucleic Acids Res.* **11**, 837–851; 10.1093/nar/11.3.837 (1983).
93. Marinus, M. G. & Morris, N. R. Isolation of deoxyribonucleic acid methylase mutants of *Escherichia coli* K-12. *J. Bacteriol.* **114**, 1143–1150 (1973).

94. Marinus, M. G. & Morris, N.R. Biological function for 6-methyladenine residues in the DNA of *Escherichia coli* K12. *J. Mol. Biol.* **85**, 309–322; 10.1016/0022-2836(74)90366-0 (1974).
95. Egan, E. S., Duigou, S. & Waldor, M. K. Autorepression of RctB, an initiator of *Vibrio cholerae* chromosome II replication. *J. Bacteriol.* **188**, 789–793; 10.1128/JB.188.2.789-793.2006 (2006).
96. Saberi, F., Kamali, M., Najafi, A., Yazdanparast, A. & Moghaddam, M. M. Natural antisense RNAs as mRNA regulatory elements in bacteria: a review on function and applications. *Cell. Mol. Biol. Lett.* **21**, 6; 10.1186/s11658-016-0007-z (2016).
97. Afonyushkin, T., Večerek, B., Moll, I., Bläsi, U. & Kaberdin, V. R. Both RNase E and RNase III control the stability of *sodB* mRNA upon translational inhibition by the small regulatory RNA RyhB. *Nucleic Acids Res.* **33**, 1678–1689; 10.1093/nar/gki313 (2005).
98. Thomason, M. K. & Storz, G. Bacterial antisense RNAs: how many are there, and what are they doing? *Annu. Rev. Genet.* **44**, 167–188; 10.1146/annurev-genet-102209-163523 (2010).
99. Sedlyarova, N. *et al.* sRNA-mediated control of transcription termination in *E. coli*. *Cell* **167**, 111-121.e13; 10.1016/j.cell.2016.09.004 (2016).
100. Franze de Fernandez, M. T., Eoyang, L. & August, J. T. Factor fraction required for the synthesis of bacteriophage Q β -RNA. *Nature* **219**, 588–590; 10.1038/219588a0 (1968).
101. Desnoyers, G., Bouchard, M.-P. & Massé, E. New insights into small RNA-dependent translational regulation in prokaryotes. *Trends Genet.* **29**, 92–98; 10.1016/j.tig.2012.10.004 (2013).
102. Peer, A. & Margalit, H. Accessibility and evolutionary conservation mark bacterial small-rna target-binding regions. *J. Bacteriol.* **193**, 1690–1701; 10.1128/JB.01419-10 (2011).
103. Sobrero, P. & Valverde, C. The bacterial protein Hfq: much more than a mere RNA-binding factor. *Crit. Rev. Microbiol.* **38**, 276–299; 10.3109/1040841X.2012.664540 (2012).
104. Tobias, N. J. *et al.* *Photorhabdus*-nematode symbiosis is dependent on hfq-mediated regulation of secondary metabolites. *Environ. Microbiol.* **19**, 119–129; 10.1111/1462-2920.13502 (2017).
105. Janssen, K. H., Diaz, M. R., Gode, C. J., Wolfgang, M. C. & Yahr, T. L. RsmV, a Small Noncoding Regulatory RNA in *Pseudomonas aeruginosa* That Sequesters RsmA and RsmF from Target mRNAs. *J. Bacteriol.* **200**; 10.1128/JB.00277-18 (2018).
106. Janssen, K. H. *et al.* Functional Analyses of the RsmY and RsmZ Small Noncoding Regulatory RNAs in *Pseudomonas aeruginosa*. *J. Bacteriol.* **200**; 10.1128/JB.00736-17 (2018).
107. Serganov, A. & Nudler, E. A decade of riboswitches. *Cell* **152**, 17–24; 10.1016/j.cell.2012.12.024 (2013).

108. Gualerzi, C. O., Giuliodori, A. M. & Pon, C. L. Transcriptional and post-transcriptional control of cold-shock genes. *J. Mol. Biol.* **331**, 527–539; 10.1016/s0022-2836(03)00732-0 (2003).
109. Johansson, J. *et al.* An RNA thermosensor controls expression of virulence genes in *Listeria monocytogenes*. *Cell* **110**, 551–561; 10.1016/s0092-8674(02)00905-4 (2002).
110. Kortmann, J. & Narberhaus, F. Bacterial RNA thermometers: molecular zippers and switches. *Nat. Rev. Microbiol.* **10**, 255–265; 10.1038/nrmicro2730 (2012).
111. Cain, J. A., Solis, N. & Cordwell, S. J. Beyond gene expression: the impact of protein post-translational modifications in bacteria. *J. Proteomics* **97**, 265–286; 10.1016/j.jprot.2013.08.012 (2014).
112. Szymanski, C. M., Burr, D. H. & Guerry, P. *Campylobacter* protein glycosylation affects host cell interactions. *Infect. Immun.* **70**, 2242–2244; 10.1128/IAI.70.4.2242-2244.2002 (2002).
113. Gardner, J. G. & Escalante-Semerena, J. C. Biochemical and mutational analyses of AcuA, the acetyltransferase enzyme that controls the activity of the acetyl coenzyme a synthetase (AcsA) in *Bacillus subtilis*. *J. Bacteriol.* **190**, 5132–5136; 10.1128/JB.00340-08 (2008).
114. Bode, E. *et al.* Simple "on-demand" production of bioactive natural products. *Chembiochem* **16**, 1115–1119; 10.1002/cbic.201500094 (2015).
115. Bode, H. B. *et al.* Determination of the absolute configuration of peptide natural products by using stable isotope labeling and mass spectrometry. *Chemistry* **18**, 2342–2348; 10.1002/chem.201103479 (2012).
116. Bode, H. B. *et al.* Structure Elucidation and Activity of Kolossin A, the D-/L-Pentadecapeptide Product of a Giant Nonribosomal Peptide Synthetase. *Angew. Chem. Int. Ed. Engl.* **54**, 10352–10355; 10.1002/anie.201502835 (2015).
117. Brachmann, A. O. *et al.* A type II polyketide synthase is responsible for anthraquinone biosynthesis in *Photorhabdus luminescens*. *Chembiochem* **8**, 1721–1728; 10.1002/cbic.200700300 (2007).
118. Engel, Y., Windhorst, C., Lu, X., Goodrich-Blair, H. & Bode, H. B. The Global Regulators Lrp, LeuO, and HexA Control Secondary Metabolism in Entomopathogenic Bacteria. *Front. Microbiol.* **8**, 209; 10.3389/fmicb.2017.00209 (2017).
119. Bode, E. *et al.* Promoter Activation in Δ hfq Mutants as an Efficient Tool for Specialized Metabolite Production Enabling Direct Bioactivity Testing. *Angew. Chem. Int. Ed. Engl.* **58**, 18957–18963; 10.1002/anie.201910563 (2019).
120. Payelleville, A. *et al.* The complete methylome of an entomopathogenic bacterium reveals the existence of loci with unmethylated Adenines. *Sci. Rep.* **8**, 12091; 10.1038/s41598-018-30620-5 (2018).
121. Lu, S. C. S-Adenosylmethionine. *Int. J. Biochem. Cell. B.* **32**, 391–395; 10.1016/S1357-2725(99)00139-9 (2000).

122. Braaten, B. A., Nou, X., Kaltenbach, L. S. & Low, D. A. Methylation patterns in pap regulatory DNA control pyelonephritis-associated pili phase variation in *E. coli*. *Cell* **76**, 577–588; 10.1016/0092-8674(94)90120-1 (1994).
123. Braaten, B. A. *et al.* Leucine-responsive regulatory protein controls the expression of both the pap and fan pili operons in *Escherichia coli*. *Proc. Natl. Acad. Sci. USA* **89**, 4250–4254; 10.1073/pnas.89.10.4250 (1992).
124. Payelleville, A. *et al.* DNA Adenine Methyltransferase (Dam) Overexpression Impairs *Photobacterium luminescens* Motility and Virulence. *Front. Microbiol.* **8**, 1671; 10.3389/fmicb.2017.01671 (2017).
125. Fischer-Le Saux, M., Viillard, V., Brunel, B., Normand, P. & Boemare, N. E. Polyphasic classification of the genus *Photobacterium* and proposal of new taxa: *P. luminescens* subsp. *luminescens* subsp. nov., *P. luminescens* subsp. *akhurstii* subsp. nov., *P. luminescens* subsp. *laumondii* subsp. nov., *P. temperata* sp. nov., *P. temperata* subsp. *temperata* subsp. nov. and *P. asymbiotica* sp. nov. *Int. J. Syst. Bacteriol.* **49 Pt 4**, 1645–1656; 10.1099/00207713-49-4-1645 (1999).
126. Lengyel, K. *et al.* Description of four novel species of *Xenorhabdus*, family *Enterobacteriaceae*: *Xenorhabdus budapestensis* sp. nov., *Xenorhabdus ehlersii* sp. nov., *Xenorhabdus innexi* sp. nov., and *Xenorhabdus szentirmaii* sp. nov. *Syst. Appl. Microbiol.* **28**, 115–122; 10.1016/j.syapm.2004.10.004 (2005).
127. Goodman, A. L. *et al.* Identifying genetic determinants needed to establish a human gut symbiont in its habitat. *Cell Host Microbe* **6**, 279–289; 10.1016/j.chom.2009.08.003 (2009).
128. Nollmann, F. I. *et al.* A *Photobacterium* natural product inhibits insect juvenile hormone epoxide hydrolase. *Chembiochem* **16**, 766–771; 10.1002/cbic.201402650 (2015).
129. Lorenzen, W., Ahrendt, T., Bozhüyük, K. A. J. & Bode, H. B. A multifunctional enzyme is involved in bacterial ether lipid biosynthesis. *Nat. Chem. Biol.* **10**, 425–427; 10.1038/nchembio.1526 (2014).
130. Waters, C. M. & Bassler, B. L. Quorum sensing: cell-to-cell communication in bacteria. *Annu. Rev. Cell. Dev. Biol.* **21**, 319–346; 10.1146/annurev.cellbio.21.012704.131001 (2005).
131. Bankevich, A. *et al.* SPAdes: a new genome assembly algorithm and its applications to single-cell sequencing. *J. Comput. Biol.* **19**, 455–477; 10.1089/cmb.2012.0021 (2012).
132. Seemann, T. Prokka: rapid prokaryotic genome annotation. *Bioinformatics* **30**, 2068–2069; 10.1093/bioinformatics/btu153 (2014).
133. Langmead, B. & Salzberg, S. L. Fast gapped-read alignment with Bowtie 2. *Nat. Methods.* **9**, 357–359; 10.1038/nmeth.1923 (2012).
134. Bolger, A. M., Lohse, M. & Usadel, B. Trimmomatic: a flexible trimmer for Illumina sequence data. *Bioinformatics* **30**, 2114–2120; 10.1093/bioinformatics/btu170 (2014).

References

135. Li, H. *et al.* The Sequence Alignment/Map format and SAMtools. *Bioinformatics* **25**, 2078–2079; 10.1093/bioinformatics/btp352 (2009).
136. Liao, Y., Smyth, G. K. & Shi, W. featureCounts: an efficient general purpose program for assigning sequence reads to genomic features. *Bioinformatics* **30**, 923–930; 10.1093/bioinformatics/btt656 (2014).
137. Fröhlich, K. S., Haneke, K., Papenfort, K. & Vogel, J. The target spectrum of SdsR small RNA in *Salmonella*. *Nucleic Acids Res.* **44**, 10406–10422; 10.1093/nar/gkw632 (2016).
138. Gibson, D. G. Synthesis of DNA fragments in yeast by one-step assembly of overlapping oligonucleotides. *Nucleic Acids Res.* **37**, 6984–6990; 10.1093/nar/gkp687 (2009).
139. Dunn, A. K., Millikan, D. S., Adin, D. M., Bose, J. L. & Stabb, E. V. New rfp- and pES213-derived tools for analyzing symbiotic *Vibrio fischeri* reveal patterns of infection and lux expression in situ. *Appl. Environ. Microbiol.* **72**, 802–810; 10.1128/AEM.72.1.802-810.2006 (2006).
140. Corcoran, C. P. *et al.* Superfolder GFP reporters validate diverse new mRNA targets of the classic porin regulator, MicF RNA. *Mol. Microbiol.* **84**, 428–445; 10.1111/j.1365-2958.2012.08031.x (2012).
141. Wright, P. R. *et al.* CopraRNA and IntaRNA: predicting small RNA targets, networks and interaction domains. *Nucleic Acids Res.* **42**, W119-23; 10.1093/nar/gku359 (2014).
142. Shi, Y.-M. *et al.* Dual phenazine gene clusters enable diversification during biosynthesis. *Nat. Chem. Biol.* **15**, 331–339; 10.1038/s41589-019-0246-1 (2019).
143. Heinrich, A. K., Glaeser, A., Tobias, N. J., Heermann, R. & Bode, H. B. Heterogeneous regulation of bacterial natural product biosynthesis via a novel transcription factor. *Heliyon* **2**, e00197; 10.1016/j.heliyon.2016.e00197 (2016).
144. Thoma, S. & Schobert, M. An improved *Escherichia coli* donor strain for diparental mating. *FEMS Microbiol. Lett.* **294**, 127–132; 10.1111/j.1574-6968.2009.01556.x (2009).
145. Chao, Y. & Vogel, J. The role of Hfq in bacterial pathogens. *Curr. Opin. Microbiol.* **13**, 24–33; 10.1016/j.mib.2010.01.001 (2010).
146. Joyce, S. A. & Clarke, D. J. A hexA homologue from *Photobacterium* regulates pathogenicity, symbiosis and phenotypic variation. *Mol. Microbiol.* **47**, 1445–1457; 10.1046/j.1365-2958.2003.03389.x (2003).
147. Papenfort, K. *et al.* Specific and pleiotropic patterns of mRNA regulation by ArcZ, a conserved, Hfq-dependent small RNA. *Mol. Microbiol.* **74**, 139–158; 10.1111/j.1365-2958.2009.06857.x (2009).
148. Killiny, N. Generous hosts: Why the larvae of greater wax moth, *Galleria mellonella* is a perfect infectious host model? *Virulence* **9**, 860–865; 10.1080/21505594.2018.1454172 (2018).

149. Mashhoon, N. *et al.* Functional characterization of *Escherichia coli* DNA adenine methyltransferase, a novel target for antibiotics. *J. Biol. Chem.* **279**, 52075–52081; 10.1074/jbc.M408182200 (2004).
150. Wilf, N. M. *et al.* The RNA chaperone, Hfq, controls two luxR-type regulators and plays a key role in pathogenesis and production of antibiotics in *Serratia sp.* ATCC 39006. *Environ. Microbiol.* **13**, 2649–2666; 10.1111/j.1462-2920.2011.02532.x (2011).
151. Wang, G. *et al.* The RNA chaperone Hfq regulates antibiotic biosynthesis in the rhizobacterium *Pseudomonas aeruginosa* M18. *J. Bacteriol.* **194**, 2443–2457; 10.1128/JB.00029-12 (2012).
152. Xu, G., Zhao, Y., Du, L., Qian, G. & Liu, F. Hfq regulates antibacterial antibiotic biosynthesis and extracellular lytic-enzyme production in *Lysobacter enzymogenes* OH11. *Microb. Biotechnol.* **8**, 499–509; 10.1111/1751-7915.12246 (2015).
153. Santiago-Frangos, A. & Woodson, S. A. Hfq chaperone brings speed dating to bacterial sRNA. *Wiley Interdiscip. Rev. RNA* **9**, e1475; 10.1002/wrna.1475 (2018).
154. Argaman, L. *et al.* Novel small RNA-encoding genes in the intergenic regions of *Escherichia coli*. *Curr. Biol.* **11**, 941–950; 10.1016/S0960-9822(01)00270-6 (2001).
155. Mandin, P. & Gottesman, S. Integrating anaerobic/aerobic sensing and the general stress response through the ArcZ small RNA. *EMBO J.* **29**, 3094–3107; 10.1038/emboj.2010.179 (2010).
156. Cavaliere, P. *et al.* The stress sigma factor of RNA polymerase RpoS/ σ S is a solvent-exposed open molecule in solution. *Biochem. J.* **475**, 341–354; 10.1042/BCJ20170768 (2018).
157. Lango-Scholey, L., Brachmann, A. O., Bode, H. B. & Clarke, D. J. The expression of stlA in *Phototrhhabdus luminescens* is controlled by nutrient limitation. *PLoS one* **8**, e82152; 10.1371/journal.pone.0082152 (2013).
158. Battesti, A., Majdalani, N. & Gottesman, S. The RpoS-mediated general stress response in *Escherichia coli*. *Annu. Rev. Microbiol.* **65**, 189–213; 10.1146/annurev-micro-090110-102946 (2011).
159. Schellhorn, H. E. Elucidating the function of the RpoS regulon. *Future Microbiol.* **9**, 497–507; 10.2217/fmb.14.9 (2014).
160. Brameyer, S., Kresovic, D., Bode, H. B. & Heermann, R. LuxR solos in *Phototrhhabdus* species. *Front. Cell. Infect. Microbiol.* **4**, 166; 10.3389/fcimb.2014.00166 (2014).
161. Heermann, R. & Fuchs, T. M. Comparative analysis of the *Phototrhhabdus luminescens* and the *Yersinia enterocolitica* genomes: uncovering candidate genes involved in insect pathogenicity. *BMC genomics* **9**, 40; 10.1186/1471-2164-9-40 (2008).
162. Sharma, I. M., Korman, A. & Woodson, S. A. The Hfq chaperone helps the ribosome mature. *EMBO J.* **37**; 10.15252/emboj.201899616 (2018).

163. Andrade, J. M., Dos Santos, R. F., Chelysheva, I., Ignatova, Z. & Arraiano, C. M. The RNA-binding protein Hfq is important for ribosome biogenesis and affects translation fidelity. *EMBO J.* **37**; 10.15252/embj.201797631 (2018).
164. Maguire, B. A. Inhibition of bacterial ribosome assembly: a suitable drug target? *Microbiol. Mol. Biol. Rev.* **73**, 22–35; 10.1128/MMBR.00030-08 (2009).
165. Stokes, J. M., Selin, C., Cardona, S. T. & Brown, E. D. Chemical inhibition of bacterial ribosome biogenesis shows efficacy in a worm infection model. *Antimicrob. Agents Chemother.* **59**, 2918–2920; 10.1128/AAC.04690-14 (2015).
166. Chen, J.-J. & London, I. M. Regulation of protein synthesis by heme-regulated eIF-2 α kinase. *Trends Biochem. Sci.* **20**, 105–108; 10.1016/S0968-0004(00)88975-6 (1995).
167. Qi, Z., Hamza, I. & O'Brian, M. R. Heme is an effector molecule for iron-dependent degradation of the bacterial iron response regulator (Irr) protein. *Proc. Natl. Acad. Sci. USA* **96**, 13056–13061; 10.1073/pnas.96.23.13056 (1999).
168. Wenger, R. H. Mammalian oxygen sensing, signalling and gene regulation. *J. Exp. Biol.* **203**, 1253–1263 (2000).
169. Rao, A. U., Carta, L. K., Lesuisse, E. & Hamza, I. Lack of heme synthesis in a free-living eukaryote. *Proc. Natl. Acad. Sci. USA* **102**, 4270–4275; 10.1073/pnas.0500877102 (2005).
170. Bolla, R. Developmental nutrition of nematodes: the biochemical role of sterols, heme compounds, and lysosomal enzymes. *J. Nematol.* **11**, 250–259 (1979).
171. Zeng, Q., McNally, R. R. & Sundin, G. W. Global small RNA chaperone Hfq and regulatory small RNAs are important virulence regulators in *Erwinia amylovora*. *J. Bacteriol.* **195**, 1706–1717; 10.1128/JB.02056-12 (2013).
172. Shanks, R. M. Q. *et al.* Suppressor analysis of eepR mutant defects reveals coordinate regulation of secondary metabolites and serralyisin biosynthesis by EepR and HexS. *Microbiology* **163**, 280–288; 10.1099/mic.0.000422 (2017).
173. Fineran, P. C. *et al.* Draft Genome Sequence of *Serratia sp.* Strain ATCC 39006, a Model Bacterium for Analysis of the Biosynthesis and Regulation of Prodigiosin, a Carbapenem, and Gas Vesicles. *Genome Announc.* **1**; 10.1128/genomeA.01039-13 (2013).
174. Matilla, M. A., Leeper, F. J. & Salmond, G. P. C. Biosynthesis of the antifungal haterumalide, oocydin A, in *Serratia*, and its regulation by quorum sensing, RpoS and Hfq. *Environ. Microbiol.* **17**, 2993–3008; 10.1111/1462-2920.12839 (2015).
175. Wilf, N. M. *et al.* RNA-seq reveals the RNA binding proteins, Hfq and RsmA, play various roles in virulence, antibiotic production and genomic flux in *Serratia sp.* ATCC 39006. *BMC genomics* **14**, 822; 10.1186/1471-2164-14-822 (2013).
176. Helwak, A., Kudla, G., Dudnakova, T. & Tollervey, D. Mapping the human miRNA interactome by CLASH reveals frequent noncanonical binding. *Cell* **153**, 654–665; 10.1016/j.cell.2013.03.043 (2013).

177. Iosub, I. A. *et al.* *Hfq CLASH uncovers sRNA-target interaction networks involved in adaptation to nutrient availability* (2018).
178. Man, S. *et al.* Artificial trans-encoded small non-coding RNAs specifically silence the selected gene expression in bacteria. *Nucleic Acids Res.* **39**, e50; 10.1093/nar/gkr034 (2011).
179. Na, D. *et al.* Metabolic engineering of *Escherichia coli* using synthetic small regulatory RNAs. *Nat. Biotechnol.* **31**, 170–174; 10.1038/nbt.2461 (2013).
180. Crawford, J. M., Kontnik, R. & Clardy, J. Regulating alternative lifestyles in entomopathogenic bacteria. *Curr. Biol.* **20**, 69–74; 10.1016/j.cub.2009.10.059 (2010).
181. Fujita, Y., Matsuoka, H. & Hirooka, K. Regulation of fatty acid metabolism in bacteria. *Mol. Microbiol.* **66**, 829–839; 10.1111/j.1365-2958.2007.05947.x (2007).
182. Pramanik, A., Pawar, S., Antonian, E. & Schulz, H. Five different enzymatic activities are associated with the multienzyme complex of fatty acid oxidation from *Escherichia coli*. *J. Bacteriol.* **137**, 469–473 (1979).
183. Herbert, E. E. & Goodrich-Blair, H. Friend and foe: the two faces of *Xenorhabdus nematophila*. *Nat. Rev. Microbiol.* **5**, 634–646; 10.1038/nrmicro1706 (2007).
184. Beisel, C. L. & Afroz, T. Rethinking the Hierarchy of Sugar Utilization in Bacteria. *J. Bacteriol.* **198**, 374–376; 10.1128/JB.00890-15 (2016).
185. Klein, W., Horlacher, R. & Boos, W. Molecular analysis of treB encoding the *Escherichia coli* enzyme II specific for trehalose. *J. Bacteriol.* **177**, 4043–4052; 10.1128/jb.177.14.4043-4052.1995 (1995).
186. Boos, W. & Shuman, H. Maltose/maltodextrin system of *Escherichia coli*: transport, metabolism, and regulation. *Microbiol. Mol. Biol. Rev.* **62**, 204–229 (1998).
187. Zhou, Q. *et al.* Structure and biosynthesis of xenoamicins from entomopathogenic *Xenorhabdus*. *Chemistry* **19**, 16772–16779; 10.1002/chem.201302481 (2013).
188. McInerney, B. V., Taylor, W. C., Lacey, M. J., Akhurst, R. J. & Gregson, R. P. Biologically active metabolites from *Xenorhabdus spp.*, Part 2. Benzopyran-1-one derivatives with gastroprotective activity. *J. Nat. Prod.* **54**, 785–795; 10.1021/np50075a006 (1991).
189. Urig, S. *et al.* The *Escherichia coli* Dam DNA Methyltransferase Modifies DNA in a Highly Processive Reaction. *J. Mol. Biol.* **319**, 1085–1096; 10.1016/S0022-2836(02)00371-6 (2002).
190. Marinus, M. G. & Casadesus, J. Roles of DNA adenine methylation in host-pathogen interactions: mismatch repair, transcriptional regulation, and more. *FEMS Microbiol. Rev.* **33**, 488–503; 10.1111/j.1574-6976.2008.00159.x (2009).
191. Low, D. A., Weyand, N. J. & Mahan, M. J. Roles of DNA adenine methylation in regulating bacterial gene expression and virulence. *Infect. Immun.* **69**, 7197–7204; 10.1128/IAI.69.12.7197-7204.2001 (2001).

192. Heinrich, A. K., Hirschmann, M., Neubacher, N. & Bode, H. B. LuxS-dependent AI-2 production is not involved in global regulation of natural product biosynthesis in *Photorhabdus* and *Xenorhabdus*. *PeerJ* **5**, e3471; 10.7717/peerj.3471 (2017).
193. Zamora-Lagos, M.-A. *et al.* Phenotypic and genomic comparison of *Photorhabdus luminescens* subsp. *laumondii* TT01 and a widely used rifampicin-resistant *Photorhabdus luminescens* laboratory strain. *BMC genomics* **19**; 10.1186/s12864-018-5121-z (2018).
194. Avcilar-Kucukgoze, I. *et al.* Discharging tRNAs: a tug of war between translation and detoxification in *Escherichia coli*. *Nucleic Acids Res.* **44**, 8324–8334; 10.1093/nar/gkw697 (2016).
195. Sakai, Y., Kimura, S. & Suzuki, T. Dual pathways of tRNA hydroxylation ensure efficient translation by expanding decoding capability. *Nat. Commun.* **10**, 2858; 10.1038/s41467-019-10750-8 (2019).
196. Vigil-Stenman, T., Ininbergs, K., Bergman, B. & Ekman, M. High abundance and expression of transposases in bacteria from the Baltic Sea. *ISME J.* **11**, 2611–2623; 10.1038/ismej.2017.114 (2017).
197. Vigil-Stenman, T. *Effects and dynamics of insertion sequences in the evolution of cyanobacteria* (Department of Ecology, Environment and Plant Sciences, Stockholm University, Stockholm, 2015).
198. Dodson, K. W. & Berg, D. E. Factors affecting transposition activity of IS50 and Tn5 ends. *Gene* **76**, 207–213; 10.1016/0378-1119(89)90161-3 (1989).
199. Reznikoff, W. S. The Tn5 transposon. *Annu. Rev. Microbiol.* **47**, 945–963; 10.1146/annurev.mi.47.100193.004501 (1993).
200. Roberts, D. IS10 transposition is regulated by DNA adenine methylation. *Cell* **43**, 117–130; 10.1016/0092-8674(85)90017-0 (1985).
201. Heusipp, G., Fälker, S. & Schmidt, M. A. DNA adenine methylation and bacterial pathogenesis. *Int. J. Med. Microbiol.* **297**, 1–7; 10.1016/j.ijmm.2006.10.002 (2007).
202. Reisenauer, A., Kahng, L. S., McCollum, S. & Shapiro, L. Bacterial DNA methylation: a cell cycle regulator? *J. Bacteriol.* **181**, 5135–5139 (1999).
203. Stephens, C., Reisenauer, A., Wright, R. & Shapiro, L. A cell cycle-regulated bacterial DNA methyltransferase is essential for viability. *Proc. Natl. Acad. Sci. USA* **93**, 1210–1214; 10.1073/pnas.93.3.1210 (1996).
204. Marinus, M. G. & Løbner-Olesen, A. DNA Methylation. *EcoSal Plus* **6**; 10.1128/ecosalplus.ESP-0003-2013 (2014).
205. Collier, J. Epigenetic regulation of the bacterial cell cycle. *Curr. Opin. Microbiol.* **12**, 722–729; 10.1016/j.mib.2009.08.005 (2009).
206. Brachmann, A. O., Forst, S., Furgani, G. M., Fodor, A. & Bode, H. B. Xenofuranones A and B: phenylpyruvate dimers from *Xenorhabdus szentirmaii*. *J. Nat. Prod.* **69**, 1830–1832; 10.1021/np060409n (2006).

207. Tobias, N. J. *et al.* Cyclo(tetrahydroxybutyrate) production is sufficient to distinguish between *Xenorhabdus* and *Photorhabdus* isolates in Thailand. *Environ. Microbiol.* **21**, 2921–2932; 10.1111/1462-2920.14685 (2019).
208. Cai, X. *et al.* Biosynthesis of the Antibiotic Nematophin and Its Elongated Derivatives in Entomopathogenic Bacteria. *Org. Lett.* **19**, 806–809; 10.1021/acs.orglett.6b03796 (2017).
209. Crawford, J. M., Portmann, C., Kontnik, R., Walsh, C. T. & Clardy, J. NRPS substrate promiscuity diversifies the xenematides. *Org. Lett.* **13**, 5144–5147; 10.1021/ol2020237 (2011).
210. Park, D. *et al.* Genetic analysis of xenocoumacin antibiotic production in the mutualistic bacterium *Xenorhabdus nematophila*. *Mol. Microbiol.* **73**, 938–949; 10.1111/j.1365-2958.2009.06817.x (2009).
211. Reimer, D., Nollmann, F. I., Schultz, K., Kaiser, M. & Bode, H. B. Xenortide Biosynthesis by Entomopathogenic *Xenorhabdus nematophila*. *J. Nat. Prod.* **77**, 1976–1980; 10.1021/np500390b (2014).
212. Kegler, C. *et al.* Rapid determination of the amino acid configuration of xenotetrapeptide. *Chembiochem* **15**, 826–828; 10.1002/cbic.201300602 (2014).

5. Supporting information

Supplementary Table 1. Optical density values for sequencing experiments covered in topic A (chapter 3.1).

Species	OD ₆₀₀ value	Purpose
<i>P. laumondii</i> replicate A	5.8	sRNA sequencing
<i>P. laumondii</i> replicate B	5.4	sRNA sequencing
<i>X. szentirmaii</i> replicate A	5.5	sRNA sequencing
<i>X. szentirmaii</i> replicate B	6.1	sRNA sequencing
<i>P. laumondii</i> replicate A	4	RNA-sequencing
<i>P. laumondii</i> replicate B	4.3	RNA-sequencing
<i>P. laumondii</i> Δ <i>arcZ</i> replicate A	3.8	RNA-sequencing
<i>P. laumondii</i> Δ <i>arcZ</i> replicate B	4.1	RNA-sequencing
<i>P. laumondii</i> knock-in replicate A	5.2	RNA-sequencing
<i>P. laumondii</i> knock-in replicate B	4.6	RNA-sequencing
<i>X. szentirmaii</i> replicate A	4.3	RNA-sequencing (control for Δ <i>arcZ</i> mutant)
<i>X. szentirmaii</i> replicate B	3.8	RNA-sequencing (control for Δ <i>arcZ</i> mutant)
<i>X. szentirmaii</i> replicate A	4.5	RNA-sequencing (control for Δ <i>hfq</i> mutant)
<i>X. szentirmaii</i> replicate B	4.5	RNA-sequencing (control for Δ <i>hfq</i> mutant)
<i>X. szentirmaii</i> Δ <i>arcZ</i> replicate A	4.8	RNA-sequencing
<i>X. szentirmaii</i> Δ <i>arcZ</i> replicate B	4.3	RNA-sequencing
<i>X. szentirmaii</i> Δ <i>hfq</i> replicate A	4.8	RNA-sequencing
<i>X. szentirmaii</i> Δ <i>hfq</i> replicate B	4.7	RNA-sequencing
<i>X. szentirmaii</i> knock-in replicate A	3.6	RNA-sequencing
<i>X. szentirmaii</i> knock-in replicate B	3.8	RNA-sequencing

Supporting Information

Species	OD600 value	Purpose
<i>P. laumondii</i> replicate A	0.5	RIP-Seq
<i>P. laumondii</i> replicate B	0.5	RIP-Seq
<i>P. laumondii</i> replicate A	5	RIP-Seq
<i>P. laumondii</i> replicate B	5	RIP-Seq

Supplementary Table 2. Compounds quantified by Target analysis.

Compound Name	<i>m/z</i>	Ion	Reference
<i>P. laumondii</i>			
Isopropylstilbene (IPS)	255.1	[M+H] ⁺	62
Anthraquinone 284 (AQ-284)	285.1	[M+H] ⁺	117
Anthraquinone 270a (AQ-270a)	271.1	[M+H] ⁺	117
GameXPepptide A (GXP-A)	586.4	[M+H] ⁺	115
GameXPepptide B (GXP-B)	600.4	[M+H] ⁺	115
GameXPepptide C (GXP-C)	552.4	[M+H] ⁺	115
GameXPepptide D (GXP-D)	566.4	[M+H] ⁺	115
Photopyrone C (PPY-C)	281.2	[M+H] ⁺	61
Photopyrone D (PPY-D)	295.2	[M+H] ⁺	61
Photopyrone E (PPY-E)	309.2	[M+H] ⁺	61
Photopyrone F (PPY-F)	323.3	[M+H] ⁺	61
Desmethyl-Phurealipide A (dmPLA-A)	215.2	[M+H] ⁺	128
Phurealipide A (PL-A)	229.2	[M+H] ⁺	128
Phurealipide B (PL-B)	243.2	[M+H] ⁺	128
Phurealipide C (PL-C)	257.3	[M+H] ⁺	128
Mevalagmapeptide (MVAP)	334.8	[M+2H] ⁺⁺	115

Supporting Information

Compound Name	m/z	Ion	Reference
<i>X. szentirmaii</i>			
Xenofuranone A (XF-A)	281.1	[M+H] ⁺	206
Tetrahydrobutyrate	367.1	[M+H] ⁺	207
GameXPepptide C (GXP-C)	552.4	[M+H] ⁺	115
Protoporphyrin IX (PPIX)	563.3	[M+H] ⁺	
Xenoamicin A (XA-A)	650.9	[M+2H] ⁺⁺	187
Xenoamicin B (XA-B)	657.8	[M+2H] ⁺⁺	187
Rhabdopeptide 659 (RXP-659)	659.5	[M+H] ⁺	64
Rhabdopeptide 673 (RXP-673)	673.5	[M+H] ⁺	64
Rhabdopeptide 772 (RXP-772)	772.4	[M+H] ⁺	64
<i>X. nematophila</i>			
Nematophin (NMP)	273.2	[M+H] ⁺	208
Rhabdopeptide 574 (RXP-574)	574.4	[M+H] ⁺	64
Rhabdopeptide 588 (RXP-588)	588.4	[M+H] ⁺	64
Rhabdopeptide 687 (RXP-687)	687.5	[M+H] ⁺	64
Rhabdopeptide 701 (RXP-701)	701.5	[M+H] ⁺	64
Rhabdopeptide 800 (RXP-800)	800.6	[M+H] ⁺	64
Rhabdopeptide 814 (RXP-814)	814.6	[M+H] ⁺	64
Xenematide A (XNM-A)	663.3	[M+H] ⁺	209
Xenocoumacin I (XNCI)	466.3	[M+H] ⁺	210
Xenocoumacin II (XNCII)	407.7	[M+H] ⁺	210
Xenortid A (XND-A)	410.3	[M+H] ⁺	211
Xenortid B (XND-B)	449.3	[M+H] ⁺	211
Xenoamicin (XA-1258)	630.4	[M+2H] ⁺⁺	187
Xenoamicin (XA-1272)	637.4	[M+2H] ⁺⁺	187
Xenotetrapeptide (XTP)	411.3	[M+H] ⁺	212

Supplementary Table 3. Optical density values for sequencing experiments covered in topic B (chapter 3.2).

Species	OD₆₀₀ value (induction)	Final OD₆₀₀ value
<i>P. laumondii</i> replicate A	2.5	3.4
<i>P. laumondii</i> replicate B	2.4	3
<i>P. laumondii</i> + insect homogenate replicate A	2.6	n.d.
<i>P. laumondii</i> + insect homogenate replicate B	2.3	n.d.
<i>X. szentirmaii</i> replicate A	3.2	4.3
<i>X. szentirmaii</i> replicate B	3.5	4.8
<i>X. szentirmaii</i> + insect homogenate replicate A	3.7	n.d.
<i>X. szentirmaii</i> + insect homogenate replicate B	3.6	n.d.
<i>X. nematophila</i> replicate A	3.6	4.9
<i>X. nematophila</i> replicate B	3.5	5.1
<i>X. nematophila</i> + insect homogenate replicate A	3.7	n.d.
<i>X. nematophila</i> + insect homogenate replicate B	3.6	n.d.

1 **6. Appendix**

2 The Appendix of this work contains the manuscript as well as the supporting
3 information part of the manuscript “Small RNA directs symbiosis, virulence, and natural
4 products biosynthesis in entomopathogenic bacteria” by Nick Neubacher[#], Nicholas J.
5 Tobias[#], Michaela Huber[#] (#co-first authors), Xiaofeng Cai, Sacha J. Pidot, Timothy P.
6 Stinear, Anna Lena Lütticke, Kai Papenfort and Helge B. Bode* (*corresponding
7 author). This manuscript is currently under revision in Nat. Microbiol. The manuscript
8 including all supplementary tables are also available digitally on the attached CD.

9

33 **Abstract**

34 Rapid modulation of gene expression is a key feature for the success of bacteria, particularly
35 for those that rapidly have to adapt to different niches. The lifecycles of *Photorhabdus* and
36 *Xenorhabdus* involve a mutualistic association with nematodes as well as an
37 entomopathogenic phase^{1,2}, both of which rely on the production of numerous specialized
38 metabolites (SMs)^{3,4}. Several regulators have been previously implicated in the regulation of
39 SM production in these genera^{3,4}. However, the molecular underpinnings regulating SM
40 production and the role of small regulatory RNAs (sRNAs) in this process are unknown. Here
41 we describe the mechanism underlying RNA-mediated control of SM synthesis. We show that
42 the Hfq-dependent sRNA, ArcZ, is an essential requirement for SM production. We discovered
43 that ArcZ directly base-pairs with the mRNA encoding HexA, a key repressor of SM genes. We
44 further demonstrate that the ArcZ regulon is not restricted to SM production, but rather
45 modulates up to ~15% of the transcriptional output in both *Photorhabdus* and *Xenorhabdus*.
46 Together, our study shows that sRNAs are crucial for SM production in these species, reveals
47 previously unknown targets for biosynthetic pathway manipulations, and offers a new tool for
48 the (over)production, isolation and identification of unknown natural products.

49

50

51 Regulation via *trans*-encoded sRNAs typically occurs by imperfect base-pairing of sRNAs with
52 their mRNA targets and can be mediated by RNA chaperones such as Hfq and ProQ^{13,14}. RNA
53 duplex formation is usually short (6 to 12 nucleotides) and can result in conformational
54 changes in RNA secondary structure with various regulatory outcomes⁵. The RNA chaperone
55 Hfq is highly conserved throughout the bacterial kingdom⁶. Several complex phenotypes have
56 been attributed to Hfq with its regulatory roles being achieved by stabilizing sRNAs and/or
57 mRNAs, mediating base-pairing of sRNAs and their targets, modulation of mRNA translation⁶,
58 as well as accelerating the degradation of sRNAs and their targets⁷. Expression of sRNAs is
59 highly dynamic, with sRNA profiles in *Salmonella* shown to be strongly dependent on the
60 bacterial growth phase⁸. ArcZ is one of the few Hfq-bound sRNAs whose expression remains
61 relatively constant in *Salmonella* throughout the growth phases, making up ~7-12% of all reads
62 identified by Hfq co-immunoprecipitation experiments⁸. ArcZ is transcribed as a 129 nt
63 primary transcript (Figure 1A) and processed into a stable short form (~50 nt)⁸⁻¹⁰. The
64 processed short form of ArcZ directly activates *rpoS* translation¹⁰ and inhibits the expression
65 of several other genes¹⁰. In *E. coli*, the expression of *arcZ* is repressed by the ArcA-ArcB two-
66 component system under anaerobic conditions. In a negative feedback loop, *arcZ* represses,
67 and is repressed by *arcB* transcription¹⁰. Although there is a wealth of research on ArcZ in *E.*
68 *coli* and *Salmonella*⁸⁻¹⁰, its function in other bacteria remains unclear.

69

70 SM in bacteria are often responsible for ecologically important activities¹¹. In the case of
71 *Xenorhabdus* and *Photorhabdus*, SMs play an essential role in cross-kingdom interactions with
72 nematodes, various insects, as well as bacterial and fungal species competing for the same
73 food source¹². Our earlier work on *Photorhabdus* showed that deletion of *hfq* resulted in
74 severe perturbation of gene networks, including several key regulators⁴. This led to an overall

75 decrease in SM production and a failure of the bacteria to support their obligate symbiosis
76 with nematodes. Despite SMs playing a central role in the life cycle of the symbiosis, the exact
77 ecological function for many of these compounds remained unknown. Over the past years,
78 significant advances have been made towards finding bioactivities for many of the SMs, with
79 assigned functions including cell-cell communication (photopyrones, dialkylresorcinols^{13,14}),
80 nematode development (isopropylstilbene¹⁵), defense against food-competitors
81 (isopropylstilbene, rhabdopeptides^{15,16}), or insect pathogenicity (rhabduscin, rhabdopeptides,
82 glidobactin¹⁶⁻¹⁸). However, understanding the full potential of SMs in these bacteria is still
83 hampered by a somewhat limited understanding of when individual SMs are produced, and
84 their regulation in general. Regulation of SM in *Photorhabdus* and *Xenorhabdus* so far
85 implicated the regulators Hfq, HexA (also LrhA), LeuO and Lrp^{3,4,19,20}. Deletion of *hfq* in
86 *Photorhabdus* resulted in complex regulatory changes, including a strong up-regulation of
87 HexA, a known repressor of SM production⁴. Consequently, SM production was completely
88 abolished in this strain and nematode development was severely restricted.

89
90 Given the overlapping lifecycles and niche occupation, we hypothesized that deletion of *hfq*
91 in *Xenorhabdus* would have a similar effect on the production of SMs and the transcriptome.
92 We confirmed this in *X. szentirmaii* DSM16338 using both high-performance LCMS/MS and
93 RNA-seq (Supplementary Results, Supplementary Table S1). To further elucidate the
94 mechanism of SM regulation, we investigated Hfq binding partners. To this end, we sequenced
95 both *X. szentirmaii* and *P. laumondii* using a sRNA sequencing protocol and combined this with
96 CappableSeq data to globally annotate transcriptional start sites belonging to coding
97 sequences or potential novel sRNAs (Supplementary Results, Supplementary Table S2). We
98 confirmed expression of several of these sRNAs by Northern blot analysis (Supplementary

99 Figures S1 & S2). To identify RNA-protein interactions on a global scale, we next employed
100 RNA immunoprecipitation followed by high-throughput sequencing (RIPseq) using
101 chromosomally produced Hfq:3xFLAG protein as bait. We performed these experiments at
102 two different cell densities (*i.e.* OD₆₀₀ 0.5 and OD₆₀₀ 5.0, for a full list of ODs from different
103 experiments, see Supplementary Table S3). From the corresponding sequencing data, we first
104 identified regions of 5 bp or more that were enriched in our tagged Hfq strain (see Methods).
105 We then searched for sRNAs (see Supplementary Results) that were specifically enriched in
106 the tagged samples, when compared to the untagged samples. We identified a total of 37
107 binding sites in annotated sRNAs (35 unique sRNAs) at OD₆₀₀ 0.5 and 37 binding sites (34
108 unique) at OD₆₀₀ 5.0 that were enriched by at least three-fold in both replicates (Figure 1B,
109 Supplementary Table S4). During early exponential growth, 11 sRNAs (out of 35) were
110 identified that are described to associate with Hfq in other species, while 10 (out of 34) are
111 known from those that were enriched at OD₆₀₀ 5.0. As a second step, we examined mRNAs
112 enriched in the data. At OD 5.0, 402 mRNAs and 32 annotated 5'-UTRs were identified to
113 associate with Hfq. At OD 0.5 a total of 1,003 mRNAs and 29 5'-UTRs were detected (Figure
114 1C, Supplementary Table S5).

115

116 We hypothesized that the performed Hfq RIP-seq analysis would allow us to identify key
117 sRNAs involved in SM repression. However, our analysis identified >50 potential sRNAs binding
118 Hfq (across both ODs, Figure 1B). Therefore, rather than individually deleting each sRNA, we
119 constructed a transposon mutant library using pSAM-BT_Kan (see Methods and
120 Supplementary Results) and searched for phenotypes consistent with that of the Δhfq strain.
121 The red color afforded to the bacteria by anthraquinone (AQ) production makes the strain
122 especially suitable for transposon mutagenesis when screening for mutants defective in SM

123 biosynthesis. We screened approximately 60,000 clones for obvious phenotypic alterations.
124 Several mutants were defective in some facets of SM production and showed growth defects
125 (Supplementary Results, Supplementary Figure S3, Supplementary Table S6), however, only
126 one displayed the desired phenotype. Re-sequencing of this strain followed by read mapping
127 revealed that the transposon was inserted within an intergenic region associated with the *arcZ*
128 sRNA gene (Supplementary Figure S4).

129

130 ArcZ is a well-known Hfq-associated sRNA, which also appeared in our list of Hfq-bound sRNAs
131 in *P. laumondii* (Figure 1B, Supplementary Table S4). To verify that the observed phenotype
132 was derived from the transposon-insertion, we generated a $\Delta arcZ$ mutant by deleting the
133 major part of the sRNA (Supplementary Figure S4) and a complemented strain by
134 reintroducing an intact version of *arcZ* at the original locus. Northern blot analysis was
135 performed to verify the absence of ArcZ in the deletion mutant and the presence of ArcZ in
136 the WT and the complementation mutant (Figure 2A). RNA sequencing of $\Delta arcZ$ mutant
137 showed severe transcriptomic changes compared to the WT and $\Delta arcZ::arcZ$ mutant of *P.*
138 *laumondii*, reminiscent of that seen in *P. laumondii* Δhfq (Supplementary Results,
139 Supplementary Tables S7 & S8). SM production titers in the $\Delta arcZ$ strain were strongly
140 decreased, similar to that seen in the transposon-insertion mutant and the complementation
141 strain restored SM production (Figure 2B-H).

142

143 To corroborate the role of ArcZ in SM production, ArcZ mRNA targets were predicted using
144 CopraRNA²¹ (Supplementary Table S9 & S10). One hit, warranting further investigation was
145 *hexA* (*IrhA*), which was previously identified as a highly upregulated gene in our strains and

146 which represses SM production in both *P. laumondii*²² and *Xenorhabdus*³. CopraRNA predicted
147 a 9 bp-long binding site in the 5'-UTR of *hexA* (Figure 3A). We also identified a corresponding
148 enriched RNA sequence upstream of the *hexA* CDS at OD₆₀₀ 0.5 in the RIPseq experiments
149 (Figure 1C, Supplementary Figure S5). We hypothesized that, through Hfq, ArcZ might bind to
150 the *hexA* transcript leading to repression of HexA. In lab cultures, where SMs are produced,
151 we hypothesized that Hfq and ArcZ prevent HexA production, allowing the strain to synthesize
152 SM. However, if either *hfq* or *arcZ* were deleted, we would expect that *hexA* is no longer
153 repressed, resulting in severely reduced SM production. To test this idea, we altered the
154 predicted site of the ArcZ-*hexA* interaction to a *PacI* restriction site (TTAATTAA) and created a
155 knock-in of *hexA* with the modified sequence in a $\Delta hexA$ strain (Supplementary Figure S6A&B).
156 We predicted that a knock-in of *hexA* with an altered 5'-UTR would result in a failure of ArcZ
157 to bind, leading to reduced SM titers. Indeed, the SM production titers in the knock-in mutant
158 with the altered binding site upstream of *hexA* were greatly reduced (Figure 2C-H).

159

160 To verify the proposed interaction region, we conducted a compensatory base mutation study
161 in *E. coli*. The fifth base-pair of the proposed interaction region was exchanged in the *arcZ*
162 sequence, the *hexA* 5'UTR, or both by site directed mutagenesis (Figure 3A). The *hexA* 5' UTR
163 sequence was fused to *gfp*. The GFP output was measured to determine the efficiency of
164 inhibition (Figure 3B & C). For the control, the GFP signal derived from the expression of
165 *hexA::gfp* was measured and set to 1. When p-*arcZ* was expressed together with *hexA::gfp*,
166 HexA repression was increased 5.7-fold compared to the control. Additionally, when p-*arcZ**
167 (G79C) was expressed, ArcZ* was no longer able to repress HexA. For *hexA*::gfp* (C-46G) in
168 combination with the native ArcZ, HexA repression was only slightly increased compared to
169 the control, suggesting that ArcZ can still bind to the 5' UTR of *hexA* but with a much reduced

170 efficiency. When combining p-*arcZ** (G79C) with *hexA*::gfp* (C-46G), HexA::GFP repression
171 was increased almost 10-fold, which confirms our hypothesis that ArcZ binds to the 5'-UTR of
172 *hexA* to repress HexA production. Of note, this base-pairing sequence is located ~50 nts
173 upstream of the *hexA* translational start site (Fig. 3A) and thus ArcZ binding is unlikely to
174 compete with recognition of the mRNA by 30S ribosomes²³. Instead, alignment of the *P.*
175 *laumondii hexA* 5' UTR revealed that the ArcZ binding site is CA-rich and highly conserved
176 among other SM-producing bacteria (Supplementary Figure S7). CA-rich sequences located in
177 proximity to translation initiation sites are well-known translational enhancers and
178 sequestration of these regulatory elements by sRNAs has been reported to down-regulate
179 gene expression^{24,25}, which might also be relevant for the ArcZ-*hexA* interaction reported
180 here. In addition, we conducted a proteomic analysis with the WT, Δ *arcZ*, Δ *hfq* and
181 Δ *hexA::hexA_PacI_UTR* strains of *P. laumondii*. We used a label free quantification of
182 quadruplicate samples to determine the HexA abundance in each strain. HexA levels were
183 significantly elevated in all mutant strains (11.8 to 22.7 fold, Supplementary Table 11)
184 compared to the WT, further supporting this mechanism of regulation for SM production.

185

186 The *arcZ* gene and its genomic organization are highly conserved among enterobacterial
187 species⁹ (Figure 1A). Since the control of SMs in *Photorhabdus* relays a fundamental ability for
188 these bacteria to occupy their specific niche, we investigated the possibility that the same
189 mechanism occurs in the closely related *Xenorhabdus*. Given the SM reduction in *X. szentirmaii*
190 Δ *hfq*, we constructed a Δ *arcZ* mutant in *X. szentirmaii* in a similar fashion to *P. laumondii*, by
191 deleting 90bp of the predicted *arcZ* sequence. We verified via Northern blots that ArcZ was
192 no longer produced by the deletion mutant and that complementation of the deletion led to
193 production of ArcZ again (Figure 3D). Subsequently, we investigated the transcriptome and

194 SM profile of the WT, deletion and complementation mutant. (Figure 3E, Supplementary Table
195 S12). Consistent with *P. laumondii*, deletion of *arcZ* resulted in a global effect on the
196 transcriptome as well as severely reduced SM titers, both of which was complemented in the
197 $\Delta arcZ::arcZ$ complementation mutant (Figure 3E, Figure 4).

198

199 Our results highlight the critical role of ArcZ in regulating specialized metabolism in these
200 strains. In fact, the critical nature of SM from *Photorhabdus* and *Xenorhabdus* in modulating
201 the insect immune response indicated that ArcZ might be required for niche occupation by
202 these bacteria. In the *P. laumondii* $\Delta arcZ$ strain, we observed an inability to support nematode
203 development (Supplementary Figure S8), consistent with our earlier observations in the Δhfq
204 mutant⁴. However, the same was not seen in *X. szentirmaii*. We suspect this might be because
205 of the observed increase in protoporphyrin IX (PPIX) production in the *X. szentirmaii* $\Delta arcZ$
206 strain. PPIX is a precursor of heme, which is an important cofactor for key biological processes
207 such as oxidative metabolism²⁶, protein translation²⁷, maintaining protein stability²⁸ and many
208 others. However, PPIX cannot be synthesized *de novo* by *Caenorhabditis elegans* and other
209 nematodes²⁹. The nematodes therefore rely on external PPIX sources (such as from symbiotic
210 bacteria), which positively affects their growth, reproduction and development³⁰. It is
211 interesting that despite *P. laumondii* also being capable of producing PPIX, the *Heterorhabditis*
212 nematode reproduction was not supported in either the $\Delta arcZ$ mutant, nor the Δhfq strain.
213 This is possibly indicative of the nematode specific requirements for reproduction, which may
214 also include isopropylstilbene as an essential factor in *Heterorhabditis*¹⁵, where no analogous
215 compound is yet known to be required for *Steinernema*.

216

217 In both *Xenorhabdus* and *Photorhabdus*, nearly all analyzed SM-related genes were found to
218 be down-regulated in the $\Delta arcZ$ mutant, in accordance with the impaired SM production
219 (Figure 4A & B). This provides a chemical background that is devoid of natural products, which
220 allows for isolation and identification of a desired compound due to the absence of
221 compounds with similar retention times. Therefore, $\Delta arcZ$ mutants could offer a powerful tool
222 for (over-) production and identification of new natural products. As a proof of concept, we
223 conducted a promotor exchange in front of *gxpS* in both *X. szentirmaii* $\Delta arcZ$ and *X. szentirmaii*
224 Δhfq and compared GXP-C production after induction to the WT (Figure 4C). GXP-C production
225 was found to be increased 90.4 (\pm 4.7)-fold in *X. szentirmaii* $\Delta arcZ::pCEP_GxpS$ and increased
226 138.6 (\pm 17.1)-fold in *X. szentirmaii* $\Delta hfq::pCEP_GxpS$ compared to the WT (Figure 4C). The
227 striking increase in production, as well as the dramatically reduced chemical background in
228 both strains, highlights the potential of exploiting this regulatory cascade for selective SM
229 production in a strain well-suited for natural product detection. Recently, we showed that this
230 strategy could be applied in a high-throughput manner for rapid screening of bioactivities³¹.
231 The same strategy used here in a $\Delta arcZ$ strain, demonstrates an alternative route to activation,
232 without the complex perturbations associated with deleting the major RNA chaperone in
233 these bacteria. Interestingly, some comparisons between these mechanisms can be drawn in
234 other SM-producing Enterobacteriaceae (Figure 1A). *Erwinia* is a genus of plant pathogenic
235 bacteria that produce SMs, where Hfq and ArcZ have both been implicated in virulence³²,
236 while HexA is a negative regulator of secondary metabolites in these bacteria³³. Similar
237 parallels can also be seen from *Serratia*³⁴⁻³⁶ and *Pseudomonas*³⁷, two other prolific SM
238 producers. Although further investigations will be required to ascertain whether these
239 apparent similarities represent identical mechanisms, the conserved nature of ArcZ in other

240 SM-producing Enterobacteriaceae could suggest that this strategy may yield new avenues for
241 rapid investigation into SM biosynthesis in other taxa.

242

243

244 **Materials & Methods**

245 **Bacterial culture conditions**

246 All *Photorhabdus* and *Xenorhabdus* strains were grown in LB with shaking for at least 16 hours
247 at 30°C. *E. coli* strains were grown in LB with shaking for at least 16 hours at 37°C. The medium
248 was supplemented with chloramphenicol (34 µg/ml), ampicillin (100 µg/ml), rifampicin
249 (50µg/ml) or kanamycin (50 µg/ml) when appropriate. Promotor exchange mutants were
250 induced by adding L-arabinose (2%, v/v) to the cultures. All plasmids and strains used in this
251 study are listed in Supplementary Table S13 & S14.

252

253 **Nematode bioassays**

254 All nematodes were cultivated in *Galleria mellonella* and collected on white traps as previously
255 described. Nematode bioassays were also performed as described elsewhere⁴.

256

257 **Creation of transposon mutant library**

258 For the transposon mutagenesis, the plasmid pSAM_Kan (containing the mariner transposon)
259 was constructed using pSAM_BT³⁸ as a template. To do this, the plasmid was linearized using
260 the primers NN191/NN192. The kanamycin resistance cassette was amplified from the
261 pCOLA_ara_tacl plasmid using the primers NN193/NN194 introducing complementary
262 overhangs to pSAM_BT at both ends of the PCR fragment. The kanamycin resistance cassette
263 was fused with the linearized pSAM_BT plasmid using Hot Fusion cloning thereby replacing
264 the erythromycin resistance cassette with kanamycin resistance. *E. coli* ST18 was transformed
265 with the plasmid pSAM_Kan and further used for the creation of the transposon mutant

266 library of *P. laumondii* TTO1 through conjugation. Transposon-insertion mutants were
267 selected on LB agar containing kanamycin. All primer sequences are listed in Supplementary
268 Table S15.

269

270 **Construction of mutant strains**

271 For the deletion of the majority of ArcZ in *P. laumondii* TTO1, a 1123 bp upstream and a 1014
272 bp downstream product was amplified using the primers NN276/NN277 and NN278/NN279,
273 respectively. The PCR products were fused using the complementary overhangs introduced
274 by the primers and cloned into the *Pst*I and *Bgl*III linearized pEB17 plasmid. The resulting
275 plasmid was used for transformation of *E. coli* s17-1 λ pir. Conjugation of the plasmid in *P.*
276 *laumondii* strains and generation of deletion strains by homologous recombination through
277 counter selection was done as previously described³⁹. Deletion mutants were verified by PCR
278 using the primers NN281/NN282 yielding a 632 bp fragment for mutants genetically equal to
279 the WT and a 502 bp fragment for the desired deletion mutant. Complementation of the ArcZ
280 deletion was achieved by inserting the full and intact version of ArcZ at the original locus. To
281 do this, a 2207 bp PCR product was amplified using the primers NN276/NN279 including the
282 upstream and downstream region required for homologous recombination and the full length
283 ArcZ. The fragment was cloned into pEB17 as described above. The verified plasmid construct
284 was used for transformation of *E. coli* s17-1 λ pir cells. The plasmid was transferred into *P.*
285 *laumondii* Δ arcZ by conjugation and integrated into the genome of *P. laumondii* Δ arcZ by
286 homologous recombination. The knock-in mutant was generated by a second homologous
287 recombination through counter selection on LB plates containing 6% sucrose. Knock-in
288 mutants were verified by PCR using the primers NN281/NN282 yielding a 632 bp fragment.

289 The same strategy was used for the construction of the mutant strains in *X. szentirmaii*. To
290 generate the promotor exchange mutants in front of *gxpS*, the plasmid pCEPKMR_ORF00346
291 was transferred into *X. szentirmaii* Δ *arcZ* and *X. szentirmaii* Δ *hfq* by conjugation and integrated
292 into the genome by homologous recombination.

293

294 **DNA extraction**

295 Genomic DNA was extracted using the Gentra Puregene Yeast/Bact Kit (Qiagen) following the
296 manufacturer's instructions. For sequencing of transposon-insertion mutants, genomic DNA
297 was extracted using the DNeasy Blood & Tissue Kit (Qiagen).

298

299 **DNA sequencing and identification of transposon insertion site**

300 DNA isolated from the transposon-insertion mutants was sequenced on the Illumina NextSeq
301 platform. DNA libraries were constructed using the Nextera XT DNA preparation kit (Illumina)
302 and whole genome sequencing was performed using 2 x 150bp paired-end chemistry. A
303 sequencing depth of >50× was targeted for each sample. Genomes were assembled with
304 SPAdes (v 3.10.1)⁴⁰ and annotated with Prokka v 1.12⁴¹.

305 Completed genome sequences were analysed and viewed in Geneious v9.1
306 (<https://www.geneious.com>).

307

308 **RNA extraction, sequencing and analysis**

309 Pre-cultures of *P. laumondii* TTO1, *X. szentirmaii* DSM16338, and their respective ArcZ
310 deletion and knock-in mutants were grown in LB broth overnight with shaking, at 30 °C. The
311 following day, the pre-cultures were used to inoculate fresh LB at an OD₆₀₀ of 0.3. Cells were
312 grown to mid-exponential phase (OD values for each experiment can be found in
313 Supplementary Table S3). RNA was extracted using the RNeasy Mini Kit (Qiagen) following the
314 manufacturer's instructions. To facilitate cell lysis, the cells were pelleted and snap frozen in
315 liquid nitrogen for 1 min after removing the supernatant. After thawing and resuspending in
316 lysis buffer, the cells were vortexed for 30 sec before proceeding with the protocol. RNA for
317 small RNA libraries were extracted in duplicate, during the mid-exponential phase for *P.*
318 *laumondii* TTO1 and *X. szentirmaii*.

319 RNA was sequenced with 150bp paired-end sequencing by Novogene following rRNA
320 depletion with a RiboZero kit and library preparation following the Illumina protocol for
321 strand-specific libraries. Raw data was trimmed using Trimmomatic⁴² and mapped to the
322 reference genome downloaded from NCBI (NC_005126.1 for *P. laumondii* and
323 NZ_NIBV00000000.1 for *X. szentirmaii*) using bowtie2 (v2.3.4.3)⁴³. Resulting .sam files were
324 converted to .bam files using samtools (v1.8)⁴⁴ and featureCounts (a part of the subread
325 package)⁴⁵ was used to count reads mapping to annotated genes. Count files were then
326 uploaded to degust (<http://degust.erc.monash.edu/>) and analyzed using the voom/limma
327 method of normalization. Only genes with an absolute fold change >2 and false discovery rate
328 < 0.01 were considered significantly regulated.

329

330

331 **Northern blot analysis**

332 For Northern blot analysis, total RNA was prepared and analyzed as described previously⁴⁶.
333 Briefly, RNA samples were separated on 6% polyacrylamide / 7 M urea gels and transferred to
334 Hybond–XL membranes (GE Healthcare) by electro-blotting. Membranes were hybridized in
335 Roti-Hybri-Quick buffer (Roth) at 42°C with gene-specific [³²P] end-labeled DNA
336 oligonucleotides, and washed in three subsequent steps with SSC (5x, 1x, 0.5x) / 0.1% SDS
337 wash buffer. Signals were visualized on a Typhoon FLA 7000 phosphorimager (FUJIFILM).
338 Oligonucleotides for Northern blot analyses are listed in Supplementary Table S15.

339

340 **Compensatory base mutation and GFP fluorescence assay**

341 Plasmids pMH078 and pMH079 were generated using Gibson assembly⁴⁷. For plasmid
342 pMH078 the *arcZ* gene was amplified using *P. laumondii* TT01 genomic DNA with
343 oligonucleotides KPO-6147 and KPO-6148 and fused into a pEVS143 vector backbone⁴⁸,
344 linearized with KPO-0092 and KPO-1397. To construct plasmid pMH079, the 5'UTR and the
345 first 20 aa of *hexA* were amplified using *P. laumondii* TT01 genomic DNA with KPO-6145 and
346 KPO-6146, and the pXG10-*gfp* vector⁴⁹ was linearized with KPO-1702 and KPO-1703. pMH078
347 and pMH079 served as templates to insert single point mutations in the *arcZ* gene as well as
348 the *hexA* 5'UTR using site-directed mutagenesis and oligonucleotide combinations KPO-
349 6156/KPO-6157 and KPO-6164/KPO-6165, respectively, yielding plasmids pMH080 and
350 pMH081.

351 Target regulation using GFP reporter fusions was analyzed as described previously⁴⁹. *E. coli*
352 Top10 cells were grown overnight in LB medium (37°C, 200 rpm shaking conditions). Three
353 independent cultures were used for each strain. Cells were washed in PBS and GFP

354 fluorescence intensity was determined using a Spark 10 M plate reader (TECAN). Control
355 samples not expressing fluorescence proteins were used to subtract background fluorescence.

356

357 **CappableSeq analysis**

358 Cappable seq was performed as previously described⁵⁰ by Vertis Biotechnologies (Germany).

359 Raw sequences were trimmed with Trimmomatic⁴² and mapped with bowtie2⁴³ to

360 NC_005126.1 for *P. laumondii* and NZ_NIBV00000000.1 for *X. szentirmaii*. Transcriptional start

361 sites were detected using readXplorer's (v2.2.3)⁵¹ built in TSS detection function with the

362 following settings: use only single perfect matches, minimum number of read starts = 100,

363 minimum percent coverage increase = 750, detect novel transcripts, min. transcript extension

364 = 40, max distance to feature of leaderless transcripts = 5, associate neighbouring TSS within

365 3bp.

366

367 **RIP-seq analysis**

368 Overnight cultures of *P. laumondii* TTO1 (WT and Hfq^{3xFLAG}) were inoculated into fresh LB

369 media in duplicate and grown at 30 °C with shaking at 200 rpm. Bacteria were harvested by

370 centrifugation at 4°C, 4000 rpm for 15 min when cells reached OD₆₀₀=0.5 and OD₆₀₀=5.0. Cell

371 pellets were resuspended in 1 mL lysis buffer (20 mM Tris pH 8.0, 150 mM KCl, 1 mM MgCl₂,

372 1 mM DTT) and pelleted again by centrifugation (5 min, 11,200 g, 4°C). The supernatants were

373 discarded and the pellets were snap-frozen in liquid nitrogen. After thawing on ice, cells were

374 resuspended in 800 µl lysis buffer and transferred into tubes containing 300 µl glass beads to

375 break cells via a Bead Ruptor (150 sec, twice, 2 min break on ice in between). After short

376 centrifugation (15,000 g, 4°C), lysates were transferred into fresh precooled tubes and

Appendix

377 centrifuged for 30 minutes at 15,200 g at 4°C. The cleared lysates were transferred into new
378 tubes and incubated with 35 µl FLAG-antibody (Monoclonal ANTI-FLAG M2, Sigma, #F1804)
379 with rotation for 45 min at 4°C, followed by addition of 75 µl Protein G Sepharose (Sigma,
380 #P3296) and rotating for 45 min at 4°C again. After five wash steps with lysis buffer (via
381 inverting the tube gently and centrifuging for 4 min at 4° C), samples were subjected to RNA
382 and protein separation by Phenol:Chloroform:Isoamylalcohol (P:C:I; 25:24:1, pH 4.5, Roth)
383 extraction. The upper phase (~ 500 µl) was transferred into to a new tube and precipitated
384 overnight at -20°C with 1.5 ml EtOH:Na(acetate) (30:1) and 1.5 µl GlycoBlue (#AM9516,
385 Ambion). After centrifugation for 30 minutes at 11,200 rpm at 4°C, RNA pellets were washed
386 with 500 µl 70% EtOH, dried and resuspended in 15.5 µl nuclease-free H₂O. RNA was treated
387 with 2 µl DNase I, 0.5 µl RNase inhibitor and 2 µl 10x DNase buffer at 37°C for 30 min.
388 Afterwards, samples were supplemented with 100 µl H₂O, and again subjected to P:C:I
389 extraction. The upper phase (~120 µl) was transferred into a new tube with addition of 2.5-3
390 volumes (~350 µl) of EtOH:Na(acetate) (30:1) and stored at -20°C overnight for RNA
391 precipitation. RNA pellets were harvested via centrifugation for 30 min at 13,000 rpm, 4 °C,
392 and washed with 500 µl 70% EtOH, dried and resuspended in nuclease-free H₂O. cDNA
393 libraries were prepared using the NEBNext Small RNA Library Prep Set for Illumina (NEB,
394 #E7300S) according to the manufacturer's instructions and sequenced on a HiSeq 1500 system
395 in single-read mode with 100 nt read length.

396 For RIPseq analysis, the enriched/control sample pairs were normalized by the number of raw
397 reads present after trimming. Depth counts of all samples were obtained using samtools
398 (v1.8)⁴⁴. Only nucleotide positions with a depth of at least 50 reads in the enriched samples
399 were taken for further analysis. The corresponding depth in the unenriched samples was
400 matched for each nucleotide. A region was considered to be enriched if the enrichment factor

401 was at least three and the corresponding 'enriched' nucleotide was present in both sample
402 pairs. Finally, we considered a region to be enriched if more than five consecutive nucleotides
403 were identified as enriched.

404

405 **ArcZ binding prediction**

406 ArcZ from *E. coli* was used to define the boundaries of ArcZ in *Xenorhabdus* and *Photorhabdus*.
407 We then took our annotated ArcZ sequence together with several ArcZ homologs from other
408 Enterobacteriaceae (listed in Supplementary Table S9) and used the online CopraRNA tool²¹,
409 a part of the Freiburg RNA tools suite⁵², with default parameters.

410

411 **Metabolite extraction and HPLC-MS/MS analysis**

412 Fresh 10 ml of LB was inoculated with an overnight culture to an OD₆₀₀ = 0.1. After 72 h of
413 cultivation at 30°C with shaking, 1 ml of the culture was removed from the culture, centrifuged
414 for 20 min at 13,300 rpm and the supernatant was directly subjected for HPLC-UV/MS analysis
415 using a Dionex Ultimate 3000 system with a Bruker AmaZon X mass spectrometer. The
416 compounds peak areas were quantified using TargetAnalysis 1.3 (Bruker). All analyzed
417 compounds are listed in Supplementary Table S16.

418

419 **Proteome analysis**

420 The detail of the proteomics procedure can be assessed in
421 (<https://pubs.acs.org/doi/abs/10.1021/acs.jproteome.8b00216>). In short, to extract proteins
422 from *E.coli*, frozen cell pellets 300 μ L lysis buffer (0.5% Na-desoxycholate in 100 mM NH_4HCO_3)
423 were added to the cell pellet, and incubated at 95°C for 10. The protein concentration in the
424 supernatant was determined with a BCA Protein Assay Kit (Thermo Fisher, #23252). Reduction
425 and alkylation was performed at 95 °C using 5mM TCEP and 10mM Chloroacetamide for
426 15min. 50 μ g of protein was transferred to new reaction tubes and protein digestion was
427 carried out overnight at 30 °C with 1 μ g trypsin (Promega). After digest, the peptides were
428 desalted using CHROMABOND Spincolumns (Macherey-Nagel) that were conditioned with
429 500 μ L of acetonitrile and equilibrated with 500 μ L and 150 μ L 0.1% TFA. After loading the
430 peptides were washed with 500 μ L 0.1% TFA in 5:95 acetonitrile:water, peptides were eluted
431 with 400 μ L 0.1% TFA in 50:50 acetonitrile:water. Peptides were concentrated and dried under
432 vacuum at 50°C and dissolved in 100 μ L 0.1% TFA by 25 s of sonication and incubation at 22°C
433 under shaking at 1200 rpm for 5 min. 1 μ g peptide was analyzed using liquid chromatography-
434 mass spectrometry (LC-MS/MS).

435 The LC-MS/MS analysis including label-free quantification was carried out as previously
436 described in (<https://pubs.acs.org/doi/abs/10.1021/acs.jproteome.8b00216>) with minor
437 modifications.

438 LC-MS/MS analysis of protein digests was performed on Q-Exactive Plus mass spectrometer
439 connected to an electrospray ion source (Thermo Fisher Scientific). Peptide separation was
440 carried out using Ultimate 3000 nanoLC-system (Thermo Fisher Scientific), equipped with
441 packed in-house C18 resin column (Magic C18 AQ 2.4 μ m, Dr. Maisch). The peptides were first

442 loaded onto a C18 precolumn (preconcentration set-up) and then eluted in backflush mode
443 with a gradient from 98 % solvent A (0.15 % formic acid) and 2 % solvent B (99.85 %
444 acetonitrile, 0.15 % formic acid) to 35 % solvent B over 30 min. Label-free quantification was
445 done using Progenesis QI software (Nonlinear Dynamics, v2.0), MS/MS search was performed
446 in MASCOT (v2.5, Matrix Science) against the Uniprot *Photorhabdus laumondii* protein
447 database. The following search parameters were used: full tryptic search with two missed
448 cleavage sites, 10ppm MS1 and 0.02 Da fragment ion tolerance. Carbamidomethylation (C) as
449 fixed, oxidation (M) and deamidation (N,Q) as variable modification. Progenesis outputs were
450 further processed with SafeQuant (<https://www.ncbi.nlm.nih.gov/pubmed/23017020>).

451

452 **Data availability**

453 All .mzXML files from HPLC-MS runs are available at MassIVE (<https://massive.ucsd.edu>) under
454 the ID MSV000084163. Raw sequence data is available at the European nucleotide archive
455 under project accession numbers PRJEB33827 and PRJEB24159. Updated annotation files are
456 available in .gff format under Supplementary Tables S17 (*P. laumondii*) and S18 (*X.*
457 *szentirmaii*). The proteomic data can be accessed at PRIDE (<https://www.ebi.ac.uk/pride/>)
458 with the project accession number PXD019095.

459

460 **Acknowledgements**

461 This work was funded in part by the DFG (SFB 902, Project B17) and the LOEWE Centre for
462 Translational Biodiversity Genomics (TBG) supported by the State of Hesse. K.P. acknowledges
463 funding by DFG (EXC 2051, Project 390713860), the Vallee Foundation, and the European

464 Research Council (StG-758212). We thank Andrew Goodman for providing pSAM-BT and
465 helpful discussions. We thank Laura Pöschel and Antje K. Heinrich for plasmid construction.

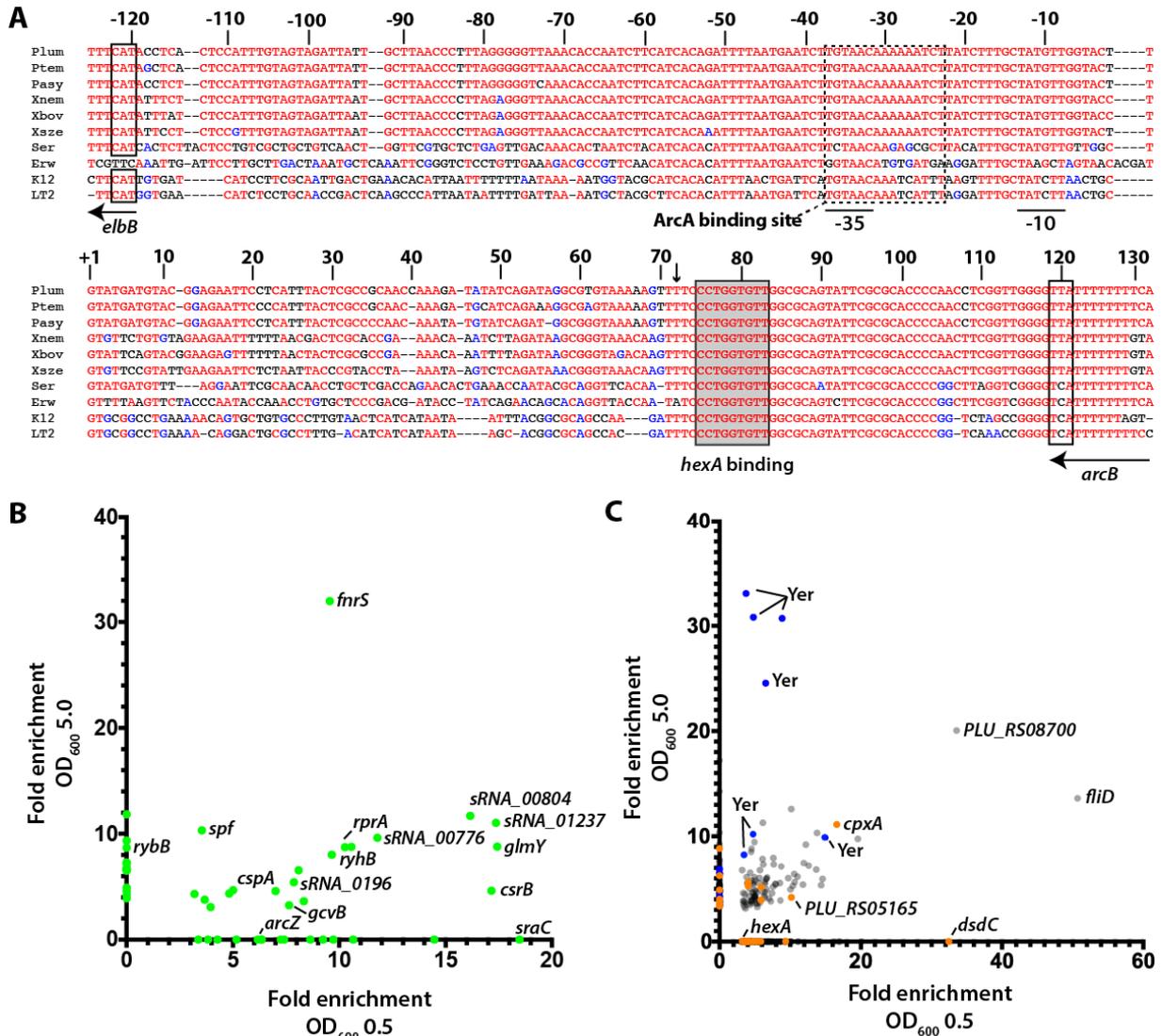
466

467 **References**

- 468 1. Stock, S. P., Campbell, J. F. & Nadler, S. A. Phylogeny of *Steinernema travassos*, 1927
469 (Cephalobina: Steinernematidae) inferred from ribosomal DNA sequences and
470 morphological characters. *J. Parasitol.* **87**, 877–889 (2001).
- 471 2. Forst, S., Dowds, B., Boemare, N. & Stackebrandt, E. Xenorhabdus and *Photorhabdus*
472 spp.: bugs that kill bugs. *Annu. Rev. Microbiol.* **51**, 47–72 (1997).
- 473 3. Engel, Y., Windhorst, C., Lu, X., Goodrich-Blair, H. & Bode, H. B. The Global Regulators
474 Lrp, LeuO, and HexA Control Secondary Metabolism in Entomopathogenic Bacteria.
475 *Frontiers in Microbiology* **8**, 209 (2017).
- 476 4. Tobias, N. J. *et al.* *Photorhabdus*-nematode symbiosis is dependent on *hfq*-mediated
477 regulation of secondary metabolites. *Environ. Microbiol.* **19**, 119–129 (2017).
- 478 5. Carrier, M.-C., Lalaouna, D. & Massé, E. Broadening the Definition of Bacterial Small
479 RNAs: Characteristics and Mechanisms of Action. *Annu. Rev. Microbiol.* **72**, 141–161
480 (2018).
- 481 6. Vogel, J. & Luisi, B. F. Hfq and its constellation of RNA. *Nat. Rev. Microbiol.* **9**, 578–589
482 (2011).
- 483 7. Santiago-Frangos, A. & Woodson, S. A. Hfq chaperone brings speed dating to bacterial
484 sRNA. *Wiley Interdiscip Rev RNA* **9**, e1475 (2018).
- 485 8. Chao, Y., Papenfort, K., Reinhardt, R., Sharma, C. M. & Vogel, J. An atlas of Hfq-bound
486 transcripts reveals 3' UTRs as a genomic reservoir of regulatory small RNAs. *EMBO J.* **31**,
487 4005–4019 (2012).
- 488 9. Papenfort, K. *et al.* Specific and pleiotropic patterns of mRNA regulation by ArcZ, a
489 conserved, Hfq-dependent small RNA. *Mol. Microbiol.* **74**, 139–158 (2009).
- 490 10. Mandin, P. & Gottesman, S. Integrating anaerobic/aerobic sensing and the general
491 stress response through the ArcZ small RNA. *EMBO J.* **29**, 3094–3107 (2010).
- 492 11. Beemelmans, C., Guo, H., Rischer, M. & Poulsen, M. Natural products from microbes
493 associated with insects. *Beilstein J Org Chem* **12**, 314–327 (2016).
- 494 12. Shi, Y.-M. & Bode, H. B. Chemical language and warfare of bacterial natural products in
495 bacteria-nematode-insect interactions. *Nat. Prod. Rep.* **35**, 309–335 (2018).
- 496 13. Brachmann, A. O. *et al.* Pyrones as bacterial signaling molecules. *Nat. Chem. Biol.* **9**,
497 573–578 (2013).
- 498 14. Brameyer, S., Kresovic, D., Bode, H. B. & Heermann, R. Dialkylresorcinols as bacterial
499 signaling molecules. *Proc. Natl. Acad. Sci. U.S.A.* **112**, 572–577 (2015).
- 500 15. Joyce, S. A. *et al.* Bacterial biosynthesis of a multipotent stilbene. *Angew. Chem. Int. Ed.*
501 *Engl.* **47**, 1942–1945 (2008).
- 502 16. Cai, X. *et al.* Entomopathogenic bacteria use multiple mechanisms for bioactive peptide
503 library design. *Nat Chem* **9**, 379–386 (2017).
- 504 17. Crawford, J. M., Portmann, C., Zhang, X., Roeffaers, M. B. J. & Clardy, J. Small molecule
505 perimeter defense in entomopathogenic bacteria. *Proc. Natl. Acad. Sci. U.S.A.* **109**,
506 10821–10826 (2012).
- 507 18. Theodore, C. M., King, J. B., You, J. & Cichewicz, R. H. Production of cytotoxic
508 glidobactins/luminmycins by *Photorhabdus asymbiotica* in liquid media and live
509 crickets. *J. Nat. Prod.* **75**, 2007–2011 (2012).
- 510 19. Lango-Scholey, L., Brachmann, A. O., Bode, H. B. & Clarke, D. J. The expression of *stIA* in
511 *Photorhabdus luminescens* is controlled by nutrient limitation. *PLoS ONE* **8**, e82152
512 (2013).

- 513 20. Kontnik, R., Crawford, J. M. & Clardy, J. Exploiting a global regulator for small molecule
514 discovery in *Phototrhobdus luminescens*. *ACS Chem. Biol.* **5**, 659–665 (2010).
- 515 21. Wright, P. R. *et al.* CopraRNA and IntaRNA: predicting small RNA targets, networks and
516 interaction domains. *Nucleic Acids Res.* **42**, W119–23 (2014).
- 517 22. Joyce, S. A. & Clarke, D. J. A *hexA* homologue from *Phototrhobdus* regulates
518 pathogenicity, symbiosis and phenotypic variation. *Mol. Microbiol.* **47**, 1445–1457
519 (2003).
- 520 23. Bouvier, M., Sharma, C. M., Mika, F., Nierhaus, K. H. & Vogel, J. Small RNA binding to 5'
521 mRNA coding region inhibits translational initiation. *Mol. Cell* **32**, 827–837 (2008).
- 522 24. Sharma, C. M., Darfeuille, F., Plantinga, T. H. & Vogel, J. A small RNA regulates multiple
523 ABC transporter mRNAs by targeting C/A-rich elements inside and upstream of
524 ribosome-binding sites. *Genes Dev.* **21**, 2804–2817 (2007).
- 525 25. Yang, Q., Figueroa-Bossi, N. & Bossi, L. Translation enhancing ACA motifs and their
526 silencing by a bacterial small regulatory RNA. *PLoS Genet.* **10**, e1004026 (2014).
- 527 26. Wenger, R. H. Mammalian oxygen sensing, signalling and gene regulation. *J. Exp. Biol.*
528 **203**, 1253–1263 (2000).
- 529 27. Chen, J. J. & London, I. M. Regulation of protein synthesis by heme-regulated eIF-2
530 alpha kinase. *Trends Biochem. Sci.* **20**, 105–108 (1995).
- 531 28. Qi, Z., Hamza, I. & O'Brian, M. R. Heme is an effector molecule for iron-dependent
532 degradation of the bacterial iron response regulator (Irr) protein. *Proc. Natl. Acad. Sci.*
533 *U.S.A.* **96**, 13056–13061 (1999).
- 534 29. Rao, A. U., Carta, L. K., Lesuisse, E. & Hamza, I. Lack of heme synthesis in a free-living
535 eukaryote. *Proc. Natl. Acad. Sci. U.S.A.* **102**, 4270–4275 (2005).
- 536 30. Bolla, R. Developmental nutrition of nematodes: the biochemical role of sterols, heme
537 compounds, and lysosomal enzymes. *J. Nematol.* **11**, 250–259 (1979).
- 538 31. Bode, E. *et al.* Promoter Activation in Δhfq Mutants as an Efficient Tool for Specialized
539 Metabolite Production Enabling Direct Bioactivity Testing. *Angew. Chem. Int. Ed. Engl.*
540 **58**, 18957–18963 (2019).
- 541 32. Zeng, Q., McNally, R. R. & Sundin, G. W. Global Small RNA Chaperone Hfq and
542 Regulatory Small RNAs Are Important Virulence Regulators in *Erwinia amylovora*. *J.*
543 *Bacteriol.* **195**, 1706–1717 (2013).
- 544 33. Mukherjee, A., Cui, Y., Ma, W., Liu, Y. & Chatterjee, A. K. *hexA* of *Erwinia carotovora*
545 ssp. *carotovora* strain Ecc71 negatively regulates production of RpoS and rsmB RNA, a
546 global regulator of extracellular proteins, plant virulence and the quorum-sensing
547 signal, N-(3-oxohexanoyl)-L-homoserine lactone. *Environ. Microbiol.* **2**, 203–215 (2000).
- 548 34. Matilla, M. A., Leeper, F. J., Salmond, George P. C. Biosynthesis of the antifungal
549 haterumalide, oocycin A, in *Serratia*, and its regulation by quorum sensing, RpoS and
550 Hfq. *Environ. Microbiol.* **17**, 2993–3008 (2015).
- 551 35. Wilf, N. M., Salmond, George P. C. The stationary phase sigma factor, RpoS, regulates the
552 production of a carbapenem antibiotic, a bioactive prodigiosin and virulence in the
553 enterobacterial pathogen *Serratia* sp ATCC 39006. *Microbiology (Reading, Engl.)* **158**,
554 648–658 (2012).
- 555 36. Wilf, N. M. *et al.* The RNA chaperone, Hfq, controls two luxR-type regulators and plays
556 a key role in pathogenesis and production of antibiotics in *Serratia* sp ATCC 39006.
557 *Environ. Microbiol.* **13**, 2649–2666 (2011).
- 558 37. Shanks, R. M. Q. *et al.* Suppressor analysis of *eepR* mutant defects reveals coordinate
559 regulation of secondary metabolites and serralyisin biosynthesis by EepR and HexS.
560 *Microbiology (Reading, Engl.)* **163**, 280–288 (2017).

- 561 38. Goodman, A. L. *et al.* Identifying genetic determinants needed to establish a human gut
562 symbiont in its habitat. *Cell Host Microbe* **6**, 279–289 (2009).
- 563 39. Brachmann, A. O. *et al.* A type II polyketide synthase is responsible for anthraquinone
564 biosynthesis in *Photorhabdus luminescens*. *Chembiochem* **8**, 1721–1728 (2007).
- 565 40. Bankevich, A. *et al.* SPAdes: A New Genome Assembly Algorithm and Its Applications to
566 Single-Cell Sequencing. *J. Comput. Biol.* **19**, 455–477 (2012).
- 567 41. Seemann, T. Prokka: rapid prokaryotic genome annotation. *Bioinformatics* **30**, 2068–
568 2069 (2014).
- 569 42. Bolger, A. M., Lohse, M. & Usadel, B. Trimmomatic: a flexible trimmer for Illumina
570 sequence data. *Bioinformatics* **30**, 2114–2120 (2014).
- 571 43. Langmead, B. & Salzberg, S. L. Fast gapped-read alignment with Bowtie 2. *Nat. Methods*
572 **9**, 357–359 (2012).
- 573 44. Li, H. *et al.* The Sequence Alignment/Map format and SAMtools. *Bioinformatics* **25**,
574 2078–2079 (2009).
- 575 45. Liao, Y., Smyth, G. K. & Shi, W. featureCounts: an efficient general purpose program for
576 assigning sequence reads to genomic features. *Bioinformatics* **30**, 923–930 (2014).
- 577 46. Fröhlich, K. S., Haneke, K., Papenfort, K. & Vogel, J. The target spectrum of SdsR small
578 RNA in *Salmonella*. *Nucleic Acids Res.* **44**, 10406–10422 (2016).
- 579 47. Gibson, D. G. Synthesis of DNA fragments in yeast by one-step assembly of overlapping
580 oligonucleotides. *Nucleic Acids Res.* **37**, 6984–6990 (2009).
- 581 48. Dunn, A. K., Millikan, D. S., Adin, D. M., Bose, J. L. & Stabb, E. V. New rfp- and pES213-
582 derived tools for analyzing symbiotic *Vibrio fischeri* reveal patterns of infection and lux
583 expression in situ. *Appl. Environ. Microbiol.* **72**, 802–810 (2006).
- 584 49. Corcoran, C. P. *et al.* Superfolder GFP reporters validate diverse new mRNA targets of
585 the classic porin regulator, MicF RNA. *Mol. Microbiol.* **84**, 428–445 (2012).
- 586 50. Tobias, N. J., Linck, A. & Bode, H. B. Natural Product Diversification Mediated by
587 Alternative Transcriptional Starting. *Angew. Chem. Int. Ed. Engl.* **57**, 5699–5702 (2018).
- 588 51. Hilker, R. *et al.* ReadXplorer 2-detailed read mapping analysis and visualization from
589 one single source. *Bioinformatics* **32**, 3702–3708 (2016).
- 590 52. Smith, C., Heyne, S., Richter, A. S., Will, S. & Backofen, R. Freiburg RNA Tools: a web
591 server integrating INTARNA, EXPARNA and LOCARNA. *Nucleic Acids Res.* **38**, W373–7
592 (2010).
- 593 53. Tobias, N. J. *et al.* Cyclo(tetrahydroxybutyrate) production is sufficient to distinguish
594 between *Xenorhabdus* and *Photorhabdus* isolates in Thailand. *Environ. Microbiol.* **121**,
595 303 (2019).
- 596



598

599 **Figure 1A.** Alignment of *arcZ* sequences from *P. laumondii* TTO1, *P. temperata*, *P. asymbiotica*,

600 *X. nematophila*, *X. bovienii*, *X. szentirmaii*, *Serratia marcescens*, *Erwinia amylovora*, *E. coli* K12

601 and *Salmonella typhimurium* LT2. Numbers refer to *P. laumondii* sequence. The +1 indicates

602 the transcriptional start of the 129 nt *arcZ* sequence. Indicated are the start codon of *elbB* and

603 the stop codon of *arcB*, -10 and -35 binding regions, as well as the conserved ArcA binding

604 region¹⁰ and the region of base-pairing to *hexA*. The site of ArcZ cleavage is indicated by an

605 arrow. **B** RIPseq enrichment in regions of sRNAs and **C** mRNAs in a strain containing Hfq^{3xFLAG}

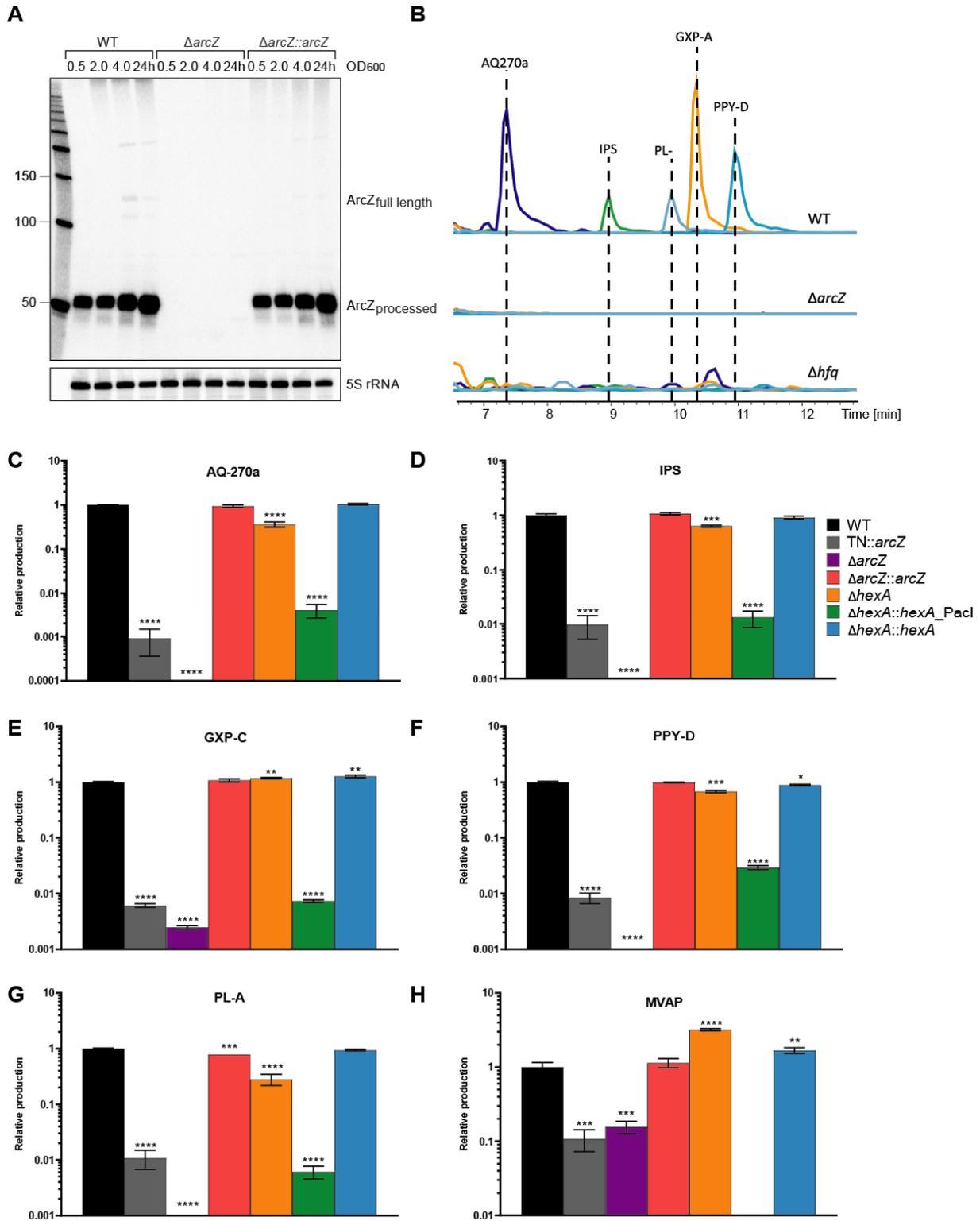
606 when compared to the untagged control strain at both optical densities. For a complete list of

607 enriched regions see Supplementary Tables S4 and S5. Blue dots represent SM-related mRNAs,
608 while orange dots represent mRNAs associated with annotated regulators.

609

610

611



612

613 **Figure 2A.** ArcZ expression in *P. laumondii* WT, $\Delta arcZ$ and $\Delta arcZ::arcZ$ cells detected by

614 Northern blot analysis. Total RNA samples were collected at three different OD₆₀₀ values (0.5;

615 2 and 4) and after 24 h of growth. Probing for 5S rRNA served as loading control. **B** Comparison
616 of relative production titers of the major SMs produced by *P. laumondii* WT, $\Delta arcZ$ and Δhfq .
617 Depicted are the extracted ion chromatograms of anthraquinone (AQ-270a), isopropylstilbene
618 (IPS), phurealipid A (PL-A), GameXPeptide A (GXP-A) and photopyrone D (PPY-D) in the WT
619 and the mutant strains. **C-H**. HPLC-MS quantification of **C**. AQ-270a, **D**. IPS, **E**. GXP-A, **F**. PPY-
620 D, **G**. PL-A and **H**. MVAP in *P. laumondii* WT (black), TN::*arcZ* (grey), $\Delta arcZ$ (purple), $\Delta arcZ::arcZ$
621 (red), $\Delta hexA$ mutant (orange), $\Delta hexA::hexA_{Pacl}$ (green) and $\Delta hexA::hexA$ (blue). All bars
622 represent relative production in comparison to the wild type. Error bars represent the
623 standard error of the mean. Asterisks indicate statistical significance (* $p < 0.05$, ** $p < 0.005$,
624 *** $p < 0.0005$, **** $p < 0.00005$) of relative production compared to WT production levels.
625 Details of all analyzed compounds can be found in Supplementary Table S14.

626

627

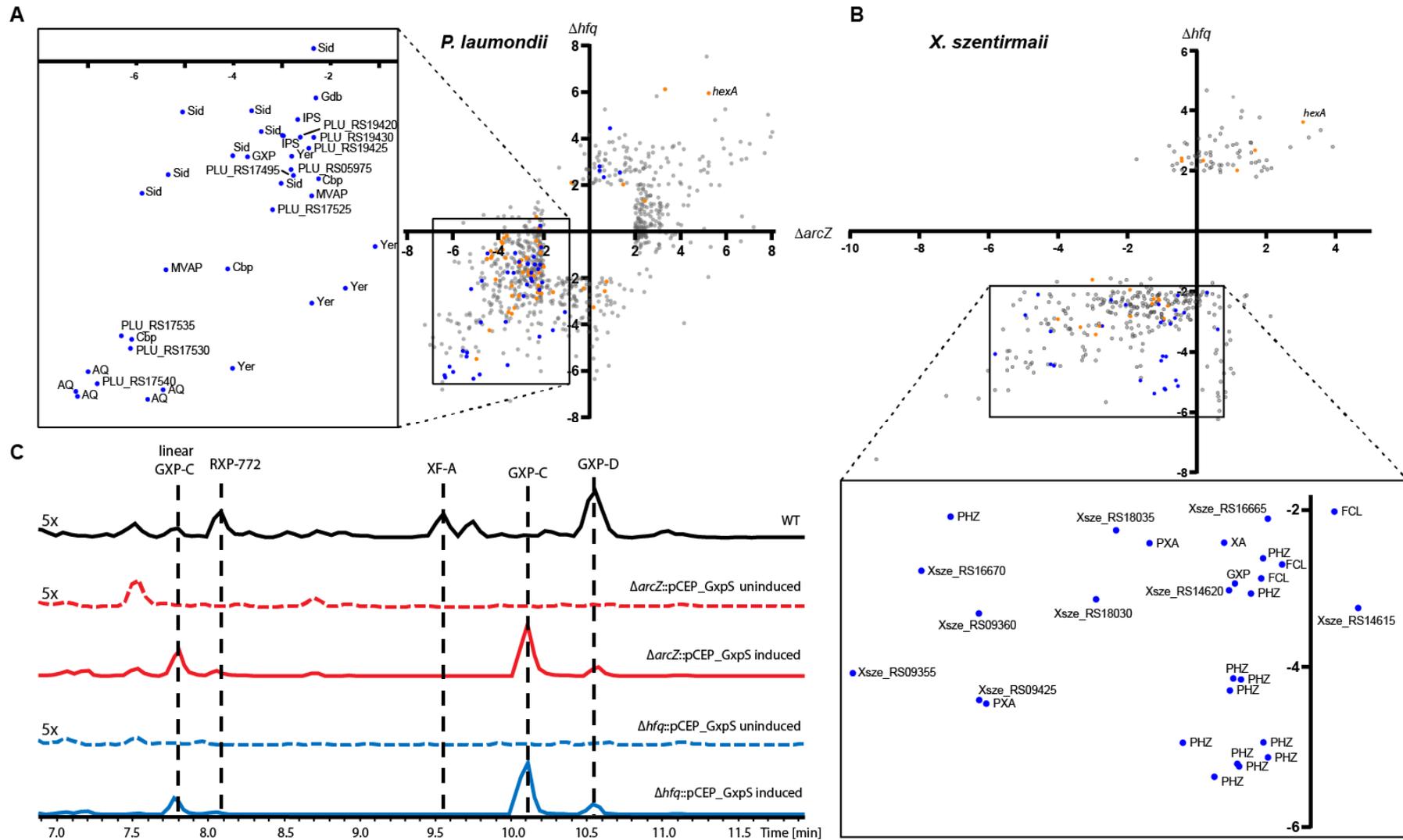
628

641 (orange) complemented *arcZ* knock-in (green) and $\Delta hexA$ mutant (blue). All bars represent
642 relative production in comparison to the wild type and were analyzed in triplicate. Shown is
643 the relative production of xenofuranone A (XF-A), GameXPeptide C (GXP-C), protoporphyrin
644 IX (PPIX), xenoamicin A (XA-A) and rhabdopeptide 772 (RXP-772). See also Supplementary
645 Table S6. Error bars represent the standard error of the mean. Asterisks indicate statistical
646 significance (* $p < 0.05$, ** $p < 0.005$, *** $p < 0.0005$, **** $p < 0.00005$) of relative production
647 compared to WT production levels.

648

649

Appendix



650

651

Figure 4. Comparison of ArcZ and Hfq regulon in **A** *P. laumondii* and **B** *X. szentirmaii*. Scatterplots show individual coding sequences and their corresponding regulatory changes compared to wild type in either the $\Delta arcZ$ (x-axis) or Δhfq (y-axis) mutants, with SMs (blue dots) and regulators (orange dots) highlighted. The inset shows only SM-related coding sequences, including those associated with anthraquinone (AQ), mevalagmapeptide (MVAP), carbapenem (Cbp), yersiniabactin (YER), GameXPeptide (GXP), siderophore (SID), isopropylstilbene (IPS) and glidobactin (Gdb), phenazine (PHZ), fabclavine (FCL), xenoamicin (XA) and pyrrolizixenamide (PXA). **C** Base peak chromatograms (BPCs) of *X. szentirmaii* WT (black), $\Delta arcZ::pCEP_GxpS$ uninduced (red dotted line), $\Delta arcZ::pCEP_GxpS$ induced (red solid line), $\Delta hfq::pCEP_GxpS$ uninduced (blue dotted line) and $\Delta hfq::pCEP_GxpS$ induced (blue solid line). Peaks corresponding to (cyclo)tetrahydroxybutyrate (THB⁵³), Linear GameXPeptide C (GXP-C), rhabdopeptide 772 (RXP), xenofuranone A (XF-A), as well as cyclic GXP-C and GXP-D. Five times zoom was applied to base peak chromatograms in the uninduced and wild type samples.

Supplementary Information

Supplementary Table S1. Significantly affected genes in *X. szentirmaii* (Δhfq RNASeq)

Supplementary Table S2. Transcriptional start sites identified for *X. szentirmaii*

Supplementary Table S3. OD₆₀₀ values of cultures from all experiments

Supplementary Table S4. Enriched sRNA sequences from RIPseq experiment

Supplementary Table S5. Enriched mRNA and 5'-UTR sequences from RIPseq experiment

Supplementary Table S6. OD₆₀₀ of *P. laumondii* WT and TN-mutants after 72 h of cultivation.

Supplementary Table S7. Significantly affected genes in TT01 Δhfq and $\Delta arcZ$

Supplementary Table S8. Significantly affected genes in TT01 only $\Delta arcZ$

Supplementary Table S9. ArcZ sequences used in Copra analysis

Supplementary Table S10. Top 200 hits defined by Copra as potentially interacting with ArcZ

Supplementary Table S11. Proteomic analysis of *P. laumondii* WT, $\Delta arcZ$, Δhfq and $\Delta hexA::hexA_PacI_UTR$

Supplementary Table S12. Significantly affected genes in *X. szentirmaii* ($\Delta arcZ$ RNASeq)

Supplementary Table S13. Plasmids used in this study

Supplementary Table S14. Strains used in this study

Supplementary Table S15. Primer sequences used in this study

Supplementary Table S16. Compounds targets used in HPLC-MS analyses

Supplementary Table S17. Updated *P. laumondii* TTO1 annotation formatted as .gff

Supplementary Table S18. Updated *X. szentirmaii* DSM16338 annotation formatted as .gff

Supplementary Figure S1. Expression of various sRNAs in *P. laumondii* at different time points

Supplementary Figure S2. Expression of various sRNAs in *X. szentirmaii* at different time points.

Supplementary Figure S3. Phenotype of transposon insertion mutants of *P. laumondii*

Supplementary Figure S4. Sequence of region in *P. laumondii* TTO1 containing predicted *arcZ* sequence

Supplementary Figure S5. RIPseq enrichment around the region of *hexA*

Supplementary Figure S6. 5' UTR of *hexA* including predicted ArcZ binding site

Supplementary Figure S7. Alignment of the *hexA* 5' UTR from different species

Supplementary Figure S8. Nematode development assays

Supplementary Figure S9. The ArcZ and Hfq regulon in *P. laumondii*

Supplementary Results

Hfq is involved in SM biosynthesis in *Xenorhabdus*. To confirm if Hfq is also involved in SM regulation in *Xenorhabdus*, we created a knockout of *hfq* in *X. szentirmaii* DSM16338 and performed HPLCMS/MS and RNAseq on the confirmed deletion strains (Supplementary Table S1). In contrast to *Photorhabdus*, the *X. szentirmaii* Δhfq strain only revealed 312 coding sequences significantly regulated compared to the wild type at mid-exponential phase. In accordance with our hypothesis, *hexA* was significantly upregulated (8.4x, FDR<0.01, Supplementary Table S1). Consistent with this observation, the production of nearly all known SMs were decreased (Figure 3E), suggesting a conserved mode of action in *Xenorhabdus*.

Identification of sRNAs in *Photorhabdus* and *Xenorhabdus*. Only very little is known about sRNAs from entomopathogenic bacteria. To identify potential Hfq-binding sRNAs and consequently the Hfq-based regulation of SMs in general, we sequenced the RNA of *P. laumondii* (formerly *P. luminescens*) and *X. szentirmaii* using a library preparation protocol specific for sRNAs. Sequences of the sRNAs from two libraries from each of *Photorhabdus* and *Xenorhabdus* yielded a total of 26,784,563 (13,204,857 and 13,579,706) and 28,813,442 (13,472,683 and 15,340,759) raw reads, respectively. Additionally, we prepared samples from *X. szentirmaii* for CappableSeq, a protocol that differentiates between primary and secondary transcripts ¹. We recently reported a data set from *P. laumondii*, which identified 15,500 primary and 3,741 secondary transcripts ². Here, we reanalyzed these data using stricter cutoff criteria (see Methods) resulting in a total of 6,174 TSSs. The *X. szentirmaii* CappableSeq data led to the identification of 2,196 TSSs (Supplementary Table S2).

By combining data from the CappableSeq experiments data along with RNAseq data from Δhfq and wild type strains (also $\Delta hfq\Delta hexA$ and $\Delta hfq::hfq$ in *Photorhabdus* from our previous study³), we were able to annotate putative transcripts, 5'-untranslated regions (UTRs), 3'-UTRs and sRNAs using ANNOgesic⁴ (Supplementary Table S17 and S18). The annotated sRNAs were added to those described in the Bacterial sRNA Database (BSRD)⁵ yielding a total of 280 and 130 candidates for sRNAs in *Photorhabdus* and *Xenorhabdus*, respectively (Supplementary Table S17 & S18).

Transposon mutant library screen. A transposon mutant library was constructed to identify genes defective in SM production. Many of the analysed mutant strains showed severely reduced SM production titers in comparison to the WT strain. In most cases, multiple SM classes were affected by the transposon insertion (Supplementary Figure S3). On rare occasions, the transposon insertion led to an increase in production of certain SMs. For example, dmPLA-A and MVAP levels were elevated in mutant strain 9 and IPS titers were slightly raised in the TN-mutant strains 10 and 11. Interestingly, the remaining SMs were negatively affected in those strains. As the growth appeared to be affected by the transposon insertion (Supplementary Table S6, it remains uncertain how the growth defects correlate with SM production. For further analysis, we decided to focus on strain 3 that showed only moderate growth defects while at the same time producing reduced SM titers, consistent with the phenotype of the *hfq* deletion mutant.

The ArcZ regulon in *Photorhabdus* and *Xenorhabdus*. Since there is a clear overlap between the regulons and functions of Hfq and ArcZ, we performed RNAseq on the $\Delta arcZ$ strains of *P. laumondii* and *X. szentirmaii*, as well as on their respective knock-in complementation mutants. RNAseq analysis on the deletion of *arcZ* in *Photorhabdus* revealed an even broader effect than in our Δhfq mutant, significantly affecting the transcriptional level of 735 coding sequences in *P. laumondii* (FDR<0.01; \log_2 fold change >2, Figure 4A, Supplementary Table S7 & S8). In *X. szentirmaii*, a global effect of the *arcZ* deletion was also observed, albeit only 191 genes were affected in this strain (Supplementary Table S12). In both deletion strains however, the majority of affected coding sequences were downregulated (Figure 4A & B, Supplementary Table S8 & S12). In an attempt to identify broader effects, we grouped all the genes that were significantly changed into eight different categories based on their known or proposed function: SM, regulators, virulence, phage related, cell wall, cell processes, hypothetical proteins and unknown. We first included only those genes that were significantly regulated in the *arcZ* deletion mutant and not in the *hfq* deletion mutant (Supplementary Figure S9A). In all cases (except for virulence related and unknown) a clear trend towards downregulation of the transcriptional level could be observed in the deletion of *arcZ*. This trend was also observed in the *hfq* deletion mutant, although somewhat weakened compared to the *arcZ* deletion strain. The knock-in complementation restored the vast majority of observed changes back to WT level (Supplementary Figure S9A). Finally, we looked at genes whose expression was significantly altered in both the *arcZ* and *hfq* deletion strain. The individual categories clustered very closely together as indicated by the median (Supplementary Figure 9B).

Effect of *arcZ* deletion in *Xenorhabdus*. The drastic reduction in SMs in the deletion mutant was restored with a knock-in complementation of *arcZ* (Supplementary Figure S3). We also observed that protoporphyrin IX (PPIX), the direct precursor for heme, was highly overproduced (~30-fold) in the $\Delta arcZ$ strain of *X. szentirmaii* compared to the WT, suggesting that the regulatory functions of ArcZ in *Photorhabdus* and *Xenorhabdus* possibly go beyond SM production. Since heme is reported to play an important role in nematode growth and development, we used the deletion mutants and complemented strains and performed nematode development assays. Both the WT and $\Delta arcZ$ strain of *X. szentirmaii* were able to support nematode development after 4 days of inoculation. However, the $\Delta arcZ$ strain of *P. laumondii* showed a significantly reduced capability to support nematode development (Supplementary Figure S8), consistent with our data showing that isopropylstilbene falls under the Hfq-ArcZ regulatory umbrella (Figure 4A, Supplementary Tables S7 & S8).

Supplementary Table S3. Optical density values for sequencing experiments

Species	OD ₆₀₀ value	Purpose
<i>P. laumondii</i> replicate A	5.8	sRNA sequencing
<i>P. laumondii</i> replicate B	5.4	sRNA sequencing
<i>X. szentirmaii</i> replicate A	5.5	sRNA sequencing
<i>X. szentirmaii</i> replicate B	6.1	sRNA sequencing
<i>P. laumondii</i> replicate A	4	RNA-sequencing
<i>P. laumondii</i> replicate B	4.3	RNA-sequencing
<i>P. laumondii</i> $\Delta arcZ$ replicate A	3.8	RNA-sequencing
<i>P. laumondii</i> $\Delta arcZ$ replicate B	4.1	RNA-sequencing
<i>P. laumondii</i> knock-in replicate A	5.2	RNA-sequencing
<i>P. laumondii</i> knock-in replicate B	4.6	RNA-sequencing
<i>X. szentirmaii</i> replicate A	4.3	RNA-sequencing (control for $\Delta arcZ$ mutant)
<i>X. szentirmaii</i> replicate B	3.8	RNA-sequencing (control for $\Delta arcZ$ mutant)
<i>X. szentirmaii</i> replicate A	4.5	RNA-sequencing (control for Δhfq mutant)
<i>X. szentirmaii</i> replicate B	4.5	RNA-sequencing (control for Δhfq mutant)
<i>X. szentirmaii</i> $\Delta arcZ$ replicate A	4.8	RNA-sequencing
<i>X. szentirmaii</i> $\Delta arcZ$ replicate B	4.3	RNA-sequencing
<i>X. szentirmaii</i> Δhfq replicate A	4.8	RNA-sequencing
<i>X. szentirmaii</i> Δhfq replicate B	4.7	RNA-sequencing
<i>X. szentirmaii</i> knock-in replicate A	3.6	RNA-sequencing
<i>X. szentirmaii</i> knock-in replicate B	3.8	RNA-sequencing
<i>P. laumondii</i> replicate A	0.5	RIP-Seq
<i>P. laumondii</i> replicate B	0.5	RIP-Seq
<i>P. laumondii</i> replicate A	5	RIP-Seq
<i>P. laumondii</i> replicate B	5	RIP-Seq

Supplementary Table S6. OD₆₀₀ of *P. laumondii* WT and TN-mutants after 72 h of cultivation.

Strain	OD ₆₀₀
WT	14.5
1	9.8
2	8.9
3	7.6
4	1.7
5	3.9
6	12.5
7	3.5
8	14.8
9	5.4
10	9.2
11	4.8

Supplementary Table S13. Plasmids used in this study

Plasmid	Genotype	Reference
pSAM_BT	R6K ori, Amp ^R , oriT, Himar1C9 transposase, transposon containing <i>ermG</i>	⁶
pSAM_KAN	R6K ori, Amp ^R , oriT, Himar1C9 transposase, mariner transposon containing Kan ^R	This study
pCK_cipB	R6K ori, CM ^R , oriT, <i>sacB</i> , <i>tral</i>	⁷
pCOLA_ara_tacl	cola oriR, Kan ^R	⁸
pCKcipB_Δ <i>arcZ</i> _TT01	R6K ori, CM ^R , oriT, <i>sacB</i> , <i>tral</i> , containing a 1083 bp upstream and a 994 bp downstream region of <i>arcZ</i>	This study
pCKcipB_Δ <i>arcZ</i> _XSZ_DSM	R6K ori, CM ^R , oriT, <i>sacB</i> , <i>tral</i> , containing a 860 bp upstream 965 bp downstream region of <i>arcZ</i>	This study
pCKcipB_hfq_flag_TT01	R6K ori, CM ^R , oriT, <i>sacB</i> , <i>tral</i> , containing the upstream and downstream region of <i>hfq</i> including a 3xFLAG tag that was introduced via primers	This study
pEB17	R6K ori, Kan ^R , oriT, <i>sacB</i> , <i>tral</i>	This study
pEB17_Δ <i>arcZ</i> _TT01	R6K ori, Kan ^R , oriT, <i>sacB</i> , <i>tral</i> , containing a 2207 bp fragment including a 1083 bp upstream and a 994 bp downstream region of <i>arcZ</i> and the full version of <i>arcZ</i>	This study
pEB17_Δ <i>arcZ</i> _XSZ_DSM	R6K ori, Kan ^R , oriT, <i>sacB</i> , <i>tral</i> , containing a 1915 bp fragment	This study

Appendix

	including a 860 bp upstream and a 965 bp downstream region of <i>arcZ</i> and the full version of <i>arcZ</i>	
pEB17_Δ <i>hexA</i> _XSZ	R6K ori, Kan ^R , oriT, <i>sacB</i> , <i>tral</i> , containing a 1110 bp upstream 1036 bp downstream region of <i>hexA</i>	This study
pEB17_HexA_Pacl_TT01	R6K ori, Kan ^R , oriT, <i>sacB</i> , <i>tral</i> , containing a 2141 bp fragment (includes upstream region of <i>hexA</i> , the complete <i>hexA</i> gene and downstream region of <i>hexA</i> with the introduced <i>Pacl</i> restriction site instead of the predicted ArcZ binding site)	This study
pCEPKMR_ORF00346	R6K ori, Kan ^R , oriT, <i>tral</i> , containing a 618 bp fragment homologous to <i>gxpS</i> required for homologous recombination	This study
pMH078	p- <i>arcZ</i> , constitutive sRNA expression plasmid, P15A, Kan ^R	This study
pMH079	pXG10- <i>hexA</i> :: <i>gfp</i> , containing the 5'UTR and the first 20 aa of <i>hexA</i> , pSC101*, Cm ^R	This study
pMH080	p- <i>arcZ</i> * (G79C), constitutive sRNA expression plasmid, P15A, Kan ^R	This study
pMH081	pXG10- <i>hexA</i> :: <i>gfp</i> (C-46G), containing the 5'UTR and the first 20 aa of <i>hexA</i> , pSC101*, Cm ^R	This study
p-ctr	pCMW-1, control plasmid, P15A, Kan ^R	⁹

Supplementary Table S14. Bacterial strains used in this study

Strain	Genotype/Description	Reference
<i>Escherichia coli</i> S17-1 λpir	Tp ^R Sm ^R <i>recA, thi, pro, hsdR</i> -M+RP4: 2- Tc:Mu:Km Tn7 λ pir	Invitrogen
S17-1 λ pir + pCKcipB_Δ <i>arcZ</i> _TT01	S17-1 λ pir + pCKcipB_Δ <i>arcZ</i> _TT01, Cm ^R , R6K ori	This study
S17-1 λ pir + pCKcipB_Δ <i>arcZ</i> _XSZ_DSM	S17-1 λ pir + pCKcipB_Δ <i>arcZ</i> _XSZ_DSM, Cm ^R , R6K ori	This study
S17-1 λ pir + pEB17_Δ <i>arcZ</i> _TT01	S17-1 λ pir + pEB17_Δ <i>arcZ</i> _TT01, Kan ^R , R6K ori	This study
S17-1 λ pir + pEB17_Δ <i>arcZ</i> _XSZ_DSM	S17-1 λ pir + pEB17_Δ <i>arcZ</i> _XSZ_DSM, Kan ^R , R6K ori	This study
S17-1 λ pir + pEB17_Δ <i>hexA</i> _XSZ_DSM	S17-1 λ pir + pEB17_Δ <i>hexA</i> _XSZ_DSM, Kan ^R , R6K ori	This study
S17-1 λ pir + pEB17_Δ <i>hexA</i> _Pacl_TT01	S17-1 λ pir + pEB17_Δ <i>hexA</i> _Pacl_TT01, Kan ^R , R6K ori	This study
S17-1 λ pir + pCEPKMR_ORF00346	S17-1 λ pir + pCEPKMR_ORF00346, Kan ^R , R6K ori	This study
<i>E. coli</i> ST18	S17 λ pir Δ <i>hemA</i>	10
ST18 + pCKcipB_hfq_flag_TT01	ST18 + pCKcipB_hfq_flag_TT01	This study
<i>E. coli</i> Top10	<i>F</i> - <i>mcrA</i> Δ(<i>mrr-hsdRMS-mcrBC</i>) <i>φ80lacZΔM15 ΔlacX74 nupG recA1</i> <i>araD139 Δ(ara-leu)7697 galE15 galK16</i> <i>rpsL(StrR) endA1 λ</i> -	Invitrogen
Top10 + pMH079 + p-ctr	Top10 + pXG10- <i>hexA</i> ::gfp+ p-ctr	This study
Top10 + pMH079 + pMH078	Top10 + pXG10- <i>hexA</i> ::gfp+ p- <i>arcZ</i>	This study
Top10 + pMH079 + pMH080	Top10 + pXG10- <i>hexA</i> ::gfp+ p- <i>arcZ</i> *	This study

Appendix

Top10 + pMH081 + p-ctr	Top10 + pXG10- <i>hexA</i> *::gfp+ p-ctr	This study
Top10 + pMH081 + pMH078	Top10 + pXG10- <i>hexA</i> *::gfp+ p- <i>arcZ</i>	This study
Top10 + pMH081 + pMH080	Top10 + pXG10- <i>hexA</i> *::gfp+ p- <i>arcZ</i> *	This study
<i>Photorhabdus laumondii</i> WT, Rif ^R		11
<i>subsp. laumondii</i> TT01		
TN:: <i>arcZ</i>	Mariner transposon insertion in <i>ArcZ</i> (insertion site: 4692989)	This study
Δ <i>arcZ</i>	Deletion starting from 4692930 to 4693059	This study
Δ <i>arcZ</i> :: <i>arcZ</i>	Complementation of TT01 Δ <i>arcZ</i> by insertion of full length <i>ArcZ</i> sequence	This study
Δ <i>hexA</i>	TT01 Δ <i>hexA</i> (<i>plu3090</i>)	3
Δ <i>hexA</i> :: <i>hexA</i> _Pacl_UTR	Knockin of <i>hexA</i> with an altered sequence in the 5'-UTR	This study
<i>hfq</i> ^{3xFLAG}	Δ <i>hfq</i> :: <i>hfq</i> ^{3xFLAG}	This study
<i>Xenorhabdus szentirmaii</i> WT, Amp ^R		12
DSM16338		
Δ <i>hfq</i>	Δ <i>hfq</i> (<i>Xsze_00563</i>)	13
Δ <i>hfq</i> ::pCEP_GXPS	Promotor exchange in front of <i>gxps</i>	This study
Δ <i>arcZ</i>	Deletion starting from 3833948 to 3833859	This study
Δ <i>arcZ</i> :: <i>arcZ</i>	Complementation of XSZ Δ <i>arcZ</i> by insertion of full length <i>ArcZ</i> sequence	This study
Δ <i>arcZ</i> ::pCEP_GXPS	Promotor exchange in front of <i>gxps</i>	This study
Δ <i>hexA</i>	Δ <i>hexA</i> (<i>Xsze_03702</i>)	This study

Supplementary Table S15. Oligonucleotides used in this study

Name	Sequence (5'-3')	Purpose
NN191	TATAACCTCTCCTTAATTTATTGC	Linearization of pSAM_Bt
NN192	AAACAATAGGCCACATGC	
NN193	TAAATTAAGGAGAGGTTATACTGCGTCT AGCATGCCTA	Amplification of Kan ^R
NN194	TTGCATGTGGCCTATTGTTTTTAGAAAAA CTCATCGAGCATC	
NN276	ATCGATCCTCTAGAGTCGACCCTGAATG ATTTTGATTACGCT	Deletion of <i>arcZ</i> : amplification of <i>upstream</i> region of <i>arcZ</i> (TT01)
NN277	GACGCTGAAAAAAAAATAACCCAAAGATA AGATTTTTTGTTACAAGATTC	
NN278	GGTTATTTTTTTTCAGCGTCC	Deletion of <i>arcZ</i> : amplification of <i>downstream</i> region of <i>arcZ</i> (TT01)
NN279	TCCCGGAGAGCTCAGATCTCGATGTAT TATCAAGTGAAAGGC	
NN281	GGCAGACTCCTGTAGAACG	Verification primer for TT01Δ <i>arcZ</i>
NN282	CGCATAAGATAAAAGGTGCTGC	
NN315	TCCTCTAGAGTCGACCTGCACGAAAAAC GATAAAGTTGTGAGC	Deletion of <i>arcZ</i> : amplification of <i>upstream</i> region of <i>arcZ</i> (XSZ DSM)
NN316	GGAACACAAGTACCAACATAGC	
NN317	TATGTTGGTACTTGTGTTCCCACCCAAC TTCGGTTGG	Deletion of <i>arcZ</i> : amplification of <i>downstream</i> region of <i>arcZ</i> (XSZ DSM)
NN318	GGAATTCCCGGGAGAGCTCAGCAACAG GAACGGGCATTG	
NN329	CGACACTTCAGCACCAAG	Verification primer for XSZΔ <i>arcZ</i>
NN330	GCGAGAGATCAGAAAGGAATTAC	
NN333	ATCGATCCTCTAGAGTCGACGCACTGCTA AAACGTGTCAG	Knockin of <i>hexA_PacI</i> _UTR: amplification of <i>upstream</i> region of <i>arcZ</i> (TT01)

Appendix

NN334	TTAGTTAGTAATTTAAAATCAAAAAAAGT GATG	
NN335	TGATTTTAATTACTAACTAATTAATTAATT TACGTAAGCACTATCAAATTAATTAACA TC	Knockin of <i>hexA_Pacl</i> _UTR: amplification of <i>downstream</i> region of <i>arcZ</i> (TT01)
NN336	GGAATTCCCGGGAGAGCTCACCTCCCTC TGAATGTTTTGAAG	
NN346	ATCGATCCTCTAGAGTCGACGCTTTGCGT GCAGAATATAAC	Deletion of <i>hexA</i> : amplification of <i>upstream</i> region of <i>hexA</i> (XSZ DSM)
NN347	CCTGGTGTTTTTACTTCAGC	
NN348	GCTGAAGTAAAAACACCAGGGTATTACG TATTTATAGGCTAATGTTTTCC	Deletion of <i>hexA</i> : amplification of <i>downstream</i> region of <i>hexA</i> (XSZ DSM)
NN349	GGAATTCCCGGGAGAGCTCACCAATAAC ACCAAATGAAAATGC	
NN359	CAGAATAAGGTGAATTTAGTTGATG	Sequencing of <i>hexA_Pacl</i> _UTR
NN357	GATGCAGAAGGTGAACTAAG	knockin part 1
NN358	CCAGCATACTTTCAATAAACTG	Sequencing of <i>hexA_Pacl</i> _UTR
NN356	GGTTCAATAGGTAAAAAACAGC	knockin part 2
X.sz_CI2_ORF0		
0346_fw_gib_L	TTTGGGCTAACAGGAGGCTAGCATATGA	
P	AAGATAGCAAGGTTGCT	Promotor exchange in front of
X.sz_CI2_ORF0	TCTGCAGAGCTCGAGCATGCACATGGTA	<i>gxpS</i>
0346_rv_gib_L	TACATGATGTACGCTGG	
P		
X.sz_CI2_ORF0		
0346_ver_fw_		
LP	GGCTGCTGGGAATGACAAT	Verification primer for
X.sz_CI2_ORF0	GATAACGAGCCGGACTACAGC	pCEPKMR_ORF00346
0346_ver_rv_L		
P		

Appendix

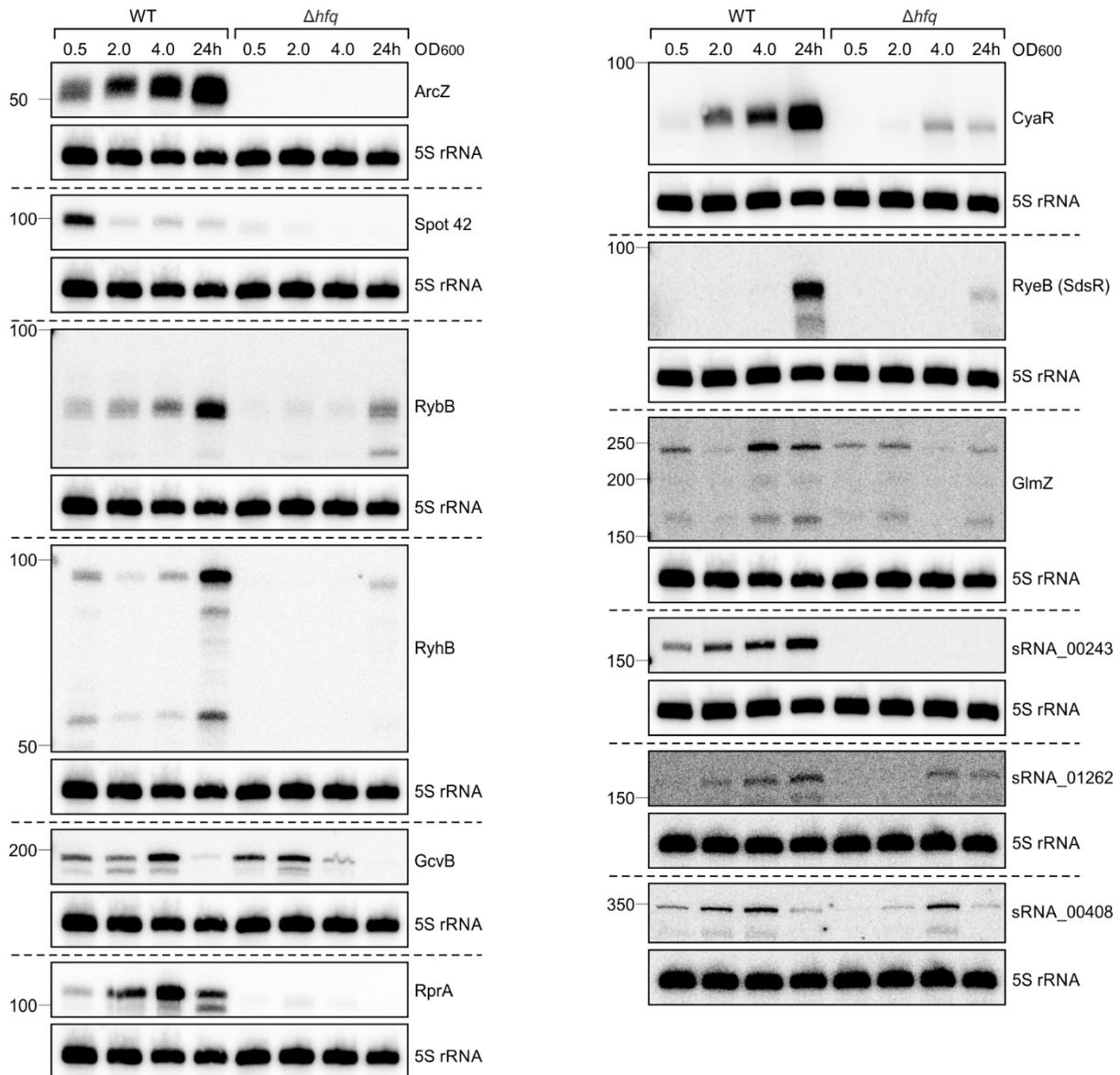
KPO-0009	CTACGGCGTTTCACTTCTGAGTTC	5S oligoprobe (<i>E. coli</i>)
KPO-0092	CCACACATTATACGAGCCGA	construction of pMH078 (p- <i>arcZ</i>)
KPO-1397	GATCCGGTGATTGATTGAGC	
KPO-1702	ATGCATGTGCTCAGTATCTCTATC	construction of pMH079 (pXG10- <i>hexA::gfp</i>)
KPO-1703	GCTAGCGGATCCGCTGG	
KPO-3024	CAATATGGGGATATCAAAGAAAAGC	RybB oligoprobe (TT01)
KPO-3109	GGACTACACACAGCAATATAGG	RprA oligoprobe (TT01)
KPO-3110	GCTGATTCACTTTTCGTTCCG	GcvB oligoprobe (TT01)
KPO-3111	CTTACCTCTGTACCCTACGC	Spot 42 oligoprobe (TT01 and XSZ)
KPO-5989	GAATACTGCGCCAACACCAG	ArcZ oligoprobe (TT01 and XSZ)
KPO-6007	AACTACCATCGGCGCTAC	5S oligoprobe (TT01 and XSZ)
KPO-6061	CTAAAGTAAACTGGAAGCAATG	RyhB oligoprobe (TT01)
KPO-6062	GCCTGTTGTTTATCTACAGTCAG	GlmZ oligoprobe (TT01)
KPO-6130	AGACAGGGATGGTGTCTATG	CpxQ oligoprobe (XSZ)
KPO-6132	TTAAGAGCCGTGCGCTAAAAG	RyeB (SdsR) oligoprobe (TT01)
KPO-6145	GAGATACTGAGCACATGCATGTCAGAAA ACAAAATAACCAA	construction of pMH079 (pXG10- <i>hexA::gfp</i>)
KPO-6146	CCAGCGGATCCGCTAGCAACAAAAGTTC TTAGCAGATCG	
KPO-6147	GGCTCGTATAATGTGTGGGTATGATGTA CGGAGAATTCC	construction of pMH078 (p- <i>arcZ</i>)
KPO-6148	GCTCAATCAATCACCGGATCCAAGAATG GAGAAAGGATACG	
KPO-6149	CAATATGGGGACATCAAAGAAAAG	RybB oligoprobe (XSZ)
KPO-6156	GTTTTCCCTGCTGTTGGCGCAGTATTCGC G	construction of pMH080 (p- <i>arcZ</i> *)
KPO-6157	GCGCCAACAGCAGGGAAAACTTTTTACA CGC	

Appendix

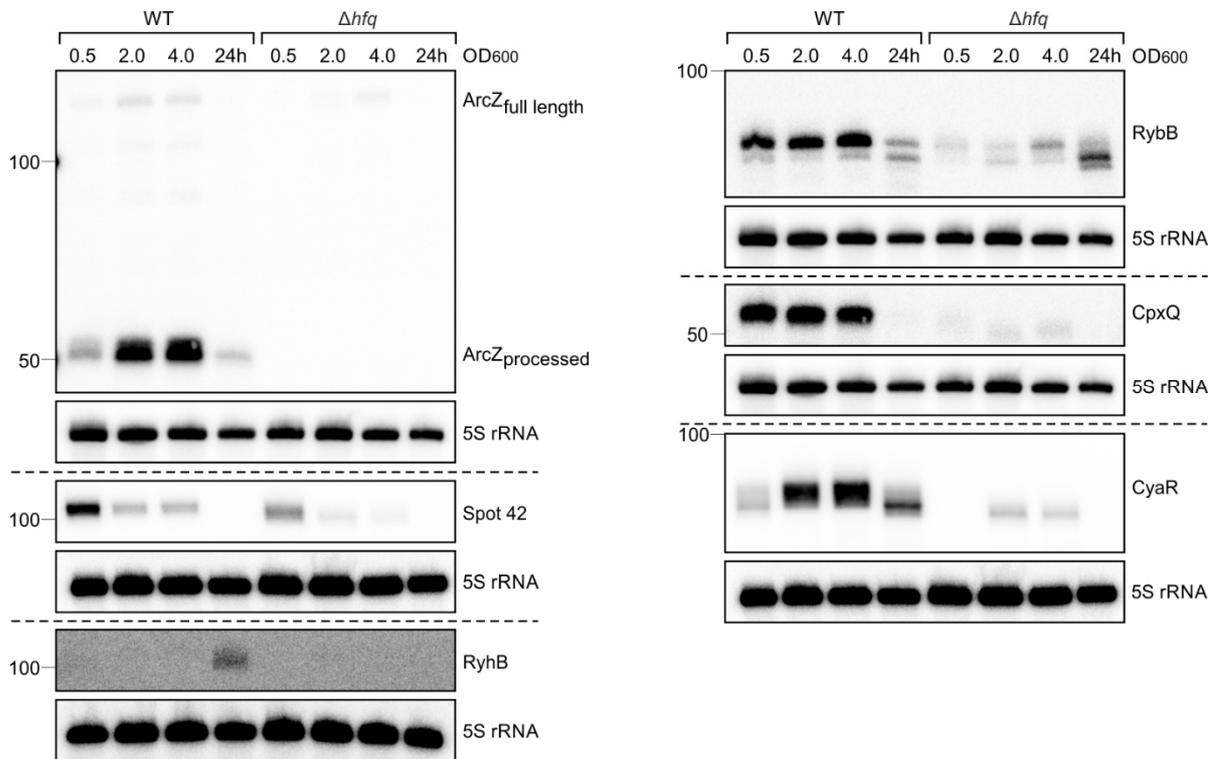
KPO-6164	CGTAAAAACAGCAGGTTAGTTAGTAATT AAAATC	construction of pMH081 (pXG10- <i>hexA*::gfp</i>)
KPO-6165	CTAACTAACCTGCTGTTTTTACGTAAGCA CTATC	
KPO-6166	CTGGTGTTGACGGAAATAAGC	sRNA_00243 oligoprobe (TT01)
KPO-6169	GAGGTGGTTCCTAGTCTTAC	CyaR oligoprobe (TT01 and XSZ)
KPO-6171	CGCGAATACTGCGCCAACA	ArcZ* oligoprobe
KPO-6303	GATACACGGTCAGAACACTATC	sRNA_00408 oligoprobe (TT01)
KPO-6305	CCGTAGCGCTGATTGATACC	sRNA_01262 oligoprobe (TT01)
AHp292	TCCTCTAGAGTCGACCTGCACATCAATTT GCTATTGCACC	
AHp293	GTAGTCGATATCATGATCTTTATAATCAC CGTCATGGTCTTTGTAGTCTTCAGTGCCA TCACTTTCC	Introduction of <i>hfq</i> ^{3xFLAG} : amplification of <i>upstream</i> product
AHp294	TTATAAAGATCATGATATCGACTACAAAG ATGACGACGATAAATAGTAAGTTTGAGA TCAGTAATAGAATGAAG	Introduction of <i>hfq</i> ^{3xFLAG} : amplification of <i>downstream</i> product
AHp295	GGAATTCCCGGGAGAGCTCATATATCCC ACCAGTGAAACC	
AHp142	CGGTTATCGTCAGATGTGG	Verification Primer for
AHp143	CAACAAAATATTTTCGGATGAGG	Introduction of <i>hfq</i> ^{3xFLAG}

Supplementary Table S16. Compounds analyzed by Target analysis.

Compound Name	<i>m/z</i>	Ion	Reference
Isopropylstilbene (IPS)	255.1	[M+H] ⁺	14
Anthraquinone 270a (AQ-270a)	271.1	[M+H] ⁺	15
GameXPepptide A (GXP-A)	586.4	[M+H] ⁺	16
Photopyrone D (PPY-D)	295.2	[M+H] ⁺	17
Phurealipide A (PL-A)	229.2	[M+H] ⁺	7
Mevalagmapeptide (MVAP)	334.8	[M+2H] ⁺⁺	16
Xenofuranone A (XF-A)	281.1	[M+H] ⁺	18
GameXPepptide C (GXP-C)	552.4	[M+H] ⁺	16
Protoporphyrin IX (PPIX)	563.3	[M+H] ⁺	
Xenoamicin A (XA-A)	650.9	[M+2H] ⁺⁺	19
Rhabdopeptide 772 (RXP-772)	772.4	[M+H] ⁺	20

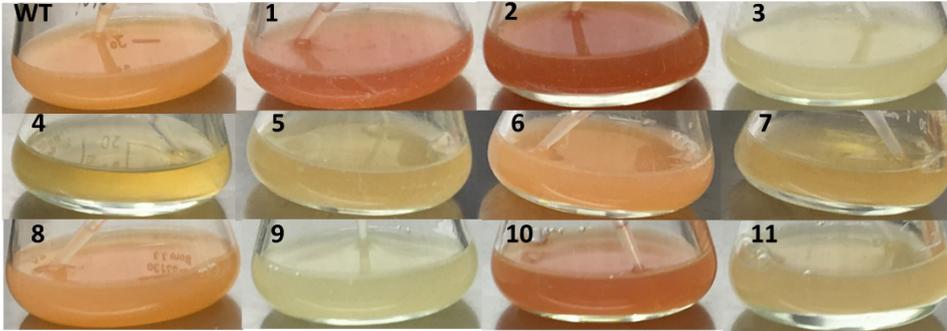


Supplementary Figure S1. Expression of various sRNAs in *P. laumondii* at different time points. RNA samples of *P. laumondii* WT and Δhfg strains were taken at three different OD₆₀₀ values (0.5, 2 and 4) and after 24 h of growth. The RNA was loaded on Northern blots and probed for the indicated sRNAs. Probing for 5S rRNA served as loading control.

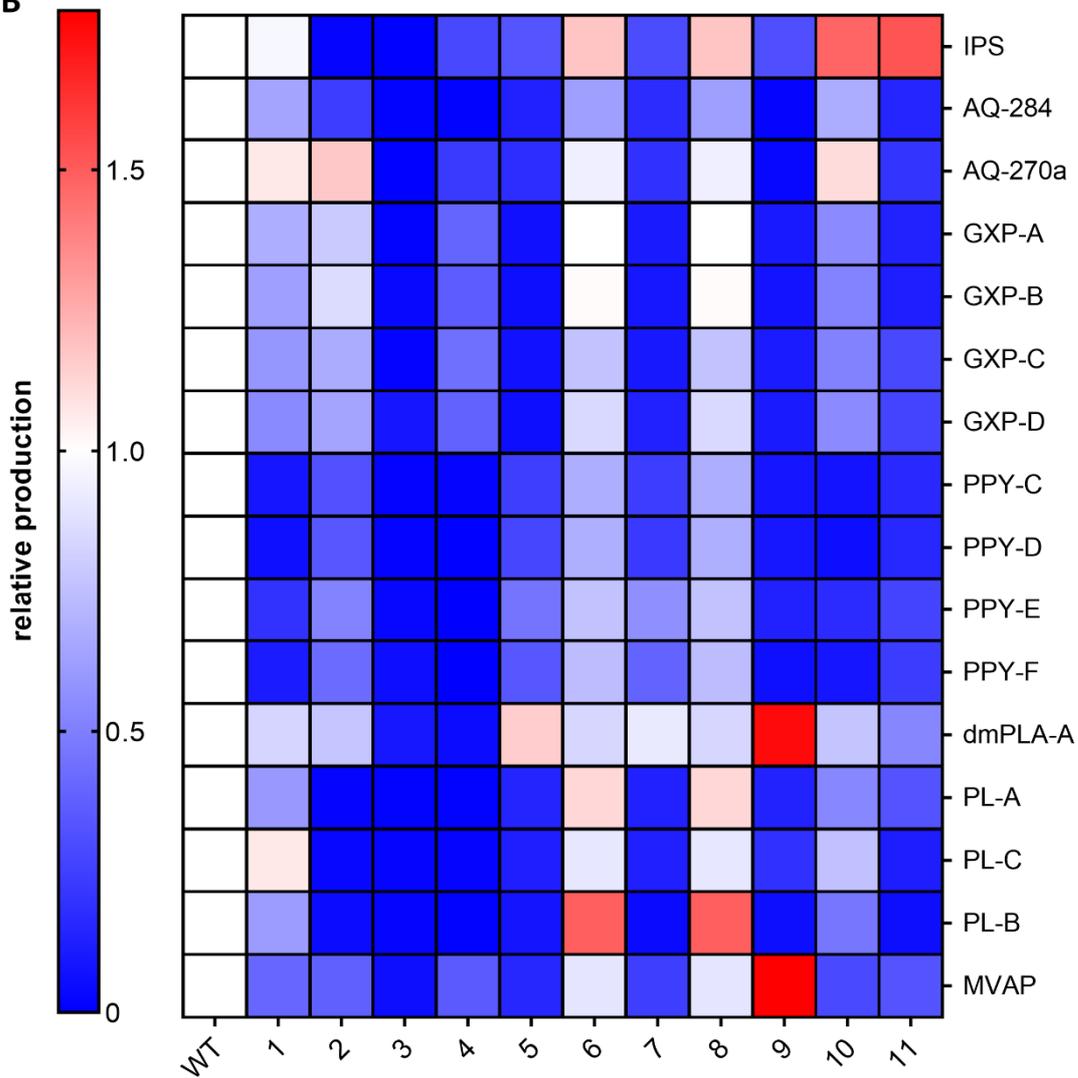


Supplementary Figure S2. Expression of various sRNAs in *X. szentirmaii* at different time points. RNA samples of *X. szentirmaii* WT and Δhfq strains were taken at three different OD₆₀₀ values (0.5, 2 and 4) and after 24 h of growth. The RNA was loaded on Northern blots and probed for the respective sRNAs. Probing for 5S ribosomal RNA served as loading control.

A

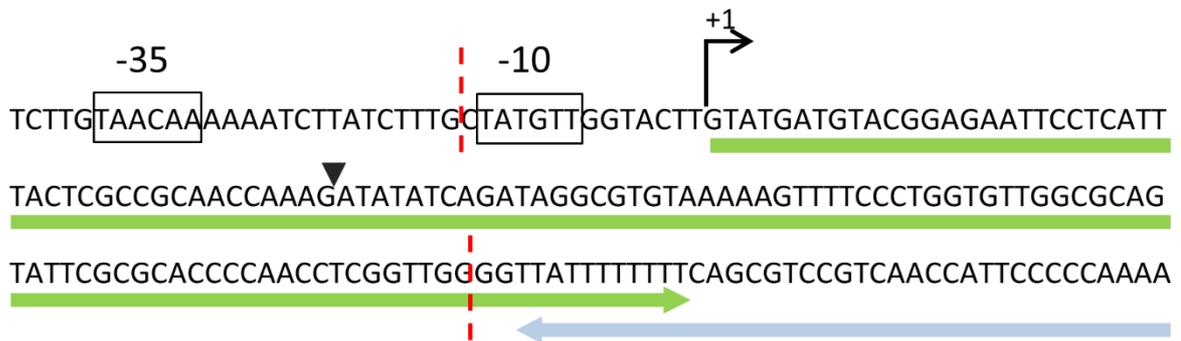


B

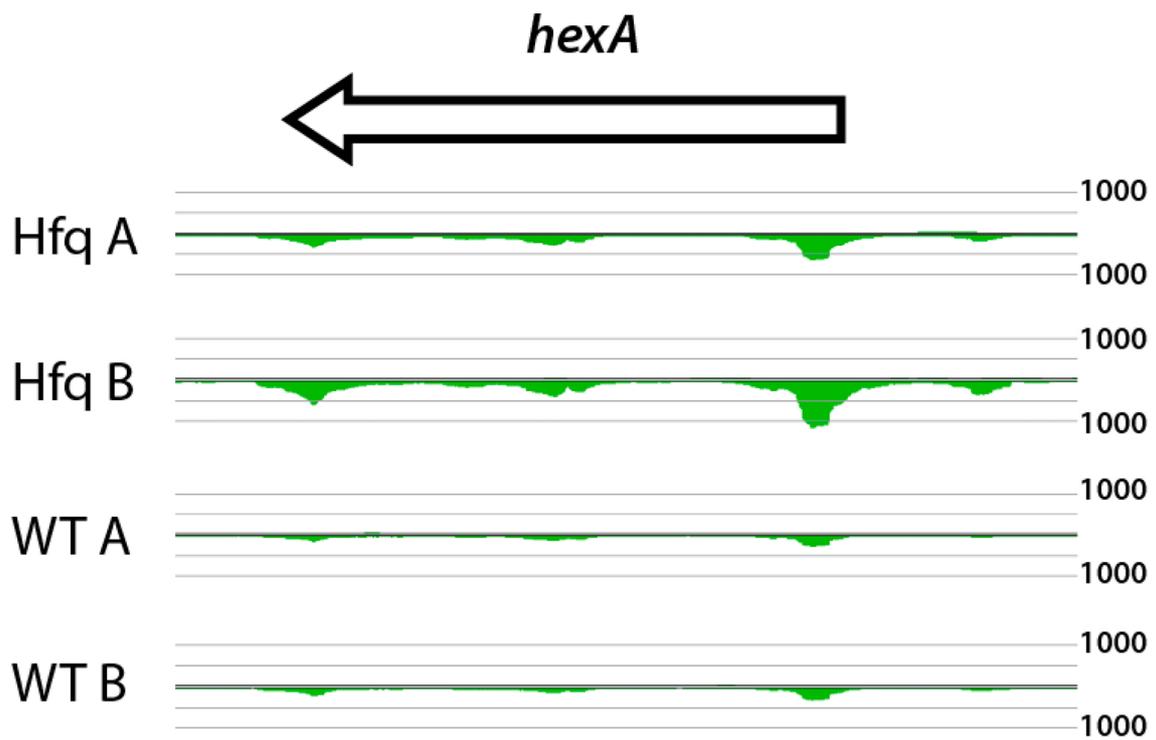


Supplementary Figure S3. Phenotype of transposon insertion mutants of *P. laumondii*. **A.** Differences in pigmentation of transposon insertion mutant liquid cultures compared to

WT. Depicted are eleven transposon insertion mutants and a WT culture after 3 d of cultivation at 30°C with shaking. **B.** SM- profiles of the transposon insertion mutants. Relative SM production was quantified from duplicates using TargetAnalysis (Bruker) and compared to the WT of *P. laumondii* after 72 h cultivation at 30°C with shaking. Mutant 3 was analysed further and the transposon insertion was identified in the *arcZ* gene.



Supplementary Figure S4. Sequence of region in *P. laumondii* TTO1 containing predicted *arcZ* sequence (green arrow). The 3' end of *arcB* (blue arrow) is also shown. Dotted red lines indicate region of *arcZ* that was deleted. Also indicated is the site of insertion from transposon sequencing (inverted black triangle), as well as the -35 and -10 promoter regions and the transcriptional start site (+1).



Supplementary Figure S5. RIPseq enrichment around the region of *hexA* in Hfq^{3xFLAG} samples (Hfq A & B) and untagged samples (WT A & B). Plots indicate the strand reads map to (bottom = reverse, top = forward). Scale represents perfectly mapped reads. For all enriched regions, see Supplementary Tables S11 and S12.

A HexA_UTR

ATGTTAATTTAATTTGATAGTGCTTACGTAAA**AACACCAGG**TTAGTTAGTAATTA

AAATCAAAAAAAGTGATGAATAACAATG



B HexA_PacI_UTR

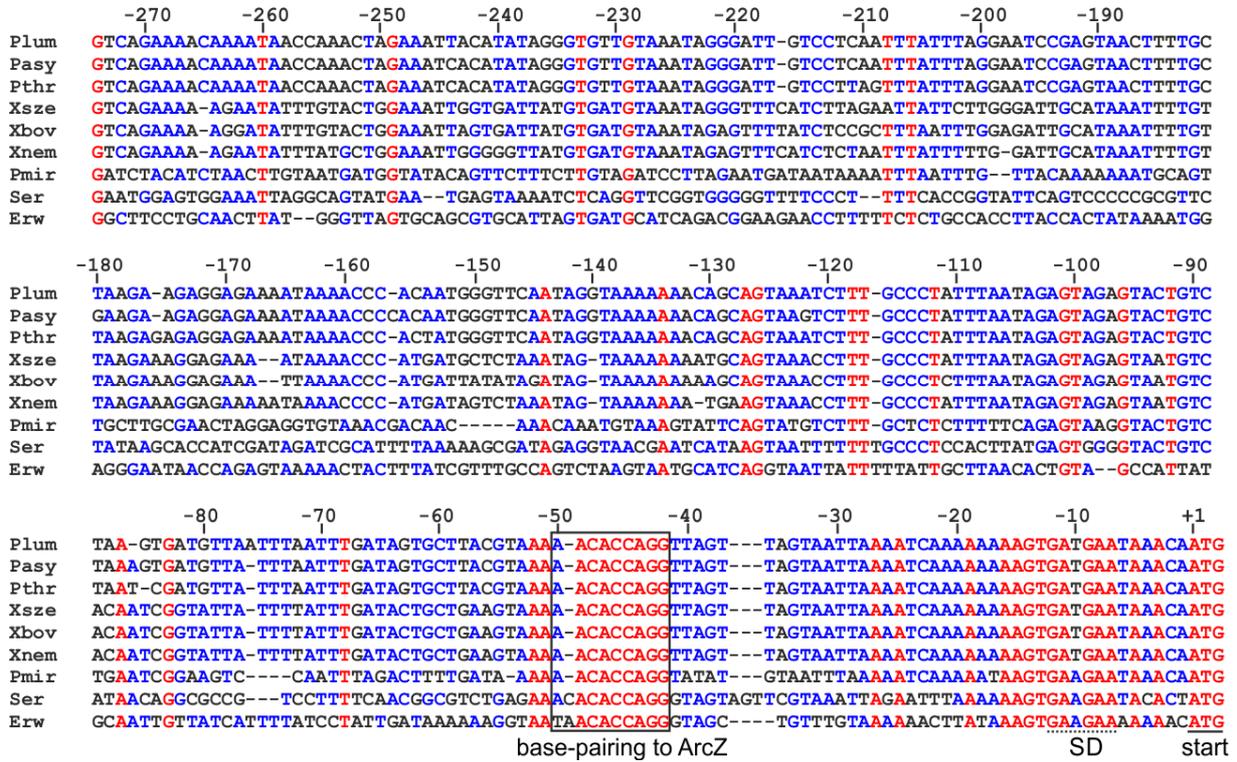
ATGTTAATTTAATTTGATAGTGCTTACGTAAA**TTAATTAA**TTAGTTAGTAATTA

ATCAAAAAAAGTGATGAATAACAATG

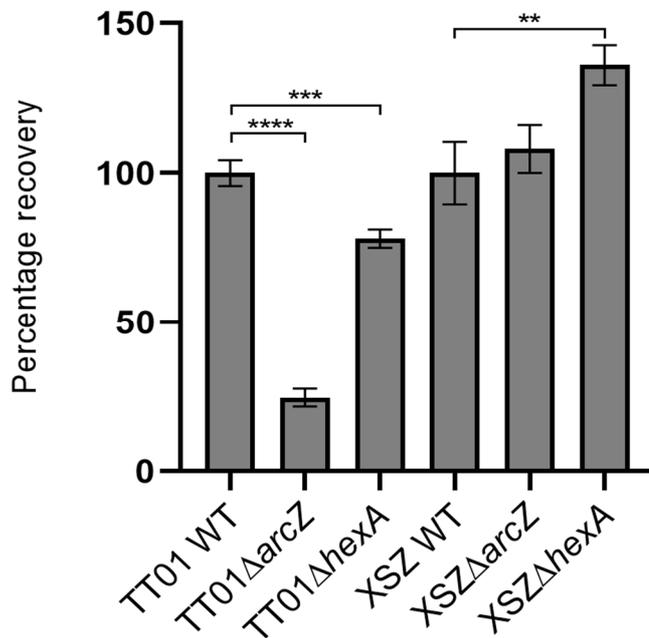


Supplementary Figure S6. A 5'-UTR of *hexA* including the predicted ArcZ binding site (red). The arrow indicates the start of the *hexA* coding sequence. **B** The predicted ArcZ binding site (AACACCAGG) was exchanged to a *PacI* restriction site (TTAATTAA) as shown.

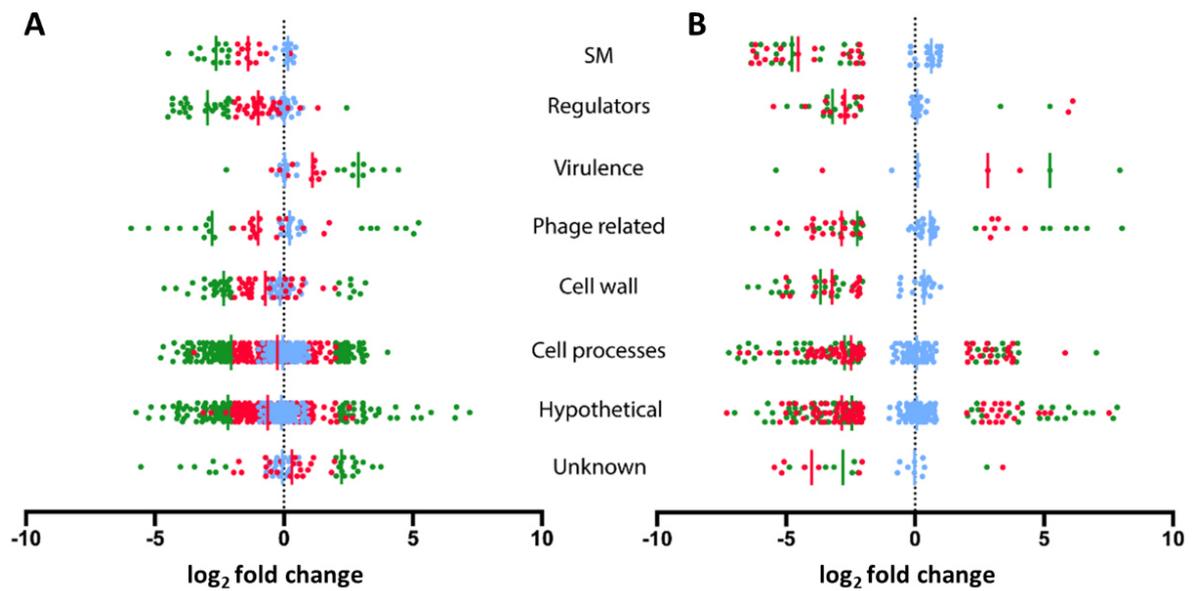
Appendix



Supplementary Figure S7. Alignment of the *hexA* 5' UTR from *P. laumondii* TT01, *P. asymbiotica*, *P. thracensis*, *X. szentirmaii*, *X. bovienii*, *X. nematophila*, *Proteus mirabilis*, *Serratia marcescens* and *Erwinia* sp. J780, beginning with the transcriptional start site. The sequences were aligned using the Multalign Algorithm²¹. Black box indicates the region of base-pairing to ArcZ. SD sequence and start codon of *hexA* are underlined. Numbers indicate distance to the start codon.



Supplementary Figure S8. Infective juvenile development to hermaphrodites with strains of *P. laumondii* and *X. szentirmaii*. Bars represent mean values of 10 individual experiments. Error bars represent the standard error of the mean. Asterisks indicate statistical significance (* $p < 0.05$, ** $p < 0.005$, *** $p < 0.0005$, **** $p < 0.00005$) of relative recovery compared to WT recovery levels.



Supplementary Figure S9A. Genes that were significantly affected in the $\Delta arcZ$ strain and not the Δhfq strain or **B** affected in both $\Delta arcZ$ and Δhfq strains. The coding sequences associated with $\Delta arcZ$ of *P. laumondii* (green), Δhfq (red) or $\Delta arcZ::arcZ$ (blue) compared to the WT were grouped into eight different categories: specialized metabolites (SM), regulators, virulence, phage related, cell wall, cell processes, hypothetical and unknown based on their annotations. Vertical lines represent the median for each group. Complete lists of regulated genes for *P. laumondii* mutants can be seen in Supplementary Tables S14-S15.

References

1. Ettwiller, L., Buswell, J., Yigit, E. & Schildkraut, I. A novel enrichment strategy reveals unprecedented number of novel transcription start sites at single base resolution in a model prokaryote and the gut microbiome. *BMC Genomics* **17**, 199 (2016).
2. Tobias, N. J., Linck, A. & Bode, H. B. Natural Product Diversification Mediated by Alternative Transcriptional Starting. *Angew. Chem. Int. Ed. Engl.* **57**, 5699–5702 (2018).
3. Tobias, N. J. *et al.* *Photorhabdus*-nematode symbiosis is dependent on *hfq*-mediated regulation of secondary metabolites. *Environ. Microbiol.* **19**, 119–129 (2017).
4. Yu, S.-H., Vogel, J. & Förstner, K. U. ANNOgesic: a Swiss army knife for the RNA-seq based annotation of bacterial/archaeal genomes. *Gigascience* **7**, 673 (2018).
5. Li, L. *et al.* BSRD: a repository for bacterial small regulatory RNA. *Nucleic Acids Res.* **41**, D233–D238 (2013).
6. Goodman, A. L. *et al.* Identifying genetic determinants needed to establish a human gut symbiont in its habitat. *Cell Host Microbe* **6**, 279–289 (2009).
7. Nollmann, F. I. *et al.* A *Photorhabdus* Natural Product Inhibits Insect Juvenile Hormone Epoxide Hydrolase. *Chembiochem* **16**, 766–771 (2015).
8. Lorenzen, W., Ahrendt, T., Bozhueyuek, K. A. J. & Bode, H. B. A multifunctional enzyme is involved in bacterial ether lipid biosynthesis. *Nat. Chem. Biol.* **10**, 425–427 (2014).
9. Waters, C. M. & Bassler, B. L. The *Vibrio harveyi* quorum-sensing system uses shared regulatory components to discriminate between multiple autoinducers. *Genes Dev.* **20**, 2754–2767 (2006).
10. Thoma, S. & Schobert, M. An improved *Escherichia coli* donor strain for diparental mating. *FEMS Microbiol. Lett.* **294**, 127–132 (2009).
11. Fischer-Le Saux, M., Viillard, V., Brunel, B., Normand, P. & Boemare, N. E. Polyphasic classification of the genus *Photorhabdus* and proposal of new taxa: *P-luminescens* subsp *luminescens* subsp nov., *P-luminescens* subsp *akhurstii* subsp nov., *P-luminescens* subsp *laumondii* subsp nov., *P.temperata* sp nov., *P.temperata* subsp *temperata* subsp nov and *P-asympiotica* sp nov. *Int. J. Syst. Bacteriol.* **49**, 1645–1656 (1999).
12. Lengyel, K. *et al.* Description of four novel species of *Xenorhabdus*, family Enterobacteriaceae: *Xenorhabdus budapestensis* sp nov., *Xenorhabdus ehlersii* sp nov., *Xenorhabdus innexi* sp nov., and *Xenorhabdus szentirmaii* sp nov. *Syst. Appl. Microbiol.* **28**, 115–122 (2005).
13. Bode, E. *et al.* Promoter Activation in Δhfq Mutants as an Efficient Tool for Specialized Metabolite Production Enabling Direct Bioactivity Testing. *Angew. Chem. Int. Ed. Engl.* **58**, 18957–18963 (2019).
14. Joyce, S. A. *et al.* Bacterial biosynthesis of a multipotent stilbene. *Angew. Chem. Int. Ed. Engl.* **47**, 1942–1945 (2008).
15. Brachmann, A. O. *et al.* A type II polyketide synthase is responsible for anthraquinone biosynthesis in *Photorhabdus luminescens*. *Chembiochem* **8**, 1721–1728 (2007).

16. Bode, H. B. *et al.* Determination of the Absolute Configuration of Peptide Natural Products by Using Stable Isotope Labeling and Mass Spectrometry. *Chemistry* **18**, 2342–2348 (2012).
17. Brachmann, A. O. *et al.* Pyrones as bacterial signaling molecules. *Nat. Chem. Biol.* **9**, 573–578 (2013).
18. Brachmann, A. O., Forst, S., Furgani, G. M., Fodor, A. & Bode, H. B. Xenofuranones A and B: Phenylpyruvate dimers from *Xenorhabdus szentirmaii*. *J. Nat. Prod.* **69**, 1830–1832 (2006).
19. Zhou, Q. *et al.* Structure and Biosynthesis of Xenoamicins from Entomopathogenic *Xenorhabdus*. *Chemistry* **19**, 16772–16779 (2013).
20. Cai, X. *et al.* Entomopathogenic bacteria use multiple mechanisms for bioactive peptide library design. *Nat Chem* **9**, 379–386 (2017).
21. Corpet, F. Multiple sequence alignment with hierarchical clustering. *Nucleic Acids Res.* **16**, 10881–10890 (1988).

Curriculum vitae

Nick Larry Valentin Neubacher

Adresse Alte Postgasse 11
69469 Weinheim
Tel. +49 175 20 61 220
E-Mail neubacher@bio.uni-frankfurt.de
Geburtsdatum 14.02.1992, Weinheim
Nationalität Deutsch

Akademischer Werdegang

- 03/2017-heute** Promotion am Institut für Molekulare Biowissenschaften der Johann-Wolfgang Goethe-Universität, Frankfurt am Main
Arbeitsgruppe für Molekulare Biotechnologie von Prof. Dr. Helge B. Bode
Forschungsthema: Einfluss von Insekten-Faktoren auf die Naturstoffproduktion von entomopathogenen Bakterien
- 10/2014-12/2016** **Master of Science**
Molekulare Biowissenschaften an der Johann-Wolfgang- Goethe-Universität, Frankfurt am Main
Thema der Abschlussarbeit: Untersuchung zum Einfluss neuartiger bakterieller Transkriptionsfaktoren sowie von Insektenhomogenisat auf die Naturstoffproduktion und Virulenz von Xenorhabdus
Abschluss: **Master of Science**
Gesamtnote: 1,5
- 10/2011-07/2014** **Bachelor of Science**
Biowissenschaften an der Johann-Wolfgang-Goethe-Universität, Frankfurt am Main
Thema der Abschlussarbeit: Einfluss von Hfq und LuxS auf die Produktion von Sekundärmetaboliten in entomopathogenen Bakterien
Abschluss: **Bachelor of Science**
Gesamtnote: 1,8

09/2002– 05/2011

Abitur

Werner-Heisenberg-Gymnasium Weinheim, Weinheim

Abschluss **Allgemeine Hochschulreife**

Gesamtnote: 2,2

Publications

Heinrich, Antje K.; Hirschmann, Merle; Neubacher, Nick; Bode, Helge B. (2017): LuxS-dependent AI-2 production is not involved in global regulation of natural product biosynthesis in *Photorhabdus* and *Xenorhabdus*. In: *PeerJ* **5**, e3471. DOI: 10.7717/peerj.3471.

Shi, Yi-Ming; Brachmann, Alexander O.; Westphalen, Margaretha A.; Neubacher, Nick; Tobias, Nicholas J.; Bode, Helge B. (2019): Dual phenazine gene clusters enable diversification during biosynthesis. In: *Nat. Chem. Biol.* **15** (4), S. 331–339. DOI: 10.1038/s41589-019-0246-1.

Tobias, Nicholas J.; Heinrich, Antje K.; Eresmann, Helena; Wright, Patrick R.; Neubacher, Nick; Backofen, Rolf; Bode, Helge B. (2017): *Photorhabdus*-nematode symbiosis is dependent on *hfq*-mediated regulation of secondary metabolites. In: *Environ. Microbiol.* **19** (1), S. 119–129. DOI: 10.1111/1462-2920.13502.

Neubacher, Nick; Tobias, Nicholas J.; Huber, Michaela; Cai, Xiaofeng; Pidot, Sacha J.; Stinear, Timothy P.; Lütticke, Anna Lena; Papenfort, Kai; Bode, Helge B.: Small RNA directs symbiosis, virulence, and natural products biosynthesis in entomopathogenic bacteria. Under Revision (*Nat. Microbiol.*)

Neubacher, Nick; Tobias, Nicholas J.; Lalk, Michael; Bode, Helge B.: Components of insect larvae modulate SM production in *Xenorhabdus* and *Photorhabdus*. Manuscript in preparation.

Poster presentations

“Global –omics approaches reveal possible key genes of entomopathogenic bacteria required for both sensing of and adaptation to insect hosts“, MaxQuant Summer School, 08.07 – 13.07.2018, Barcelona, Spain.

“Global –omics approaches reveal possible key genes of entomopathogenic bacteria required for both sensing of and adaptation to insect hosts“, VAAM Workshop “On the biology of bacteria producing natural products“, 31.08 – 02.09.2018, Frankfurt, Germany.

Oral presentation

“RNA-based regulation of natural product biosynthesis in entomopathogenic bacteria“, SFB902 kickoff meeting, 23.09-24.09.2019, Bad Homburg, Germany.

Danksagung

Ich danke **Prof. Dr. Helge B. Bode** für motivierende Worte in den nicht ganz so leichten Zeiten, spannende Forschungsthemen sowie für die Unterstützung und Inspiration, die jetzt schon mehr als ein halbes Jahrzehnt anhält.

Bei **Prof. Dr. Eckhard Boles** bedanke ich mich für die Übernahme des Zweitgutachtens dieser Arbeit.

Ein großer Dank geht an **Dr. Yi-Ming Shi**, **Dr. Nicholas J. Tobias** sowie an meine Freundin **Jessi** für das Korrekturlesen dieser Arbeit. Des Weiteren danke ich **Dr. Gina Grammbitter** für viele hilfreiche Tipps in der heißen Phase des Schreibens.

Insbesondere möchte ich mich bei der ganzen **Arbeitsgruppe Bode** für die konstruktive Zusammenarbeit und für das angenehme Arbeitsklima bedanken. Außerdem danke ich allen **Kooperationspartner**, **Co-Autoren** und **Studenten/Studentinnen** für die super Zusammenarbeit.

Ein besonderer Dank geht an meine „Heimarena“ (Büro 0.03). Neben den herausragenden wissenschaftlichen Fähigkeiten zeichneten sich die Mitglieder des Teams „OnlyHereForTheBeer“ (**Siyar „Kavakli“ Kavakli**, **Lukas „Hering“ Kreling**, **Andreas „Doktorandi“ Tietze**, **Sebastian „Zippler“ Wenski** und **Janik „Schaffner“ Kranz**) als Volleyball-Koryphäen aus, indem sie **alle** Uni-weiten Turniere gewannen (insgesamt eins). An dieser Stelle möchte ich auch **Margaretha Westphalen** und **Moritz Drechsler** danken für viele hilfreiche fachliche Diskussionen und natürlich für Weltklasse Tennismatches.

Mein größter Dank gilt meinen Freunden und meiner Familie, die viel Geduld mit mir hatten und mich stets unterstützt haben.